INFORMATION TO USERS

The most advanced technology has been used to photograph and reproduce this manuscript from the microfilm master. UMI films the original text directly from the copy submitted. Thus, some dissertation copies are in typewriter face, while others may be from a computer printer.

In the unlikely event that the author did not send UMI a complete manuscript and there are missing pages, these will be noted. Also, if unauthorized copyrighted material had to be removed, a note will indicate the deletion.

Oversize materials (e.g., maps, drawings, charts) are reproduced by sectioning the original, beginning at the upper left-hand corner and continuing from left to right in equal sections with small overlaps. Each oversize page is available as one exposure on a standard 35 mm slide or as a 17″ × 23″ black and white photographic print for an additional charge.

Photographs included in the original manuscript have been reproduced xerographically in this copy. 35 mm slides or 6″ × 9″ black and white photographic prints are available for any photographs or illustrations appearing in this copy for an additional charge. Contact UMI directly to order.

Accessing the World's Information since 1938

300 North Zeeb Road, Ann Arbor, MI 48106-1346 USA

Order Number 8801682

Spatial and spectral properties of the goldfish retina

Bilotta, Joseph, Ph.D.

City University of New York, 1987

Copyright ©1987 by Bilotta, Joseph. All rights reserved.

U·M·I
300 N. Zeeb Rd.
Ann Arbor, MI 48106

PLEASE NOTE:

In all cases this material has been filmed in the best possible way from the available copy. Problems encountered with this document have been identified here with a check mark ✓.

1. Glossy photographs or pages _____
2. Colored illustrations, paper or print _____
3. Photographs with dark background _____
4. Illustrations are poor copy _____
5. Pages with black marks, not original copy _____
6. Print shows through as there is text on both sides of page _____
7. Indistinct, broken or small print on several pages ✓
8. Print exceeds margin requirements _____
9. Tightly bound copy with print lost in spine _____
10. Computer printout pages with indistinct print _____
11. Page(s) _____ lacking when material received, and not available from school or author.
12. Page(s) _____ seem to be missing in numbering only as text follows.
13. Two pages numbered _____. Text follows.
14. Curling and wrinkled pages _____
15. Dissertation contains pages with print at a slant, filmed as received ✓
16. Other _____

_____

_____

U·M·I

SPATIAL AND SPECTRAL PROPERTIES OF THE GOLDFISH RETINA

by

Joseph Bilotta

A dissertation submitted to the Graduate Faculty in Psychology in partial fulfillment of the requirements for the degree of Doctor of Philosophy, The City University of New York.

1987

© 1987

Joseph Bilotta

All Rights Reserved

This manuscript has been read and accepted for the Graduate Faculty in Psychology in satisfaction of the dissertation requirement for the degree of Doctor of Philosophy.

7/1/87
date

Chair of Examining Committee

7/29/87
date

Herbert D. Saltzstein
Executive Officer

Dr. Israel Abramov

Dr. Louise Hainline

Dr. Anthony Sclafani

Dr. James Gordon

Dr. David H. Raab

Supervisory Committee

The City University of New York

Abstract

Spatial and Spectral Properties of the Goldfish Retina

by

Joseph Bilotta

Adviser: Professor Israel Abramov

Most studies of retinal ganglion cells have concentrated on either spatial or spectral properties, even though the same cells are involved in processing both types of information. This project examined the relationship of spatial and spectral processing in goldfish ganglion cells. Responses of single ganglion cells from an excised, isolated retina were recorded while various spatial and spectral stimuli were presented to the retina. Each cell was classified by its spatial properties (e.g., linearity of spatial summation and spatial contrast sensitivity (S-CSF)) and its spectral properties (spectral class or long-wavelength center response and spectral opponency/ nonopponency).

Results show that X-, Y-, and W-like cells exist in the goldfish retina. Goldfish X-like cells, like cat X-cells, possess a null point, while Y-like cells respond with a frequency doubling at all spatial positions at high spatial frequencies; W-like cells' properties were similar to the "not-X" cells found in the eel retina. These spatial classes were independent of spectral class and spectral opponency.

The shape of the cell's S-CSF depended on various stimulus parameters (e.g., stimulus drift rate) and on the intrinsic properties of its receptive field components. The S-CSFs of X- and Y-like cells also differed as a function of spectral class and spectral opponency. These differences can be explained by differences in receptive field center size across spectral class and by antagonistic interactions between the center's chromatic mechanisms in spectrally opponent cells. Sensitivity to a drifting grating varied as a function of stimulus orientation and direction. Some X-like cells and virtually all Y- and W-like cells displayed orientation tuning; however, this tuning depended on the spatial frequency of the stimulus. Many Y-like cells and all W-like cells displayed direction selectivity; this also varied with stimulus spatial frequency but in a different fashion than orientation tuning.

In conclusion, goldfish ganglion cells, like those in mammalian retina, can be subdivided into X-, Y-, and W-like cells based on their spatial summation properties. Differences in S-CSFs across stimulus variations and the cell's spectral properties can be explained by a "difference of two Gaussian distributions" receptive field model with slight modifications.

To Martin S. Lindauer, Ph.D.,

my friend and colleague.

ACKNOWLEDGEMENTS

One of the more difficult tasks of writing this thesis was to make the acknowledgements shorter than the body of text. Any scientific endeavor requires support and guidance from many sources. Although it would be impossible to name them all or even to do justice to their contributions, there are several I would like to take a moment to thank.

When I was just a young undergraduate, I marvelled at the work and accomplishments of scientists like Hubel and Wiesel. I thought, 'how exciting it must be to enter the world of a neuron and watch as it communicates to other neurons'. Well, I was right, it is exciting and even now, I still find myself watching in amazement the responses of a neuron during a recording session. I thank Issy Abramov for allowing me the opportunity to fulfill a dream. As my adviser, he has provided me with the opportunity, guidance and support to accomplish this goal.

I would also like to acknowledge the contributions of the other members of my committee. Jim Gordon provided me a "sounding board" throughout this project. He has smoothed many of the "rough edges" in my ideas and thinking and has made me a better scientist. Louise Hainline has always been very supportive throughout my graduate career. She has helped in all aspects of my work, from helping me fix my computer to reading my manuscripts to make sure they made sense. Tony Sclafani has been a steady source of support and assistance. Tony expected hard work and only the best from me because thats what he gave to me. Finally, aside from the wisdom and advice, Dave

Raab has shown me that you can possess excitement and enthusiasm in your work and still maintain your respect and dignity.

Ron Mackintosh showed me the "ins and outs" of single neuron electrophysiology. He taught me how to use the equipment and how to become obsessed with the data -- where would I be without Mack? Chris Harris and Ed Donahue, my fellow graduate students, have helped me on the many occasions I ran into problems. Oh, and special thanks to Ed for helping me align that mirror.

Throughout this project I have had a number of graduate and undergraduate assistants; a very special thanks goes to the following: Faun Tabin has been more than just a colleague to me. She has been a true friend and confidant throughout the years. She was always there when I needed a friend and was not afraid to be brutally honest when necessary. I thank her for everything and wish her a very happy life. One could not ask for better help than Ali Shan Khan, Fritzgerald Francois, Kahang Chang and Laura Kelly. These individuals helped to get the project successfully underway. They spent most of their time with tedious checking, calculating and analyzing only to find a better way to do it. I thank them with all my heart and hope they realize how important they are to me. Jeff Farbman took over where they left off. He helped me through the middle years with constant discussion and assistance. A special thanks goes to Jeff for his help with the Appendix. I am touched that he has "seen the light" and is pursuing a career in vision. Christina Pansarasa provided me with support and hard work during the "home stretch". I owe much of the last part of the results to her dedication

and perserverence. I wish her the best of luck in her career even though she really doesn't need it. I thank her for her friendship and support as well as her scientific contributions. I would also like to thank Christina's daughter, Ashley for helping me to keep things in perspective.

I would like to thank my parents and relatives for all of their support. A special thank you goes to Grandma Pizzuti who was always there when I needed her. Two friends who have stood by me throughout the years are Tom Ziuko and John Koury.

Finally, my wife Elizabeth has helped me in this endeavor in so many ways that I could not possibly begin to thank her. Aside from reading and re-reading every page of this manuscript, she has been supportive, understanding and caring throughout. She has suffered all of my disappointments, shared in all my joy. It became a part of her life as well as mine. No one could ask any more of a person. Thank you, Elizabeth.

TABLE OF CONTENTS

LIST OF FIGURES

LIST OF TABLES

INTRODUCTION

1.1 Overview.

The world around us contains a plethora of visual images. The role of our visual system is to sort out or "filter" this infinite array of light patterns and to somehow extract information about the environment. This is not an easy task; every object or stimulus possesses a number of different visual dimensions or properties. For example, an object has a particular size, pattern or shape, contrast and color. Our visual system is able to "keep track" of all these dimensions and does so with remarkable success.

The first stage of processing in the visual system occurs in the eye, more specifically, in the neural tissue located in the back part of the inside of the eye, the retina. The retina (which is part of the central nervous system), consists of several layers of neurons, each with its own function. For example, the photoreceptors' function is to convert the light pattern falling onto the retina into neural energy. This represents the first stage of neural processing in the retina. The retina's final stage of neural processing occurs at the ganglion cells. The axons of these neurons send information to the

brain for further processing. Thus, ganglion cell responses are the output of all the processing that takes place in the retina.

All neurons communicate or send information by voltage changes throughout the various parts of the neuron. Electrical changes in one neuron can, under certain circumstances, cause changes in a neighboring neuron. Most neurons in the retina signal information by producing very small changes in electrical potential -- these neurons are physically close to one another so that small voltage changes (graded potentials) are sufficient. However, the ganglion cells face a different situation. Since they must send signals over long distances (from the eye to the brain), a regenerating electrical pulse (action potential) is sent down the axon to the brain. All action potentials are similar in their amplitude and waveform and thus, the only information the brain receives from the retina is that an action potential was sent or that it wasn't. To wit, all the information regarding the visual stimulus is somehow coded into a particular pattern (i.e., a binary code of pulse - no pulse) of action potentials.

A change in the visual stimulus must be represented by a change in the frequency of the action potentials or perhaps by a change in the firing pattern of these signals. The goal of this project is to examine the coding process in the retina. This will be accomplished by "eavesdropping" on the ganglion cells by placing microelectrodes next to these ganglion cells and recording their firing patterns as the visual stimulus is varied. Most studies of retinal ganglion cells have concentrated on either spectral (color) or spatial (pattern) properties, even though, the same cells are involved in

processing both types of information. This project examines and relates the spectral and spatial properties of goldfish ganglion cells.

The goal of this research is to provide a better understanding of the visual system, also, and more generally, to provide some insight on how neurons communicate with one another. Ganglion cells are good candidates for this type of investigation. As mentioned above, the retina is physically separate from the rest of the central nervous system. Since the ganglion cells are the final processing neurons of the retina, their responses contain the basic information about the visual stimulus prior to the brain, making the ganglion cell an important way-station in vision.

Another advantage in examining the output of the retina is that information is unidirectional. That is, for the most part, information travels from the ganglion cell to the brain. Finally, there are fewer ganglion cells than any other type of neurons in the visual system. Thus, information is represented most efficiently and with the least redundancy at this level.

In summary, the retina is a self-contained visual processing unit in which the ganglion cell response represents the output. The retina can be thought of as a system or device in which the input (the visual stimulus) is known and controlled, while the output (ganglion cell response), can be monitored and recorded. Thus, the goal of this work is to examine how the retina transforms the input into a code that the brain can use to understand the visual world.

This work will focus on the ganglion cells of the common goldfish. There are both practical and theoretical reasons for studying

the goldfish retina. Since the goldfish is a cold-blooded vertebrate, its retina can be removed, and under the proper conditions, can be kept functioning and healthy for long periods of time. This provides an opportunity to study a particular neuron for much longer periods of time than would be possible if one were studying the same neurons in an intact, anesthetized, warm-blooded animal. For most cases, the isolated goldfish retina can be maintained in good health for up to 6 hours. The retinal neurons of the goldfish are larger than those in the mammalian retina, and therefore, are easier to record from, especially, the more distal cells which provide inputs to the ganglion cells.

Another reason for choosing the goldfish for the experimental animal is that it has been widely used as a model of the vertebrate retina and therefore, many of the important characteristics are already described. It is known that the goldfish retina has the same cell types and interconnections as other vertebrates. However, one should not assume that all vertebrate retinae are the same. There are differences across species; fortunately, these differences can be useful tools in examining properties which are more difficult to study in other animals (see below).

Before progressing any further, some mention of goldfish taxonomy is in order. The common goldfish belongs to the family of Cyprinid fishes, commonly refered to as carps or minnows. Cyprindae are part of a large group of fresh-water fishes, known as teleosts. The goldfish belongs to the genus Carassius. There are two members of the Carassius genus, the common goldfish (Carassius

auratus) and the crucian carp (Carassius carassius). For the most part, visual processing across the cyprinid family is very similar. Because of this, references will be made to the other cyprindae when information is lacking in the goldfish. Since there are some subtle differences across these fishes, however, the species from which the information was obtained will be explicitly stated.

The primary reason for using the goldfish for this work stems from the fact that the goldfish has color vision. There is both physiological and psychophysical evidence that the goldfish has the necessary mechanisms for color vision. In fact, goldfish color vision appears to be very similar, at least qualitatively, to primate color vision, including that of humans. Goldfish possess the same types of photoreceptors (rods and cones) as primates. However, primate and goldfish photoreceptors differ in their spectral sensitivities. The spectra of the individual cone photopigments are more separated in goldfish than in primates. Because of this separation of the cone types across the spectrum, goldfish are capable of responding to infra-red wavelengths of light, making it much simpler to identify which cone types are contributing to the responses of any ganglion cell.

1.2 Goldfish Retinal Anatomy.

The broad principles of retinal processing appear to hold across species since most vertebrate retinae possess the same types of neurons and interconnections (see Walls, 1942). The vertebrate retina consists of five different classes of neurons (Boycott and Dowling,

1969). Three of these neuron types, receptors, bipolar cells and ganglion cells are commonly referred to as the direct neural pathway; that is, information travels from the receptors directly to the bipolar cells and then to the ganglion cells which send their information to the brain. The remaining neurons, horizontal and amacrine cells, provide lateral transfer throughout the retina. Horizontal cells are located between the receptors and the bipolar cells, and the amacrine cells are between bipolar and ganglion cells.

The retina can also be divided into several layers. The three nuclear layers, starting from the back of the eye, are the outer nuclear layer, the inner nuclear layer, and the ganglion cell layer. As is apparent from their names, the nuclear layers consist of the cell bodies of the various neurons. The outer nuclear layer contains the cell bodies of the receptors (i.e., the rods and cones). The inner nuclear layer is where the cell bodies of the horizontal, bipolar and amacrine cells are located, and of course, the ganglion cell bodies are found in the ganglion cell layer.

There are two plexiform layers between the nuclear layers, the outer plexiform layer, located between the outer and inner nuclear layers, consists of synaptic connections among the receptors, bipolar cells and horizontal cells. The inner plexiform layer, consists of the synaptic connections among bipolar, amacrine and ganglion cells, and is found between the inner nuclear layer and the ganglion cell body layer. A schematic illustration of the anatomy of the goldfish retina is shown in Figure 1.

Of major importance to this work, as well as to any visual physi-

Figure 1

Schematic illustration of the anatomy of the goldfish retina. This figure is a composite from several sources. For a general description, see Rodieck (1973), Dowling (1970) and DeTesta (1966). The features of the receptors and the outer nuclear layer are redrawn from Scholes (1975). Information regarding the outer plexiform and inner nuclear layers can be found in Stell and Kock (1983) and Stell and Lightfoot (1975). The interconnections among bipolar, amacrine and ganglion cells are derived from Famiglietti, Kaneko and Tachibana (1977). Pure cone bipolar cells are not included in this figure since information regarding their anatomical connections is sparse. The illustration is not drawn to scale -- its purpose is to show the anatomical connections within the goldfish retina.

Anatomy of the Goldfish Retina

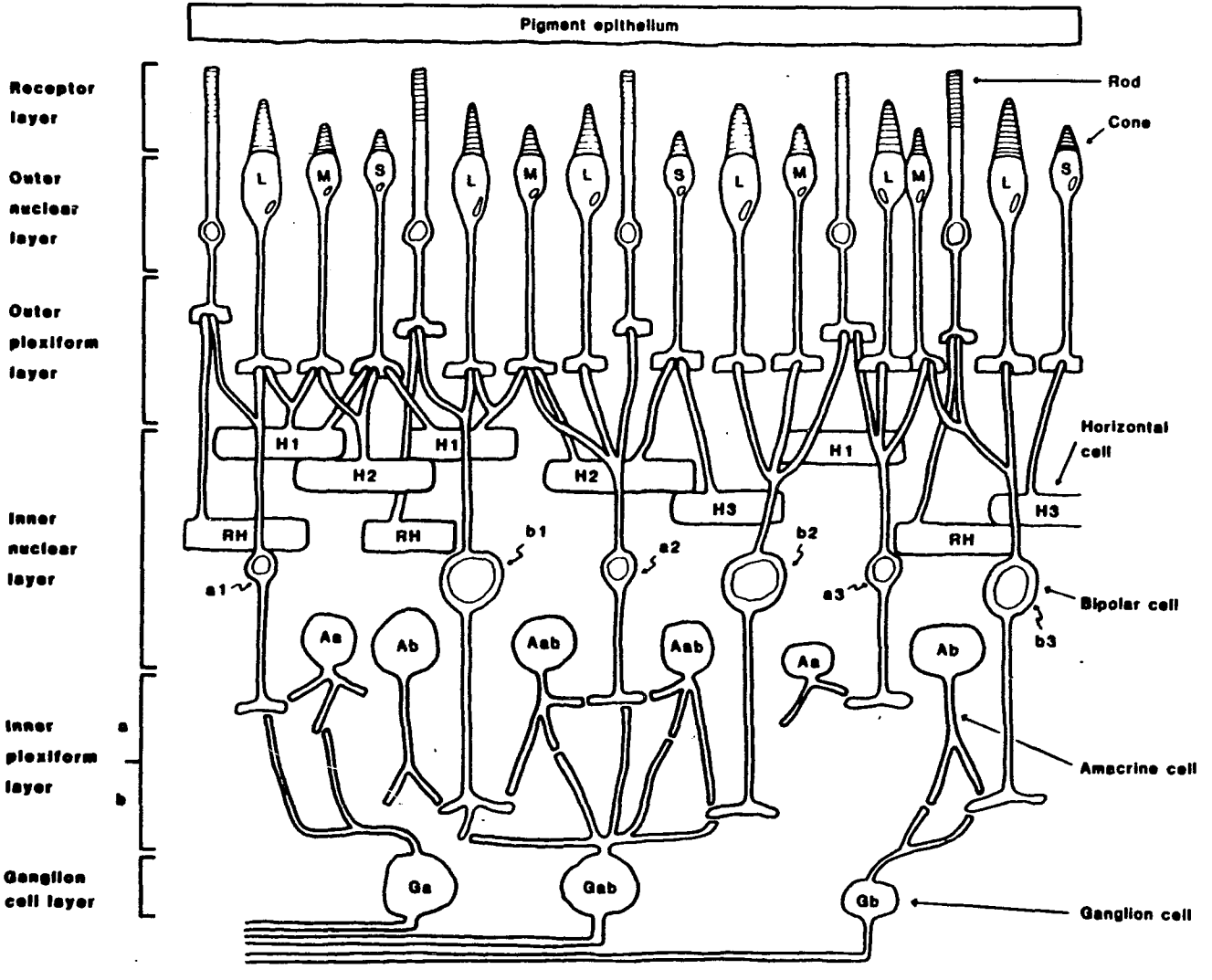

ology, is the concept of a cell's receptive field. The most general definition is: any area on the retina, that, when stimulated by light, produces an electrical change or response in the particular cell of interest. Since only the receptors are capable of changing light energy to neural energy, the receptive field of any neuron is ultimately a function of the receptors it contacts. However, due to the lateral connections that occur in the retina, the receptive field of a neuron can contain regions antagonistic to one another. That is, one area of the receptive field, when stimulated by light, can produce an increase in the response of that neuron, while another portion of the receptive field can cause a decrease in the cell's response.

1.2.1 Photoreceptors and Photopigments.

The goldfish retina is similar to the primate retina in that it is a duplex retina. However, unlike the primate retina which has a fovea containing the vast majority of cones, the goldfish rods and cones appear to be evenly distributed across the retina (Marc and Sperling, 1976) with a slightly higher density of rods and cones at the temporal-dorsal side (Schellart, 1973). There are at least six morphologically distinct types of cones in the goldfish retina, although there do not appear to be any functional differences across the different types (Marc, 1977). The only functional difference among the cones is that they each possess one of three different photopigments (Harosi, 1976; Marc, 1977; Marc and Sperling, 1976; Stell and Harosi, 1976). Through the use of microspectrophotometry, the λ-max, or peak sensitivity, of three of the goldfish cone types has been deter-

mined to be 450 nm, 533 nm and 625 nm (Harosi, 1976). These cone types will be designated as the short-wavelength cones (S-cones), middle-wavelength cones (M-cones), and long-wavelength cones (L-cones), respectively, to refer to the portion of the spectrum in which their peak sensitivities are found. The proportions of the three cone types in the retina have been determined to be 45% L-cones, 35% M-cones and 20% S-cones (Marc and Sperling, 1976).

The adult goldfish retina contains a substantial number of rods (Stell and Harosi, 1976), but the rods do not appear to have any different structural types as do the cones. Bridges (1967) has determined the spectral sensitivity of the goldfish rod photopigment by means of pigment extraction and bleaching of the rod pigments contained in the crucian carp. The goldfish rods contain the photopigment porphyropsin, which is commonly found in fresh-water fishes and has a λ-max of 520 nm. (Walls, 1942).

About half the cones in the goldfish retina are twin or double cones. Double cones consist of two cones juxtaposed at the ellipsoid and myoid portion (Marc, 1977). The longer outer segment of a double cone contains the L-cone photopigment while the shorter outer segment contains the M-cone photopigment (Stell and Harosi, 1976). The long, single cones can possess either the L- or M-cone photopigment; S-cone photopigment is found only in the short and miniature cone types (Marc and Sperling, 1976; Stell and Harosi, 1976).

The cone pedicles of the goldfish (Stell, 1972) possess invaginated synapses and within any one cross-section contains a bipolar cell dendrite situated between two horizontal cell dendrites. This

"triad" arrangement in the cone pedicles is very common in many species (Scholes, 1975; Stell, 1967). There is also evidence that the receptors make reciprocal contacts with other receptors in a variety of species. Scholes (1976) found that the rudd (which is a cyprinid fish) possesses invaginating cone-to-cone interactions that occur across the different cone types in a particular arrangement. M-cones invaginate into L-cones, L-cones into M-cones, and S-cones invaginate into M-cones. Similar interconnections have been found in the goldfish with the addition that L- and M-cones invaginated into S-cones (Lockhart and Stell, 1979).

The receptors' outer segments and the pigment ephithelium of goldfish, as well as those of many other fish, migrate depending upon the lighting conditions of the environment. The results of these movements is that the outer segment is surrounded by the pigment ephithelium which acts as a "sheath" of absorbing pigment; a possible consequence of this being that the receptor's sensitivity to light is reduced. These "retinomotor movements" are the result of changes in the lighting conditions and are also a function of a circadian rhythm or day/night cycle (Ali, 1975). In daylight, the cone myoids (the portion of the receptor that connects the outer segment to the inner segment) shorten leaving the cone ellipsoids near the external limiting membrane, and retracted from the pigment ephithelium. The rod myoids, on the other hand, lengthen, placing the rod ellipsoids and the outer segments near the pigment ephithelium to protect the highly sensitive rods from bleaching by strong light (Ali, 1975). In darkness, the retinal movements are just the opposite for both types of

receptors exposing the rods to function at scotopic light levels.

Recently, there have been several psychophysical reports of a possible fourth receptor in goldfish (Hawryshyn and Beauchamp, 1985; Neumeyer, 1985). This receptor type is sensitive to ultraviolet (U.V.) light, has a λ-max at about 380 nm and is sensitive up to about 420 nm (Hawryshyn and Beauchamp, 1985). Although there is no direct evidence from microspectrophotometry for such a receptor in goldfish, there have been reports of U.V.-sensitive photopigments in other cyprinid fishes (Avery, Bowmaker, Djamgoz and Downing, 1982; Harosi and Hashimoto, 1983). In both cases, the U.V.-sensitive receptor was found in the smaller cone types. This may account for their elusiveness in other microspectrophotometry studies. It is also interesting to note that although the U.V. receptor is apparent in psychophysical measures, there is only one report of any electrophysiological evidence. Fukurtani and Hashimoto (1984) found U.V. responses from horizontal cells in several fish species (none of which were goldfish). There is certainly no evidence for a U.V. receptor input at the level of the ganglion cell or optic nerve in the range from 400 to 720 nm in the goldfish (Beauchamp and Lovasik, 1973; Mackintosh, Bilotta and Abramov, 1987; Spekreijse, Wagner and Wolbarsht, 1972).

1.2.2 Horizontal Cells.

The horizontal cell layer in the teleost fish comprises one-third of the entire retina. These giant cells have cell bodies that range from 15 to 40 μm in diameter (Schellart, 1973). There are four types

of horizontal cells based on their morphology and arborizations; each forming a layer laterally across the retina. Lateral transmission of information between horizontal cells may be in the form of conventional synapses (Witkovsky and Dowling, 1969) as well as by electrical coupling (Kaneko, 1971a).

The four horizontal cells types also differ in their specific receptor connections. Starting from the most sclerad layer in the retina: H1 cells make direct connections with all cone types (S-, M-, and L-cones, including double cones). H2 cells synapse to all M- and S-cone types (including short, double cones which contain the M-cone pigment), and H3 cells synapse only to S-cones (short, single and miniature cone types). (See Stell and Lightfoot, 1975, for more details.) The fourth type, RH, make connections only to the rods. All cone-to-horizontal cell synapses are sign conserving (Stell and Lightfoot, 1975); that is, both the receptors and their corresponding horizontal cells hyperpolarize to light. The cone horizontal cell (H1, H2, H3) response can be altered by the influence of other cone horizontal cell types by means of feedback synapses of horizontal cells to the cones (Stell and Lightfoot, 1975). This interaction among horizontal cells produces the spectral opponency response found in the biphasic (H2) and triphasic (H3) cells and will be discussed, in more detail, below. Cone horizontal cell axons appear to terminate in the inner nuclear layers of the retina (Stell, 1975); however, their specific function is still unknown. At present, there is insufficient information regarding the presence or role of rod horizontal cell axons.

1.2.3 Bipolar Cells.

There are two morphological types of bipolar cells in the goldfish retina: large bipolar cells and small bipolar cells. The diameter of the small bipolar cell body is 8 μm; whereas, the large bipolar cell body diameter is larger than 10 μm (Cajal, 1893; Stell, 1972; Witkovsky and Dowling, 1969). Due to the size of the small bipolar cell, there has been little success in determining its structure and function.

The two morphological types of bipolar cells can also be distinguished by their receptor contacts. The small bipolar cells contact exclusively cones while the large bipolar cells receive input from both rods and cones. Thus, these cells types are also referred to as pure cone and mixed bipolar cells, respectively (Scholes, 1975; Stell, 1980). Unlike mammals, teleosts possess no pure rod bipolar cells (Kolb, 1970). Stell and colleagues (see Stell and Kock, 1983 for a review) have further divided the mixed bipolar cells of the goldfish into five types. This division is based on their receptor input and their termination in the sublaminae of the inner plexiform layer (IPL). Bipolar cells that terminate in the distal sublamina "a" are designated as types a1 and a2. Bipolar cells terminating in the proximal sublamina "b" are designated as types b1, b2, and b3. Subtypes a1 and b1 contact rods and L-cones, while subtypes a2, a3, b2, and b3 synapse on rods, M-cones and L-cones. Stell and Kock (1983) have postulated a sixth type of bipolar cell based on studies using carp (Saito, Kujiraoda and Yonaha, 1983). They have suggested that the new type of bipolar cell should be labelled as a3 based on their cone

inputs, dendritic field size and response type (i.e., OFF-center).

The size of the goldfish mixed bipolar cell dendritic tree diameter varies linearly with the number of individual cones contacted. However, there is no correlation between dendritic field size and the number of rods contacted or the ratio of rods to cones contacted (Ishida, Stell and Lightfoot, 1980). Also, the dendritic arborization of the mixed bipolar cell is slightly elliptical and may produce an "orientation bias" even at this level of the retina. However this degree of ellipticity is not enough to account for the orientation tuning found in ganglion cells since the dendritic spread of a single bipolar is smaller than the receptive field center of a goldfish ganglion cell. More will be said regarding this bias in Section 1.5.2.

The pure cone bipolar cell dendritic field is much larger than that of the mixed bipolar cell (Scholes, 1975). At present, only pure S- and M-cone bipolar cells have been found. There has been no evidence for a pure L-cone bipolar cell, however, it has been speculated that this type does exist. Pure cone bipolar cell termination appears to be somewhere in the inner synaptic layer, but details about this cell type are unclear. One final point worth mentioning about the bipolar cells is that the S-cone inputs are completely segregated from the other cone inputs. The S-cones appear to supply information only to pure cone bipolar cells. There is no interaction of the S-cones with the other cone types at the level of the bipolar cell (Scholes, 1975; Stell and Lockhart, 1975).

1.2.4 Amacrine Cells.

There appear to be four morphologically different types of amacrine cells in the goldfish retina (DeTesta, 1966). Like the horizontal cells, amacrine cells stretch laterally across the retina. Amacrine cells do not possess any type of axon, however, they have widely branched dendrites which terminate in the inner nuclear layer (INL) and inner plexiform layer (IPL). One type of amacrine cell sends its dendritic arborizations to sublamina "a" of the IPL and receives input from mixed bipolar cells that terminate in this sublamina (i.e., a1 and a2 of Stell's classification). Another type of amacrine cell has its dendrites terminate in sublamina "b" of the IPL and thus, receives information from b1, b2, and b3 mixed bipolar cells. A third type of amacrine cell sends dendritic arborizations to both sublaminae and receives input from both types of bipolar cells (Famiglietti, et al., 1977). This "wiring" produces a functional difference among the amacrine cells which will be discussed in Section 1.3.

1.2.5 Ganglion Cells.

Ganglion cell axons make up the optic nerve and therefore their responses represent the last processing before reaching the brain. Ganglion cells receive information from bipolar cells and amacrine cells. Recently, goldfish ganglion cells were classified into three morphological types (Hitchcock and Easter, 1984). This classification was based on the size of the cell body and its dendritic arborizations. Type I cells consisted of a small cell body, one to three thin primary dendrites, and small, dense arbors. Type II cells possessed a larger

cell body, two to five thick primary dendrites, and large, moderately dense arborizations. Type III cells had small somata, and one to three thin primary dendrites, but also possessed large sparse arbors. It was also found that each type contained several subtypes based upon their dendritic stratification pattern. Unfortunately, no correlation between these morphological types and their functions has been attempted in the goldfish. Since their original report, Hitchcock and Easter (1986) have found a fourth morphological class of goldfish ganglion cell. These cells are similar to the Type I cells, but are somewhat smaller in cell body size.

This relationship has been examined in the cat retina and a very strong correlation between morphological and functional cell types was found. Boycott and Wassle (1974) found that cat retinal ganglion cells could be divided into three morphological classes based on somata size and dendritic arborization. The first type, β-cells, possessed the largest cell body and a large dendritic tree. The α-type, on the other hand, had the smallest soma and the smallest dendritic tree. The third type, ɣ-cells, had a small soma like the α-cells but possessed a large dendritic tree not unlike the β-cells. Famgilietti and Kolb (1976) have elaborated on this finding by dividing the α- and β-cells into subclasses based on their dendritic branching patterns. The α-, β-, and ɣ-cell morphological classes of cat retinal ganglion cells (which correspond to the I, II, and III types, respectively, found in the goldfish retina) have been correlated with the three functional types of ganglion cells (i.e., X-, Y-, and W-cells) based on their spatial summation properties. β-cells have been posi-

tively identified as the Y-cell functional type (Cleland, Levick and Wassle, 1975). Although there has been no direct evidence relating the α-cells and X-cells, there is a strong correlation between the receptive field center size of X-cells and the dendritic spread of α-cells (Cleland and Levick, 1974a). Finally, the range of dendritic field spread of γ-cells agree with the range of receptive field centers found in W-cells. However, this is not as clear-cut since the properties of W-cells are somewhat vague. The similarities in the morphological classifications between the well-studied cat ganglion cells and the goldfish cells would predict that these three functional types should also exist and correlate with their morphological cell types.

The dendritic processes of ganglion cells, like amacrine cells, also terminate in different sublamina of the IPL. Some ganglion cells terminate in sublamina "a", some in sublamina "b" and other ganglion cells terminate in both sublaminae (Famiglietti, et al., 1977).

1.3 Physiology of the Goldfish Retina.

1.3.1 Receptors.

Tomita (1966) was the first to successfully record intracellularly from single cones. Using the carp retina, he discovered several important characteristics of the cone response. He found that all cone types show a sustained hyperpolarization to light stimulation, the consequences of this being that no one cone type is capable of wavelength discrimination since there is no means of comparison across

wavelengths. This is known as the principle of univariance (Rushton, 1965). Univariance states that once a quantum of light is absorbed by the photopigment resulting in isomerization, all information regarding the wavelength of the light is lost. Thus, receptors can only report at what rate the photopigment absorbs photons.

Tomita also found that the action spectra obtained by electrophysiological recordings from the carp cones agreed with the difference spectrum (Marks, 1965) obtained by microspectrophotometry from goldfish cones. The λ-maxs of the photopigments have also been verified by recordings in more proximal cells, such as goldfish horizontal cells (Spekreijse and Norton, 1970) and goldfish ganglion cells (Mackintosh, et al., 1987).

It was originally believed that the receptive field of a single cone was the diameter of the outer segment of the cone; however, this is not the case in many species. For example, the receptive fields of turtle cones extend up to 100 μm in diameter, well beyond the size of the individual cone outer segment. This was attributed to electrical coupling among cones of the same type (Baylor and Hodgkin, 1973). Further examination of the turtle cones revealed an antagonistic center and surround organization; light stimulation on the center of the field produced a hyperpolarization response, while stimulation on the outer portion of the receptive field area resulted in a depolarizing response (Baylor and Fuortes, 1970). This antagonistic surround is believed to be the result of a reciprocal feedback synapse to the cone from a horizontal cell. This was verified by O'Bryan (1973) who demonstrated that the surround response of the cone to

illumination had a similar time course to that of horizontal cells.

Although there is evidence that goldfish rods and cones may be electrically coupled as in the turtle cones (Nagy, Stell and Lightfoot, 1983, cited in Stell and Kock, 1983), there is no evidence of the large cone receptive fields (Kaneko, 1973). However, in other fish, such as the pike-perch, cone receptive fields may extend up to 100 µm (Burkhardt, 1977).

The response of the carp cone to light intensity is nonlinear and may be described as a compressive function (Tomita, 1972). The single receptor response conforms to the function:

$$R = \frac{v \times I^n}{k + I^n} \qquad (1)$$

where v and k are half-saturation constants, I is the light intensity and n = 0.73. When I is small, compared to k, the response rises in proportion to intensity; thus, at low intensities, the response is approximately linear. When light intensity is very high (so that k is negligible) the response saturates. This compressive function for single cones also holds for other species, such as Necturus (Werblin and Dowling, 1969) and macaque monkey (Boynton and Whitten, 1970).

1.3.2 Horizontal Cells.

The responses of horizontal cells or S-potentials (named after their discoverer, Svaetichin, 1953) can be classified into two types. The L-type (luminosity cells) responds to all wavelengths of light

with hyperpolarization (Byzov and Trifonov, 1968; Trifonov, 1968). C-type (color cells) S-potentials, however, can respond by hyperpolarizing or depolarizing depending upon the wavelength of the light; these cells are therefore, spectrally opponent. C-type cells can be further subdivided into biphasic or triphasic cells. Biphasic cells respond with hyperpolarization to middle-wavelengths and depolarization to long-wavelengths lights. Triphasic cells respond to both short- and long-wavelengths with hyperpolarization and depolarization to middle-wavelengths. The spectral opponency found in these C-units is a function of the interactions among the different horizontal cells types described in Section 1.2.2. Since cone-to-horizontal cell synapses are sign-conserving, and thus capable of only hyperpolarization, depolarization responses must develop from interactions with other horizontal cells (Stell and Lightfoot, 1975).

Stell and colleagues (see Stell and Kock, 1983, for a review) have proposed a model to account for these different response types based on what is known regarding their synaptic connections. Each horizontal cell possesses a direct non-inverting connection to a specific cone type. Each horizontal cell also contains an inverting feedback synapse to the other cone types. These inverting synapses can affect the response of the other horizontal cell types to produce a depolarizing response. For example, the H1 horizontal cell receives only a direct non-inverting input from the L-cones and thus responds with hyperpolarization across the spectrum with its maximum response at the longer wavelengths; the remaining connections to the other cone types of these H1 cells provide an inverting feedback synapse

which affects the responses of the other horizontal cell types (see below).

The H2 cell type (biphasic C-cells) receive a non-inverting input from the M-cones and thus responds with hyperpolarization at the short- and middle-wavelengths. However, due to an inverting feedback synapse from the H1 cells onto the M-cones, any long-wavelength stimulation will increase the response of the H1 cells and thus produce an opposite depolarizing response of the H2 cells. A similar, although somewhat more complicated, effect occurs with the triphasic H3 cells. These cells receive direct input from S-cones and thus hyperpolarize to short-wavelengths; but because of an inverting feedback synapse from the H2 cells onto the S-cones, the result is inputs opposite of the H2 cells (i.e., hyperpolarization at middle- and depolarization at long-wavelengths) producing depolarization at middle-wavelengths and hyperpolarization at long-wavelengths.

This model has been supported by the finding that the latencies of the chromatic responses of the horizontal cell types differ in the direction one would predict from the model. That is, direct non-inverting responses would have the shortest latency (25 msec for the "blue" component in triphasic cells, the "green" component in biphasic cells, and the "red" component for monophasic or L-type cells). The latency was found to be 50 msec for the "green" component in triphasic cells and the "red" component in biphasic cells, and the longest latency occurred with the "red" component of the triphasic cells which was 75 msec. This would be expected since this component involved "three steps" (Spekreijse and Norton, 1970).

S-potentials obey Ricco's law (area x intensity = k) over large distances across the retina implying a large receptive field. Naka and Rushton (1966a,b,c) determined that these findings were due to an electrical current across the horizontal cells. For carp horizontal cells, Ricco's law holds up to 10 mm on the retina. Exceeding this area does not result in a decrement in response and therefore demonstrates that horizontal cells have no antagonistic center and surround organization.

1.3.3 Bipolar Cells.

Bipolar cells, under most conditions, respond to light by means of a graded sustained response. This has been demonstrated in goldfish (Kaneko, 1970), carp (Kaneko and Hashimoto, 1969) and Necturus (Dowling and Werblin, 1969). Although most bipolar cells recordings have been from large bipolar cells, the responses and synaptic termination in the inner plexiform layer of small bipolar cells appear to be similar (Famiglietti, et al., 1977; Kaneko, 1971b). Bipolar cells are the first neurons in the goldfish retina to demonstrate a true center/surround spatial antagonism. They have a concentric organization in which the center is much more sensitive than the surround mechanism (Kaneko, 1970). The receptive field center of the goldfish bipolar cell is roughly 100-200 μm in diameter. This corresponds to the dendritic field of the bipolar cells and suggests that the bipolar receptive field center receives direct cone input (Kaneko, 1973; Werblin and Dowling, 1969).

The surround portion of the bipolar cell's receptive field prob-

ably results from input of the horizontal cells. To demonstrate that horizontal cells are responsible for the bipolar cell surround, Toyota (see Kaneko, 1979), while recording from a bipolar cell, electrically stimulated a horizontal cell and found the response of the bipolar cell to be similar in response to the surround when stimulated by light. Exactly how horizontal cells play a role in the surround of bipolar cells is still unclear. The surround could be formed by either direct horizontal cell influence or by means of a feedback system onto the receptors. It is also possible that feedback from amacrine cells may be responsible (Stell, 1978).

Bipolar cells can be classified into two groups based on their response properties. A bipolar cell can be an ON-type (depolarization to light illumination of the receptive field center) or an OFF-type (hyperpolarization to light in the receptive field center). The response to light in the surround portion of the receptive field of each of these two cell types is opposite to the response in the center (i.e., ON-type surround hyperpolarizes to light and OFF-type depolarizes to light). There do not appear to be any morphological differences between ON-type and OFF-type bipolar cells. The differences appear to be in the nature of the receptor-to-bipolar cell contact. For example, mixed ON-bipolar cells make either ribbon or narrow cleft contacts with rods, whereas mixed OFF-bipolar cells contact rods with only wide cleft junctions; however the exact nature of these differences is still unclear (Saito, et al., 1983; Sakai and Naka, 1983; Stell, Ishida and Lightfoot, 1977). These functional differences in ON and OFF systems are further segregated in their termination in

the inner plexiform layer. ON-bipolar cells terminate in sublamina "b" of the inner plexiform layer and OFF-bipolar cells send their processes to sublamina "a" of the inner plexiform layer (Famiglietti, et al., 1977).

Many bipolar cells are also spectrally opponent (Kaneko and Hashimoto, 1969). Using Stell's classification scheme for bipolar cells (see Section 1.2.3), types a1 and b1 appear to receive input from L-cones (as as well as the rods) while a2 and b2 receive input from both the L- and M-cone types. Stell and Kock (1983) suggest that the a2 and b2 bipolar cells may be double-opponent. These double-opponent cells are both spatially and spectrally opponent; that is, they are spectrally opponent within a receptive field area (i.e., center or surround). For example, a double-opponent cell may possess a center mechanism that will hyperpolarize to long-wavelength light (-R) and depolarize to middle-wavelength light (+G) giving an overall center response of -R+G. The surround response would be antagonistic or opposite to the center, i.e., +R-G. Double-opponent bipolar cells have been found in the carp (Kaneko and Tachibana, 1981) and in dace (Hashimoto and Inokuchi, 1981). Kaneko and Tachibana (1981) identified the cone inputs of these double-opponent cells as the L- and the M-cones. It is believed that a number of these cells are directly connected to, and may be the origin of the double-opponent ganglion cells. Finally, it should be mentioned that the L-cone input and the rod input to bipolar cells are always synergistic (Saito, Kondo and Toyoda, 1979).

1.3.4 Amacrine Cells.

Amacrine cell bodies are located in the proximal area of the inner nuclear layer. Their dendrites arborize into the inner plexiform layer where they contact bipolar and ganglion cell processes. The role of amacrine cells is not entirely clear, however, Werblin and Dowling (1969) suggest that the amacrine cell's role is to process the dynamic or transient aspects of the stimulus. Amacrine cells may also play a role in the overall adaptation level of the retina.

There are three functionally distinct types of amacrine cells: transient ON-OFF cells (Kaneko, 1970; Werblin and Dowling, 1969), sustained ON-cells, and sustained OFF-cells (Kaneko, 1973; Naka and Ohtsuka, 1975). The functional properties of these amacrine cells correspond to their synaptic contact in the inner plexiform layer. Sustained ON-cells terminate in the inner sublamina "b" and synapse with ON-type bipolar cells; sustained OFF-cells terminate in the outer sublamina "a" and make contact with OFF-type bipolar cells; ON-OFF amacrine cells arborize in both sublaminae and therefore receive input from both ON- and OFF-type bipolar cells (Famiglietti, et al., 1977).

Goldfish amacrine cells display no spatial antagonism, although Werblin and Dowling (1969) found a slight center/surround antagonism in Necturus amacrine cells. Like horizontal cells, amacrine cells display large receptive fields which is most likely due to lateral contacts among amacrine cells. It has been suggested that amacrine cells are capable of generating action potentials as well as graded potentials although it is not clear whether these cells are amacrine cells or merely displaced ganglion cells.

1.3.5 Ganglion Cells.

The ganglion cell sends information about the visual environment to the brain. It is the only retinal neuron with a typical axon. The ganglion cells' axons, which constitute the optic nerve, traverse a large distance to reach the appropriate area of the brain. Therefore, unlike the other retinal neurons, ganglion cells must produce regenerating signals down the axon to reach their objective. These action potentials (or spikes) are randomly generated even in the absence of any visual stimulation; this is the cell's spontaneous or maintained rate. Changes in the visual stimulus must be reflected by changes in pattern or rate from the cell's spontaneous rate.

Hartline (1938), recording from frog ganglion cells, found three functionally distinct types based on their response to large spots of white light: ON-cells, OFF-cells and ON-OFF cells. Light stimulation of ON-cells would increase the firing rates of these cells, while stimulation of OFF-cells would decrease their firing with reference to their spontaneous rates. ON-OFF cells would increase their firing rate both at the onset and offset of light stimulation.

Kuffler (1953) presented small spots of light to the retina while recording from cat ganglion cells and found that these cells possessed a receptive field center with an antagonistic surround. Using similar stimuli, center and surround components were also found in goldfish ganglion cells (Wagner, MacNichol and Wolbarsht, 1960). These goldfish ganglion cell receptive fields, unlike the cat cells, had a spectrally opponent center (e.g., -R+G) and a small spectrally nonopponent surround (+G).

Daw (1967a) recorded from goldfish ganglion cells using a large annular light stimulus and found that the ganglion cell receptive fields were much larger and more complex than previously believed. He found a larger surround component which was both spectrally and spatially opponent to the center mechanism. An example of these "double-opponent" ganglion cells would be +R-G in the center and -R+G in the surround mechanism. A ganglion cell with the mirror image of this cell can also exist (i.e., -R+G center and +R-G surround). Spectral sensitivities of these double-opponent cells revealed M- and L-cone inputs with antagonistic responses (Beauchamp and Lovasik, 1973; Spekreijse, et al., 1972). These double-opponent cells are believed to mediate simultaneous color contrast (Daw 1967b; 1968) since a +R-G center/-R+G surround cell would be most responsive to a red spot of light with a green surround.

Currently, it is generally accepted that there are three functionally distinct types of ganglion cells in the goldfish retina. They are usually designated as Red-ON center, Red-OFF center and ON-OFF cells. Red-ON center cells are equivalent to +R-G center with -R+G surround; Red-OFF center cells correspond to -R+G center with +R-G surround; ON-OFF cells are equivalent to Hartline's ON-OFF classification of frog ganglion cells. The L-cone component (red) is used for classification since these cone inputs are easily isolated (since only they are sensitive to long-wavelength light) and allow for a quick classification scheme of the goldfish ganglion cell. The Red-ON center cells dendritic arborizations terminate in sublamina "b" of the inner plexiform layer, while the Red-OFF center cell processes termi-

nate in sublamina "a" of the inner plexiform layer. ON-OFF ganglion cells send arborizations to both sublaminae (Famiglietti, et al., 1977). Red-ON and Red-OFF center cells have a center diameter of approximately 1 mm although the Red-ON center cell's center is generally smaller. Both cell types possess a large surround ranging from 1.5 to 6 mm in diameter. More will be said about these size differences in Section 1.6.3, below.

All goldfish ganglion cells receive inputs from both rods and cones. The diameters of the rod and cone receptive field centers of a ganglion cell are equivalent in size (Raynauld, 1969). Spectral sensitivity curves from dark-adapted ganglion cells correspond to the goldfish rod photopigment. Also, the sign of the rod response is synergistic to the L-cone input to the ganglion cell (Beauchamp and Daw, 1972; Raynauld, 1972; Shefner and Levine, 1977).

Various goldfish ganglion cells have been reported in which at least one cone input is undetected (Abramov and Levine, 1972; Adams, 1970; Daw, 1968; Spekreijse, et al., 1972). For example, the surround components and the M-cone input of the receptive field center are vulnerable to the isolation procedure when recording from the excised goldfish retina (Abramov and Levine, 1972; Shefner and Levine, 1979; Spekreijse, et al., 1972). The gas composition during the isolation procedures can convert a spectrally nonopponent cell into a spectrally opponent one. Abramov and Levine (1972) found that a gas composition of 100% oxygen produced goldfish ganglion cells that were more sensitive, had higher spontaneous rates in the dark, and were spectrally nonopponent. By changing the gas composition to

contain 2% carbon dioxide, the same cells responded with lower spontaneous rates in the dark, were less sensitive, and also became spectrally opponent. It should be noted that, although the cone inputs can be made to "disappear" in the ganglion cell response under certain conditions, the sign or nature of the cone input remains the same regardless of the manipulation (Mackintosh, et al., 1987). That is, nothing can be manipulated to convert a $^{+}$R-G center cell to a -R^{+}G center cell.

There is an obvious lack of information regarding the contribution of the S-cones to the ganglion cell. Many investigators found little evidence for S-cone input to the ganglion cell (Adams, 1970; Daw, 1967a). However, it is now apparent that the S-cones do contribute to the ganglion cell response, although, there has been some disagreement as to the "sign" of the S-cones to the ganglion cell. One group of experiments suggest that the S-cones, when they are found, are synergistic with the L-cone input (Spekreijse, et al., 1972; van Dijk and Spekreijse, 1984a). Spekreijse, et al. (1972), recording from the isolated goldfish retina found only a few ganglion cells with S-cone input and their response was always synergistic with the L-cone input; also, S-cone input was found only in the center of the receptive field. The inputs to the ganglion cells were determined using a threshold technique, in which a stimulus was presented below threshold and gradually increased in intensity until a threshold response (a change in firing rate) was reached. However, Beauchamp and Lovasik (1973) recording from the optic tract of the intact goldfish found that the majority of ganglion cells did possess

an S-cone component in both the center and surround, and this component was antagonistic to the L-cones.

In an attempt to resolve the discrepancies concerning the contribution of the S-cones to goldfish ganglion cells, Mackintosh and colleagues (Mackintosh, 1981; Mackintosh, et al., 1987) examined the S-cone inputs of over a hundred ganglion cells recorded from the excised, isolated retina across a range of different retinal preparations. Each cell was first classified into one of three cell types based on the response of the center's L-cone input. The three cell types were: $L^+/-$ center (on-excitation/ off-inhibition); $L-/^+$ center (on-inhibition/off-excitation); $L^+/^+$ center (on-excitation/off-excitation). These three cell types correspond to the Red-ON, Red-OFF and ON-OFF cell types, respectively, described in previous literature. The new terminology was used because it reflects a more accurate description of the response characteristics of the cell, since all three cell types respond to both onset and offset of a light stimulus. For example, a Red-OFF center cell (or $L-/^+$) responds with excitation at light offset but also responds with inhibition at light onset. $L^+/-$ center cells respond at light offset with inhibition as well as excitation at the onset of the stimulus.

It was found, with rare exception, that the threshold spectral sensitivities of the centers and surrounds of cells that possessed opposite ON and OFF responses ($L^+/-$ and $L-/^+$) exhibited S-cone contributions, either prior to and/or during chromatic adaptation of the M- and L-cones; the S-cone response was antagonistic with respect to the L-cones; S-cone inputs were also found in both the

center and surround components. The $L^{+}/^{+}$ center cells also possessed an S-cone input, but it was synergistic to the L-cone input at suprathreshold intensities. These findings were robust across all of the retinal preparations employed and the spectra of all isolated mechanisms agreed very well with the direct microspectrophotometric measures of goldfish cones. These results are in agreement with Beauchamp and Lovasik (1973) but disagree with Spekreijse and colleagues (Spekreijse, et al., 1972; van Dijk and Spekreijse, 1984a); one reason for the disagreement may be that Spekreijse and colleagues categorized their cells only at threshold and some of their cells may have been mistyped as $L^{+}/^{+}$ center cells.

1.3.6 Interplexiform Cells.

A fifth retinal neural type, called the interplexiform cell, has been identified in the goldfish (Dowling, Ehinger and Hedden, 1976). Its cell body is located in the inner nuclear layer and has reciprocal contacts with amacrine cells in both sublaminae of the inner plexiform layer. It possesses an axon which contacts horizontal and bipolar cells. Little is known about its function, however it is speculated that the interplexiform cell's role is to control the lateral interactions of horizontal cells (Kaneko, 1979).

1.4 Spatial Summation of Ganglion Cell Receptive Fields.

As mentioned above, the ganglion cell responses represent the final processing by the retina before information is sent to the brain.

Therefore, only information that reaches the ganglion cell can ultimately reach the brain. Since there are many more receptors than ganglion cells, an enormous amount of spatial summation must take place at the ganglion cell level. For example, the human retina contains 6.5 million cones, 120 million rods but only 1 million ganglion cells (see Abramov and Gordon, 1973). It is therefore essential to understand the spatial properties of the ganglion cells. There have been volumes of literature regarding this topic, but the research seems to lack cohesiveness. There are so many variations of stimuli that it becomes difficult to compare across studies. This review does not intend to be exhaustive; its purpose is to review the work relevant to this project. This section will be divided into two broad categories; the earlier studies which examined linearity using small spots of light, and the more recent studies involving spatial frequency analysis.

The underlying question is whether the spatial summation of the ganglion cell is linear or nonlinear. Inquiring about the cell's linearity poses several problems. A major problem is that as early as the receptors, there are inherent nonlinearities. The receptor response as a function of light intensity is clearly nonlinear and any nonlinearity occurring at this stage of processing should occur at all later stages. (An exception to this would be a situation in which a subsequent stage imposes an inverse transform.) However, this response approximates a linear function at stimulus intensities near threshold and at low stimulus intensities. Therefore, the response vs. intensity function can appear to behave linearly over a range of

intensities. The nonlinearity will be more obvious using brief flashes so that adaptational mechanisms cannot come into play. Also, the range over which responses are linear depends on the size of the stimulus -- small stimuli will extend the linear range.

1.4.1 Spatial Summation Using Small Spots of Light.

Much of the early work on spatial summation was performed on cat ganglion cells. Like those of the goldfish, most cat ganglion cell receptive fields consist of a center and an antagonistic surround region. One technique used to examine spatial summation is to determine if the algebraic sum of the responses to two separate spots of light, yields the same response as when the same two spots of light are presented simultaneously. This can be represented, formally, in the following manner:

$$R_{1+2} = R_1 + R_2 \qquad (2)$$

If the previous equation is found to be valid, then the subareas are linearly adding their signals.

Cleland and Enroth-Cugell (1968) found this relationship to hold in cat ganglion cells using spots of light placed in different areas within the receptive field center. However, linearity was tested only at threshold which does not necessarily imply that these findings will hold at higher stimulus intensities. Stone and Fabian (1968) found that linear spatial summation does not hold at higher intensities. They used a technique similar to the previous study with the excep-

tion that the relationship was tested over a wide range of luminances and found that linearity did not persist over the entire range of luminances. They contended that these nonlinearities were not the result of the nonlinearity at the receptor level, since any nonlinearity occurring as early as the receptors would be present on both sides of the equation. Thus, these nonlinearities must occur at some later stage of processing. Grusser, Schaible and Vierkant-Glathe (1970) found similar results using a slightly different procedure; instead of varying luminance, the luminance of each spot remained the same, but they increased the number of spots. Like Stone and Fabian (1968), they found that with more spots, the algebraic sum of the spots was greater than the response to the spots presented simultaneously.

Several studies have investigated the spatial interactions between the center and surround mechanisms of the receptive field. For example, Enroth-Cugell and Pinto (1972a, b), found that the interactions between the center and surround areas were linear; that is, the algebraic sum of a spot in the center and a spot in the surround was similar to the response when the spots were simultaneously illuminated. Similar results occurred even under a moderate range of illumination (Maffei and Cervetto, 1968).

Turning to the goldfish literature, Levine and Abramov (Abramov and Levine, 1975; Levine, 1972; Levine and Abramov, 1975), examined spatial summation in goldfish ganglion cells using small spots of long-wavelength light (710 nm). Long-wavelength stimuli were used because the authors were interested in examining the characteristics of a single receptor type without the complexities of

spectral interactions. They analyzed their results in terms of response summation (as in the previous work) and also in terms of sensitivity summation. That is, does the algebraic summation of the sensitivities of the two areas, stimulated separately, have the same sensitivity as when both spots are simultaneously presented? These two analyses together were used to examine at which stages the nonlinearities, if any, existed in the output of the ganglion cell. For example, any nonlinearities before the first interaction of the areas would be apparent in the response summation analysis; nonlinearities before the final summation, would be revealed in the sensitivity summation analysis. They found linear spatial summation within the different subareas, but nonlinearities both before and after summation. Prior to summation, the nonlinearity was described as a square root function probably at the level of the receptors (a square root function is a compressive function) and another negatively accelerated function following summation. These nonlinearities were most apparent at higher intensities; at lower intensities, the responses were approximately linear. All of these findings for the goldfish correspond to the results obtained from cat ganglion cells. That is, at low intensity levels, spatial summation is linear, but at higher stimulus intensities, summation is nonlinear and can be described as a compressive function that cannot be due solely to the nonlinearity found at the receptor level.

Another technique for determining the spatial summation properties is to examine the conditions under which Ricco's law holds. Ricco's law asserts that there is a reciprocal relationship between the

area being stimulated and the stimulus intensity. Thus, to maintain a constant response, an increase in area can be compensated for by the appropriate decrease in stimulus intensity. The usual procedure for determining Ricco's law for a given area is to measure some criterion response (e.g., threshold) as a function of increasing spot diameter. If Ricco's law applies, then increasing spot diameter will result in less stimulus intensity necessary to produce the criterion response. The result will be a linear function up to a point where increasing the spot diameter no longer produces a decrease in intensity to reach criterion. The spot diameter where the slope of the function approaches zero is the limit of Ricco's area.

Easter (1967, 1968) demonstrated Ricco's law to hold within the center portion of goldfish ganglion cells. He found that stimulus diameters of up to 1 mm obeyed Ricco's law. This diameter corresponds to the average ganglion cell center diameter. Easter's findings have since been verified by Spekreijse, et al., (1972). However, Easter discovered an extra "wrinkle" in his findings. When using one spot which varied in diameter, Ricco's law was upheld; however, small spots of light, placed in areas separate from one another but still within Ricco's area, did not summate their signals linearly. This was not the case when the same experiments were performed on cat ganglion cells (Cleland and Enroth-Cugell, 1968). For cat ganglion cells, Ricco's law was valid for circular concentric stimuli as well as for small spots placed in separate areas. It should be pointed out that Ricco's law does not necessarily demonstrate linearity: receptors can be nonlinear and the spatial summation at a later

stage can be the inverse of the receptor function. (See Levine, 1972, for more details.)

1.4.2 Spatial Frequency Analysis.

Spatial frequency analysis has been used in optics to determine the output or transform of lenses. This technique has been applied to the optics of the eye and has been used in human psychophysics. Spatial frequency analysis involves the presentation of sinusoidal patterns of light and dark bars (gratings) to the particular system being studied and then determining the characteristics or transform of the output of that system. Once this is complete, the response of that system to any stimulus can be predicted by the transform. For an excellent review of the use of spatial frequency analysis in vision, see Barlow and Mollon (1982).

Spatial frequency analysis has now focused on the processing of single neurons. Robson (1975) points out that there are many advantages to this type of investigation. First, it appears that most visual neurons respond to the presentation of a drifting grating across the receptive field (Maffei and Fiorentini, 1973) even though they may not respond to small spots of light. A second advantage is that due to the repetitive nature of the stimulus (sinusoidal patterns), data can be collected and averaged at a much faster rate. Also, sinusoidal patterns of light can be used to stimulate the entire receptive field, providing more accurate information about the neuron as a whole rather than information about segments or portions of the receptive field.

One drawback of using spatial frequency analysis is that a major assumption of the analysis is that the system under investigation is linear. As mentioned above, the visual system is not linear, but can approximate linearity under certain conditions. If the system is working near threshold or at low stimulus intensity levels, then the ganglion cell response is approximately linear. Approximating linearity can also be accomplished by modulating the contrast of a sinusoidal stimulus around some constant mean luminance, thus maintaining the cell at the same adaptation level. This allows for a direct examination of the spatial summation properties of the neuron while keeping the nonlinearities of the gain control constant (see Shapley and Enroth-Cugell, 1984, for an exhaustive review of retinal gain control).

Spatial Null Point. There are several methods that can be used to determine the spatial summation properties of a neuron. The most commonly accepted measure is to determine if the cell possesses a spatial null point. This section describes the rationale behind this technique and the implications of its results.

One method of determining a ganglion cell's spatial summation properties is to present two small spots of light at two separate locations on the cell's receptive field and then determine the algebraic sum of the responses to the two spots separately and compare this value with the response of the cell when both spots are presented simultaneously. If the two values are equal, then the cell possesses linear spatial summation. If the two values are not the same, then the cell is adding the signals nonlinearly.

This can also be tested, using the same two spots of light, by presenting both spots of light simultaneously, waiting until the cell adapts to this change in luminance, and then, modulating the luminance of the spots 180 degrees out of phase. By doing so, as the intensity of one light is decreased, the intensity of the second spot is increased at the same rate. If the cell possesses linear spatial summation, and assumming that all stages prior to spatial summation are approximately linear, then this manipulation will produce no change in response. The cell will respond as if there were no change in the stimulus.

The two spots of light can be replaced with two adjacent semi-circles of light that cover the entire receptive field center (assuming a circular and symmetric center area) so that each semi-circle of light falls directly on only one-half of the receptive field center. The luminances of these semi-circles are modulated out-of-phase so that as one increases, the other decreases at the same rate. If the cell is linear, then this stimulus will also produce no change in response -- i.e., the cell possesses a null point. The implication is that the increased signals for one-half of the receptive field center are being compensated for by a decrease in the signals from the other side of the receptive field.

If the modulated semi-circles of light are positioned just slightly off the midpoint of the receptive field center so that one semi-circle stimulates more of the center area than the other, then the cell will respond to the stimulus modulation. If the cell is linear, then the response pattern will correspond to the stimulus modulation. The

largest response to these stimuli will occur when only one of the semi-circles is positioned on the center mechanism.

Thus, any stimulus which equally stimulates both halves of the receptive field mechanism can be used to determine the existence of a spatial null point. The most commonly used stimulus for this procedure is a spatial sinusoidal grating (light and dark bars of light) centered around the midpoint of the receptive field. The advantage of this stimulus is that the spatial frequency (number of bars of light per unit on the retina) can be controlled; by manipulating the spatial frequency of the grating, one can obtain a better understanding of the exact nature of the summation properties of the cell as will be demonstrated below.

It is also important to point out that the spatial null test only describes the spatial summation properties within a given mechanism. For example, if a spatial null point is found, using a stimulus that stimulates the entire receptive field, for a cell that possesses a center and antagonistic surround, the implications are that the signals within the center summate linearly, and the signals within the surround summate linearity. It does not necessarily imply that the center and surround signals summate linearly. If the center and surround signals are "nulled" prior to interaction, and the null points of both mechanisms are located in the same position, then it is not possible to determine the process or operation by which they interact. It is quite likely that these mechanisms in the ganglion cells summate prior to their interaction since they receive their inputs from different classes of neurons; the center mechanism receives its signals directly

from bipolar cells while the surround probably receives its input from amacrine cells.

Receptive Field Spatial Summation of Cat Ganglion Cells. Enroth-Cugell and Robson (1966) presented sinusoidal patterns of light to cat ganglion cells and found two distinct functional types based on their spatial summation properties. Cells that appeared to behave linearly were labelled X-cells and cells that appeared to function nonlinearly were classified as Y-cells. This dichotomy was determined by flashing a stationary sinusoidal grating at various positions (spatial phase) across the receptive field. For X-cells, when the position of the sinusoidal pattern was directly centered on the receptive field, there was no change in the firing rate of the cell. This was the cell's spatial null point and implied that the receptive field was linearly adding its signals. Placing the sinusoidal grating at any other location in the receptive field did not produce a "null" effect. For Y-cells, there was no position on the receptive field where a null point could be found. Therefore, Y-cell spatial summation was not linear.

Enroth-Cugell and Robson then presented sinusoidal drifting gratings across the receptive field of the ganglion cell. The reason for using a drifting grating as opposed to a stationary grating was to eliminate any adaptation effects. They found that X-cells responded only at the modulated stimulus frequency. That is, the firing rate of the ganglion cell corresponded with the temporal modulation produced by drifting the grating across the receptive field. A criterion for a linear system, in general, is that the frequency of a system's output

is the same as the input frequency. Hence, X-cells are linear cells. The Y-cells' response, on the other hand, did not correspond to the sinusoidal grating drifting across the receptive field at all spatial frequencies. At low spatial frequencies, drifting gratings produced a response modulated at the stimulus frequency; however, at higher spatial frequencies, the cell responded with an elevated discharge or increase in firing rate. That is, the average firing rate of the cell increased, but, there was no pattern or modulation to the response.

Hochstein and Shapley (1976a) have elaborated on the X/Y dichotomy in the cat ganglion cell by presenting counterphase modulated gratings to the cell's receptive field. A counterphase modulated grating is an alternating phase grating or contrast-reversal grating, in which the contrast at a particular point in space varies as a sinusoidal function in time. Presenting these contrast-reversal gratings as a function of spatial phase produced results similar to the Enroth-Cugell and Robson study; there were two functionally distinct types of cat ganglion cell based on their spatial summation properties. Hochstein and Shapley performed a Fourier analysis on the responses of X- and Y-cells. Since a linear cell should respond only at the modulation frequency (f) of the stimulus, X-cells should have most of their power at the fundamental frequency. This was found to be the case. Also, the amplitude of the fundamental component of the response was a sinusoidal function of the spatial phase of the grating; moving the grating away from the null position produced an increase in the amplitude of the fundamental component which reached its maximum amplitude at a position 90 degrees away on either side of

the null position. A Fourier analysis on Y-cells revealed that the Y-cell response contains most of its power at double the modulation frequency or 2f. Y-cells were found to be nonlinear even at low contrasts and the amplitude of the second harmonic was independent of the spatial position of the grating. The fundamental component of Y-cells, however, resembled the spatial phase sensitivity of X-cells in that its amplitude was a sinusoidal function of the position of the stimulus. This suggests that there are both linear and nonlinear components in the Y-cell response.

This was also supported by the fact that at low spatial frequencies, even Y-cells contained a strong fundamental component at most spatial positions; only at the null position of the fundamental component was there a slight, but substantial, second harmonic component. More extensive testing by Hochstein and Shapley (1976b) showed that the nonlinearities of Y-cells were caused by small, nonlinear subunits in the receptive field. These units extend across the center, surround and even beyond. They possess the same sign or response as the center mechanism and act as rectifiers thus producing a nonlinear response. This explains why the nonlinearities appear primarily at high spatial frequencies for both contrast-reversal and drifting gratings (the elevated discharge at high spatial frequencies), since these small subareas would be most responsive at high spatial frequencies.

Since the discovery of the X/Y dichotomy, there have been attempts to differentiate these cells along other dimensions. Cleland, Dubin and Levick (1971), found that cat ganglion cells could be distinguished by their response patterns; that is, they could be classi-

fied as either sustained or transient response types. X-cells appeared to possess a sustained response, while Y-cells responded in a transient pattern. However, X-cells are not always sustained and Y-cells are not always transient in their responses. Hochstein and Shapley (1976a) demonstrated that, under certain conditions, X-cells could produce a transient response. Therefore, the X/Y and sustained/transient dichotomies should not be considered synonomous.

Clelend and Levick (1974a) found that X-cells were primarily located in the central retina of the cat and that most project to the lateral geniculate nucleus (LGN). Fukuda and Stone (1974) found that Y-cells project to both the midbrain and the LGN. Y-cell receptive fields are generally larger than X-cells and therefore it was concluded that Y-cells have larger cell bodies. This was confirmed by Boycott and Wassle (1974) who found morphological differences among ganglion cells which correspond to the functional differences of the X- and Y-cells.

Because of this apparent dichotomy between the ganglion cells, many have speculated as to the purpose of this parallel pathway. On the surface, it appears that the function of X-cells is visual acuity. This is based on the following: that the majority of X-cells are found in the area centralis, they possess smaller receptive fields, hence better spatial acuity, and their pathway to the brain (directly to the LGN) is considered to be the "primary" visual pathway. The Y-cells, on the other hand, have large receptive fields, are located in the more peripheral areas of the retina and project not only to the primary visual pathway but also to the midbrain or reticular formation.

Many have speculated that the role of the Y-cells is to provide sensory information to the eye movement system since eye movements are believed to be generated by the midbrain. The fact that Y-cells have a faster conduction velocity than X-cells also supports the notion that Y-cells are involved in informing the eye movement system where to move the eyes so that the image falls on the fovea which contains the high acuity X-cells.

More recently, a third functional type of cat ganglion cell, W-cells, has been found. These W-cells have slower conducting axons and smaller cell bodies than either X- or Y-cells (Stone and Fukuda, 1974). They appear to project into the superior colliculus (Fukuda and Stone, 1974) and are sensitive to moving patterns and directions (Cleland and Levick, 1974a, b). W-cells are morphologically different from X- and Y-cells as well (Boycott and Wassle, 1974). The role of these W-cells is unclear and unpredictable (hence, their designation as W or weird). They appear to possess such diffuse characteristics that many believe that they are just an amalgamate of several classes. It is also very difficult to record from these cells due to the fact that they have very small cell bodies.

Ganglion Cell Spatial Summation in Other Species. Although the majority of work on ganglion cell spatial summation has been done with the cat, some investigators have examined the linear/nonlinear dichotomy in other species. Gouras (1968, 1969) found that monkey ganglion cells could be divided into tonic and phasic types (similar to the sustained/transient dichotomy in the cat) based on their response to prolonged stimuli. The tonic cells had smaller axons than the pha-

sic cells and were located in the fovea. X-like and Y-like cells have been found in the monkey LGN based on tests similar to those used on cat ganglion cells, including testing for a spatial null point (Dreher, Fukuda and Rodieck, 1976; Kaplan and Shapley, 1982).

Shapley and Gordon (1978) found X-like cells in the eel retina using contrast-reversal gratings; although no Y-like cells were found, a type of cell resembling a cat W-cell was found. Ganglion cells of Necturus (Tuttle and Scott, 1978) and frog (Gordon and Shapley, 1978) can also be classified into X-like and Y-like cells.

Turning to the goldfish literature, Spekreijse and van den Berg (1971) examined phasic ganglion cells of the goldfish to determine the spatial summation of the various receptive field components and mechanisms. They found that for the center and surround, as well as Red and Green components, there was a linear spatial summation for the various interactions. Thus, they concluded that all goldfish ganglion cells are X-like; there was no report of cells that did not follow linear summation. However, the statement made regarding linearity in this study may be misleading since a "null point" was demonstrated for a specific set of stimuli. This was accomplished, for example, by superimposing temporally modulated lights (500 nm and 650 nm to test the linear combination of the Red and Green components) and adjusting both the modulation and relative phases until a null response was obtained. However, as pointed out in a later paper by Hochstein and Shapley (1976a), one null response, at one particular contrast does not imply linearity. One must examine the response at several contrasts to determine whether a null response is a true

null or just a matter of serendipity. This was not attempted in the Spekreijse and van den Berg experiment. Also, their stimuli consisted of large checkerboard patterns, which consist primarily of low spatial frequency components. It is possible that if there are nonlinearities due to the small subunits as those found in the cat retina, then they would be insensitive to these stimuli.

Levine and Shefner (1979) distinguished between X-like and not-X-like ganglion cells in the goldfish by using a pinwheel of light whose position could be shifted within the center mechanism of the ganglion cell. Shifting the pinwheel position did not change the amount of light stimulating the center and, therefore, if the spatial summation of the cell were linear, there should be no change in the response pattern. They found that out of 24 ganglion cells tested, 9 were X-like and 15 were not-X-like. Although this pinwheel technique is useful in determining if the cell is linear or X-like it can say nothing about the characteristics of the not-X-like cells other than that they are nonlinear. Also, this study only examined the linearity of the center mechanism. In a later study, Levine (1982), using the pinwheel technique on goldfish ganglion cell centers, found that of 10 Red-OFF center cells, 3 were X-like, 6 were not-X-like and one was unclassified. For the 3 Red-ON center cells tested, 1 was X-like and 2 were not-X-like. These findings are in disagreement with Spekreijse and van den Berg (1971) since over half of the cells observed by Levine were nonlinear.

1.5 Difference of Gaussians Receptive Field Model.

Most of the work concerned with spatial processing of ganglion cells has focused on the cat retina. Thus, this section summarizes what is known about cat ganglion cells with an occasional reference to other species. Goldfish ganglion cells are somewhat more complex, since many of the cells are double opponent (making it difficult to separate the spatial and spectral properties). What is known about their spatial properties and receptive field arrangement will be discussed in Section 1.6.3.

1.5.1 Spatial Contrast Sensitivity Functions.

The Receptive Field Model. It has been known for some time that sensitivity across the center mechanism is not uniform. For example, using small spots of light to map the receptive field centers of cat ganglion cells, Cleland and Enroth-Cugell (1968), found sensitivity maximum in the middle of the center component and decreased away from the middle of the field. Similar findings have been reported for the surround mechanism (Hammond, 1973). Most vertebrate ganglion cell receptive fields are organized in a concentric center/surround pattern where the surround responses are opposite to the center responses. A useful model of the receptive field is the "difference of two Gaussian distributions" (Rodieck, 1965). In this model, both center and surround distributions are centered on the entire field, each with its maximal sensitivity located in the middle. The center distribution is narrower, but its amplitude is larger than

that of the surround distribution. Rodieck (1965) has suggested that if the sensitivity profile of the ganglion cell receptive field were known, then its response to any stimulus could be determined. Unfortunately, it is difficult to test this model using spots of light since any stimulus that stimulates the center mechanism must inevitably stimulate the surround mechanism.

However, spatial frequency analysis can be very useful in relating a cell's responses to its sensitivity profiles (Shapley and Lennie, 1985). One way to accomplish this is to determine the cell's sensitivity to sinusoidal gratings of various spatial frequencies. This can be obtained by drifting sinusoidal gratings of different spatial frequencies at a constant temporal rate across the receptive field and determining the contrast necessary to reach a criterion response. This Spatial Contrast Sensitivity Function (S-CSF) is extremely useful, especially if the cell's responses are linear. When the cell's S-CSF is known, the response of the cell to any stimulus can be predicted, since, according to Fourier's theorem, any stimulus can be decomposed into a particular combination of sinusoids. Also, the S-CSF of a neuron is valuable since it can be directly compared with the S-CSF obtained behaviorally from the entire organism (Braddick, Campbell and Atkinson, 1978).

Testing the Model. The S-CSFs derived from single ganglion cells are qualitatively similar to the psychophysically determined S-CSF (see Maffei, 1978, for a review). There is a drop in sensitivity at the higher spatial frequencies expected of any optical imaging device, as well as attenuation of sensitivity at low spatial frequencies,

which is believed to be the product of neural inhibition (Ratliff, 1965).

Enroth-Cugell and Robson (1984) have illustrated how a ganglion cell's S-CSF can be derived from a "difference of Gaussians" receptive field model. Figure 2 shows the S-CSFs of the center alone, the surround alone, and the entire receptive field based on a difference of Gaussians model. Examining the center S-CSF first, one can see that when the light portion of the stimulus covers the entire center area maximal responses will be produced. Thus, the center mechanism will be maximally sensitive to a stimulus consisting of a spatial frequency whose period is one-half the exact diameter of the receptive field center or lower. As spatial frequency is increased, the center mechanism will never be "filled" by the light portion of the stimulus, so sensitivity decreases until the spatial frequency is high enough so that the center mechanism can no longer "discriminate" this stimulus from a uniform stimulus. This is the acuity limit of the center mechanism. Similar findings occur when the surround mechanism is stimulated alone; however, since the surround diameter is larger than the center, the spatial frequency which covers the entire surround is larger; thus, sensitivity begins to drop at a lower spatial frequency than the center mechanism. Because of this, the surround has poorer spatial resolution than the center and is virtually insensitive at the higher spatial frequencies where the center is still responsive.

The overall S-CSF of the neuron must inevitably result from the interaction of the center and surround components. Since the spatial

Figure 2

Hypothetical S-CSFs derived from the different receptive field components of a ganglion cell. Shown here are the functions obtained from stimulating the entire receptive field (solid line), the center mechanism alone (dotted line), and the surround mechanism alone (dashed and dotted line). Note that when both the center and surround are examined separately, there is no low frequency attenuation. However, when the entire receptive field is stimulated, the interaction between the two antagonistic mechanisms (center and surround) produces lateral inhibition at the spatial frequencies where they are both sensitive (i.e., low spatial frequencies). This figure is redrawn and modified from Enroth-Cugell and Robson (1984).

S-CSFs of Receptive Field Components

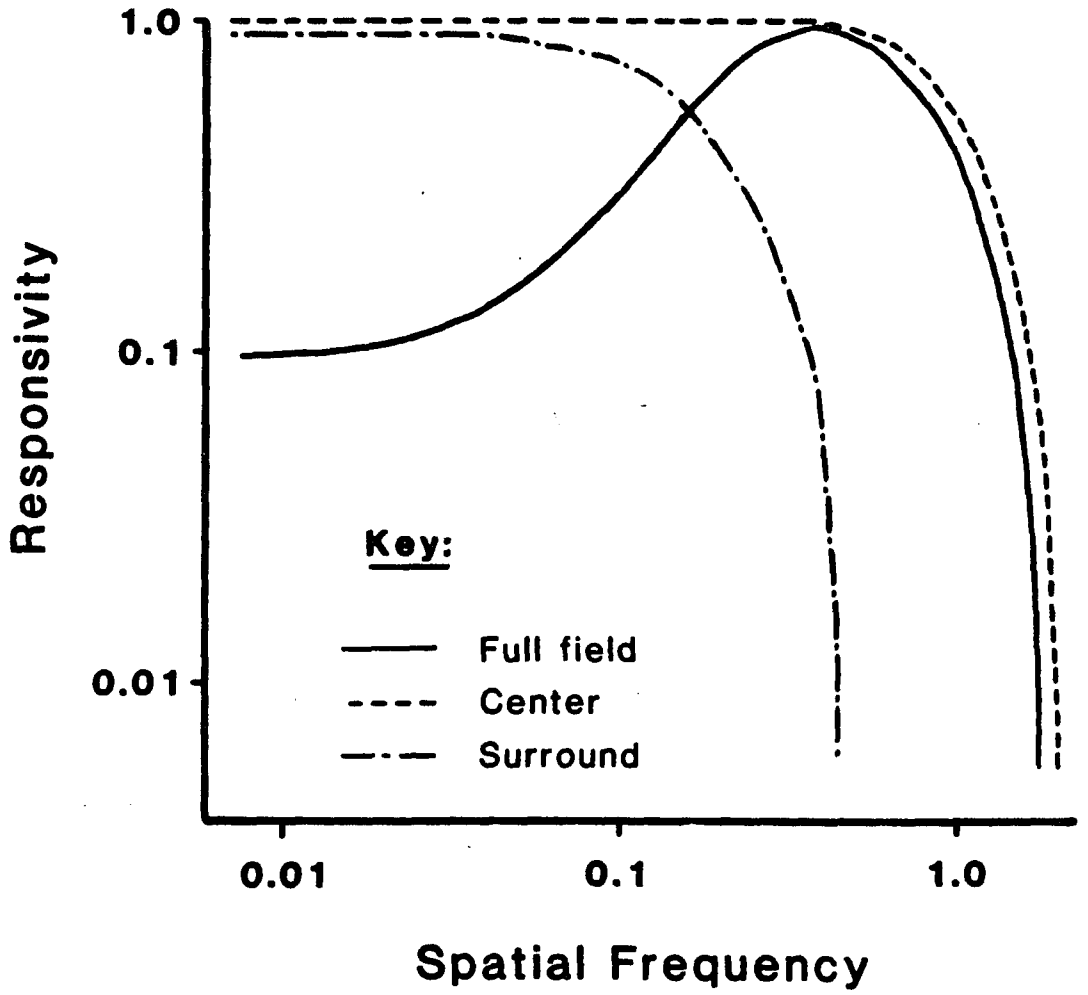

resolution of the surround is less than the center, sensitivity at high spatial frequencies is due solely to the center component. Because the center and surround components are antagonistic, any stimulus which activates both mechanisms will produce antagonistic responses resulting in the neuron to be less sensitive to these stimuli. This explains the drop in sensitivity of the overall S-CSF of the cell at low spatial frequencies. At low frequencies, sensitivity is reduced because of the interaction between the antagonistic center and surround mechanisms. Gordon and Shapley (1978) found evidence to support the notion that low frequency attenuation is due to the antagonistic center and surround interactions in frog and eel ganglion cells; cells that displayed no apparent surround also had S-CSFs with no low frequency attenuation.

The difference of Gaussians model has been tested, at least indirectly, by examining S-CSFs across cell types and different stimulus conditions. For example, cat X-cells possess better spatial resolution than Y-cells. This has been determined by comparing their S-CSFs at high spatial frequencies (Enroth-Cugell and Robson, 1984). Since the sensitivity at high spatial frequencies is due to the center mechanism, X-cells should possess smaller center diameters than Y-cells. Linsenmeier, Frishman, Jakiela and Enroth-Cugell (1982) derived the sensitivity profiles of X- and Y-cells by decomposing their S-CSFs using an iterative process to find the best fit Gaussian profiles to the S-CSFs. Their findings suggest that X-cells have smaller receptive field centers than Y-cells.

The interaction between the center and surround components may

also vary as a function of the stimulus and background conditions. For example, the shape of the S-CSF varies as a function of stimulus drift rate (Dawis, Shapley, Kaplan and Tranchina, 1984). Derrington and Lennie (1982) found that changes in stimulus temporal frequency produced dramatic changes in cat ganglion cell S-CSFs. However, these changes were found only at low spatial frequencies; changing the temporal frequency of the stimulus did not alter the peak of the S-CSF or the shape of the function at high spatial frequencies. On the other hand, sensitivity at low spatial frequencies increased with increasing temporal frequency. That is, the low frequency attenuation diminished with increasing temporal frequency. They suggested that these results could be explained by the fact that the center and surround components possess different temporal characteristics. This also explains why the function is unaffected by high temporal frequencies at the high spatial frequencies, since the surround is insensitive at the high spatial frequencies; the response at this point is due only to the center component.

There is physiological evidence of a phase delay in the surround in cat ganglion cells (Rodieck and Stone, 1965). Enroth-Cugell, Robson, Schweitzer and Watson (1983) have proposed that spatio-temporal interactions can be explained by a signal delay of a few milliseconds in the surround response. They derived S-CSFs at various temporal frequencies, using contrast-reversal gratings instead of drifting gratings. Contrast-reversal gratings were used because they provide more accurate information regarding the phase lag of the response than drifting gratings. To verify that the responses to contrast-

reversal gratings were similar to responses obtained from drifting gratings, S-CSFs were derived from both stimuli and compared for each cell. They found no difference between the relative S-CSFs across the different stimuli. Unfortunately, the S-CSFs were compared after each function was normalized; although the shapes of the two functions obtained were virtually identical, their absolute sensitivities were not compared. This is important since a contrast-reversal grating is physically equivalent to two drifting gratings moving in opposite directions. Thus, a drifting grating stimulus would possess one-half the contrast of the corresponding contrast-reversal grating. Differences in absolute sensitivities could also arise from the asymmetries found in the center and surround mechanisms which can produce directionally selective responses (Dawis, et al., 1984). It should also be mentioned that they only examined cells that possessed linear spatial summation. However, if the responses were confined to only the center and surround components of the receptive field, Y-cells should produce the same findings. For Y-cells, this can be accomplished by examining only the fundamental component of the response.

Enroth-Cugell, et al. (1983) also found that the cell's phase lag to sinusoidal gratings of high spatial frequencies corresponded to the response of the center mechanism; that is, an ON-center cell responded in-phase to the contrast-reversal grating. However, when stimulated with lower spatial frequencies, the response was slightly out-of-phase. They attributed this change in phase lag to the presence of the surround response interacting with the center mechanism.

In summary, it is not possible to separate the spatial and the temporal properties of a cell's response. The interaction between the center and surround components appears to change as a function of both the spatial and temporal properties of the stimulus. These spatio-temporal interactions have also been found in human psychophysics (Kelly, 1974).

Finally, the mean level of illumination also affects the S-CSF of a neuron. When the mean level of illumination is low, low frequency attenuation disappears in the S-CSF of cat ganglion cells (Enroth-Cugell and Robson, 1966; Kaplan, Marcus and So, 1979). This also reflects differences in the interactions between the center and surround mechanisms. It has been shown that the surround mechanism is virtually insensitive at low light levels (Barlow, Fitzhugh and Kuffler, 1957). Thus, one would predict that if low frequency attenuation is due to the center and surround interactions, there would be no low frequency attenuation at low light levels.

1.5.2 Orientation and Direction Selectivity.

Cat Ganglion Cells. The difference of Gaussians model proposed by Rodieck assumes a concentric center and surround organization. With this arrangement, an individual ganglion cell would be incapable of providing any orientation information. That is, a bar of light or a grating, drifted across the ganglion cell receptive field, would yield the same response regardless of which orientation or direction the stimulus crossed the field. Despite the fact that cortical cells invari-

ably are orientation selective, ganglion cells were believed to be concentric and symmetrical. Careful investigation of cat ganglion cell receptive fields, however, has revealed that this is not the case. For example, when the center mechanisms of cat ganglion cells were mapped with small spots of light, it was found that the center was not circular but elliptical (Hammond, 1974).

Levick and Thibos (1982) drifted sinusoidal gratings at different orientations across the receptive field of cat ganglion cells and found that the majority of cells were indeed orientation selective. However, orientation tuning was found only when gratings of high spatial frequency were presented. At low spatial frequencies, the cells behaved as if they were circularly and concentrically organized while at high spatial frequencies, they clearly responded as if the receptive fields were elliptical. To account for these findings, Levick and Thibos proposed that cat ganglion cell centers were elliptical while the surround mechanisms were circular. At low spatial frequencies, where there is no apparent orientation tuning, the surround component dominates the response; at high spatial frequencies, only the elliptical center component responds producing orientation tuning. This is consistent with Hammond's (1974) finding that the center component is elliptical in shape. Levick and Thibos also found no evidence of direction selectivity in cat ganglion cells. That is, a grating at a particular orientation moving in one direction produced the same response as the same grating, at the same orientation, but moving in the opposite direction. Unfortunately, none of the cells in this study were tested for linearity of spatial summation. Therefore, it is not

known whether orientation tuning is dependent on the spatial summation properties of the cell or even if all the classes were examined.

Soodak, Kaplan and Shapley (1985) have continued to investigate orientation tuning in the cat retina and lateral geniculate nucleus (LGN). They confirmed the findings of Levick and Thibos that ganglion cells are orientation tuned because of an elliptical center mechanism; orientation tuning occurred with stimuli of high spatial frequencies, but not with stimuli of low spatial frequencies. They also discovered that the cell's response as a function of orientation changed from a function containing two peaks at orientations 180 degrees apart to a function with four or more peaks at very high spatial frequencies. They believe that this change in the orientation tuning curve is a result of the fact that the center component is not a single, uniform mechanism but consists of smaller subareas. The four peaked orientation tuning curve found at high spatial frequencies can be best explained by the fact that the center consists of two adjacent circular subareas (Soodak, 1986). Thus, at moderate spatial frequencies, the center will appear elliptical and only at high spatial frequencies will the subareas become apparent. These subareas are not the small, nonlinear subunits discussed above since these findings are robust for both X- and Y-cells; however, like these nonlinear subunits, these subareas respond primarily at high spatial frequencies.

In a following paper, Soodak, Shapley and Kaplan (1986) examined the orientation tuning of the small, nonlinear subunits found in

Y-cells. They were able to eliminate the center and surround component responses by using contrast-reversal gratings and "nulling" their responses, leaving only the response of the nonlinear subunits. By varying the orientation of the grating, they found that the nonlinear subunits were also orientation tuned, but in a different fashion from the center component.

Although most of their cells were clearly orientation tuned, there were very few cases in which they were also direction selective. Unfortunately, due to the nature of their recording technique, no W-cells were examined (W-cells axons are relatively small and therefore difficult to isolate when recording at the level of the LGN); W-cells are the most likely candidates for direction selectivity in the retina (see Rodieck, 1979).

There is some evidence that direction selectivity exists in the cat retina. Dawis, et al. (1984) found that most X-cells in the cat retina are somewhat asymmetric. Thus, a grating drifting across the receptive field in one direction produced a different response than if the same grating was drifted in the opposite direction.

Goldfish Ganglion Cells. There has been very little evidence that goldfish ganglion cells are orientation or direction selective. Despite the fact that orientation and direction selective cells are found in the higher visual centers, i.e., the optic tectum (Cronly-Dillon, 1964; Jacobson and Gaze, 1964; Riemslag and Schellart, 1978; Wartzok and Marks, 1973), there have been few examples of these cells in the retina. Direction selective cells have been found occasionally in optic nerve recordings (Daw and Beauchamp, 1972); orien-

tation selective cells are also just as rare in the optic nerve (Daw and Beauchamp, 1972; Riemslag and Schellart, 1978).

This lack of tuning at the ganglion cell level is quite puzzling, since there is both anatomical and physiological evidence that, at the very least, orientation tuning should be found at this level. For example, the dendritic spread of teleost bipolar cells clearly shows asymmetries in the form of elliptical fields (Stell and Kock, 1983). Similar findings have been reported in carp ganglion cells (Kock and Reuter, 1978).

Levine and Zimmerman (1986) have investigated the responses of the subareas of the center and surround portions of the goldfish ganglion cell. By examining the ON and OFF responses to small spots of light, they were able to map the response characteristics of the subareas. They found that the subareas were not uniform in their responses within the center and surround mechanisms. In fact, many of the cells examined revealed that their properties were much more complicated than the difference of Gaussians model would predict. The receptive field components were generally elongated and not concentric as the model would suggest. They also found fields that were asymmetrical. Elliptical fields and asymmetries within the fields would suggest that goldfish ganglion cells should possess orientation and direction selectivity. However, like the cat cells, the tuning characteristics of these cells may depend on the particular stimuli.

It is clear from these studies of the cat and goldfish retina that the receptive field is not as simple as proposed by the difference of Gaussians model. The receptive field is not as symmetrical and uni-

form as originally proposed and these variations can produce subtle and sometimes dramatic changes in response for a particular set of stimuli. Yet, one should not completely discard the model since it does explain many of the phenomena associated with the receptive field responses. However, the model does have its drawbacks and does not completely describe the receptive field properties.

1.6 Cone Contributions to Ganglion Cells.

Very little effort has been made to examine the relationship between the spatial and spectral properties of ganglion cells. One reason for this lack of information is that much of the work on ganglion cell spatial processing has been done with the cat, an animal not known for its color vision. However, when this relationship has been investigated, the results have proven to be interesting.

De Valois and De Valois (1975) presented two types of stimuli to the receptive fields of LGN cells of the macaque monkey. (Macaque LGN neurons are similar in response to their ganglion cells in that they are concentrically organized and color coded.) One stimulus consisted of a white bar of light while the other stimulus was a red bar of light surrounded on both sides by green bars of light (a third stimulus consisting of a green bar of light flanked by red bars of light was also used). The red and green lights were equated for luminance so that the stimulus represented only a change of color. The stimulus was centered on the receptive field and responses were recorded. The line widths were then increased to determine which

width produced the greatest response. As expected, the white stimulus' optimum width roughly corresponded to the size of the receptive field center, and responses decreased as the width was increased to also stimulate the surround portion of the field. The pure color stimulus, on the other hand, produced different results. As the center bar width increased so did the cell's response, even when the center bar encroached into the surround. For the color stimulus, stimulating the surround actually enhanced the response, whereas, for the white light stimulus, the surround antagonized the center mechanism. They concluded that for the LGN cells of the macaque, the center and surround are antagonistic for luminance changes but synergistic for color stimuli. Examining these results closely, the synergism between the center and surround mechanisms becomes apparent; for a +R center and -G surround cell, as the red center bar spills over into the surround, there will be less green light in the surround producing less inhibition and therefore stronger excitation.

Gouras and Zrenner (1979) demonstrated that the center and surround interactions were dependent upon both the temporal and spectral properties of the stimulus. They presented various spectral stimuli at varying flicker rates and found that at high flicker rates, not only did color coded ganglion cells lose their spectral opponency, but the center and surround responses were actually synergistic. Their results can be explained by a frequency dependent phase shift between the center and surround spectral mechanisms. The above experiments illustrate that there are interactions between the chro-

matic, spatial, and temporal channels in the ganglion cell and that the channels are not separable.

1.6.1 Spatial Summation and Cone Interactions.

It was originally believed that the X/Y distinction was related to whether the cell was spectrally opponent or nonopponent (Schiller and Malpeli, 1977). Dreher, et al. (1976) attempted to classify LGN cells of old world monkeys into X- and Y-cells as well as into spectral classes. The spectral classification was based on the classification of Wiesel and Hubel (1966). They found that types I and II of Wiesel and Hubel's classification were X-like while type IV appeared to be Y-like. Type III cells were subdivided into IIIx and IIIy cells. However their stimuli consisted of spots of light and they classified the cells into X- and Y-like based on the basis of the sustained/ transient criterion. Thus, spatial summation was not directly tested. Also, spectral classification was based on the response to several wavelengths of light; no action spectra were obtained to verify exactly which cone inputs were present.

Only one experiment to date has attempted any further investigation to relate the spectral properties of a cell and its linearity of spatial summation. de Monasterio (1978) found that the segregation of the two dichotomies (X/Y and spectrally opponent/nonopponent) is not as clear-cut as originally proposed. Recording from macaque ganglion cells, he categorized each cell using Wiesel and Hubel's (1966) classification scheme for macaque LGN cells. Once classified along this dimension, each cell was examined for its overall linearity as well as

the linearity of its center and surround mechanisms separately. The results were that only type I cells (i.e., cells that received only one cone input within a receptive field mechanism) had overall linearity, type III and type IV cells were classified as Y-like cells even though type IV cells were spectrally opponent. By presenting stimuli of different wavelengths on different chromatic backgrounds, de Monasterio was also able to examine the properties of the individual cone inputs. For spectrally opponent cells (type I and IV) it was found that only cone inputs that were specific to a particular mechanism (i.e., center or surround) were linear. For example, in a type IV cell (which consists of both Red and Green excitatory components in the center (+RG) and an inhibitory Red component in the surround (-R)) only the Green component appeared to be linear. For type I cells (+R in the center and -G in the surround) both components were linear. To demonstrate this further, de Monasterio examined the sensitivity profiles of the type I receptive fields and found the surround mechanism to have a bimodal profile; that is, the surround mechanism does not overlap the center component; for these cells the center and surround portions were completely separate.

There are several problems with this study. Although spectral sensitivities were obtained initially to classify the cell, there is no indication that any spectral sensitivities were determined during chromatic adaptation. Therefore, there is no way of knowing which cone types were contributing to the output of the cell. For example, de Monasterio, Gouras and Tolhurst (1976) found concealed color opponency in rhesus monkey ganglion cells. It is possible that concealed

cone inputs, revealed by chromatic adaptation, may have influenced the responses of the cells. This can only be determined by examining the spectral sensitivities of the cell during chromatic adaptation. A second problem has to do with the "closeness" of the spectral sensitivities of the primate cones. Any attempt to chromatically adapt one cone type will inevitably affect the sensitivity of the others. This again suggests that spectral sensitivities should have been determined during chromatic adaptation to determine the "purity" of the cone inputs. Another problem is that the sensitivity profiles were examined only for cells with overt dichromatic opponency. This was done for the sake of convenience; however, this eliminates any cells with a trichromatic arrangement. The most serious problem with this study is that a bipartite field was used to test for the existence of a spatial null point. Since such a stimulus consists primarily of low spatial frequencies it might have been inadequate to activate the small, nonlinear subunits; many Y-like cells may have been misclassified as linear.

These results and shortcomings raise some interesting questions regarding goldfish ganglion cells. The majority of goldfish ganglion cells are both spatially and spectrally opponent. In fact, they are double-opponent in that they display spectral opponency within a center or surround mechanism (e.g., $^{+}$R-G in the center and -R^{+}G in the surround). It also appears that each mechanism receives input from all three cone types whether the contributions are overt or not (Mackintosh, 1981; Mackintosh, et al., 1987). If this is the case, then the results from the spectrally opponent ganglion cells of the

primate would suggest that the double-opponent ganglion cells of the goldfish are nonlinear or Y-like. This directly opposes the findings of Spekreijse and van den Berg (1971) who report that all goldfish ganglion cells are both spatially and spectrally linear. That is, not only do the spatial subareas summate linearly, but the spectral inputs (e.g., Red- and Green-components) summate their signals linearly (see Section 1.4.2).

More recently, van Dijk and Spekreijse (1984b) examined the linearity of the spectral inputs of double-opponent ganglion cells in the carp retina. Linearity was determined by algebraically combining the center responses to a 694 nm spot and a 550 nm spot presented separately and comparing them to the physiological sum resulting from presenting both spots simultaneously. Fourteen out of 49 cells tested displayed linear summation. Clearly, spatial summation is not dependent on whether only one cone mechanism is present within a receptive field area. Unfortunately, in all the studies described above, spatial summation was not rigorously and quantitatively assessed with the appropriate stimuli or procedures as has been done in the cat retina.

1.6.2 Sensitivity to Contrast.

More recent attempts to relate spatial and spectral properties have examined the cell's sensitivity to stimulus contrast. Kaplan and Shapley (1984; 1986) have been able to monitor the responses of macaque ganglion cells by recording from the LGN. The macaque LGN consists of several layers in which ganglion cell axons appear to

project to the different layers based on their spectral coding. Spectrally opponent ganglion cells project to the parvocellular layers of the LGN (P-cells), while spectrally nonopponent ganglion cells project to the magnocellular layers (M-cells). They also discovered that M-cells (spectrally nonoppponent) were also very sensitive to stimulus contrast. On the other hand, P-cells (spectrally opponent) were relatively insensitive to grating contrast. Using the appropriate quantitative measures to determine the spatial summation properties of these cells, it was found that although the majority of cells were X-like, both P- and M-cells could be Y-like. This suggests that the linearity of spatial summation is independent of whether the cell is spectrally opponent or nonopponent.

1.6.3 Spatial Contrast Sensitivity Functions.

As discussed in Section 1.5, the S-CSF of a ganglion cell is a function of its receptive field components and their interactions. Thus, any differences in receptive fields across cells should be reflected in differences in the S-CSFs. Goldfish ganglion cells provide an interesting vehicle to test the difference of Gaussians model since they provide differences across cell classes in both the spatial and spectral domains.

Ganglion Cell Color Mechanisms. Many goldfish ganglion cells are double-opponent. Each of these cells possesses a center and an antagonistic surround region as well as spectral opponency within each mechanism. In primates, double-opponent receptive fields are found only in the cortex (Hubel and Wiesel, 1968; Thorell, De Valois

and Albrecht, 1984). An example of the receptive field map of a typical goldfish double-opponent cell is shown in Figure 3a. The letters refer to the maximally effective wavelengths and the signs associated with the letters refer to an excitatory (+) or inhibitory (-) response. The two inner circles correspond to the center component while the large, outer circle represents the surround component. Note that any stimulus in the center will produce an opposite response if the same stimulus is presented in the surround -- the cell is spatially opponent. The actual response sign within each component depends on the wavelength of the stimulus. For example, a long-wavelength stimulus in the center will produce a response of excitation, while a middle-wavelength stimulus in the center will produce an inhibitory response; just the opposite is true for the surround responses. This cell is spectrally opponent. Another common arrangement of double-opponent cells is the same configuration but with all the response signs reversed (-R+G in the center and +R-G in the surround).

The smaller portion of the cell's center consists of an excitatory Red- and an inhibitory Green-component. The inhibitory component extends beyond the smaller excitatory component and forms the outer ring of the center. The smaller portion of the center is always the Red-component; the Green-component center is always slightly larger than the Red-component, regardless of the response sign. Mapping the receptive field center with small, monochromatic spots of light shows that the average size of the Red-component is roughly 1 mm in diameter (Macy and Easter, 1981). Daw (1967a, 1968) found slightly larger diameters for the Red-component (Mean: 1.35 mm) and a

Figure 3

Spatial organization of commonly found goldfish ganglion cells. The letters refer to the maximally effective wavelength and the signs associated with the letters refer to either an excitatory (+) or inhibitory (-) response. In (a), a double-opponent receptive field is shown. The two inner circles display the center component while the large outer circle represents the surround mechanism. This cell is double-opponent in that it is both spatially opponent (the response signs of the center are opposite to the response signs of the surround) as well as spectrally opponent within a given mechanism. For example, within the center mechanism, the cell responds to long-wavelength light with excitation and middle-wavelength light with inhibition. In (b), a spectrally nonopponent receptive field arrangement is shown. This cell type is not spectrally opponent since there is no change in response sign as a function of wavelength. However, this cell is spatially opponent in that it possesses a center and an antagonistic surround. For both cell types, cells with the opposite responses are also commonly found (e.g., a -R center and +R surround). The receptive field components' diameters are drawn to scale -- values were obtained from Daw (1967a; 1968).

Goldfish Ganglion Cell Types

(a)

Spectrally

Opponent

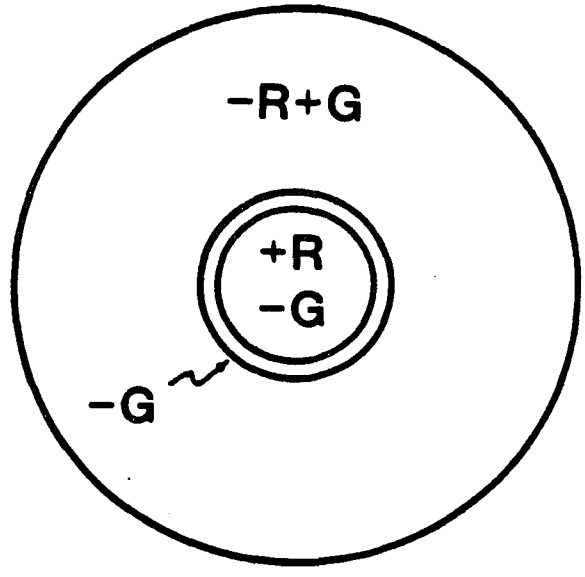

(b)

Spectrally

Nonopponent

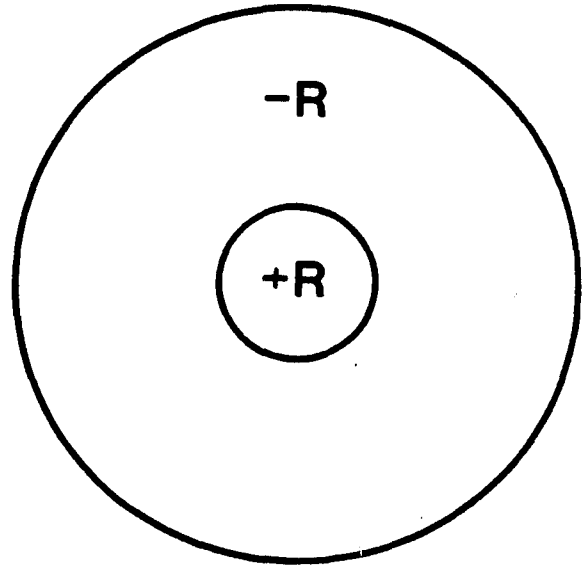

Scale

1 mm

Green-component average diameter of 1.60 mm. It is not clear why Daw's values are larger than those in other reports; however, it is likely to be due to the fact that larger fish were used in his work. Although the fish size in his original work was not reported, subsequent work (Daw and Beauchamp, 1972) reported fish sizes of 6 to 10 inches, which is somewhat large. This could account for the differences since receptive field size, measured in millimeters on the retina, increases with fish length (Macy and Easter, 1981). However, the important aspect of the above work is that the Red-component is always slightly smaller than the Green-component in the center mechanism.

Raynauld (1975) has proposed that the receptive field organization of these cells is a direct consequence of the neurons from which each mechanism receives its inputs. Figure 4a shows the receptive field of a bipolar cell with a center and surround arrangement. This bipolar cell has a Red-ON center with an antagonistic Green-OFF surround. Since the ganglion cell center receives its input directly from bipolar cells, Figure 4b shows the result of combining the inputs of a number of bipolar cells of the same type. Thus, the Red-component of the ganglion cell center is comprised of the sum of the bipolar cell centers; the outer Green-component of the ganglion cell center is comprised from the sum of the bipolar cell surrounds. This schematic is further supported by the fact that the majority of the bipolar cells studied possessed a Red-component dominated center accounting for the finding that the smallest component in ganglion cells centers are dominated by the Red-component.

Figure 4

Hypothetical model of the neural inputs to a double-opponent goldfish ganglion cell center mechanism. The letters refer to the maximally effective wavelength and the signs associated with the letters refer to either an excitatory (+) or inhibitory (-) response. In (a), the components of a +R center and -G surround bipolar cell are shown. In (b), the result of a number of these bipolar cells converging to form the input of a ganglion cell is shown. Only one-quarter of the bipolar cells necessary to form the entire ganglion cell is presented for clarity. With the entire complement of bipolar cell inputs, the ganglion cell receptive field center would be circular as in Figure 3a. This figure is redrawn and modified from Raynauld (1975).

Goldfish Ganglion Cell Inputs

a) Bipolar cell

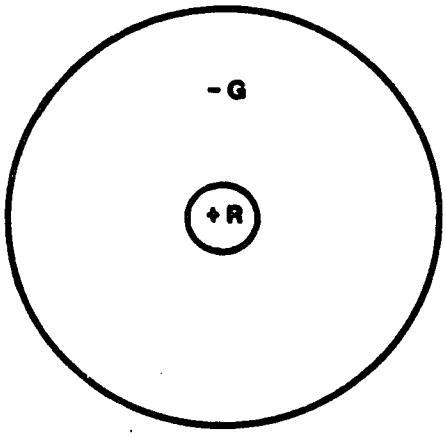

b) Ganglion cell

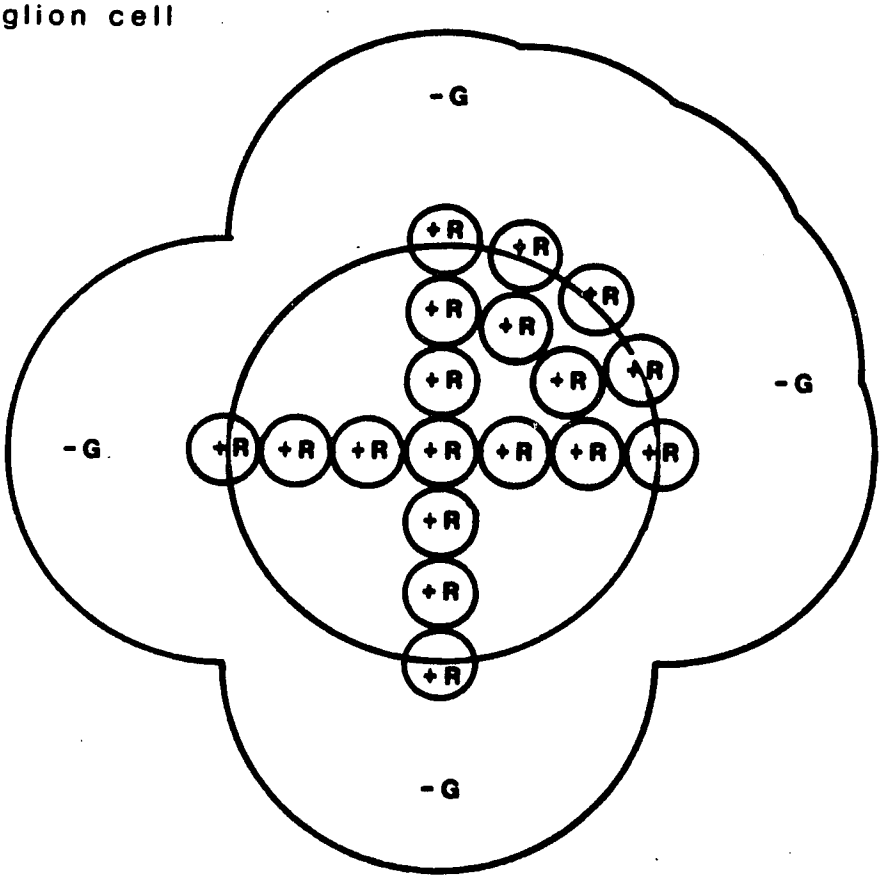

The ganglion cell surround probably receives its input from amacrine cells. This is supported by the fact the amacrine cells are most responsive to large fields and insensitive to small stimuli. This would explain why the large surround component was literally undetected in early work using small spots of light (Wagner, et al., 1960) and uncovered when large annuli were presented (Daw, 1967a, 1968). The receptive field surround may be as large as 6 mm in diameter (Daw, 1967a; 1968).

Another common goldfish ganglion cell type possesses a spatially opponent, but spectrally nonopponent receptive field (see Figure 3b). In this cell type, the response to a stimulus presented to the center is opposite to the response to the same stimulus presented in the surround. However, unlike the double-opponent cells, the response within the center or surround does not depend on the stimulus wavelength. Although these cells are overtly spectrally nonopponent, it does not necessarily imply that these cells possess only one cone input. It is possible that the center may possess a relatively weak Green-component in which the Red-component dominates, or that the inputs of two cone types are combined in such a way that they behave as one cone type (Sirovich and Abramov, 1977).

Spectral Response Class. A cell's spectral response class may also influence its S-CSF. In goldfish, the size of the receptive field center's Red-component varies as a function of spectral class; the average value of the receptive field center is roughly 1 mm in diameter, but when segregated by spectral class, Red-ON center cells are smaller in size than Red-OFF center cells (Macy and Easter, 1981;

Schellart and Spekreijse, 1976). The receptive field centers of ON/OFF cells may be smaller than those of both Red-ON and Red-OFF center cells (Macy and Easter, 1981). These findings were determined by mapping the diameter of the center area with small, monochromatic spots of light. Since the Red-component of the center mechanism is the smallest subarea of the receptive field, the responses of this component should determine sensitivity at the higher spatial frequencies. Any differences in size across spectral class should also be found at the higher spatial frequencies of the S-CSFs.

This difference in center diameter across spectral class is found in both spectrally opponent and nonopponent cells, and correspond with differences in the sizes of ganglion cell bodies; Red-ON center cells have smaller cell bodies than Red-OFF cells. There is no evidence indicating that the Green-component center varies with spectral cell type.

1.7 The Study.

The goal of this project is to examine and relate the spatial and spectral properties of ganglion cells. The goldfish is the ideal candidate for this type of investigation; since it is commonly used as a model of vertebrate color vision, many of its spectral characteristics have already been examined. Also, because of its robustness and stability as a retinal preparation, each cell under investigation can be exhaustively and rigorously tested. This is of particular importance for examining the spatial properties of these cells since a thorough, quantitative assessment requires a great deal of time. In this sec-

tion, the various hypotheses to be tested will be discussed.

1.7.1 Goldfish Spatial Processing.

Although the goldfish is often used as a model for color vision, the spatial properties of its retina have been somewhat ignored. In spite of the rigorous, quantitative analyses performed on cat ganglion cells, there have been very few attempts to establish this type of investigation with goldfish ganglion cells. The few attempts that have been made have yielded completely disparate findings. For example, some reports claim that all goldfish ganglion cells are linear, others report that the majority are nonlinear. The differences are most likely due to the type of stimuli and the definition of linearity used. One aspect of this work is to "bring the goldfish up to date" regarding its spatial processing. This will be accomplished by quantitatively assessing the spatial properties of goldfish ganglion cells using the same criteria and techniques as used in the cat and monkey research. For example, linearity will be determined by presenting contrast-reversal gratings to the retina and determining whether a spatial null position can be found. The criteria (the existence of a null point is one) for X-like cells in the goldfish retina will be the same criteria used in determining X-cells in the cat retina. Only through this kind of assessment can the spatial processing of goldfish ganglion cells be unequivocally related to the cat retina's spatial processing.

Another aspect of the goldfish ganglion cell's spatial processing is its spatial filtering characteristics. This will be determined by

deriving S-CSFs for each cell. Since the receptive field properties of goldfish ganglion cells are similar to cat ganglion cell receptive fields, these functions should be similar to the S-CSFs of the cat and other species. It will also be of interest to compare the goldfish ganglion cell S-CSFs to the psychophysical S-CSF of the goldfish (Northmore and Dvorak, 1979). The goldfish psychophysical S-CSF, although shifted to lower spatial frequencies, is similar in shape to the S-CSFs of other species. By obtaining the S-CSFs of the ganglion cells, their spatial resolution can be compared to the resolution of the entire animal's visual system.

1.7.2 Testing the Difference of Gaussians Model.

Because it is possible to maintain stable isolation of goldfish ganglion cells, it is feasible to examine the responses of the same cell to a number of different stimuli. This will provide a more complete picture of the spatial characteristics of these cells. For example, it is of interest to examine the spatio-temporal interactions of a cell, not only to confirm the similarities of the goldfish cells to other species, but as a test for the difference of Gaussians model. Since the center and surround arrangement of goldfish ganglion cells is similar to other species, they should also possess the same spatio-temporal interactions. For example, if the S-CSFs of spatially opponent goldfish cells lose their low frequency attenuation at high temporal frequencies, then it would suggest that the goldfish is similar to other species and still an adequate model of a vertebrate visual system. However, if there are no differences in the S-CSFs across temporal

frequency, then one can conclude that not only is the goldfish inappropriate as a model, but also, that spatial opponency is not sufficient to account for the spatio-temporal interactions.

Another test of the difference of Gaussians model would be to derive S-CSFs for the center and surround alone and compare these functions to the S-CSF of the entire receptive field of the same cell. This has not been done successfully in the past because it requires a long isolation time to present the appropriate stimuli and also, it is difficult to isolate the center and surround since their sensitivity profiles overlap. However, maintaining isolation is no problem for the goldfish preparation, and the responses of one mechanism can be minimized by restricting the stimulus grating to a spot or annulus while maintaining the rest of the field at the same mean luminance.

Extending the spatio-temporal domain to its limit, it is of interest to examine the temporal properties of the cell with a stimulus of zero spatial frequency. This is nothing more than a uniform field which modulates around a mean luminance as a sinusoidal function of time. Each temporal frequency can be presented at several contrasts, and the sensitivity of the cell, at each temporal frequency can be derived by finding the contrast necessary to produce a criterion response. Only one study has examined the temporal properties of the goldfish ganglion cells. Schellart and Spekreijse (1972) found two classes of cells with different Temporal Contrast Sensitivity Functions (T-CSFs). These cells were designated as "spontaneous" or "silent" based on their spontaneous rates or lack thereof. However, Schellart and Spekreijse made no mention of the X/Y dichotomy and the degree or

differences of linearity of these cell types were not determined.

Orientation and direction selectivity will also be examined in this project. Although there is evidence to suggest that goldfish ganglion cells should be orientation tuned, the direct evidence is somewhat mixed. What is necessary is to examine orientation and direction selectivity using an approach similar to Levick and Thibos (1982) and others for the cat retina. If orientation tuning in the goldfish retina is a function of stimulus spatial frequency, then it is possible that the stimuli used in past work on the goldfish (spots and bars of light) are inappropriate stimuli. Evidence exists to suggest that the goldfish ganglion cell receptive field contains irregular subareas; this can only be adequately tested with stimuli of high spatial frequencies.

The most interesting question regarding orientation and direction selectivity concerns the properties of W-like cells. Although these cells are the best candidates for this type of tuning, they have not been assessed in the past. The reason for this scarcity of W-like cells in general is that they are very difficult to isolate and maintain in the cat retina and optic nerve. This should not be a problem in the goldfish preparation; if W-like cells exist in the goldfish retina, it will be of great importance to investigate all of their spatial properties and relate them to the other spatial classes.

1.7.3 Spatial and Spectral Properties.

Once the spatial properties of goldfish ganglion cells have been established, the next step is to examine the spatial properties across the various spectral properties. Each cell will be classified by its

spatial properties (linearity of spatial summation, S-CSFs, and response to contrast) as well as by its spectral properties (spectral class and spectral opponency/nonopponency). To examine the relationships across the various categories, a large database will be established. The interactions between spatial summation class and the spectral properties will be examined to determine if linearity of spatial summation depends on the cell's spectral characteristics.

Cells will also be classified by their sensitivity to contrast. It is likely that this classification is dependent upon whether the cell is spectrally opponent or nonopponent (as is the case for the macaque), however, it will also be interesting to examine the relationship between sensitivity to contrast and spectral class. There is evidence in cat ganglion cells that ON- and OFF-center cells differ in their modulation sensitivity, (Cleland and Enroth-Cugell, 1966).

It will be interesting to compare the S-CSFs across spectral class (Red-ON, Red-OFF and ON/OFF), spectral opponency (spectrally opponent and nonopponent) as well as the S-CSFs of spectral class by spectral opponency. Certainly there should be differences across spectral class (Red-ON cells should have better spatial resolution than Red-OFF cells). The more intriguing manipulation is to compare the S-CSFs of the double-opponent cells (spectrally opponent) and the nonopponent cells. Since the early work involved mapping these receptive field components separately (by using monochromatic stimuli), there is no evidence examining the overall characteristics of these cells to a stimulus with only luminance variations (e.g., white light). The center mechanism alone of these double-opponent cells

contains an antagonistic relationship between a small field and a slightly larger one. This must certainly affect the spatial resolution and the S-CSFs of these cells.

[2]
METHODS

2.1 Subject and Husbandry Procedures.

Subjects were common goldfish (Carassius auratus) measuring 10-15 cm (from tip of nose to base of tail) in length. As with many fish, the photopigments in goldfish can change back and forth between rhodopsins and porphyropsins, thereby changing the cone spectra (Bridges, 1972). Also, temperature changes can alter the overall visual sensitivity of the fish (Hester, 1968) as well as altering the sensitivity of the individual cone types (Thorpe, 1971). Therefore, great care was taken to produce a stable environment. The goldfish were acquired from a local pet store and were stored in a 75 gallon white polyethylene tank capable of housing up to 15 fish of this size. The tank contained various plastic plants and assorted colored paraphernalia to provide adequate visual stimulation to the fish. The tank was well filtered and aerated. The water used in the tank was tap water which was aerated in a filtered 25 gallon storage tank for at least 48 hours prior to entering the fish tank. Aquarium salt was added to the water whenever storage water was placed into the fish tank (1 teaspoon per 5 gallons). Every two to three weeks, fif-

teen percent of the fish tank water was changed to aid in the filtering process.

The fish tank water temperature ranged from 21-26 degrees Celsius. Any extreme temperature changes were compensated for by introducing ice cubes or warm water gradually to maintain a comfortable and safe water temperature. The condition of the tank was carefully monitored to ensure an optimum environment for the fish. For example, water hardness ($CaCO_3$ levels) ranged from less than 50 ppm to 100 ppm and the pH of the water ranged from 6.6 to 6.9. Any fluctuation was corrected by standard fish care procedures.

When fish were obtained, they were carefully acclimated to the tank water by gradually introducing small amounts of tank water to their container. This was done to avoid any dramatic changes in the fish's environment (especially water temperature) which can place a severe strain on the fish. This process took anywhere from one to four hours. When new fish entered the tank a dose of achromycin (Lederle Laboratories) was placed into the tank (250 mg per 5 gallons) as a safety measure. About three days after the introduction of the antibiotic into the tank, thirty percent of the water was changed. At this time, the regular feeding process began. The fish were fed once a day as much food (Wardley's Shrimp Pellets) as they could consume in about ten minutes. Any remaining food was removed from the tank.

The tank was illuminated by a single fluorescent bulb (G.E.; 14 W cool white) suspended above the water; it produced an illuminance of about 130 lux at the water surface. The light was attached to a

timer producing a 12 hour day/night cycle.

2.2 Apparatus.

2.2.1 Isolation Chamber.

Physiological recordings were made from excised, isolated retinae as described in Section 2.3. The retina was maintained in a gas environment and was not immersed in liquid. The retina was placed in a brass chamber with dimensions of 4.6 x 4.6 x 1.2 cm. The bottom of this chamber consisted of a glass plate on which the retina rested, receptor side up. The light stimulation of the optical system came from underneath the glass plate which corresponds to the direction the light must travel through the eye to reach the receptors in the intact eye. There were two duct systems in the brass chamber. Water, maintained at a constant temperature (Brinkman Instruments; Lauda K2/R Cooler), was circulated through one of the ducts, thereby keeping the chamber's air space and the retina at a fixed temperature. Retinal temperature was maintained at 18 degrees Celsius throughout the experiments.

The upper duct system allowed a steady flow across the retina of 100% moist oxygen from a compressed gas tank. The oxygen was moistened by passing it through a container of distilled water. After leaving the water chamber, the gas was cooled to the temperature of the recording chamber and then sent through a vial of spun glass to remove any suspended water droplets. The oxygen flowed into the chamber at a rate of 75 ml/min. Pure oxygen was used in this prep-

aration since any carbon dioxide in the gas can greatly reduce the sensitivity and the spontaneous rate of ganglion cells (Abramov and Levine, 1972; Mackintosh, et al., 1987).

The top of the chamber consisted of two microscope slides separated by a distance of about 9 mm. This gap allowed the microelectrode to be lowered into the retina and also allowed any gas or gaseous waste products from the retina to escape. The entire isolation chamber was located in a light-tight Faraday cage measuring 62 x 33 x 36 cm. To prevent the Faraday cage from collecting waste gases and stale air, a small vacuum and air pump circulated the air in the cage. With this preparation, a retina could be maintained for up to six hours.

2.2.2 Electrical Recording.

The extracellular recordings from single ganglion cells were made with glass-insulated platinum-iridium microelectrodes. The electrodes were made using the method of Wolbarsht and Wagner (1963) and Snodderly (1969) with the exception that the glass was not treated with hexamethyldisilazane, a substance used to render the glass hydrophobic. To ensure that the tip of the electrode was free of the glass-coating, it was plated with platinum black. This procedure produced electrodes with a tip diameter of less than 1 μm. Electrodes could be reused for long periods of time if gently sprayed at the end of each recording session with distilled water and occasionally replated with platinum blacking.

The electrode was lowered into the retina by a micromanipulator

(designed and built by the Rockefeller University Instrument Shop). The indifferent electrode consisted of a 10 mm bare platinum-iridium wire which was placed on the edge of the retina. Ganglion cell responses were amplified by a small, low-noise, battery powered, capacitively-coupled, pre-amplifier with a field-effect transistor input (designed by M. Rossetto of the Rockefeller University Electronics Shop). The pre-amplifier was also enclosed in the Faraday cage which shielded the pre-amplifier from any electrical noise. The signals from the pre-amplifier were amplified again and then passed into an adjustable bandpass filter (Krohn-Hite, Model 3103) to provide additional filtering of the signal. This signal was then sent to a level detector (designed by M. Rossetto) which provided an output pulse when the input signal exceeded an adjustable threshold. Both the threshold level and the amplified signal were displayed on a dual-beam oscilloscope screen. Signals from the level detector were sent to an audio speaker, a set of counters and to the digital I/O panel of a computer (DEC; PDP 8/E) which stored the data as well as stimulus information on magnetic tape after each stimulus period. Each stimulus period, whether the responses were to spectral or spatial stimuli, was stored as a string of event-interevent intervals. Each event (a neural impluse -- "spike" or some stimulus parameter such as a shutter opening) was represented by a number followed by the number of internal clock ticks of the computer that elapsed prior to the next event; this clock counted at a rate of 10 kilohertz so that the precision available to collect the events (0.1 msec) was more than sufficient.

A bank of digital timers (designed by L. Eisenberg of the Rockefeller University Electronics Shop) controlled the onset and offset of the "gate" during which data were collected and stimuli were presented, the acquisition of data by the computer, and a series of buzzers which provided auditory information to the experimenter signalling the onset and offset of the stimulus. For the spectral stimuli, timers controlled the shutters of the main optical system; for spatial stimuli, these timers controlled the onset and offset of the V2-R2 Visual Stimulator (see below).

2.2.3 Optical System.

The optical system consisted of four independent beams joined by mixing cubes and projected to the underside of the retina. Three of the beams were used to present spectral stimuli to the retina. These beams were optically identical and allowed for control of shape, position, wavelength, quantal flux and timing of the stimulus. Each beam, had as its light source, a tungsten filament quartz-halogen lamp (Sylvania Electric Products; 50 W, 60 V/T3 1/2-inch prefocused base). The filament of the bulb was imaged on the entrance slit of a grating monochromator (Jarrell-Ash; one-quarter meter Ebert-type); the half-power bandwidth of the monochromator was eight nanometers.

Upon leaving the exit slit of the monochromator, part of the light was deviated by a microscope cover slip into a feedback system which controlled the intensity level of the bulb via a photocell monitor (U.D.T.; Pin-10), with a function generator linked to the monochromator's wavelength drive (Perkin-Elmer; Vernistat Function Genera-

tor, Model DC250 and interpolating potentiometer, Model 2X5). This feedback loop ensured that the same quantal flux was delivered at each wavelength to the retina, and that the rate did not change with the life of the lamp. These wavelength-dependent settings on each beam's function generator were made with reference to a calibrated photocell placed in the recording chamber at the plane of the retina; this ensured that any wavelength-selective differences among the beams were compensated for. (The photocell was attached to a radiometer (U.D.T.; Photometer/Radiometer, Model 111A) and had been spectrally calibrated by the manufacturer.) For details of this feedback system see Rosen, Levine, Rossetto and Abramov (1970). From the photocell monitoring assembly, light passed through an assembly which allowed the introduction of spectral "blocking filters" when needed. These were used to ensure purity of the monochromatic light at wavelengths less than 480 nm (Melles Griot; 03 SWP 013) and for wavelengths greater than 630 nm (Kodak, Wratten 29).

From the blocking filters, light passed through another lens which focused the image on an electromagnetic vane shutter with a rise and fall time of less than 1 msec (Hartline and McDonald, 1947). The light then passed through two wheels containing Inconel neutral density filters (Boxton Beel Inc.). These neutral density filters allowed the experimenter to control the intensity of the light by rotating the wheels to the appropriate configuration. There were 24 possible log attenuations ranging from 0.2 to 4.8 in 0.2 log unit steps. The maximum log quantal flux (designated as 0.0) corresponded to 2.75×10^{12} quanta/cm^2/sec. The wavelength setting of

each monochromator and the positions of filter wheels in each beam were electronically coded and sent to the computer for storage with the cell's responses.

High contrast photographic transparencies were used as field stops. These field stops produced a stimulus to the center of the cell's receptive field (0.63 mm diameter spot of light) and an annulus to stimulate the surround portion of the receptive field (outer and inner diameters of 6.31 mm and 1.95 mm, respectively). These values were sufficient to stimulate either the center or surround mechanism while minimizing the influence of the other mechanism (Daw, 1968). The three beams were joined by mixing cubes and then passed to the final projection lens. The optical system had a reduction factor of 0.1 on the retinal surface. The mixing cubes also provided an observation beam in which the experimenter could check that the appropriate stimulus was presented.

The fourth beam was used to produce the appropriate spatial and temporal stimuli. This beam consisted of a high resolution oscilloscope (CRT) (Tektronix; Model 606, P31 phosphor) which displayed the output of an electronic visual stimulator (designed by N. Milkman and D. Kocsis of the Rockefeller University Electronics Shop, Model V2-R2). (See Milkman, Shapley and Schick, 1978, for more details.) This microcomputer was designed to produce sinusoidal gratings whose spatial frequency (cy/mm on the retina), orientation, contrast and temporal frequency were independently variable. Therefore, different spatial frequencies could be set at a constant temporal rate; that is, the number of cycles that crossed a point in space remained the same

regardless of the spatial frequency. The visual stimulator was also capable of producing gratings whose contrast is reversed as a sinusoidal function of time (i.e., contrast-reversal stimulus). The spatial position (phase) of this grating could also be manipulated.

Each pattern was modulated around some mean luminance to maintain a constant adaptation state. The contrast of the stimulus was defined as: Maximum luminance - Minimum luminance / Maximum luminance + Minimum luminance. The CRT's intensity was set at a predetermined value and the Z-axis was then controlled entirely by the stimulus generator. Since the CRT's Z-voltage/light intensity function was not linear, a linearizing circuit was added to correct this distortion (Harris and Abramov, 1983). With this circuit, contrasts up to 95% were possible with no more than 5% harmonic distortion. The CRT was placed into a holder underneath the Faraday cage; by reflecting the CRT's image off a mirror, the image entered the beam splitter of the main optical system and was projected to the plane of the retina. Since the optics reduced the image 0.1, the entire image of the CRT face on the retina was 10.5 x 8.5 mm. However, to produce a symmetrical and uniform stimulus, the image was restricted to a 7.5 mm diameter circle by placing an opaque cut-out on the CRT's face.

The overall mean luminance was varied by placing neutral density filters on the face of the CRT. The stimulus generator was also capable of restricting the stimulus pattern to a central area or to its surround while the remaining portion of the display was maintained at the same mean level. The size of the stimulus pattern could be

adjusted by the experimenter. The laboratory computer provided the instructions to the visual stimulator's microprocessor. The experimenter could control the instructions directly or allow a series of predetermined instructions to be generated by the computer. A schematic of the entire system is shown in Figure 5.

2.3 Procedures.

2.3.1 Isolation and Surgery Procedures.

About two to four hours prior to surgery, a fish was placed in a 10 gallon light-tight dark adaptation tank. This dark adaptation permitted the pigment epithelium to retract from the cones, allowing an easier separation of the retina from the pigment epithelium with minimum damage to the cones (Ali, 1975).

Following dark adaptation, the fish was removed from the tank and sacrificed by decapitation. The eye was enucleated by first making a small cut on the dorsal pole of the ocular orbit. This allowed the experimenter to reach behind the eyeball with a pair of iridectomy scissors and cut the optic nerve. Following this, the ocular muscles were severed and the eye then slipped out of the socket.

Once enucleated, the front half of the eye (containing the cornea and lens) was removed exposing the retina which rested in the back half of the eyecup. In order to remove the retina, a pair of iridectomy scissors was used to "peel" the retina from the back of eye and finally to cut the optic nerve which caused the retina to fall out of

Figure 5

Schematic of recording and optical set-up. Solid, dark lines refer to electrical connections within the system; dotted lines represent the light pathway to the retina. Only one beam of the three spectral beams is shown.

Recording and Optical Systems

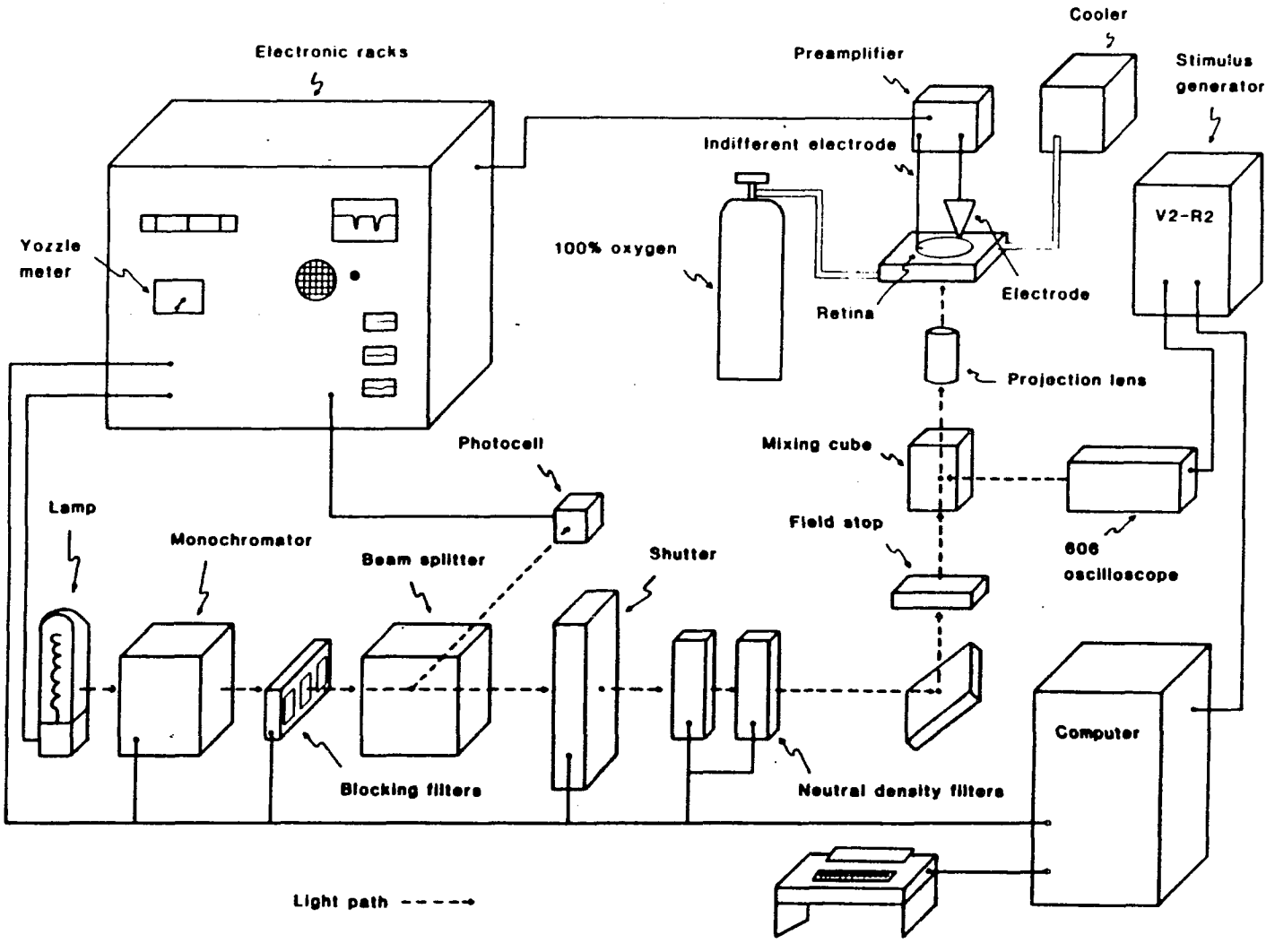

the eyecup. The retina was placed, receptor side up, on a microscope slide and then taken to the isolation chamber where it was placed gently on the glass plate at the bottom of the recording chamber. The time taken to complete the surgery and place the retina into the chamber ranged from two to five minutes.

During surgery, the only illumination on the retina was from a small, tungsten light (G.E. 6S6; 6 W/ 120 V) attached to the headband of the surgeon. This illumination greatly reduced the sensitivity of the rods, which do not recover, leaving exclusively cone driven responses at the ganglion cells (Mackintosh, 1981; Shefner and Levine, 1979). From a distance of 15 cm the light produced an irradiance of about 60 $\mu W/cm^2$ on the retina. Finally, since the surgeon worked so close to the retina, a skin-diver's snorkel and nose plugs were worn to eliminate exposing the retina to any carbon dioxide contamination from his breath (see Abramov and Levine, 1972).

While in the isolation chamber, the retina was occasionally exposed (one to two seconds in duration) to light from a small penlight. This was necessary when the experimenter was visually checking the location of the electrode on the retina. Again, allowing a distance of 15 cm, the irradiation of this light source on the retina was about 15 $\mu W/cm^2$.

Once the retina was placed in the isolation chamber it was allowed to stabilize to the environment before recording started. During this time, the experimenter cleaned the surgery tools, measured the fish length and measured the diameter of the lens; any comments regarding the surgery, retina, etc. were recorded.

A microelectrode was then inserted into the micromanipulator and lowered to the surface of the retina. The pre-amplifier was turned on and an inspection beam (a 520 nm spot of light, 0.63 mm in diameter, at 0.0 log unit intensity from one beam of the optical system) was presented briefly to the retina in order to determine where on the retina the electrode was lowered. (During the set-up procedures, the electrodes were aligned to the middle of the center spot to ensure that when a cell was isolated, the electrode was close to the cell body and the center of the receptive field (Brown and Wiesel, 1959)). Once it was established that this area of the retina was satisfactory, the inspection beam was closed (the duration of inspection was no more than one second), and the electrode was lowered through the retina to the ganglion cell layer. If there was no obvious activity in a particular area, the electrode was raised and the entire isolation chamber was shifted laterally so that the electrode could be lowered into another area of the retina. This was continued until a ganglion cell was isolated (i.e., when the amplitude of one ganglion cell's response was sufficiently large to be distinct from the noise and from the activity of other cells). Since ganglion cells are the only retinal cells that respond with true action potentials, there was very little chance that the isolated response was from any other retinal neuron.

Once a cell was isolated, general information such as the spontaneous rate, amplitude of the signal, etc. was recorded by the experimenter. Occasionally, a cell would have to be re-isolated due to the settling of the retina. At this point, the electrode was lowered or raised slightly to achieve the largest signal amplitude possible. To

ensure that the same cell was re-isolated, several stimuli were repeated and the responses were compared to the responses prior to re-isolation. Also, a device which laterally moved the electrode was employed when the isolation was no longer sufficient. These lateral movements were minimal (no more than 0.1 mm on the retina) to ensure that the electrode was still aligned with the center spot. When the cell was successfully isolated, the computer run-time program was initiated and the data collection began.

There were two phases of data collection. One consisted of the presentation of the spectral stimuli (via the main optical system); the second phase was the presentation of the spatial stimuli (via the V2-R2 stimulus generator). It should be emphasized that the following procedures represent the ideal protocol. Since the life of an isolated ganglion cell can vary, it was necessary to deviate from these procedures to obtain as much useful information about the cell as possible.

2.3.2 Spectral Stimuli.

The basic strategy of the presentation of the spectral stimuli was to present different wavelengths of light at various intensities to the center, the surround, and to the entire receptive field. From this information, spectral sensitivities could be derived and the cone contributions to the ganglion cell could be determined. Each stimulus presentation consisted of a five second gate which had a one-second pre-stimulus, a one-second stimulus and a three-second stimulus-off period. The pre-stimulus component was used to measure the sponta-

neous rate of the ganglion cell. The stimulus on component, of course, represented the "on" response of the cell and the first second of the post stimulus component represented the "off" response of the cell.

Ganglion cell responses for each gate, along with coded stimulus information were recorded by the computer for later analysis. The computer also produced a peri-stimulus-time histogram (PSTH) on a storage oscilloscope and a brief printout of the cell's response to give the experimenter some feedback regarding the cell's activity. The inter-trial interval was 25 seconds, which allowed the experimenter to set up for the next stimulus, as well as allowing the cell's response to return to its spontaneous rate.

Once a cell was isolated, stimuli of 700, 510 and 450 nm (all monochromatic stimuli were equated for equal quantal content) were presented to the center and surround portions of the cell's receptive field. These were presented at several intensities covering the range from threshold to saturation in five approximately equal logarithmic steps. These three wavelengths represented iso-absorption points along the spectral sensitivity of the L-cones (Harosi, 1976). Therefore, if only L-cones were present, then the responses at these three wavelengths would be identical. This allowed the experimenter to quickly identify the spectral characteristics of the cell.

Following this procedure, a standard wavelength-intensity series was performed. This consisted of up to 12 different wavelengths corresponding to critical points along the spectral sensitivities of the cone types. Each wavelength was presented at three intensities.

This was done for the center, the surround, and the entire receptive field.

2.3.3 Spatial Stimuli.

Following the completion of the spectral stimuli, the CRT display was turned on and a few minutes were allowed for the retina to adapt to the illumination provided by the CRT. The retinal illumination of the CRT display was 0.2 lm/m^2. At this point, the computer run-time program to control the V2-R2 stimulus generator was initiated. The response of the cell to each stimulus and stimulus information were recorded by the computer for later analysis.

The usual procedure was to present first a series of drifting gratings at different spatial frequencies at a moderate contrast. This provided information regarding the S-CSF of the cell, which aided in choosing an appropriate spatial frequency to test for linearity (i.e., a spatial frequency which lies between the peak sensitivity and the high-frequency cut-off of the cell's S-CSF); it also indicated how responsive the cell was to contrast so that an appropriate range of contrasts could be chosen. Following these stimuli, a contrast-reversal series was initiated to test the cell's linearity of spatial summation. To provide an estimate of the cell's spontaneous rate as well its variability, a contrast-reversal grating of zero contrast was presented with phase marks at a specified temporal rate for five seconds. After this "dummy" stimulus was presented, the computer performed an on-line Fourier decomposition of the averaged response, and the first and second harmonics were displayed. If the amplitude of the

components was relatively high, indicating that the cell's response had large variability, then the stimulus gate length was increased, thereby increasing the number of stimulus cycles over which the response was averaged, and the zero contrast stimulus was repeated. When the appropriate gate duration was established, contrast-reversal gratings at a particular contrast, spatial frequency and temporal frequency, determined by the experimenter, were presented at various positions or spatial phases of the cell's receptive field to establish whether or not the cell possessed a null point; that is, a position at which the cell responded as if there was no modulated stimulus.

Since there was no direct way of finding the midpoint of the cell's receptive field, an iterative process, controlled by the experimenter, was used to pinpoint the location of the null position, if one existed. This was accomplished by taking advantage of the fact that the fundamental component's amplitude and phase shift are dependent on the spatial position of the contrast-reversal grating. The amplitude of the fundamental component is a sinusoidal function of spatial phase and the phase shift of the fundamental component on one side of the midposition of the receptive field is 180 degrees out of phase with positions on the other side. Therefore, by presenting several stimuli at different spatial phases and comparing their fundamental responses, the midpoint of the receptive field can be determined quite easily. For example, if two gratings, 90 degrees apart in spatial phase (0 and 90 degrees, for example), have fundamental components which are 180 degrees out of phase to one another, then the midpoint of the receptive field must fall between these two positions. If the

phases are equal, then the stimuli are on the same side of the midpoint which must lie between spatial phases of 90 and 180 degrees. From this information the experimenter could choose the appropriate spatial position to locate the midpoint of the receptive field. Within five or six stimuli the experimenter could be reasonably certain of the cell's classification in terms of its spatial summation and could then proceed with other stimuli.

To determine the S-CSF of the cell, sinusoidal gratings, of different spatial frequencies, were drifted across the receptive field of the cell at a constant temporal rate (cycles per second across the field). Each spatial frequency was presented at several contrasts. The T-CSF was determined by presenting a uniform pattern ("blank field") whose intensity varied sinusoidally in time. The stimulus duration was varied to maintain the same number of stimulus presentations across temporal frequencies. For example, to produce 30 presentations of a 1 Hz stimulus requires 30 seconds, however, a 2 Hz stimulus needs only 15 seconds for 30 presentations. These stimuli were also presented at various contrasts.

If time permitted, the various parameters of the different spatial stimuli were varied. For example, contrast-reversal gratings were presented at different temporal and spatial frequencies to determine their influence on the spatial summation properties of the cell. Drifting gratings were presented at different drift rates to examine the affect of stimulus drift rate on the cell's S-CSF. Also, drifting gratings were restricted to the center or surround portions of the receptive field to examine the contributions of each mechanism while mini-

mizing the input of the other component. To determine if the receptive field was circular and symmetrical, drifting gratings were presented at different orientations at 45 degree steps from 0 to 135 degrees. For each orientation, the grating was drifted in each of the two possible directions. Stimuli for determining the T-CSF were also restricted to the center or surround components of the receptive field.

After obtaining all the necessary spatial information, or if the cell's isolation was lost, the CRT was turned off and another cell was isolated. To ensure that there were minimal effects of adaptation of the new cell due to the CRT, approximately ten to fifteen minutes were allowed to pass before the new cell's spectral properties were examined. For some cells, the spectral properties were determined after the spatial stimuli were presented and, as in the previous case, the CRT was turned off for ten to fifteen minutes prior to examination.

[3]
RESULTS

3.1 Spectral Classification of Cells.

3.1.1 Spectral Class.

Each cell was classified into one of three spectral classes based on its L-cone input to the center of the receptive field. This was determined by presenting a 700 nm stimulus to the center at several intensities ranging from near-threshold to suprathreshold intensities. Since only the L-cones are sensitive to this wavelength, this classification scheme unequivocally determines the response driven by a single receptor type. L-cone input was used to classify cells since it is easy to isolate (by using near-infrared stimuli) and because all goldfish ganglion cells possess L-cone input. The presence or absence of M- and S-cone contributions was used with the L-cone input to classify the cell as spectrally opponent or nonopponent (see Section 3.1.2). A cell was classified as an L-/$^+$ center cell if its response to this stimulus was ON-inhibition and OFF-excitation (-/$^+$). Cells were also classified as L-/$^+$ if only a partial response was found (i.e., OFF-excitation only, (/$^+$) or ON-inhibition only (-/)). Cells with a

partial response either had a low spontaneous rate (and thus no obvious inhibition) or different thresholds for the "on" and "off" responses. These cells were also examined at suprathreshold intensities to determine if the response became ON-excitation and OFF-excitation (+/+). If there was a discrepancy between near-threshold and suprathreshold responses, the cells were always classified by their suprathreshold responses. The second cell type was simply the reverse of the previous category: L+/- center cell. These two cell classes refer to Red-ON and Red-OFF center cells described in past literature. The third type of cell had an L-cone input that responded with both ON-excitation and OFF-excitation (L+/+ center), corresponding to Hartline's (1938) category of ON/OFF cells. Since, in some cases, only one portion of the L+/+ center cell's response was apparent at threshold, these cells could be misclassified as one of the previous categories unless examined at suprathreshold intensities (see Mackintosh, 1981; Mackintosh, et al., 1987).

3.1.2 Spectral Opponency.

Each cell was also classified as either spectrally opponent or nonopponent. A spectrally opponent cell responded with ON-excitation at some wavelengths and ON-inhibition at others (or OFF-inhibition at certain wavelengths and OFF-excitation at others). This change in response type (sign) across wavelengths was due to more than one cone type contributing to the response (for example L+/- and M-/+). A cell was classified as spectrally nonopponent if there was no change in the type of response across the spectrum. How-

ever, this does not imply that a spectrally nonopponent cell had only one cone type, but that the net result of the combined inputs produced the same response type across wavelengths. It should be noted that these two spectral classifications (L-cone center response and whether the cell is spectrally opponent or nonopponent) are independent classifications (Mackintosh, et al., 1987); that is, $L^{+/-}$, $L^{-/+}$, and $L^{+/+}$ center cells can be either spectrally opponent or nonopponent. Spectral opponency was determined separately for the center, surround, and full field of the receptive field.

3.2 Spatial Summation.

3.2.1 Criteria for Classification.

Spatial summation was tested by presenting a contrast-reversal grating at different spatial phases across the receptive field of the ganglion cell. The grating's contrast was reversed according to a specified sinusoidal temporal function. The temporal function was divided into discrete time bins and the cell's responses to each reversal cycle were superimposed to provide the average number of spikes per time bin. These values were converted into spike rates and a discrete Fourier transform (Cooley and Tukey, 1965) provided the power spectrum of the first ten harmonics.

To be classified as a linear or X-like cell, four criteria had to be met. First, there must have been a spatial position at which there was no response to the contrast-reversal grating (i.e., a null point).

Second, when the grating was positioned away from the null point, the response was modulated at the same frequency (f) as the contrast-reversal (i.e., except for high contrasts, most of the power in the response was at f). Third, the power at f was a sinusoidal function of spatial phase. Fourth, the power at f increased linearly with grating contrast, at least up to some saturation point. Cells with a low spontaneous rate presented a special problem since their response to the stimulus fell to zero and thus distorted the response waveform. This produced a response pattern resembling a half-wave rectified response. A Fourier decomposition of a half-wave rectified response will produce substantial power at the second harmonic and other even harmonics. To minimize this, contrast-reversal gratings were presented at several contrasts in an attempt to find a contrast that did not cause the response to drop to zero. However, it was not always possible to find such a contrast especially with cells that displayed no spontaneous rate.

These criteria for linearity had to be satisfied at high, but not necessarily at low, spatial frequencies. At low spatial frequencies, the responses of the small, nonlinear subunits found in Y-cells are overshadowed by the contributions of the larger center and surround components and could give the impression that the cell is linear (Hochstein and Shapley, 1976a). To be sure that the nonlinear subunits were contributing to the response, a moderately high spatial frequency was used. This was determined by choosing a spatial frequency which was located between the peak sensitivity and the high frequency cut-off of the S-CSF.

A cell was classified as Y-like if it responded at double the stimulus frequency at all spatial phases and did not possess a null point. This criterion, too, had to be met at high spatial frequencies. Cells that were neither X- nor Y-like were classified as W-like. These cells responded as X-like when the stimulus grating was placed away from the midpoint of the receptive field and responded at double the modulation frequency as the grating approached the midposition ("null point") of the receptive field. These cells possessed no true null point regardless of the spatial frequency of the stimulus.

It should be mentioned that the criteria described above are the same rigorous criteria for classifying X- and Y-cells in the cat (Hochstein and Shapley, 1976a). The only distinction between X-cells in the cat retina and X-like cells in this study is in the species in which they are found. However, for historical reasons, the terms "X-, Y-, and W-cells" are reserved only for cat neurons meeting the above criteria.

3.2.2 X-like Cells.

Twenty-seven (21%) of a total of 126 ganglion cells successfully isolated were classified as X-like cells. Figure 6 illustrates the presence of a null point and the dependence of the response on spatial phase for one of these cells. The contrast-reversal cycle was at 4 Hz, the spatial frequency of the grating was 1.52 cy/mm, and the contrast was 6 percent. The abscissa represents one reversal cycle of the stimulus grating (250 msec). The stimulus cycle was divided into 30 discrete time bins (8.3 msec each) and the response reflects

Figure 6

Averaged X-like cell responses to a contrast-reversal grating at various spatial positions on the receptive field. The stimulus consisted of a contrast-reversal grating with a spatial frequency of 1.52 cy/mm, at 6% contrast, and modulated at a rate of 4 Hz. The value above each figure refers to the position of the grating, in degrees, on the receptive field of the cell; zero degrees is the midposition or "null point" of the X-like cell. The bottom illustrations show one complete contrast-reversal cycle of the stimulus.

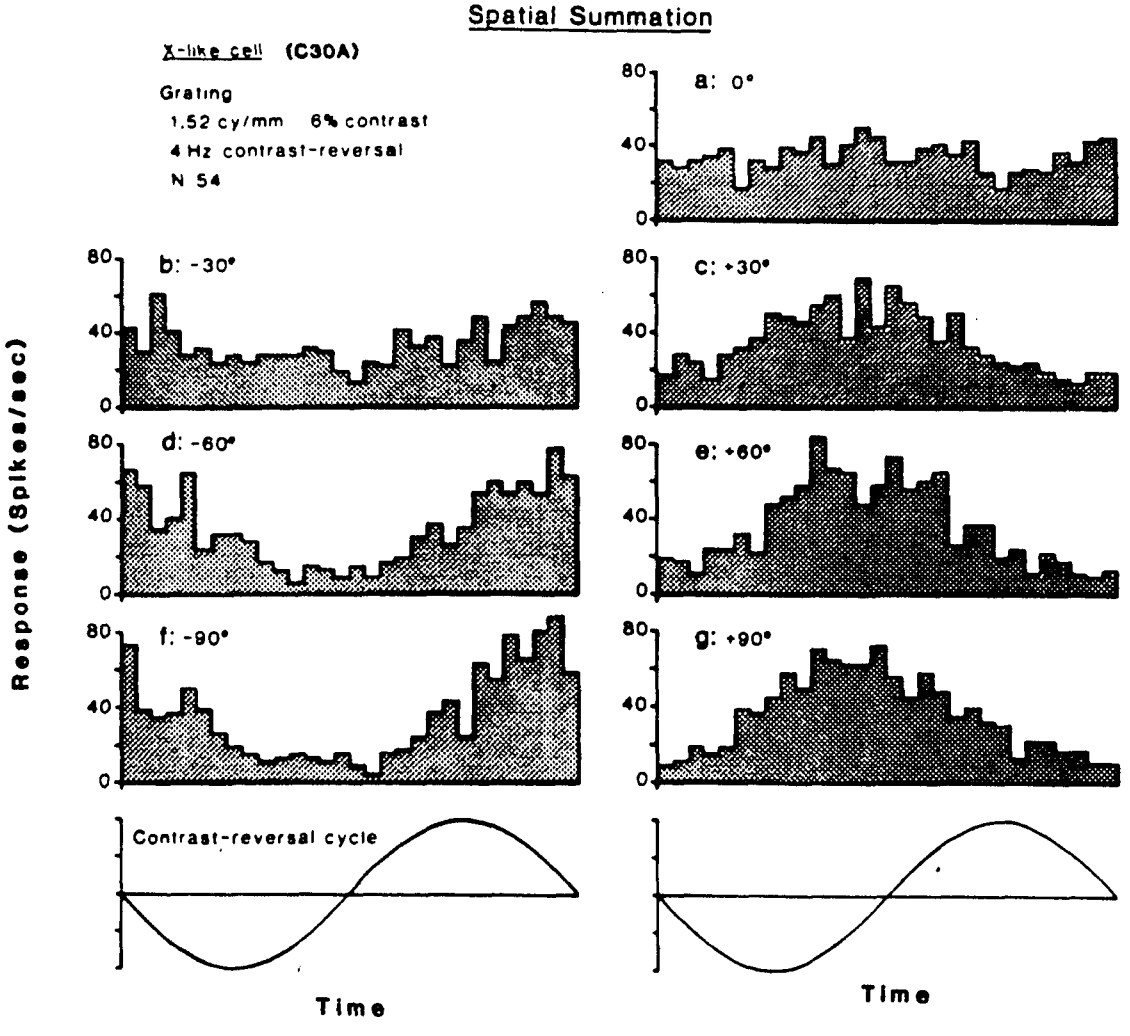
Spatial Summation
X-like cell (C30A)
Grating
1.52 cy/mm 6% contrast
4 Hz contrast-reversal
N 54
a: 0°
b: -30°
c: +30°
d: -60°
e: +60°
f: -90°
g: +90°
80
40
0
Response (Spikes/sec)
Contrast-reversal cycle
Time
Time

the average response rate per time bin. Figure 6a shows the averaged response of the cell to the contrast-reversal grating positioned at the midpoint of the cell's receptive field. At this position, there was no response to the grating. As the grating was positioned away from this null point, the cell responded to the stimulus. In Figure 6c, the grating was positioned 30 degrees away from the null point; there was clearly a response to the stimulus and the response was modulated at the same temporal frequency as the stimulus' cycle-reversal. When the grating was positioned further away from the null point (Figures 6e, g) the response still modulated at the same temporal frequency but the response amplitude was greater. When the grating was positioned on the opposite side of the null point (Figures 6b, d, f), the response amplitude, again, depended on the spatial phase of the grating; the farther away the grating was positioned from the null point, the larger the response amplitude. However, the modulation responses on one side of the null point were 180 degrees out of phase with the responses on the other side of the null.

Figure 7 shows the relative response amplitudes of the fundamental and second harmonic components as a function of spatial phase in the same cell. The amplitude of the fundamental component was a sinusoidal function of the spatial phase of the stimulus grating. Since the responses on either side of the null point were 180 degrees out of phase, one side was arbitrarily designated as a positive response and the other side as a negative response. The curve represents the best fit sinusoid; this was done by determining the exact location of the null point by interpolation of the data points and plac-

Figure 7

Relative response amplitudes of the first two Fourier components of an X-like cell's responses to a contrast-reversal grating as a function of spatial phase of the stimulus. Stimulus parameters are the same as in Figure 6. Closed circles refer to the amplitude of the fundamental component of the response; asterisks represent the amplitude of the second harmonic component of the response. The curve is the best-fit sinusoid to the data.

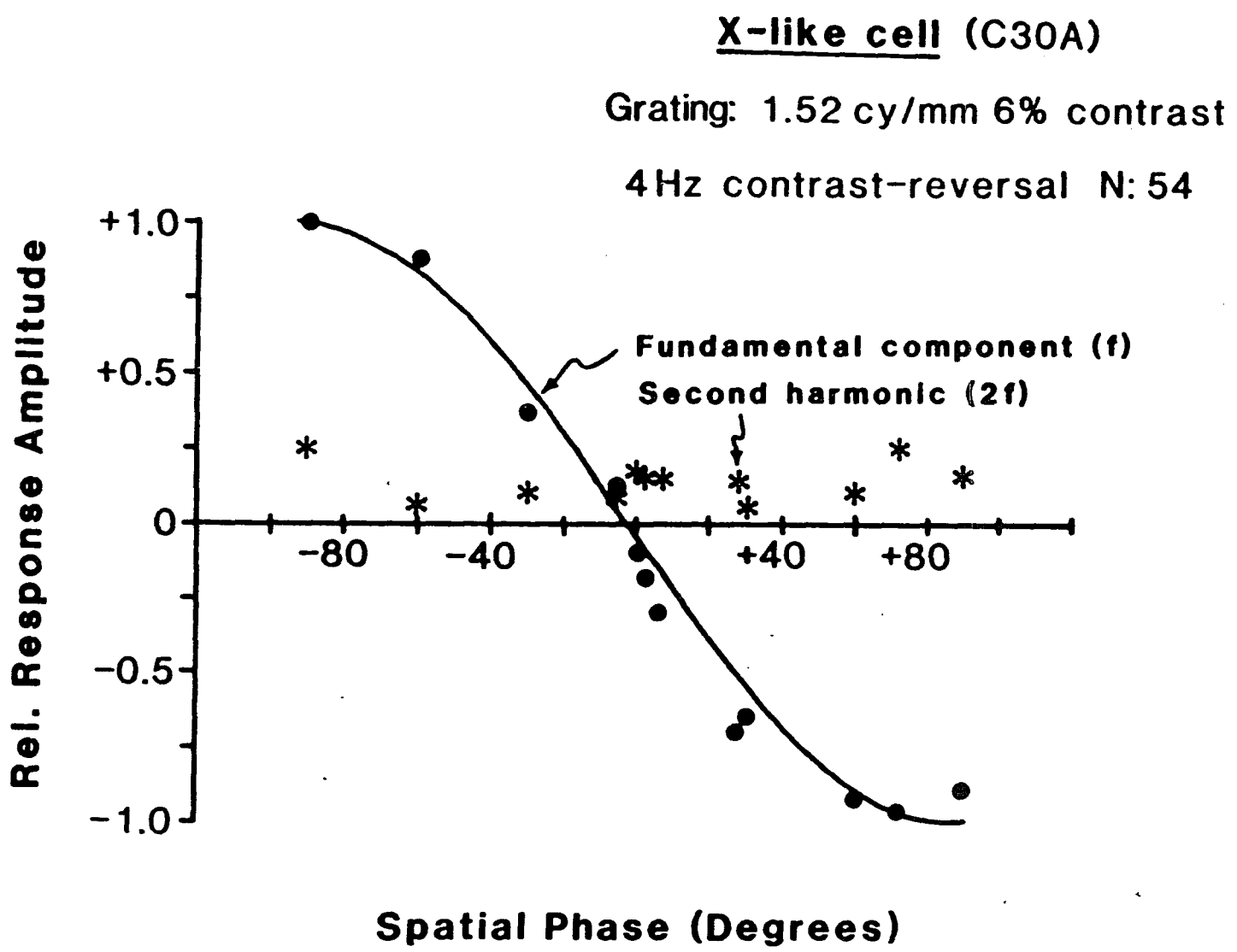
X-like cell (C30A)
Grating: 1.52 cy/mm 6% contrast
4 Hz contrast-reversal N: 54
Fundamental component (f)
Second harmonic (2f)
Rel. Response Amplitude
+1.0
+0.5
0
-0.5
-1.0
-80
-40
+40
+80
Spatial Phase (Degrees)

ing the sinusoid value of zero at that position. The second harmonic component was very low regardless of the spatial phase of the grating. Also, there was no phase shift in the second harmonic component as a function of spatial phase.

The presence of a null point was tested at different spatial frequencies, temporal frequencies and contrasts; these parameters did not affect the existence of a null point in X-like cells. The only exceptions were at very high contrasts where the cell's response approached saturation. The ratio of the second harmonic and the fundamental components (2f/f) was a good indicator of the dominant components in the response (Hochstein and Shapley, 1976a). This ratio was always less than one for X-like cells indicating that the response was dominated by the fundamental component.

3.2.3 Y-like Cells.

Fifty-three (42%) of 126 ganglion cells successfully isolated were classified as Y-like cells. Figures 8 and 9 show a typical Y-like cell's response to a contrast-reversal grating at two different spatial frequencies. The gratings were presented at 25% contrast with a reversal rate of 4 Hz. At high spatial frequencies (e.g., 3.05 cy/mm), the cell responded at twice the stimulus frequency at all spatial phases (Figures 8a, c, e; 9b). However, at low spatial frequencies (e.g., 0.38 cy/mm) a null point could be found (Figure 8d). This cell had no spontaneous rate so there were no spikes recorded at the low spatial frequency null point.

Figure 9 shows the relative response amplitudes of the funda-

Figure 8

Averaged Y-like cell responses to contrast-reversal gratings at various spatial positions on the receptive field at two different spatial frequencies. For both spatial frequencies, the contrast-reversal rate was 4 Hz at 25% contrast. The values above each figure refers to the position of the grating, in degrees, on the receptive field; zero degrees represents the best estimate of the midposition of the receptive field. The two spatial frequencies were 3.05 cy/mm (a, c, and e) and 0.38 cy/mm (b, d, and f). The bottom illustrations show one complete contrast-reversal cycle of the stimulus.

Spatial Summation

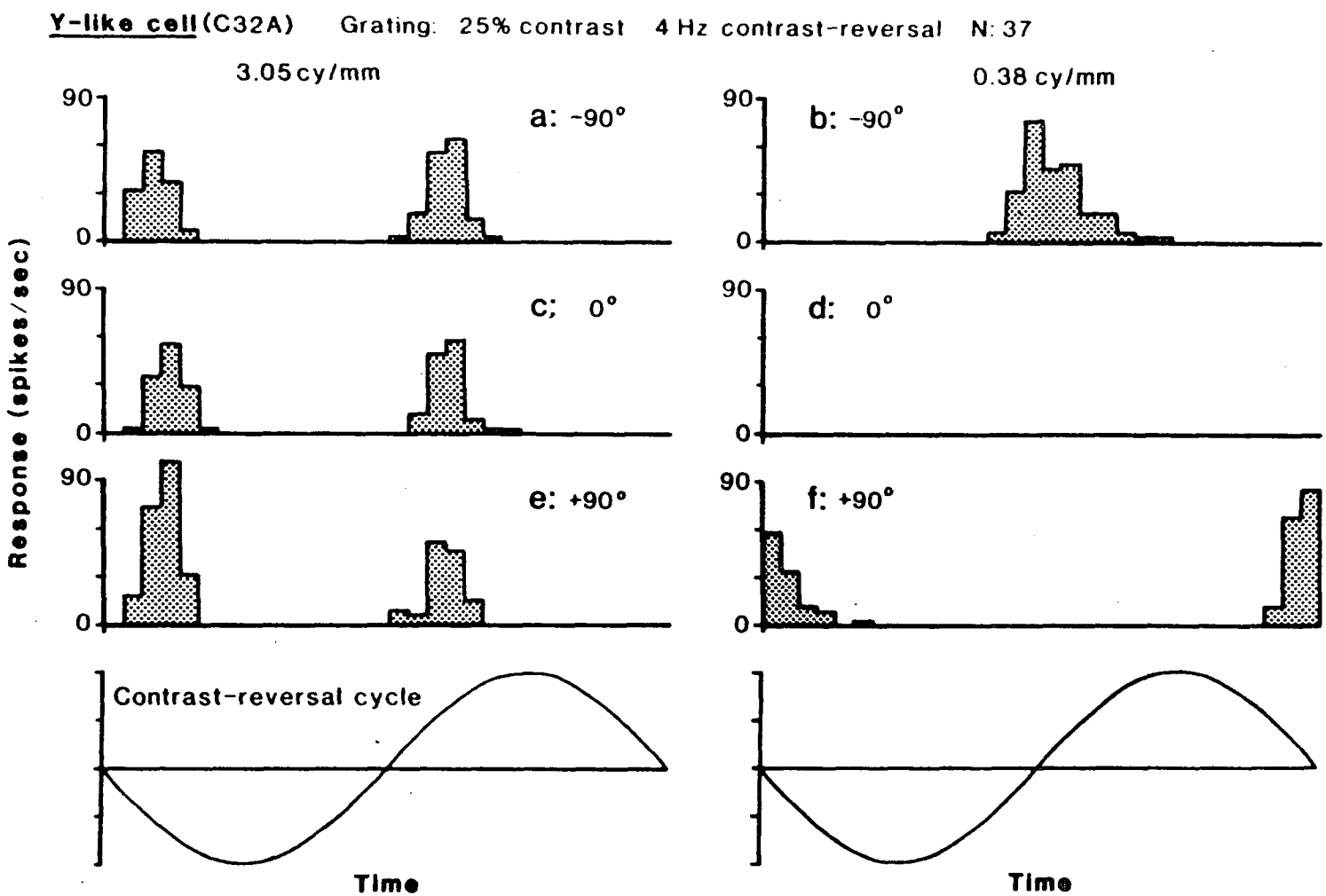

Figure 9

Relative response amplitudes of a Y-like cell to a contrast-reversal grating as a function of spatial phase at two different spatial frequencies. Stimulus parameters were the same as in Figure 8. The two spatial frequencies were 0.38 cy/mm (a) and 3.05 cy/mm (b). Closed circles refer to the amplitude of the fundamental component; asterisks represent the amplitude of the second harmonic component. Only the fundamental component is shown at the lower spatial frequency; see text for details. The curve is the best-fit sinusoid to the data.

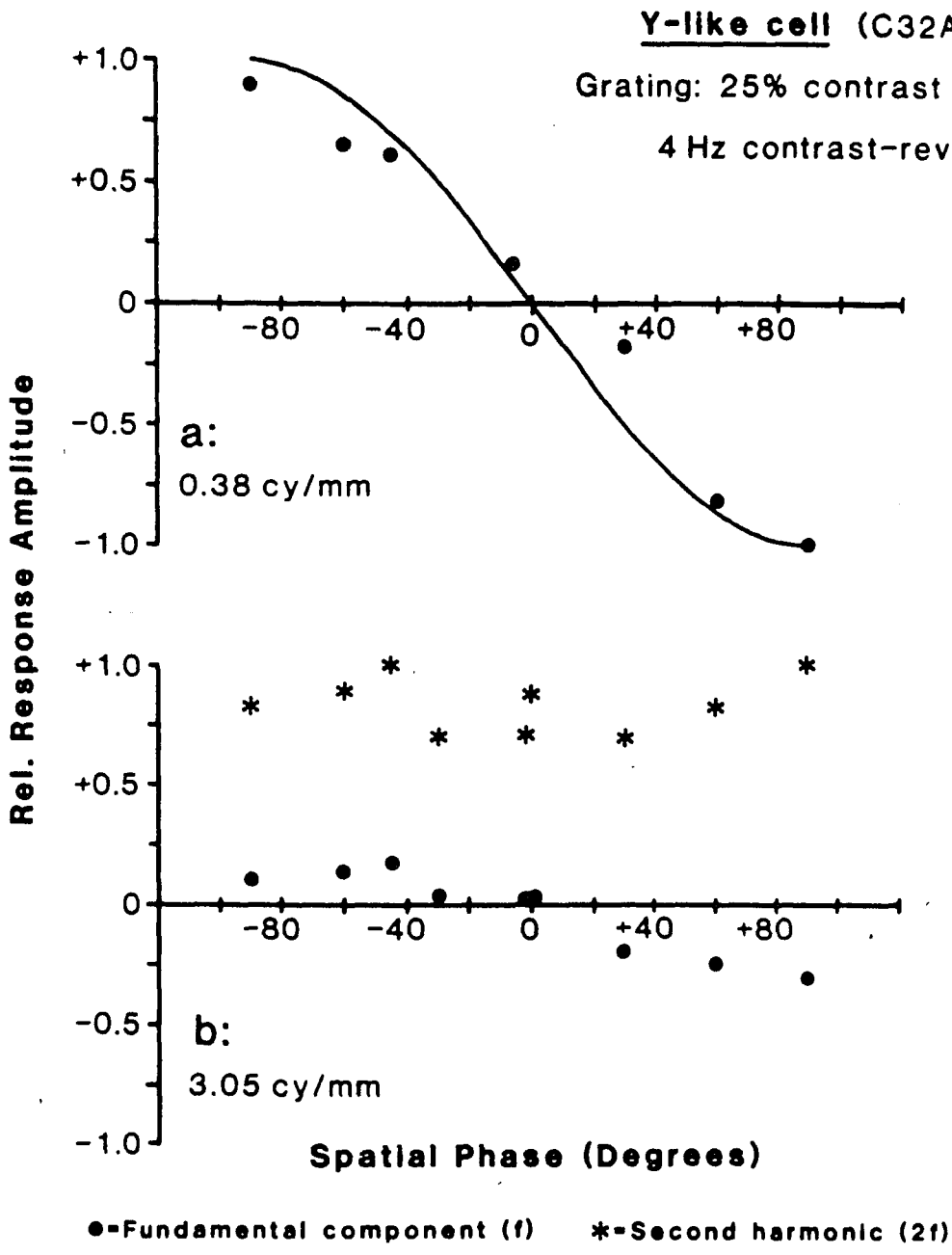
Y-like cell (C32A)
Grating: 25% contrast N: 37
4 Hz contrast-reversal
+1.0
+0.5
0
-0.5
-1.0
-80
-40
0
+40
+80
a:
0.38 cy/mm
b:
3.05 cy/mm
Rel. Response Amplitude
Spatial Phase (Degrees)
●=Fundamental component (f)
*=Second harmonic (2f)

mental and second harmonic components of the same cell as a function of spatial phase at a high spatial frequency (Figure 9b), and the fundamental amplitude as a function of spatial phase at a low spatial frequency (Figure 9a). Positive responses were again arbitrarily assigned to one side of the null position and negative responses to the other side. The curve represents the best fit sinusoid determined by the method described in Section 3.2.2. At high spatial frequencies (Figure 9b), the second harmonic component dominated the response. Note that the second harmonic response amplitude did not depend on the spatial phase of the stimulus. There was also no phase shift in the second harmonic component with spatial phase; hence all responses were arbitrarily designated as positive. The fundamental component, at high spatial frequencies was very weak, however, it was still a sinusoidal function of spatial phase.

At low spatial frequencies (Figure 9a), Y-like cells behaved like X-like cells. The fundamental component dominated the response, the cell possessed a null point, and the fundamental component amplitude was a sinusoidal function of spatial phase. The second harmonic component was not shown in this figure because its responses were somewhat distorted due to the fact that this cell had no spontaneous rate (see Section 3.2.1).

The 2f/f ratio varied as a function of the spatial frequency of the grating in Y-like cells. At low spatial frequencies, the ratio was less than one, however, as spatial frequency increased, so did the 2f/f ratio. At high spatial frequencies, this ratio typically reached values of two to three or even higher. Clearly, the mechanisms

responsible for the nonlinearities found in these Y-like cells were responsive only at high spatial frequencies. These findings were robust across different temporal frequencies and contrasts, including low contrasts.

3.2.4 W-like Cells.

Forty-six (37%) out of 126 cells were classified as W-like cells. Figure 10 illustrates a W-like cell's response to a contrast-reversal grating of 1.52 cy/mm. The stimulus was presented at 6% contrast, with a reversal rate of 4 Hz. The response of W-like cells to a contrast-reversal grating contained both fundamental and second harmonic components. At spatial phases well away from the null position the fundamental component dominated (Figures 10a, c). However, as the spatial phase of the grating approached a point midway between those extremes, a doubling of the response occurred, indicating domination by the second harmonic component (Figure 10b). This was due to the fact that the fundamental component was a function of spatial phase and the second harmonic was not. Figure 10d shows that the fundamental component was, again, a sinusoidal function of spatial phase; it also shows a relatively strong second harmonic component, compared to X-like cells, across all spatial phases. Once again, positive and negative responses were arbitrarily assigned and the curve represents the best fit sinusoid. The 2f/f ratio of W-like cells, unlike X- and Y-like cells, varied as a function of spatial phase. For example, at positions away from the null, the ratio was less than one, indicating that the fundamental component dominated; at positions

Figure 10

Averaged W-like cell responses to a contrast-reversal grating at various spatial positions on the receptive field. The stimulus consisted of a contrast-reversal grating of 1.52 cy/mm, at 6% contrast, and modulated at a rate of 4 Hz. The values above each figure (a, b, and c) refer to the position of the grating, in degrees, on the receptive field; zero degrees represents the best estimate of the midposition of the receptive field. The bottom illustration shows one complete contrast-reversal cycle of the stimulus. In (d), the relative response amplitudes of the Fourier components of a W-like cell to a contrast-reversal grating as a function of spatial phase are shown. Stimulus parameters were the same as in (a), (b), and (c). Closed circles refer to the amplitude of the fundamental component; asterisks represent the amplitude of the second harmonic component. The curve is the best-fit sinusoid to the data.

Spatial Summation

W-like cell (C27A)

Grating: 1.52 cy/mm 6% contrast

4 Hz contrast-reversal N: 37

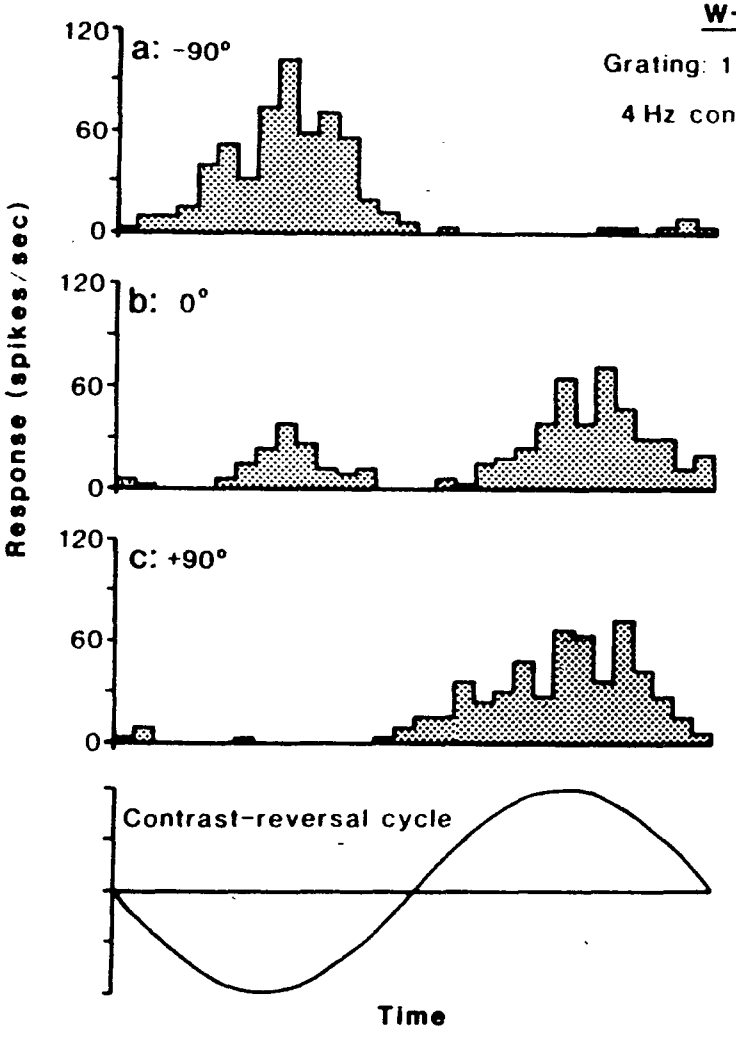

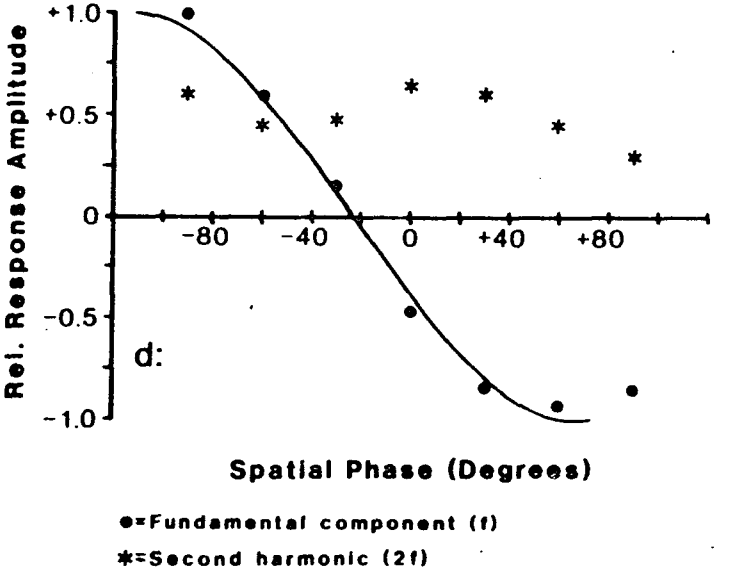

closer to the null position, the ratio became larger than one, suggesting that the second harmonic component was larger. This becomes apparent when comparing the graphs in Figure 10; away from the null (Figures 10a, c), the responses appear X-like, but closer to the null, the responses mimic Y-like cells (Figure 10b). However, the value of the 2f/f ratio was never as high as in Y-like cells. The general response characteristics of most W-like cells were independent of spatial frequency, temporal frequency and contrast. That is, whatever mechanism is responsible for the nonlinear response was not the same as Y-like cells, since Y-like cells behaved linearly at low spatial frequencies and W-like cells did not.

3.3 Spatial and Temporal Contrast Sensitivity Functions.

To derive S-CSFs, sinusoidal gratings were drifted across the receptive field of a ganglion cell at a constant temporal frequency. The drift rate provided the temporal modulation of the responses. For the majority of the cells isolated, a drift rate of 4 Hz was used to derive the S-CSF. With rare exceptions, cells were quite responsive to this temporal rate. It was important to use the same drift rate for all the cells, since average S-CSFs were calculated (see Section 3.5). When possible, different drift rates were also presented to a cell to examine the role of spatio-temporal interactions on the shape of the S-CSF. The sensitivity at each spatial frequency was derived by interpolation on the response vs. contrast curves to find the contrast for a constant response amplitude. This method of deriving sensitivity was also used to derive the T-CSF.

3.3.1 X-like Cells.

Since X-like cells are linear, the response measure was the amplitude of the fundamental component. Figure 11 shows a typical S-CSF from an X-like cell. The stimulus grating was drifted at a rate of 4 Hz. The shape of the S-CSF was similar to those obtained in other species; there was the sharp high frequency drop as well as the low frequency attenuation believed to be due to lateral inhibition within the receptive field of the cell (Ratliff, 1965).

To further illustrate the linearity of an X-like cell's response, the fundamental component of the response vs. contrast for the same cell in Figure 11 is presented in Figure 12 at several spatial frequencies. The values at zero contrast represent the fundamental component amplitude to a "dummy" stimulus; that is, a stimulus with no modulation around mean luminance. This was a measure of the cell's spontaneous rate.

The S-CSFs obtained from the single neurons are qualitatively similar to the psychophysical S-CSF of the goldfish (Northmore and Dvorak, 1979). The peak of the psychophysical S-CSF is at about 0.3 cy/deg and the acuity limit, or high frequency cut-off, is between 1 and 2 cy/deg. To compare the neuron's S-CSF to the psychophysical function, cycles per millimeter on the retina were converted to cycles per degree, using measurements obtained from the schematic eye of the goldfish (Charman and Tucker, 1973). The appropriate conversion value is about 19 deg/mm (see Appendix). Extrapolating from the cell's S-CSF, the acuity limit is between 12 and 20 cy/mm. This converts to between 0.6 and 1.0 cy/deg which

Figure 11

S-CSF of an X-like cell. The response measure was the amplitude of the fundamental component. The stimulus consisted of a 4 Hz drifting grating. Sensitivity was obtained by interpolation on the response vs. contrast curves to find the contrast necessary for a constant response amplitude.

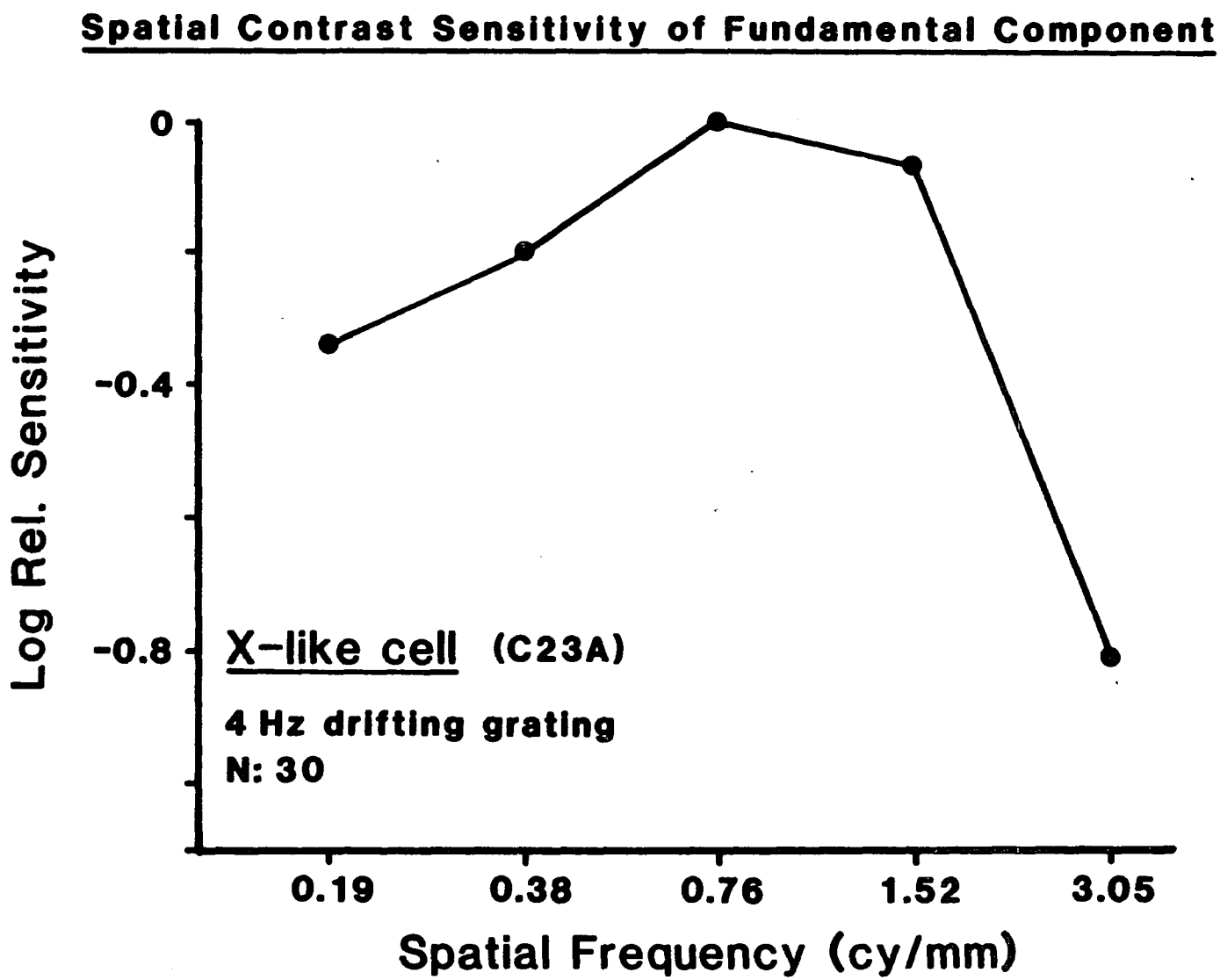
Spatial Contrast Sensitivity of Fundamental Component
0
-0.4
-0.8
Log Rel. Sensitivity
X-like cell (C23A)
4 Hz drifting grating
N: 30
0.19
0.38
0.76
1.52
3.05
Spatial Frequency (cy/mm)

Figure 12

Response vs. contrast curves of an X-like cell at several spatial frequencies. The response measure was the amplitude of the fundamental component. The stimulus consisted of a 4 Hz drifting grating. The value above each figure refers to the spatial frequency of the stimulus grating. The dotted line in each figure represents the amplitude of the fundamental component when a grating of zero contrast was presented; thus, it is a measure of the spontaneous rate of the cell.

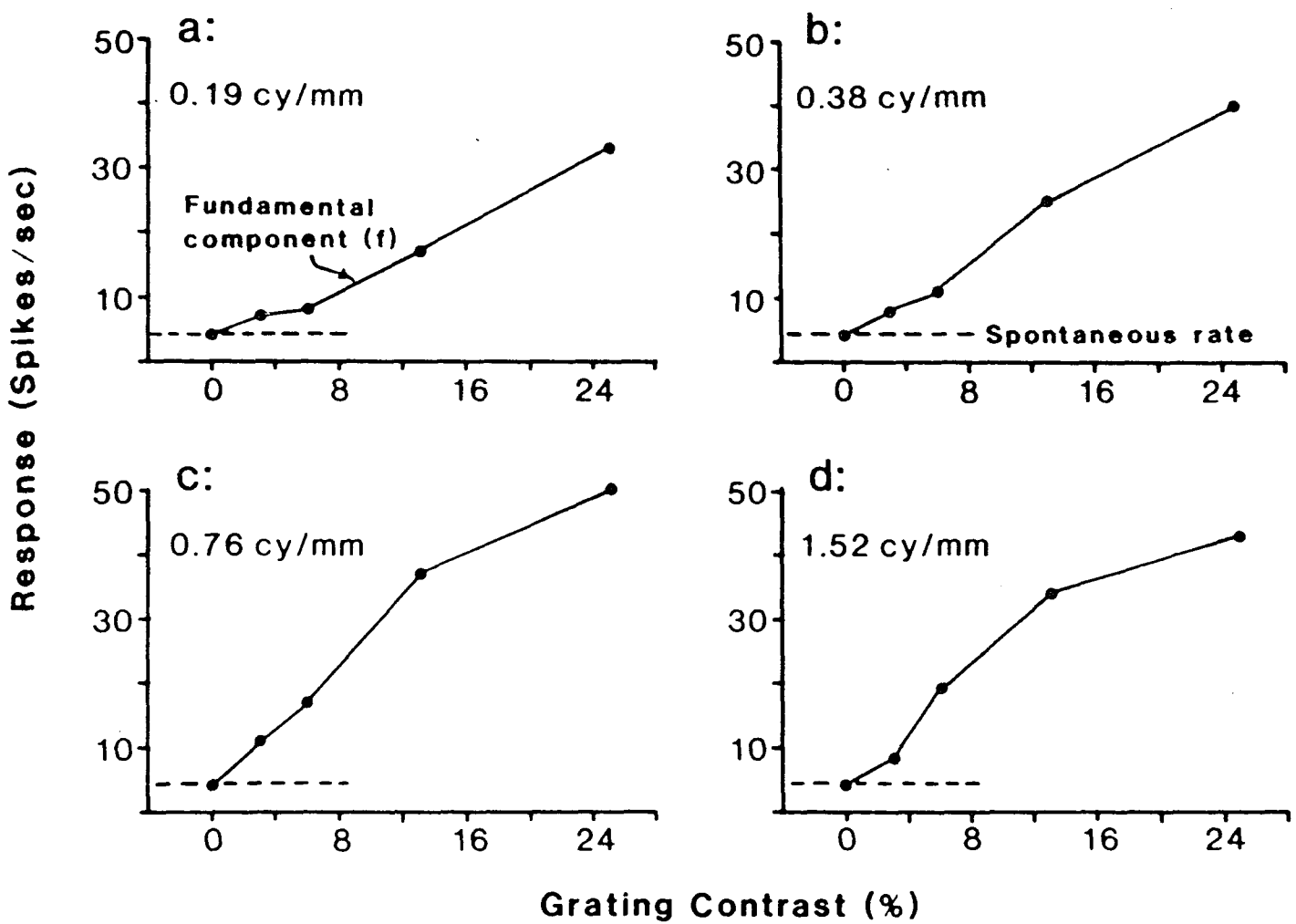
X-like cell (C23A) 4 Hz drifting grating N: 30
a:
0.19 cy/mm
Fundamental component (f)
b:
0.38 cy/mm
Spontaneous rate
c:
0.76 cy/mm
d:
1.52 cy/mm
50
30
10
0
8
16
24
Response (Spikes/sec)
Grating Contrast (%)

is close to the behavioral limit. However, the peak of the cell's S-CSF is at about 0.8 cy/mm which converts to 0.04 cy/deg, well below the behavioral peak.

Since X-like cells are linear up to moderate contrasts, their responses can be used directly as measures of sensitivity -- it is not necessary to interpolate on response vs. contrast curves functions. Figure 13 shows the S-CSFs of several X-like cells obtained at a drift rate of 4 Hz. The contrasts for each cell are indicated in the figure. To be strictly correct, since these functions were derived directly from the response measure (in this case, the fundamental amplitude), the ordinate was designated as log relative 'response' rather than 'sensitivity'. These cells were all similar in the high frequency portion of the S-CSF; however, two of the cells (Figures 13b, d) did not appear to possess any low frequency attenuation as in the other cells. It is worth noting that these two cells did not possess a surround mechanism; that is, they were spatially nonopponent. This supports the notion that the low frequency attenuation found in neurons is a result of an antagonistic interaction between the center and surround portions of the receptive field (Enroth-Cugell and Robson, 1984).

To test this hypothesis, S-CSFs were obtained separately from the center and surround mechanisms and from the entire receptive field by restricting the drifting grating to one portion of the receptive field while maintaining the same mean luminance across the remaining portion of the field. It should be mentioned that restricting the stimulus pattern to the middle portion of the receptive field does not eliminate the influence of the surround component since the

Figure 13

S-CSFs of several X-like cells. The response measure for each cell was the amplitude of the fundamental component. In all cases, the stimulus consisted of a 4 Hz drifting grating. The contrast at which each function was obtained is given at the bottom of each figure.

Spatial Contrast Sensitivity of Fundamental Component

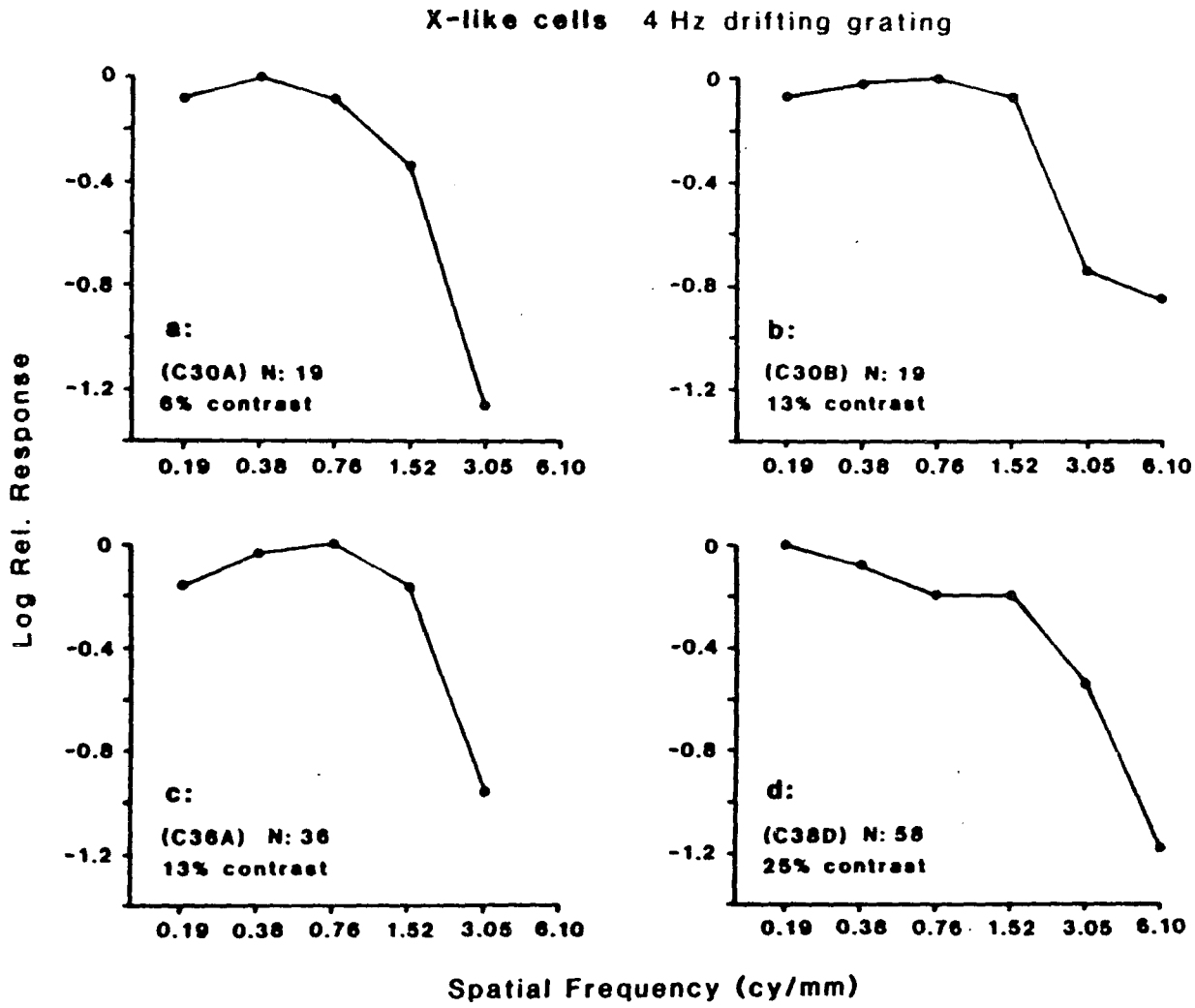

surround overlaps with the center in the middle portion of the receptive field. The intentions of this restricted pattern were to minimize the influence of one component while examining the other. A similar argument can be made for restricting the pattern to the outer, surround portion. Typical results are shown in Figure 14. The full field S-CSF was obtained by presenting the drifting gratings across the entire receptive field (7.5 mm circular aperture). The center mechanism's S-CSF for this cell was determined with the drifting grating confined to a 1 mm x 1 mm square centered on the receptive field. For the surround S-CSF, the gratings were restricted to the surrounding portion of the full aperture while the 1 mm x 1 mm center square was held at mean luminance. The drift rate for all S-CSFs was 4 Hz, and the response measure was the fundamental amplitude. All sensitivity values were normalized with respect to one maximum value. Therefore, displacement of the S-CSFs on the ordinate reflect differences in sensitivity. (For example, the surround mechanism is appoximately 1 log unit less sensitive than the center mechanism in Figure 14.) As can be seen in Figure 14, the center's sensitivity at high spatial frequencies closely matched the sensitivity of the entire receptive field suggesting that the center mechanism alone was responsible for the high frequency portion of the cell's overall S-CSF. However, the surround mechanism's sensitivity was much lower at these frequencies and probably contributed little to the response to full field stimulation. This would be expected from the larger area of the surround. At low spatial frequencies, the center and full field values became disparate in that the center was more

Figure 14

S-CSFs of an X-like cell's receptive field components. The response measure in each case was the amplitude of the fundamental component. The stimulus consisted of a 4 Hz drifting grating. Sensitivity was obtained by interpolation on the response vs. contrast curves to find the contrast necessary for a constant response amplitude. Each sensitivity value was normalized with respect to one maximum value. Closed circles represent the response of the entire receptive field. Open stars refer to the response to a grating restricted to a 1 mm by 1 mm square centered on the receptive field; enclosed stars represent the response of the cell to a grating restricted to the surrounding portion of the full aperture. In all cases, the portion of the receptive field not stimulated by the grating was maintained at mean luminance.

Spatial Contrast Sensitivity

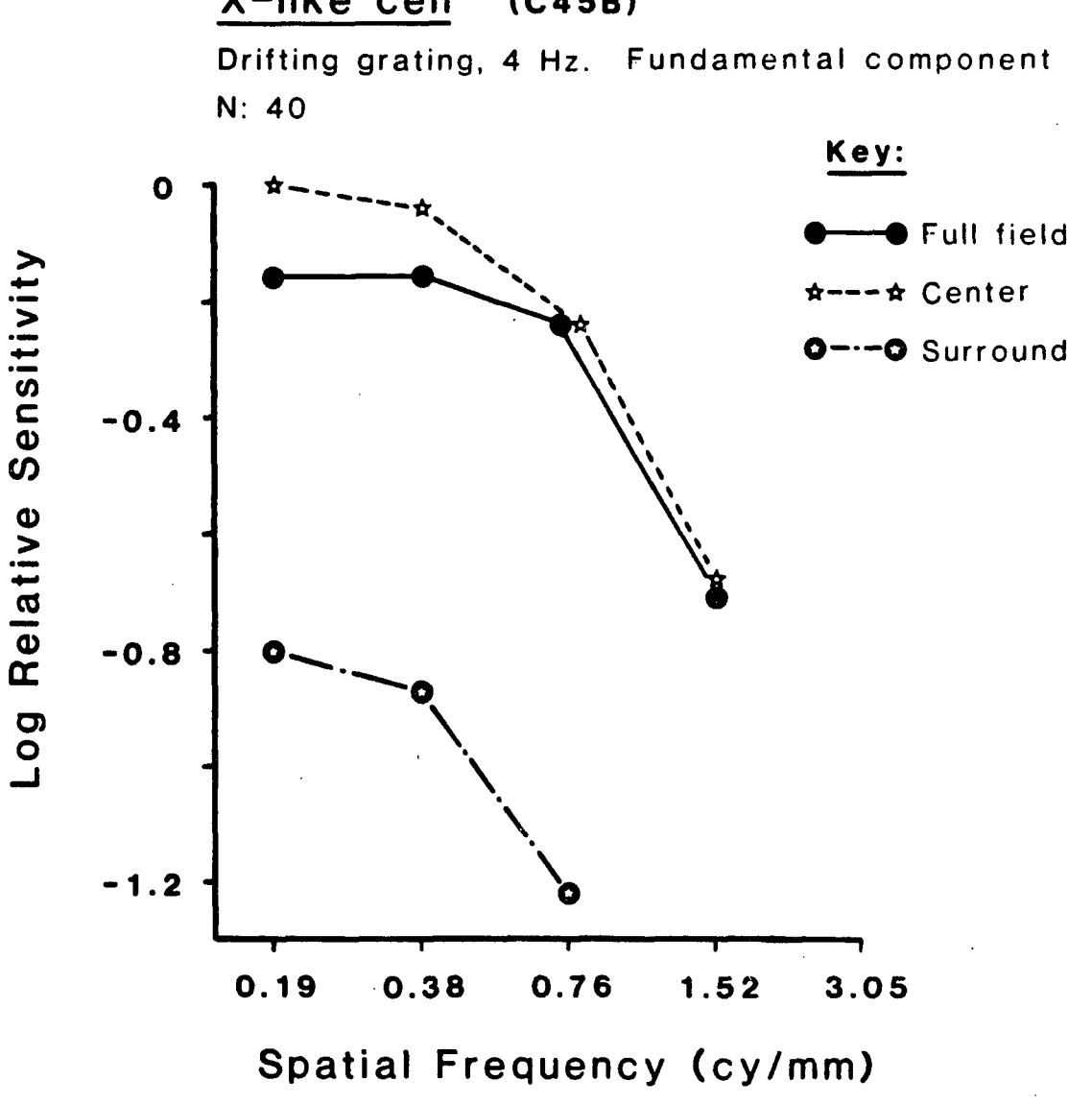

sensitive than the full field. At low spatial frequencies, the surround contributes to the response to full field stimulation, and since, in most cases, the center and surround mechanisms are antagonistic, the result is that the center response is "pulled down" by the antagonistic surround when the entire receptive field is stimulated. This was certainly the case for the cell in Figure 14 since the fundamental components of the center and surround mechanisms were 180 degrees out of phase. However, as suggested by the large displacement of the surround's S-CSF, the spatial opponency of this cell was relatively weak, and the influence of the surround was minor compared to other cells. In cells with strong spatial opponency, the full field S-CSF had a more apparent low frequency attenuation.

As discussed earlier, the S-CSF of a ganglion cell is not separable from its T-CSF. That is, the shape of the S-CSF depends on the stimulus grating's drift rate. To examine this phenomenon in goldfish ganglion cells, S-CSFs were derived at different drift rates. The results are shown in Figure 15. S-CSFs were obtained for drift rates of 1, 4 and 8 Hz at 13% contrast and all values were normalized with respect to one maximum value. The shape of the S-CSF depended on the drift rate, but only at low spatial frequencies. At high spatial frequencies, the three functions were very similar; the curves deviated only at the lower frequencies. At the lower drift rates of 1 and 4 Hz, there was strong low frequency attenuation. However, at the higher drift rate of 8 Hz, low frequency attenuation was less. Since low frequency attenuation disappears at the high drift rate, it is possible that the surround mechanism is either unable to respond to or

Figure 15

S-CSFs of an X-like cell at different stimulus drift rates. The response measure was the amplitude of the fundamental component. The stimuli consisted of a drifting grating at 1 Hz (closed triangles), 4 Hz (closed hexagons), and 8 Hz (open hexagons), at 13% contrast. Each value was normalized with respect to one maximum value.

Spatial Contrast Sensitivity

X-like cell (B99B) Drifting grating, 13% contrast.

Amplitude of Fundamental Component N: 20.

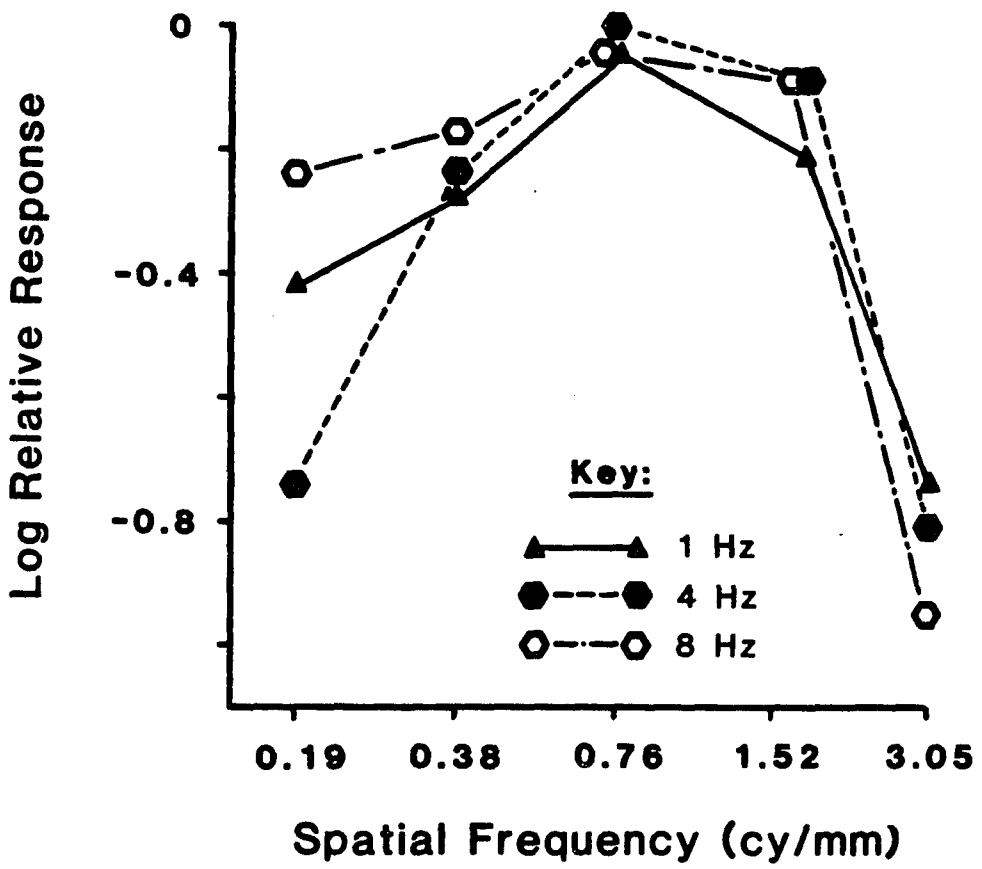

follow these frequencies, or that the center and surround components are no longer antagonistic to one another. Although there were differences at low spatial frequencies, the relative sensitivities of the different S-CSFs were quite similar. This suggests that this cell probably had a broad temporal tuning.

A typical T-CSF of an X-like cell is shown in Figure 16. The T-CSF was obtained by presenting a uniform field which varied sinusoidally in intensity. This was presented at different temporal frequencies and contrasts; sensitivity was calculated by interpolation on the amplitude of the fundamental response component vs. contrast curves, as described earlier for S-CSFs. At low temporal frequencies, the cell was relatively insensitive; however, at frequencies between 2 to 8 Hz the cell was quite responsive with a peak sensitivity at about 4 Hz.

To examine the center and surround interactions in more detail, T-CSFs from the entire field as well as from the center and surround separately were obtained. Figure 17 shows the results. The response measure was the amplitude of the fundamental component and the stimulus consisted of a uniform field which varied sinusoidally in intensity at 25% contrast. All values were normalized with respect to one maximum value. The center T-CSF was derived with the stimulus restricted to a 1 mm by 1 mm square; for the surround T-CSF, the stimulus was restricted to the surrounding portion of the full field stimulus with a center square maintained at mean luminance. The full field was a 7.5 mm diameter circular aperture. Several points are worth mentioning regarding the T-CSFs (Figure 17a). At low tempo-

Figure 16

T-CSF of an X-like cell. The response measure was the amplitude of the fundamental component. The stimuli consisted of a uniform field which varied sinsoidally in intensity. Sensitivity was obtained by interpolation on the response vs. contrast curves to find the contrast necessary for a constant response amplitude.

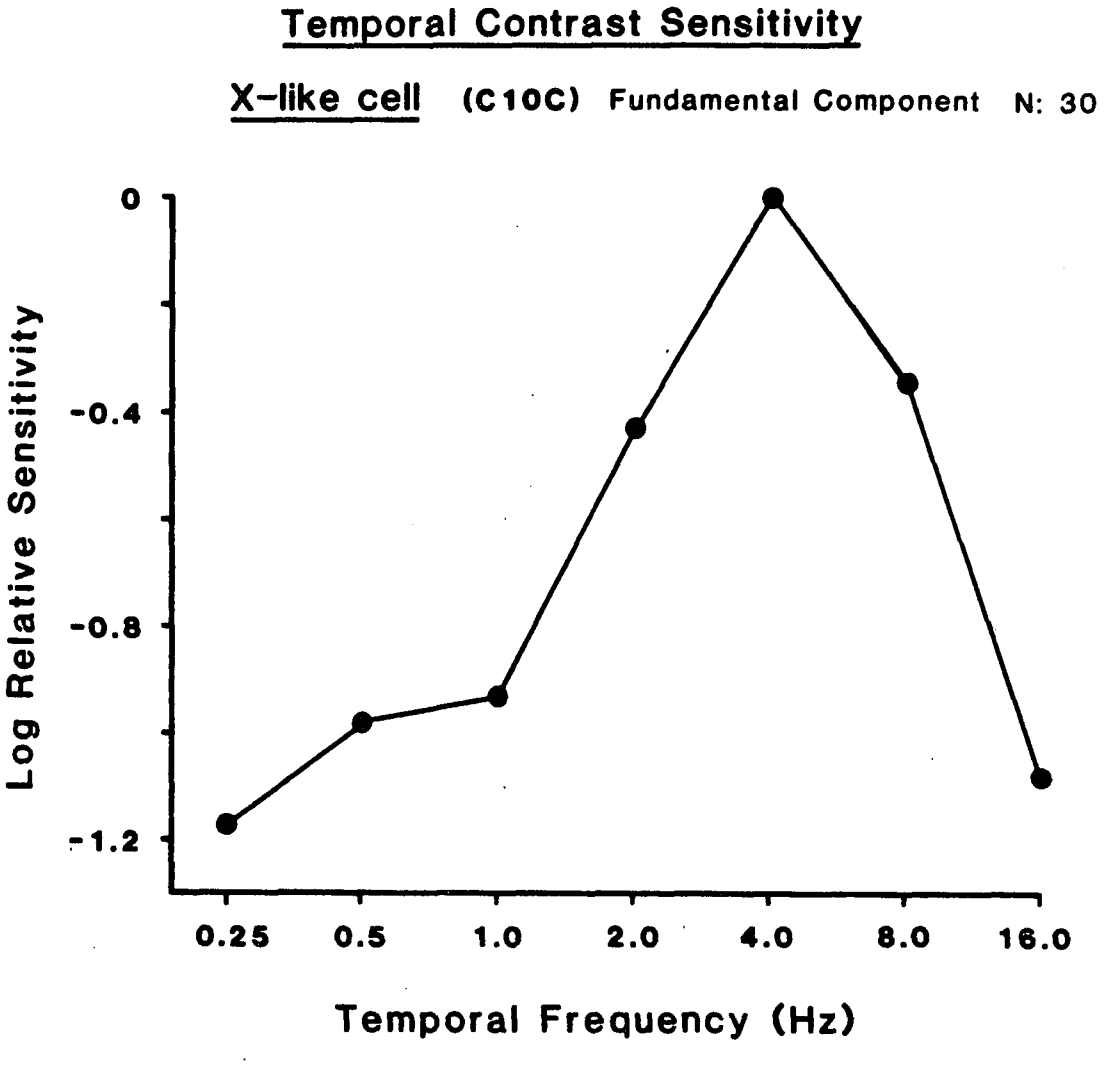
Temporal Contrast Sensitivity
X-like cell (C10C) Fundamental Component N: 30
0
-0.4
-0.8
-1.2
Log Relative Sensitivity
0.25
0.5
1.0
2.0
4.0
8.0
16.0
Temporal Frequency (Hz)

Figure 17

(a) T-CSFs of the center (open stars), surround (enclosed stars), and full field (closed circles) of an X-like cell. The response measure was the amplitude of the fundamental component; the stimulus consisted of a uniform field which varied sinusoidally in intensity. The contrast for each stimulus was 25 percent. All response values were normalized with respect to one maximum value. See text for details. (b) Fundamental component phase differences between center and surround components.

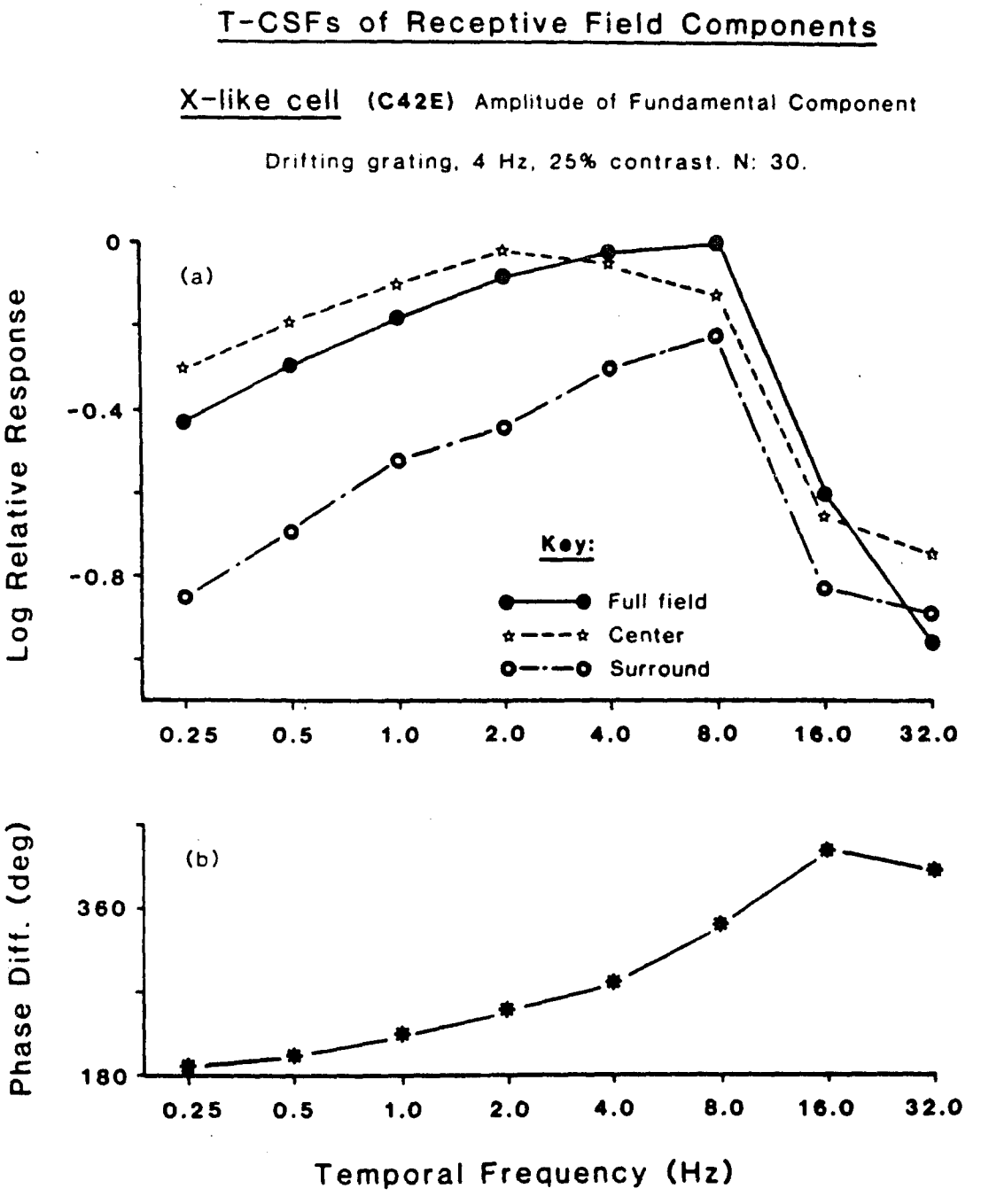
T-CSFs of Receptive Field Components
X-like cell (C42E) Amplitude of Fundamental Component
Drifting grating, 4 Hz, 25% contrast. N: 30.
(a)
0
-0.4
-0.8
Log Relative Response
Key:
Full field
Center
Surround
0.25
0.5
1.0
2.0
4.0
8.0
16.0
32.0
(b)
360
180
Phase Diff. (deg)
Temporal Frequency (Hz)

ral frequencies, the center and the full field values are similar while the surround values are much lower in sensitivity, suggesting that the center contributes more to the full field T-CSF. Also, the center is relatively more sensitive than the full field at low temporal frequencies, which suggests that there must be antagonism between the center and surround components. However, as temporal frequency increases, the center and full field values become disparate; at the same time, the sensitivity of the surround increases, and peaks at a higher temporal frequency than the center component (8 Hz). Thus, the surround is quite sensitive at high temporal frequencies, and in fact, appears to be as sensitive as the center portion at high frequencies. Also, at a temporal frequency of 8 Hz, the full field T-CSF is more sensitive than either the center of surround alone suggesting not only that there is no center and surround antagonism, but that these components must be synergistic.

This can be explained by comparing the fundamental component phase differences of the center and surround responses as in Figure 17b. At low temporal frequencies, the phases of the center and surround values are about 180 degrees out-of-phase -- thus, at these frequencies, the center and surround are antagonistic. However, as the temporal frequency of the stimulus increases, the phases of the center and surround components also change but at different rates. At 8 Hz the phases between the center and surround are similar and are now, in-phase. Thus, at 8 Hz, the center and surround components are actually synergistic and their interaction enhances sensitivity.

3.3.2 Y-like Cells.

In general, Y-like cells were much easier to isolate and record from than X-like cells. Also, isolation tended to be better maintained over longer periods of time. Perhaps, like in the cat retina (Boycott and Wassle, 1974), goldfish Y-like cells have larger cell bodies making them easier to isolate and maintain. Although there has been no correlation between spatial summation properties and anatomy in the goldfish retina, there is evidence of at least three distinct anatomical classes of ganglion cells in the goldfish retina (Hitchcock and Easter, 1984).

Since Y-like cells, by definition, are nonlinear, the amplitude of the fundamental component was not appropriate as a response measure. Three different response measures were used for Y-like cells. The fundamental response component was used to examine any linear mechanisms of the cell. This also allowed a direct comparison with X-like cells to examine whether the linear components of the Y-like cells were similar to those of X-like cells. Because there is a strong second harmonic component in Y-like cells when a contrast-reversal grating is presented, the amplitude of the second harmonic component was also examined for Y-like cells. This would provide some information concerning the nonlinearities contained in Y-like cells. A third response measure was the maximum response bin minus the minimum response bin of the stimulus cycle (max-min), or in others words, the peak-to-peak value of the averaged response. This was used as an overall measure of the cell's response, including the responses of the small nonlinear subunits like those found in Y-cells of the cat retina.

This response measure was chosen over the maximum response for several reasons. The first was that the maximum response by itself represents only one portion of the entire averaged response. Therefore, this measure would be very susceptible to random fluctuations in the response. For example, some cells had a firing pattern in which the action potentials fired in groups or multiples. This "burstiness" could have affected the maximum response measure. While the max-min response is not much better, it does represent two values of the averaged response cycle instead of just one. A more important reason for using the max-min response has to do with the variability of the cell's spontaneous rate over time. Since cells could be isolated for up to six hours, the spontaneous rate could fluctuate due to cell adjustments and, more importantly, for changes due to different adaptation levels, such as changes in mean luminance or chromatic adaptation. Any change in the spontaneous rate would affect primarily the maximum response, but not the max-min response. When cells were re-examined with the same stimuli hours later, there might be dramatic differences in the maximum response measure but not in the max-min.

Finally, since Y-like cells are nonlinear, all spatial and temporal CSFs were derived by interpolation from the response vs. contrast curves. No CSFs were obtained directly from the response measures even when the response was well within the linear response range.

Figure 18 compares a Y-like cell's S-CSF based on the fundamental component of the response and the max-min response. The drift rate of the grating was 4 Hz. The sensitivity values of the funda-

Figure 18

S-CSF of a Y-like cell. The response measures were the amplitude of the fundamental component (closed circles) and the maximum response minus the minimum response (open circles). The stimulus consisted of a 4 Hz drifting grating. Sensitivity was obtained by interpolation on the response vs. contrast curves to find the contrast necessary for a constant response amplitude.

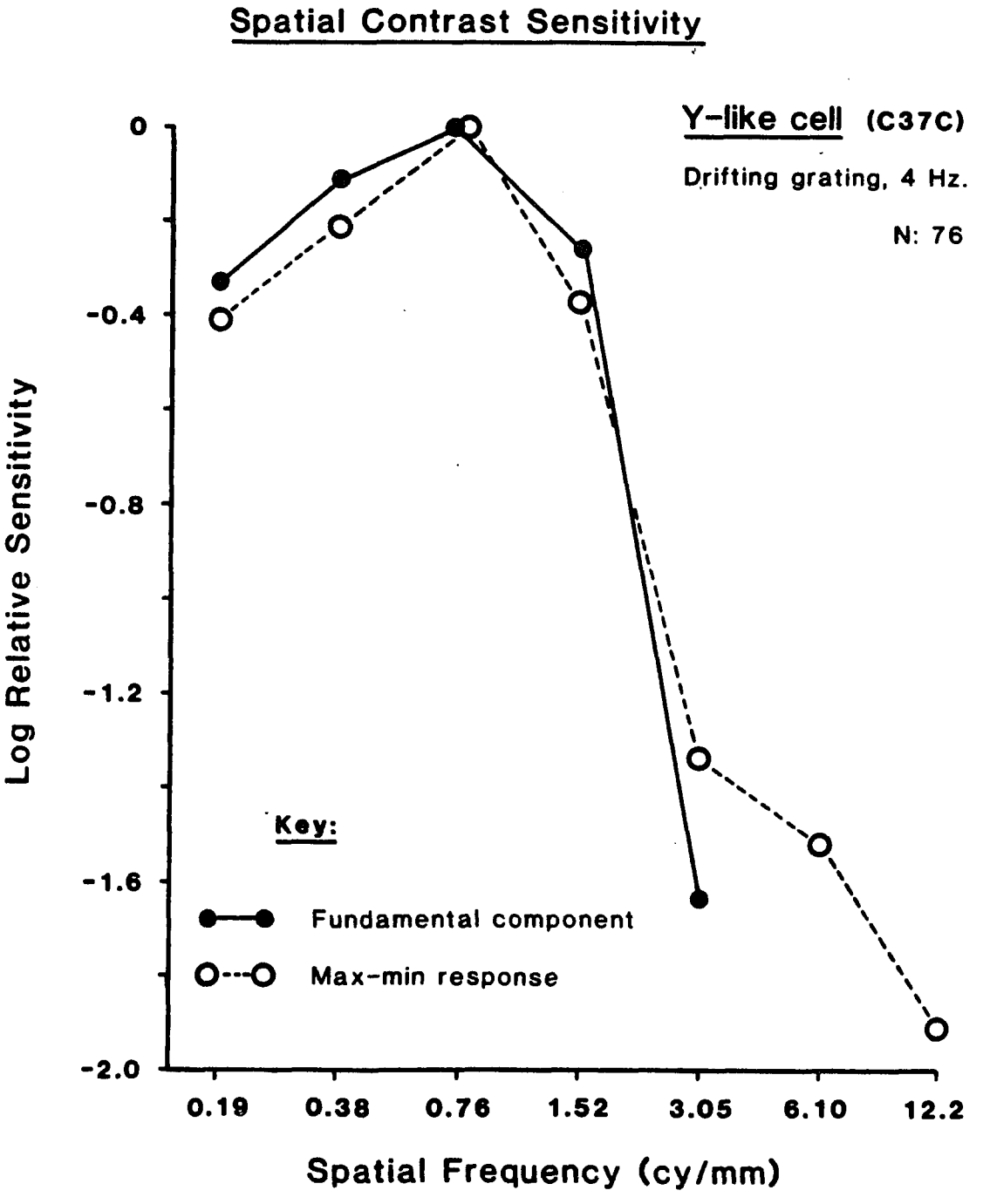
Spatial Contrast Sensitivity
Y-like cell (C37C)
Drifting grating, 4 Hz.
N: 76
Log Relative Sensitivity
0
-0.4
-0.8
-1.2
-1.6
-2.0
Key:
Fundamental component
Max-min response
0.19
0.38
0.76
1.52
3.05
6.10
12.2
Spatial Frequency (cy/mm)

mental component and the max-min response were similar at low to moderate spatial frequencies, but the curves became disparate at high spatial frequencies. At high frequencies, the fundamental component was relatively insensitive to gratings higher than 3.05 cy/mm, whereas the max-min response was still sensitive. The differences, no doubt, reflect the presence of the small nonlinear subunits similar to those found in cat Y-cells. This figure also supports the notion that the fundamental component of Y-like cells reflects the same mechanisms as those of X-like cells, at least at low to moderate spatial frequencies, since the function was similar to the S-CSF found in X-like cells. That is, the fundamental component of both X- and Y-like cells were the result of a simple interaction of the responses of the center and surround mechanisms of the receptive field.

However, unlike Y-cells in the cat, the nonlinear subunits provided more than just an elevated discharge to the overall response. There appeared to be a slight "doubling" of response when these subunits were activated. Figure 19 compares the S-CSFs of the fundamental and second harmonic components of another Y-like cell. The drift rate of the stimulus was 4 Hz and the two curves were normalized with respect to one maximum value. At the lower spatial frequencies, although the relative sensitivities differ, the fundamental and second harmonic values were similiar in shape. This was probably due to the fact that the second harmonic component was the result of the cell's response being distorted by the overdriving of the response to zero. However, the curves become disparate at 6.10 cy/mm where the second harmonic component clearly dominated the

Figure 19

S-CSFs of a Y-like cell based on the first two Fourier components. The response measures were the amplitude of the fundamental component (closed circles) and the amplitude of the second harmonic component (asterisks). The stimulus consisted of a 4 Hz drifting grating. Sensitivity was obtained by interpolation on the response vs. contrast curves to find the contrast necessary for a constant response amplitude. Each sensitivity value was normalized with respect to one maximum value.

Spatial Contrast Sensitivity

Y-like cell (C49A) Drifting grating, 4 Hz. N: 20.

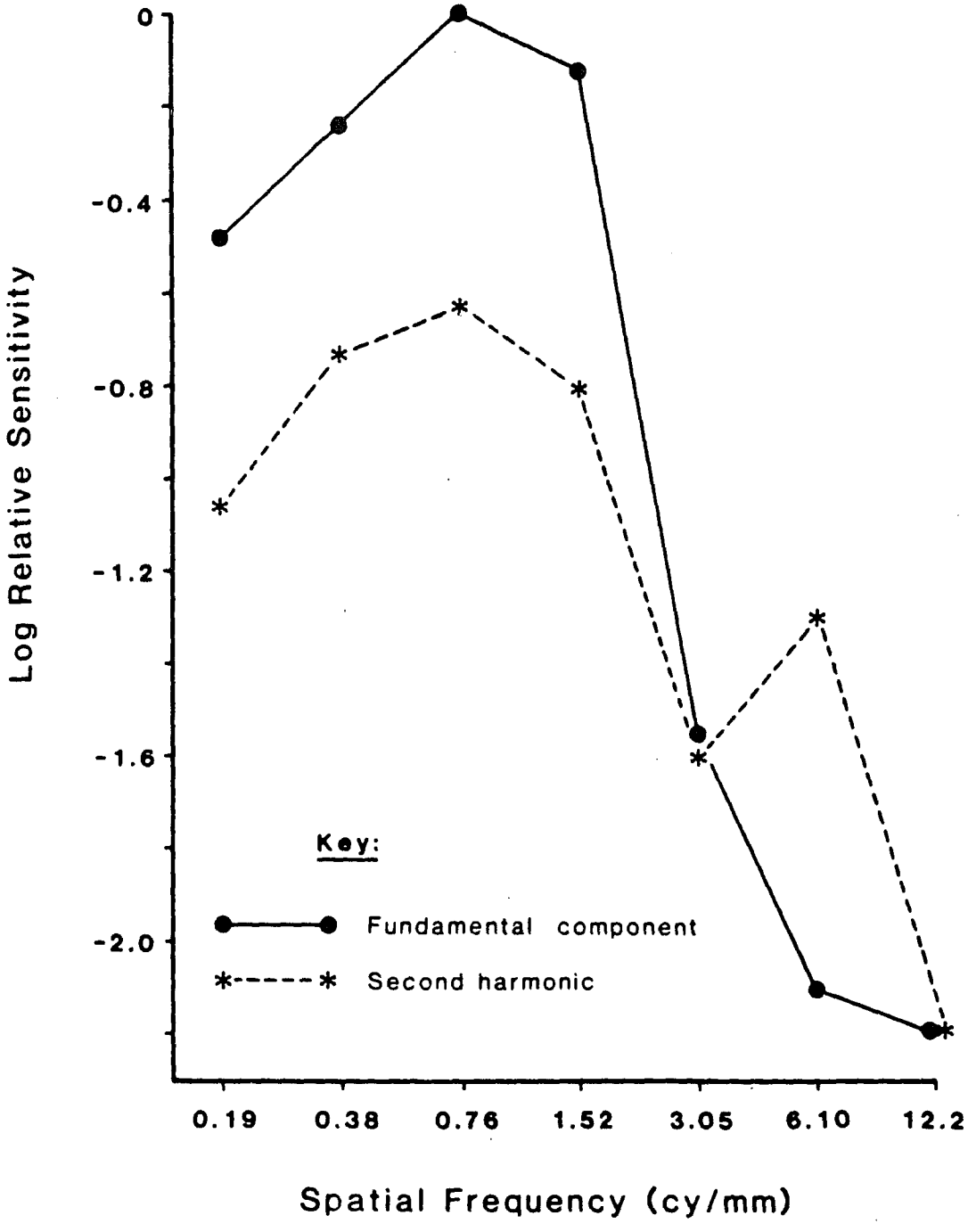

response. This increase in sensitivity, at such a high spatial frequency, must be due to the small, nonlinear subunits.

Most X- and Y-like S-CSFs were similar in shape; they possessed relatively broad-band tuning along the spatial domain. However, there were Y-like cells that displayed much more narrowly tuned functions. Figure 20 shows one of these Y-cells. The response measure was the fundamental amplitude and the drift rate was 4 Hz. This cell was insensitive to very low spatial frequencies and peaked at a spatial frequency about three octaves higher than most cells. This narrow tuning was not the result of a particular drift rate since this cell was examined at several drift rates with no dramatic change in the S-CSF.

To examine the influence of the center and surround mechanisms on the overall Y-like cell S-CSF, S-CSFs were obtained using drifting gratings restricted to the center (1 mm x 1 mm square), surround (annular portion of the entire aperture) as well as the full field (7.5 mm circular aperture). Figure 21 displays the results from three Y-like cells. The response measure was the fundamental component, the drift rate was 4 Hz, and the mean luminance was the same for all mechanisms. All values in Figures 21a and 21b were normalized with respect to one maximum value. In Figure 21c, the center and surround values were normalized with respect to each other; the full field values were normalized separately. This was done because the center and surround data were collected near the end of the recording session approximately three hours after the full field data were collected. Thus, there was a slight decrease in absolute sensitivity

Figure 20

S-CSF of a sharply-tuned Y-like cell. The response measure was the amplitude of the fundamental component. The stimulus consisted of a 4 Hz drifting grating. Sensitivity was obtained by interpolation on the response vs. contrast curves to find the contrast necessary for a constant response amplitude.

Spatial Contrast Sensitivity

Y-like cell (C02E) Amplitude of Fundamental Component

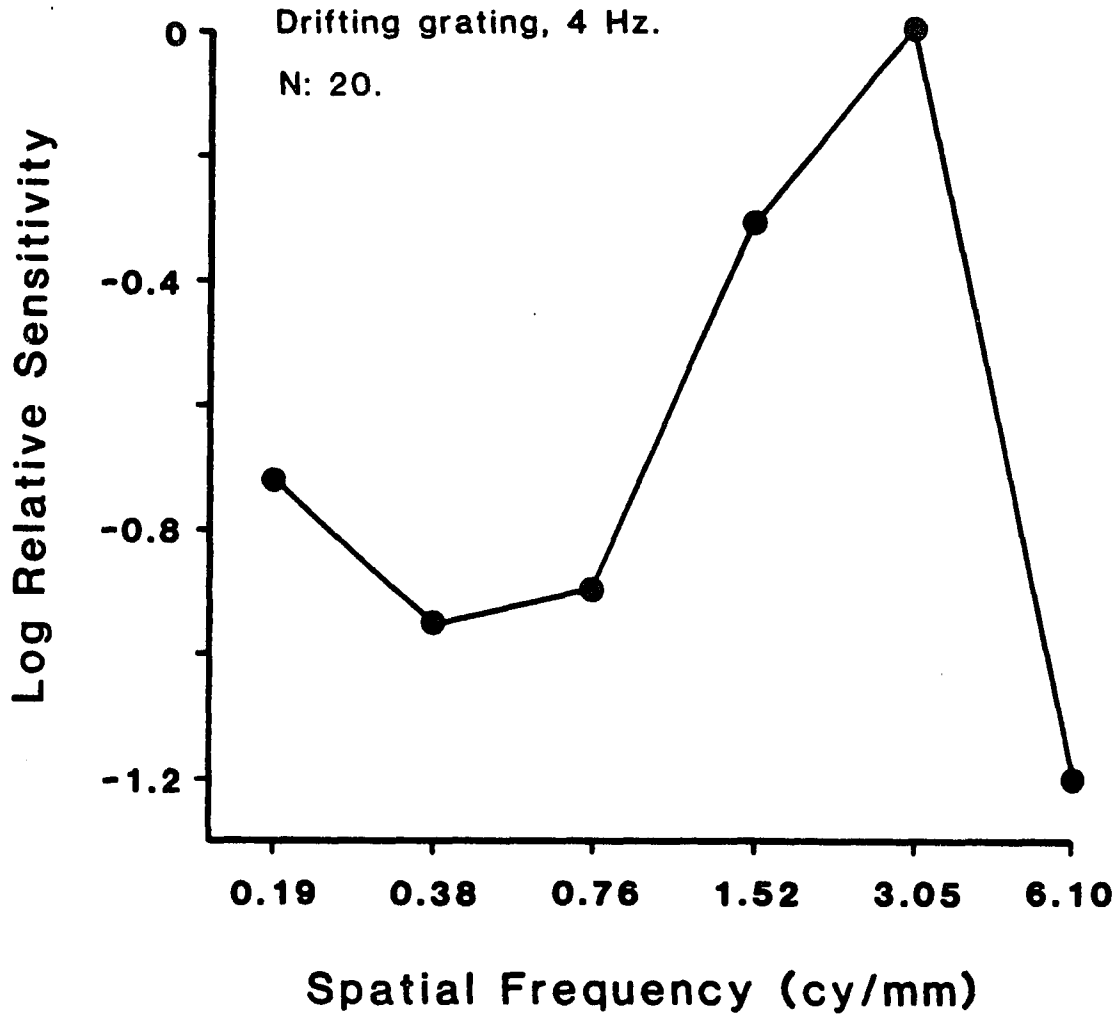

Figure 21

S-CSFs of three Y-like cells' receptive field components. The response measure was the amplitude of the fundamental component. The stimulus consisted of a 4 Hz drifting grating. Sensitivity was obtained by interpolation on the response vs. contrast curves to find the contrast necessary for a constant response amplitude. Closed circles represent the response of the entire receptive field. Open stars represent the responses to a grating restricted to a 1 mm by 1 mm square centered on the receptive field; enclosed stars refer to responses of the cell to a grating restricted to the surrounding portion of the full aperture. In all cases, the portion of the receptive field not stimulated by the grating was maintained at mean luminance. All sensitivity values in (a) and (b) were normalized with respect to one maximum value; in (c), the center and surround values were normalized together but the full field values were normalized separately (see text for details).

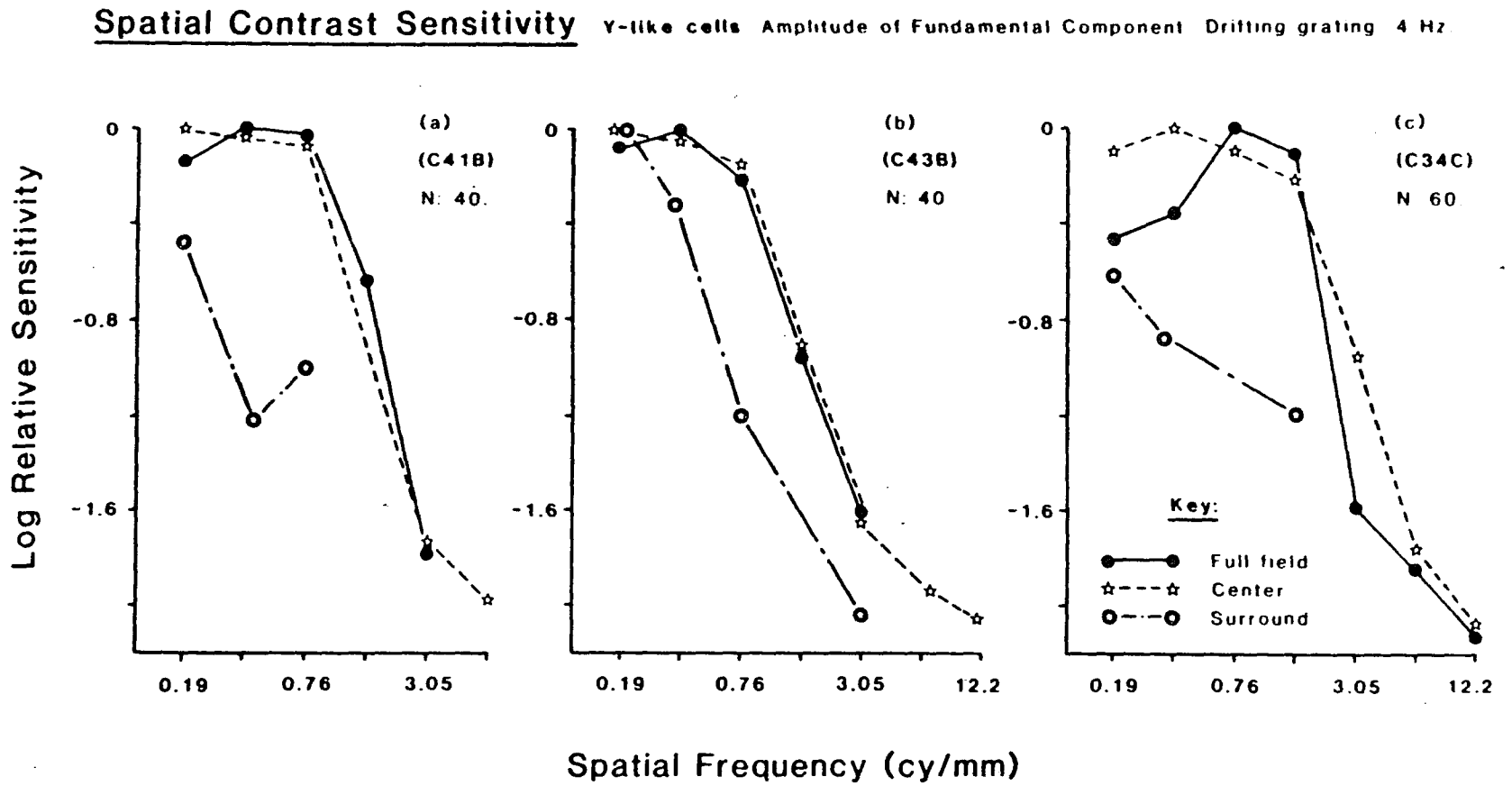
Spatial Contrast Sensitivity
Y-like cells Amplitude of Fundamental Component Drifting grating 4 Hz
Log Relative Sensitivity
0
-0.8
-1.6
(a)
(C41B)
N: 40.
(b)
(C43B)
N: 40
(c)
(C34C)
N 60
0.19
0.76
3.05
12.2
Key:
Full field
Center
Surround
Spatial Frequency (cy/mm)

in the latter functions. As in X-like cells, functions of the center and full field agreed at high spatial frequencies, indicating that the full field response at high spatial frequencies resulted from the center mechanism only, since the surround function was insensitive at these high frequencies. The functions of the center and surround stimulated alone had no low frequency attenuation, but the full field S-CSF did possess a slight attenuation at the lower frequencies. The low frequency attenuation was most apparent where the surround was most sensitive. In Figures 21a and 21c, the center and surround fundamental components were approximately 180 degrees out-of-phase with one another at low spatial frequencies. However, in Figure 21b, the phase of the fundamental component for the center and surround mechanisms were not 180 degrees out-of-phase but approximately 135 degrees at the lower spatial frequencies. Thus, the two mechanisms are not completely antagonistic nor synergistic. This could explain why there was little low spatial frequency attenuation for the full field function even though the center and surround were equally sensitive at these frequencies.

Like X-like cells, the shape of the Y-like cells' S-CSF depended on the drift rate of the stimulus grating. Figure 22 shows the S-CSF of a Y-like cell at different drift rates. The response measure for these functions was the amplitude of the fundamental component and all values were normalized with respect to one maximum value. The high frequency portion of the S-CSF was relatively unaffected by changes in the stimulus' drift rate. It was only at low spatial frequencies and high temporal frequencies (16 Hz) that there was any

Figure 22

S-CSFs of a Y-like cell at different stimulus drift rates. The response measure was the amplitude of the fundamental component. The stimuli consisted of a drifting grating at 1 Hz (closed triangles), 4 Hz (closed hexagons), and 16 Hz (open hexagons). Sensitivity was obtained by interpolation on the response vs. contrast curves to find the contrast necessary for a constant response amplitude. Each sensitivity value was normalized with respect to one maximum value.

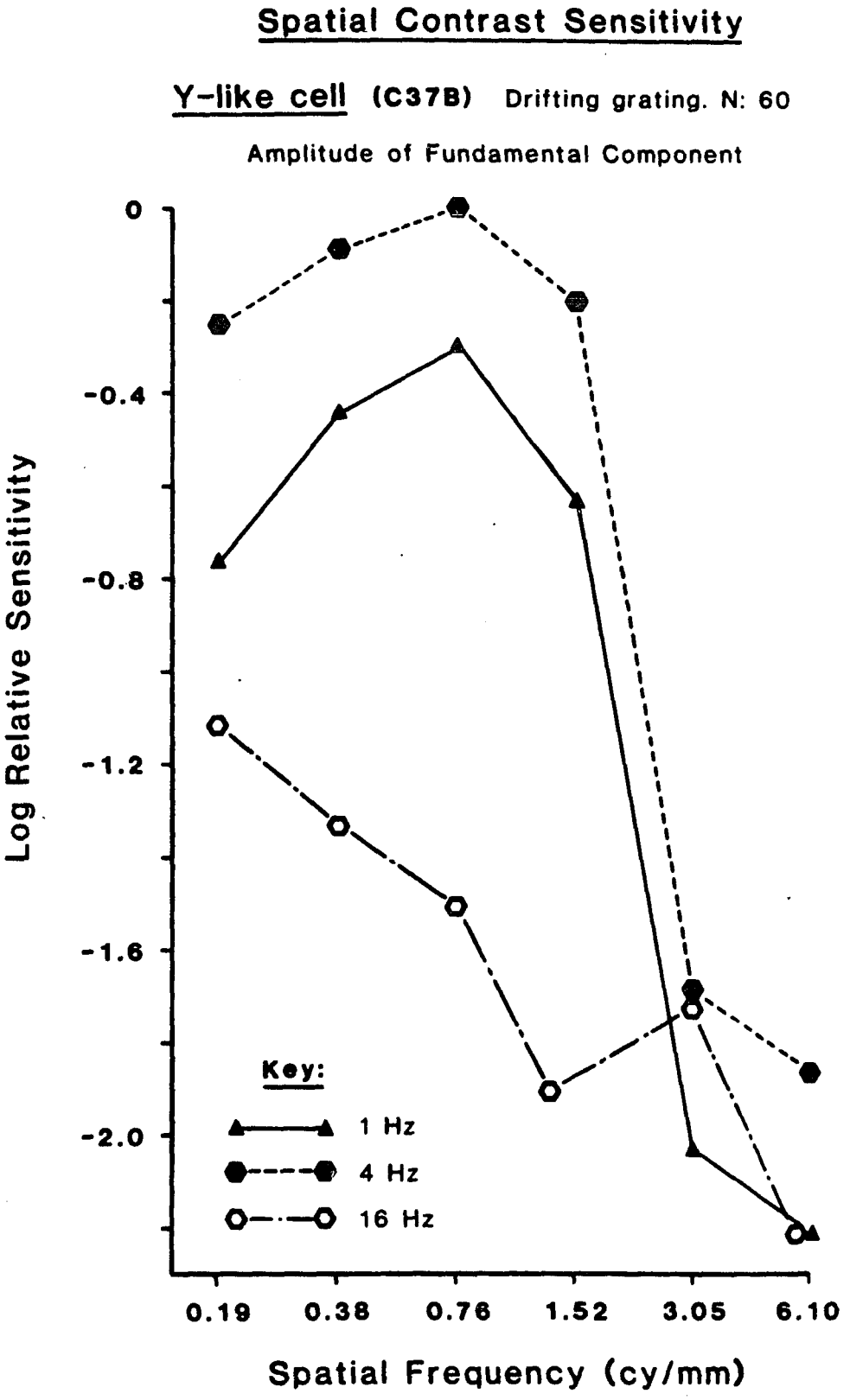
Spatial Contrast Sensitivity
Y-like cell (C37B) Drifting grating. N: 60
Amplitude of Fundamental Component
Log Relative Sensitivity
0
-0.4
-0.8
-1.2
-1.6
-2.0
Key:
1 Hz
4 Hz
16 Hz
0.19
0.38
0.76
1.52
3.05
6.10
Spatial Frequency (cy/mm)

substantial change in the function. Increasing the stimulus drift rate decreased the degree of the low frequency attenuation in the S-CSF.

T-CSFs were also obtained from Y-like cells. All Y-like cells responded to the temporal stimuli with pure sinusoidal modulation at the stimulus frequency; that is, the response's power was at the fundamental component. Although, at first, this may seem odd given that these cells are usually associated with a doubling response, it is not peculiar when the type of stimulus being presented is examined. With a contrast-reversal grating, it was found that Y-like cells responded with a doubling of the stimulus modulation. However, this doubling usually occurred at high spatial frequencies; at lower spatial frequencies, the cell did not respond at double the stimulus frequency, but responded similarly to a linear, X-like cell in that a null point could be found and the cell's response modulated at the same frequency as the stimulus cycle. Taking spatial frequency to its lowest limit, a contrast-reversal grating with zero spatial frequency is nothing more than a uniform field sinusoidally modulated in time around a mean luminance.

All Y-like cells' T-CSFs were band-pass; however, some Y-like cells were much more sharply tuned in the temporal domain than others. Figure 23 shows the T-CSFs of two Y-like cells. Figure 23a gives an example of a broad band-pass cell while Figure 23b shows a narrowly tuned Y-like cell. The response measure in both cases was the amplitude of the fundamental component. The stimulus in both cases covered the entire receptive field (7.5 mm circular aperture).

T-CSFs of a Y-like cell were determined for the center, sur-

Figure 23

T-CSFs of two Y-like cells. The response measure was the amplitude of the fundamental component. The stimulus was a uniform field which varied sinusoidally in intensity. Sensitivity was obtained by interpolation on the response vs. contrast curves to find the contrast necessary for a constant response amplitude. This figure illustrates the two types of T-CSFs found in Y-like cells, a broadly tuned function (a) and a very narrowly-tuned function (b).

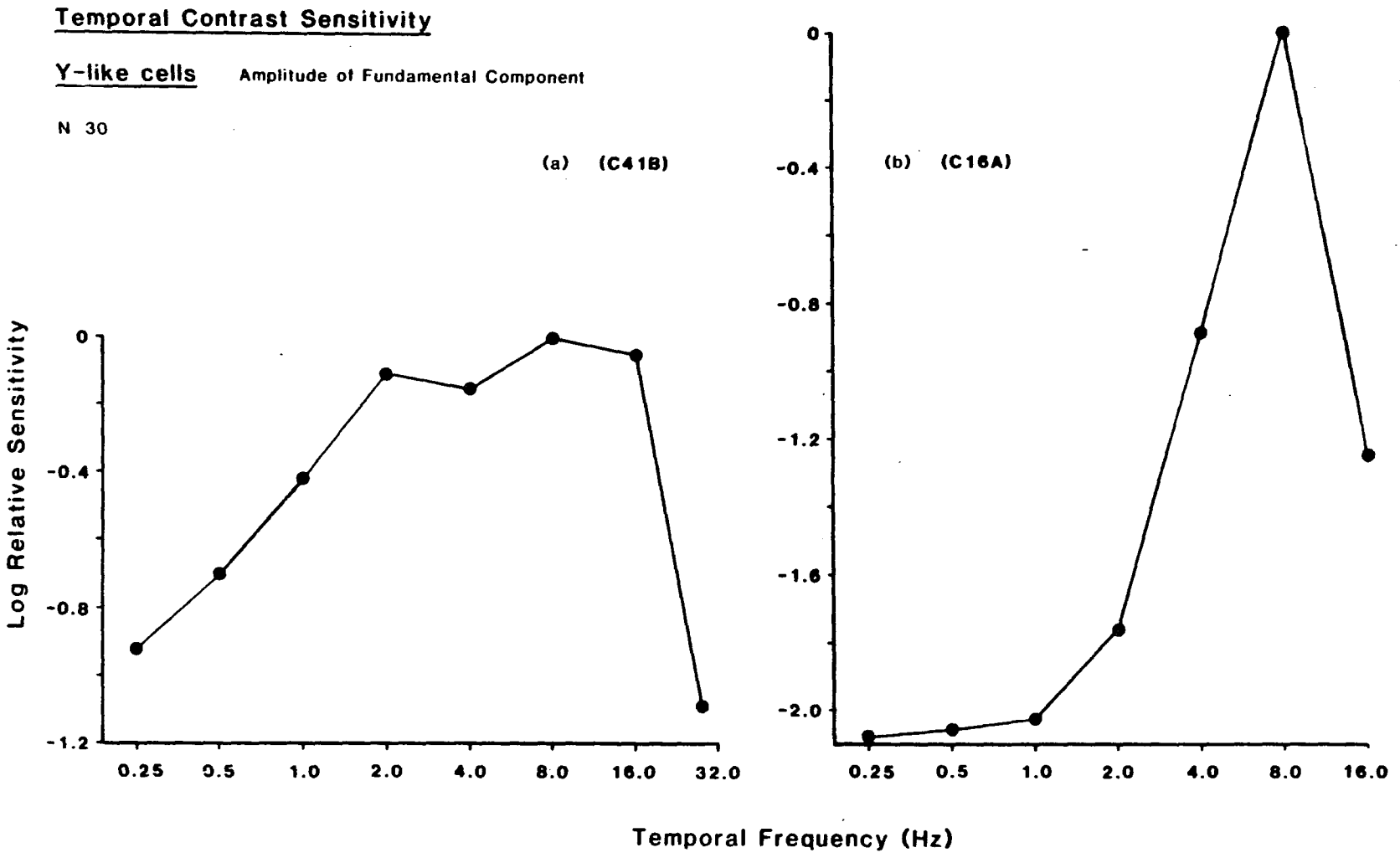
Temporal Contrast Sensitivity
Y-like cells
Amplitude of Fundamental Component
N 30
(a) (C41B)
(b) (C16A)
Log Relative Sensitivity
0
-0.4
-0.8
-1.2
-1.6
-2.0
0.25
0.5
1.0
2.0
4.0
8.0
16.0
32.0
Temporal Frequency (Hz)

round and full field components to examine their interactions as a function of temporal frequency. Figure 24 shows the results. As in X-like cells, the center and surround components are antagonistic at low temporal frequencies; that is, full field values are less sensitive than the center values and the center and surround phases are approximately 180 degrees apart. However, at high temporal frequencies, the center and surround components appear synergistic; the full field sensitivity values are higher than either the center and surround values. Also, the phases of the center and surround components coincide at the temporal frequencies in which the full field sensitivity is enhanced (i.e., 16 and 32 Hz).

3.3.3 W-like Cells.

Unlike X- and Y-like cells, which appeared to be similar in most respects except for the presence of the nonlinear subunits in Y-like cells, W-like cells were a class apart. There was so much variability across W-like cells that it is difficult to make general statements about them.

For the most part, S-CSFs could be obtained from W-like cells. Many of them had functions that were similar to X-like cells. That is, there were no indications that any W-like cells possessed the small, nonlinear subunits found in Y-like cells. The nonlinear responses of W-like cells must be due to some other aspects of the cell's mechanisms. One common finding regarding the S-CSFs of W-like cells is that they all showed a high-frequency sensitivity similar to that in X-like cells. Figure 25 shows the S-CSF of a W-like

Figure 24

(a) T-CSFs of the center, surround and full field of a Y-like cell. The response measure was the amplitude of the fundamental component and the stimulus consisted of a uniform field which varied sinusoidally in intensity at 13% contrast. All values were normalized with respect to one maximum value. The center T-CSF (open stars) was derived with the stimulus restricted to a 1 mm by 1 mm square; for the surround T-CSF (enclosed stars), the stimulus was restricted to the surrounding portion of the full field stimulus with a center square maintained at mean luminance. Full field stimulation (closed circles) was a 7.5 mm diameter circular aperture. (b) Fundamental component phase differences from the responses of the center and surround components.

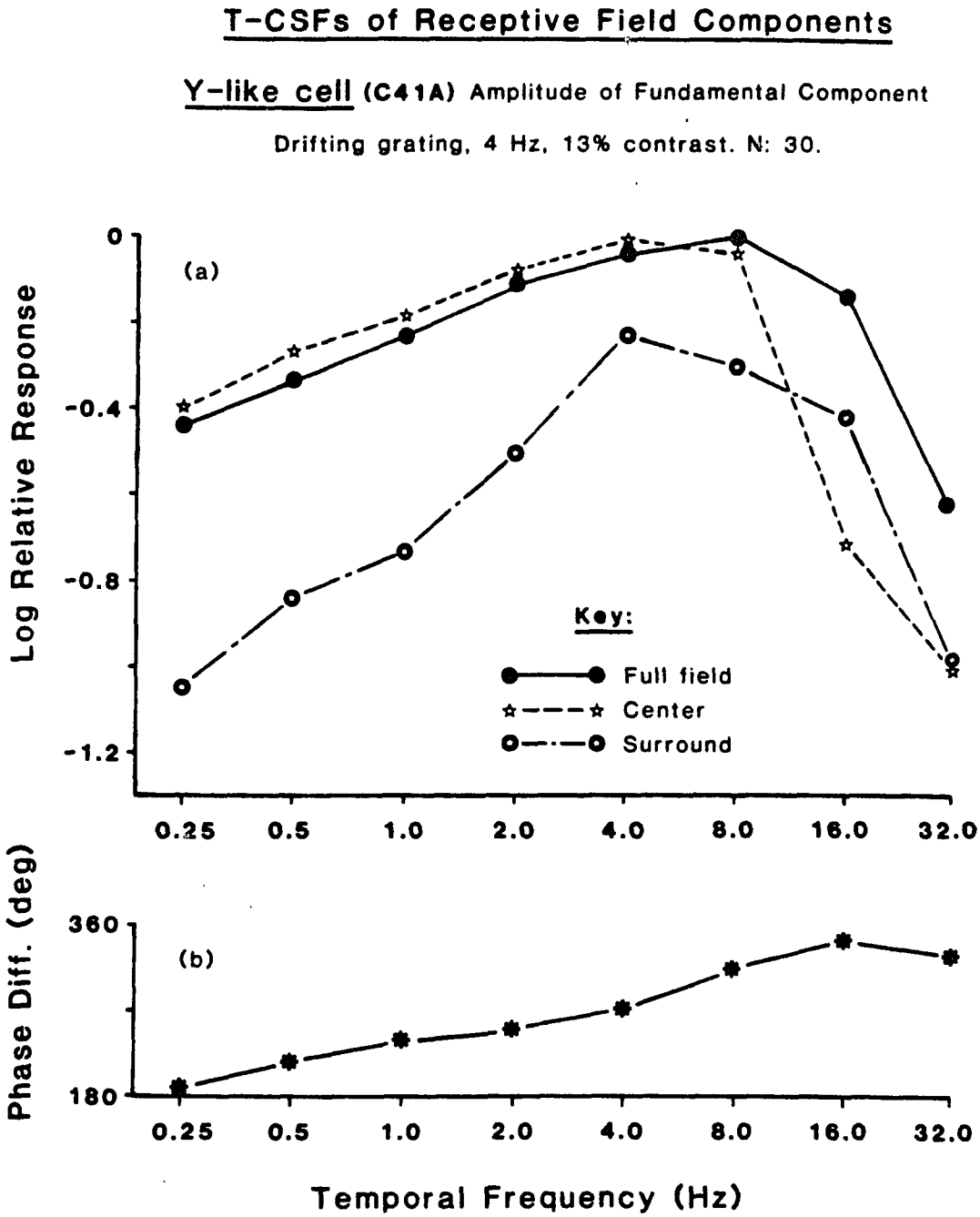
T-CSFs of Receptive Field Components
Y-like cell (C41A) Amplitude of Fundamental Component
Drifting grating, 4 Hz, 13% contrast. N: 30.
(a)
Log Relative Response
0
-0.4
-0.8
-1.2
Key:
Full field
Center
Surround
0.25
0.5
1.0
2.0
4.0
8.0
16.0
32.0
(b)
Phase Diff. (deg)
360
180
Temporal Frequency (Hz)

Figure 25

S-CSF of a W-like cell. The response measure was the maximum response minus the minimum response. The stimulus consisted of a 2 Hz drifting grating. Sensitivity was obtained by interpolation on the response vs. contrast curves to find the contrast necessary for a constant response amplitude.

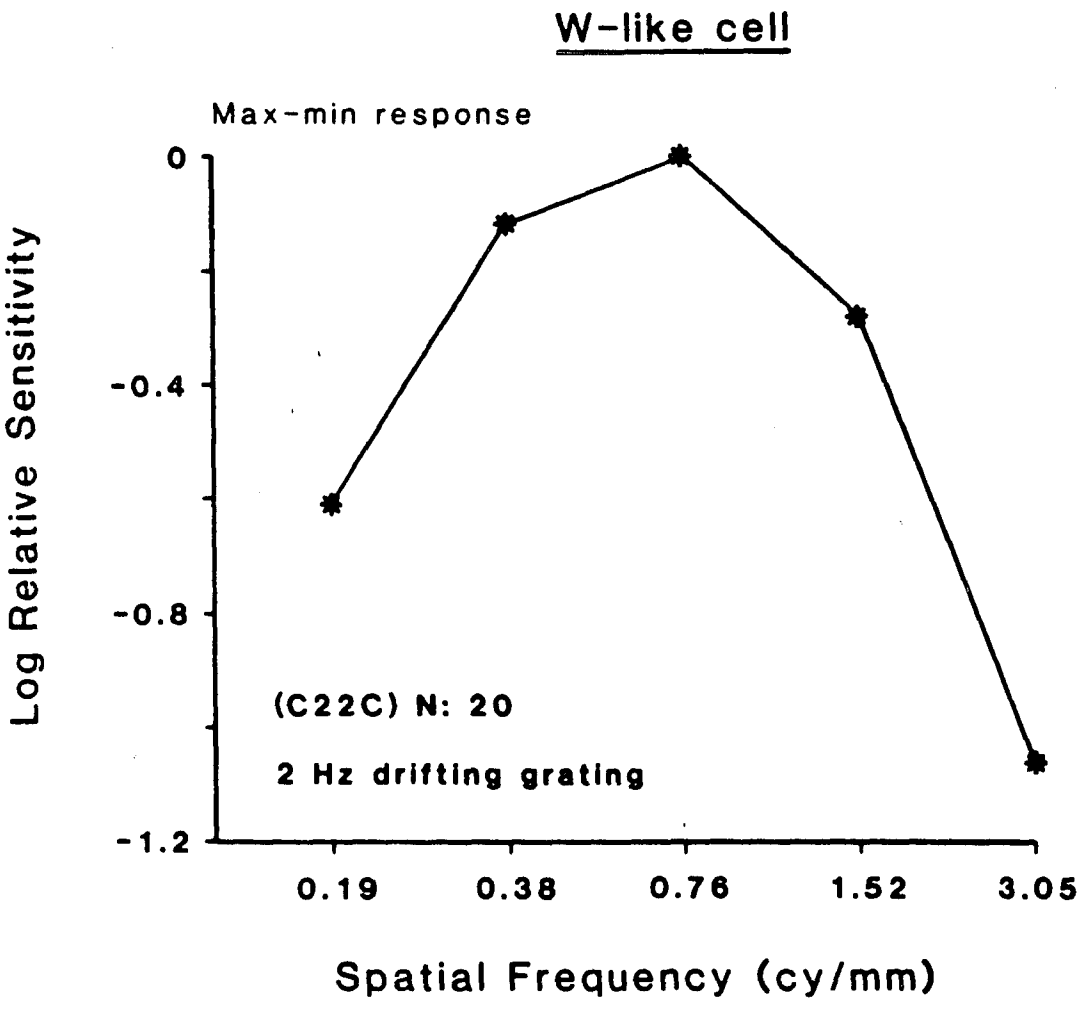
W-like cell
Max-min response
0
-0.4
-0.8
-1.2
Log Relative Sensitivity
(C22C) N: 20
2 Hz drifting grating
0.19
0.38
0.76
1.52
3.05
Spatial Frequency (cy/mm)

cell. The response measure was max-min and the drift rate was 2 Hz. Sensitivity was determined by interpolation on the response vs. contrast curves. Note that the high frequency portion of the S-CSF had no indication of the nonlinear subunits found at high spatial frequencies in Y-like cells. If present, these would certainly be apparent with the max-min response measure (compare with the Y-like cell in Figure 18).

Some, but not all, cells possessed the low frequency attenuation found in cells with an antagonistic mechanism present (e.g., the cell in Figure 25). The shape of the S-CSF for cells with an antagonistic mechanism, as with X- and Y-like cells, depended on the drift rate of the stimulus grating. Figure 26 illustrates the dependence of the S-CSF on the stimulus' drift rate. The response measure was the amplitude of the fundamental component and all values were normalized with respect to one maximum value. At high spatial frequencies, the drift rate had little effect on the S-CSFs; at low spatial frequencies, however, the S-CSF was influenced dramatically in that the slow drift rates produced large amounts of low frequency attenuation. By 8 Hz, there was no low frequency attenuation at all. Thus, the mechanism responsible for the low frequency attenuation was either insensitive to high temporal rates or that the responses of the mechanisms were no longer antagonistic at high temporal rates due to phase shift changes across temporal rates (see Sections 3.3.2 and 3.2.3). Figure 27 shows the S-CSF of another W-like cell at different drift rates (Figure 27a); the T-CSF of the same cell is also shown in Figure 27b. The response measure in both CSFs was the amplitude of the funda-

Figure 26

S-CSFs of a W-like cell at different drift rates. The response measure was the amplitude of the fundamental component. The stimuli consisted of a drifting grating of 2 Hz (closed triangles), 4 Hz (closed hexagons), and 8 Hz (open hexagons). Sensitivity was obtained by interpolation on the response vs. contrast curves to find the contrast necessary for a constant response amplitude. Each sensitivity value was normalized with respect to one maximum.

Spatial Contrast Sensitivity

W-like cell (C08A) Amplitude of Fundamental Component

Drifting grating. N: 30.

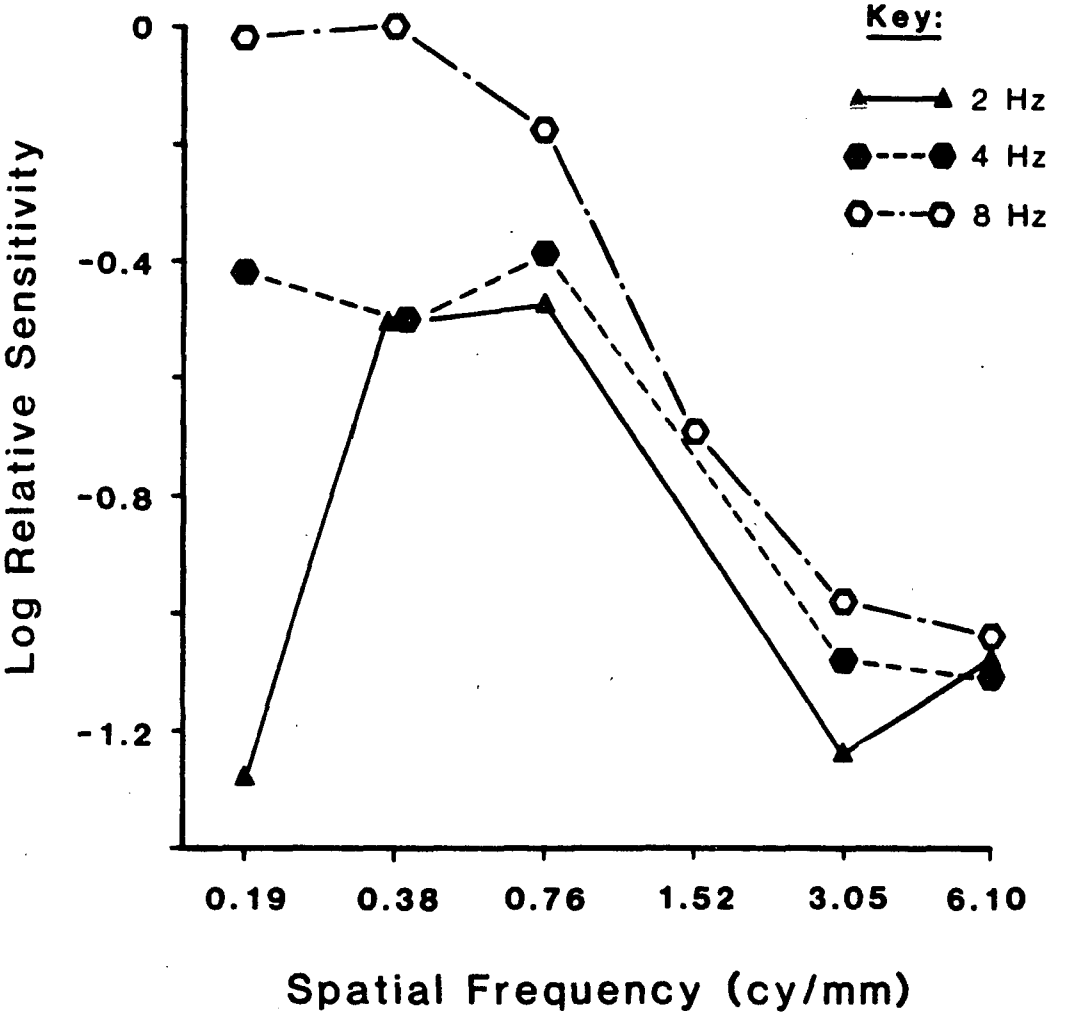

Figure 27

S-CSFs (a) and T-CSF (b) of a W-like cell. The response measure for all functions was the amplitude of the fundamental component. The stimuli for the S-CSFs consisted of a drifting grating of 2 Hz (closed triangles), 4 Hz (closed hexagons), and 8 Hz (open hexagons). For the T-CSF, the stimulus was a uniform field which varied sinusoidally in intensity (closed circles). Sensitivity was obtained by interpolation on the response vs. contrast curves to find the contrast necessary for a constant response amplitude. For the S-CSFs, all sensitivity values were normalized with respect to one maximum value.

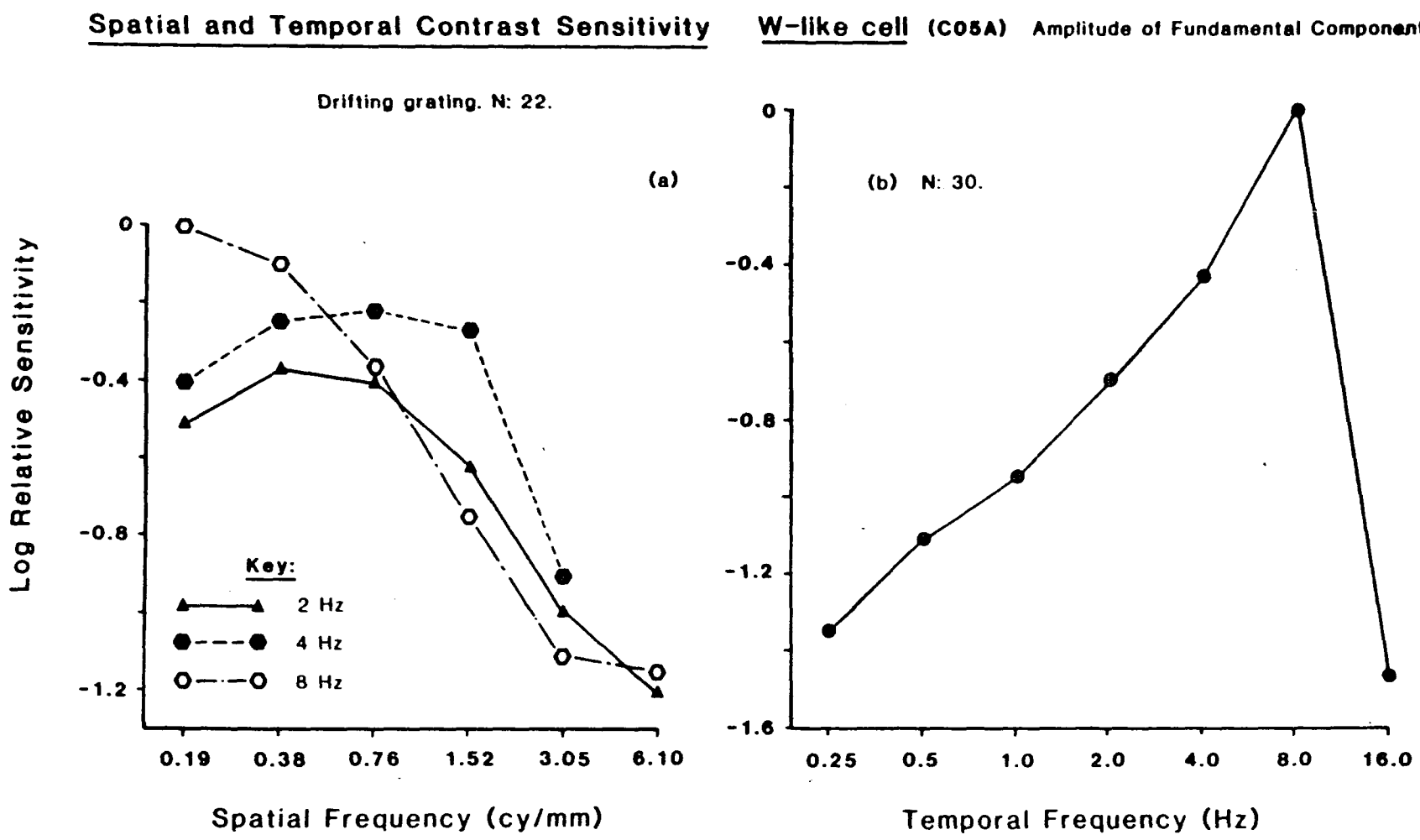
Spatial and Temporal Contrast Sensitivity
W-like cell (C05A) Amplitude of Fundamental Component
Drifting grating. N: 22.
(a)
(b) N: 30.
Log Relative Sensitivity
0
-0.4
-0.8
-1.2
-1.6
Key:
2 Hz
4 Hz
8 Hz
0.19
0.38
0.76
1.52
3.05
6.10
0.25
0.5
1.0
2.0
4.0
8.0
16.0
Spatial Frequency (cy/mm)
Temporal Frequency (Hz)

mental component and all values in Figure 27a were normalized with respect to one maximum value. The T-CSF of this cell was typical of W-like cells. Most W-like cells' T-CSF were sharply tuned to a small range of temporal frequencies. Figure 28 shows another example of a T-CSF. As with X- and Y-like cells, most of the cell's response to uniform sinusoidally modulated gratings was found in the fundamental component.

3.4 Orientation and Direction Selectivity.

Orientation and direction selectivity were examined by drifting sinusoidal gratings in opposite directions varied in 45 degree steps from 0 to 135 degrees. Spatial frequency, contrast and drift rate of the stimulus were also varied.

3.4.1 X-like Cells.

Since X-like cells are linear, the response measure used to examine orientation and direction selectivity was the amplitude of the fundamental component. Four of the ten X-like cells tested for orientation and direction selectivity displayed orientation tuning. Typical results from an X-like cell are shown in Figure 29. The drift rate of the grating was 4 Hz at 40% contrast. The ordinate is the amplitude of the fundamental component of the response. The spontaneous rate of this cell was zero. As can be seen in this figure, the degree of orientation tuning depended upon the spatial frequency of the stimulus grating. At low spatial frequencies (Figure 29a), there was little or no orientation tuning, but as the spatial frequency of the stimulus

Figure 28

T-CSF of a W-like cell. The response measure was the amplitude of the fundamental component. The stimulus was a uniform field which varied sinusoidally in intensity. Sensitivity was determined by interpolation on the response vs. contrast curves to find the contrast necessary for a constant response amplitude.

Temporal Contrast Sensitivity

W-like cell (C12B) Amplitude of Fundamental Component

N: 30.

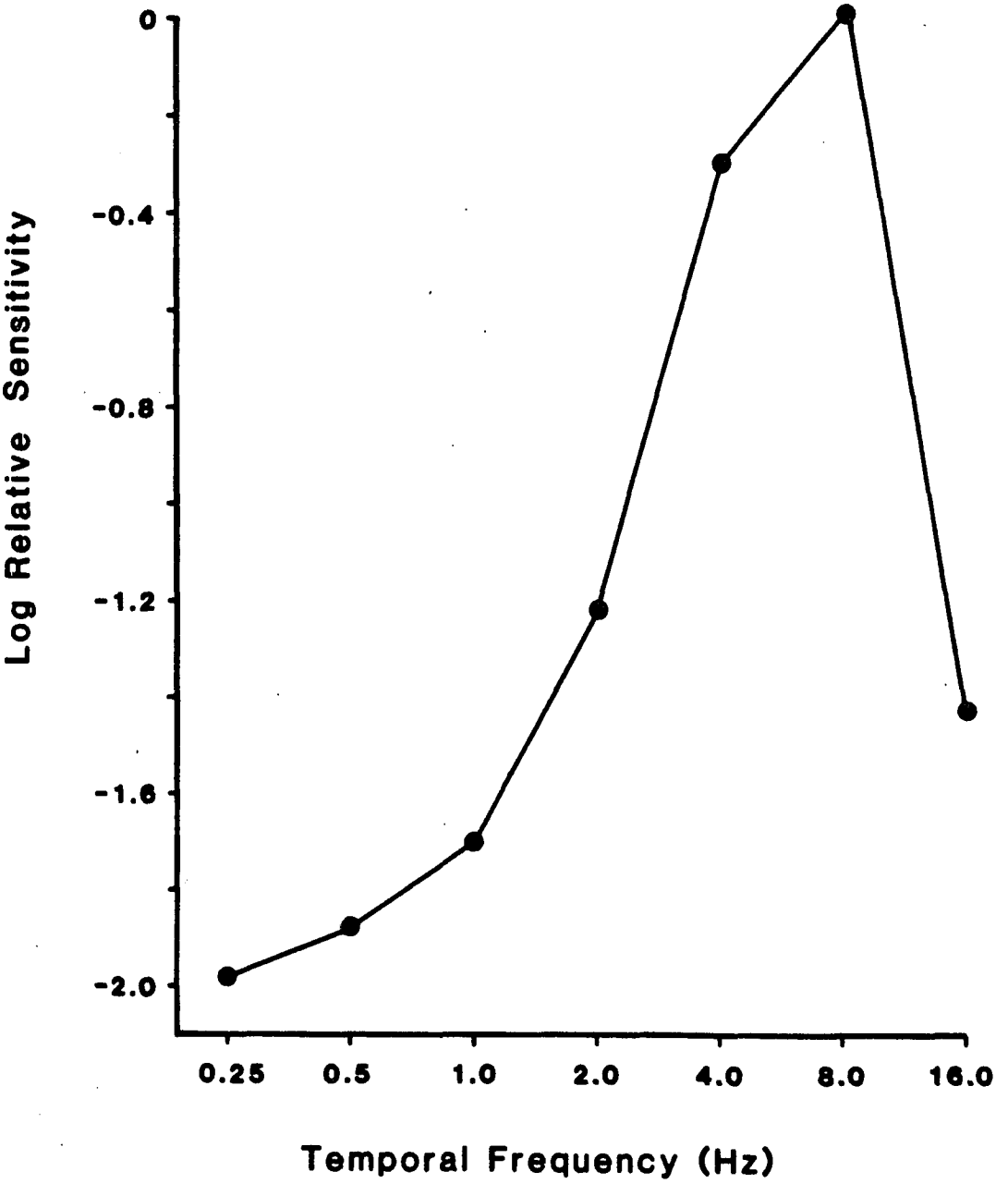

Figure 29

Orientation tuning of an X-like cell. The response measure was the amplitude of the fundamental component. The responses of the cell to a 4 Hz drifting grating at various orientations and at several spatial frequencies (a, b, and c), are shown. The stimulus contrast in each case was 40 percent. The spatial frequency of the grating is given at the bottom of each figure. This cell had no spontaneous rate. To examine direction selectivity, each orientation axis in each figure (a, b, and c) was redrawn such that orientations 180 degrees out of phase to one another were superimposed. These redrawn figures are shown in (d), (e), and (f).

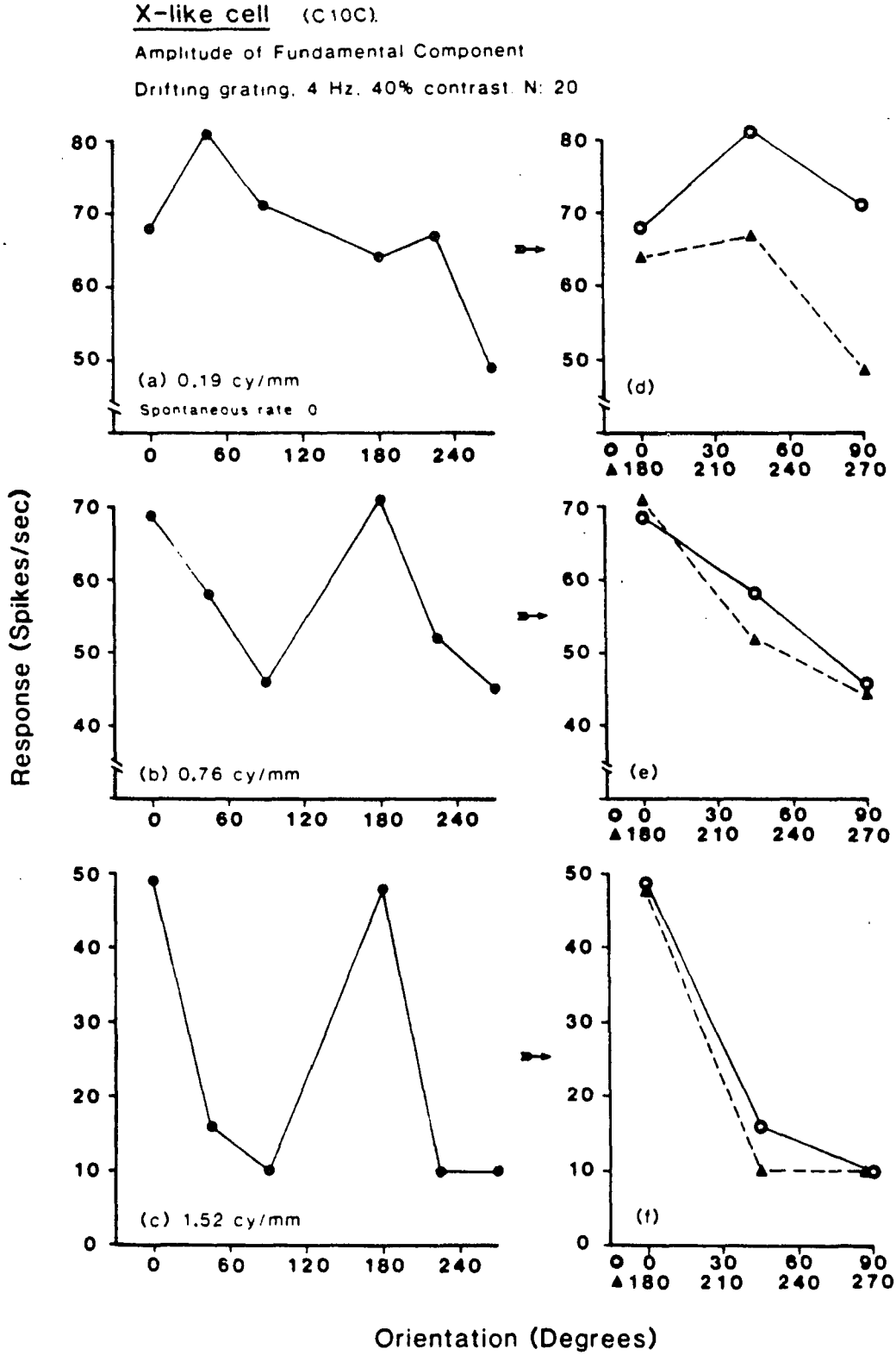
X-like cell (C10C).
Amplitude of Fundamental Component
Drifting grating. 4 Hz. 40% contrast. N: 20
(a) 0.19 cy/mm
Spontaneous rate 0
(b) 0.76 cy/mm
(c) 1.52 cy/mm
(d)
(e)
(f)
Response (Spikes/sec)
Orientation (Degrees)

was increased, orientation tuning increased (Figures 29b, c).

Since drifting gratings of 0 and 180 degrees have the same orientation but move in opposite direction the responses of these two stimuli were superimposed on the orientation axis to test for direction selectivity. This was done for all values 180 degrees out of phase. The replotted values of the data in Figures 29a, b and c are shown in Figures 29d, e and f, respectively. In Figures 29e, f, the two curves superimpose, indicating no direction selectivity. That is, the cell responded similarly to gratings at the same orientation but moving in opposite directions. From Figures 29e, f, the cell was also orientation selective, since the functions were not straight horizontal lines. However, the responses in Figure 29d showed a slight direction selectivity at low spatial frequencies since the responses to gratings 180 out of phase did not superimpose on one another. This was the only X-like cell isolated that displayed any indication of direction selectivity.

Figure 30 compares the spatial resolution of the cell in Figure 29 for gratings at the preferred and non-preferred orientations. As expected, at low spatial frequencies, the responses were similar, but as spatial frequency increased, the responses of the two orientations differed. These findings suggest that only the mechanism responsible for the responses at high spatial frequencies (i.e., the center) was not circular since this was where orientation differences occurred.

The remaining six out of ten X-like cells displayed little or no orientation tuning to a drifting grating. Figure 31 shows one such cell at several spatial frequencies. Once again the response measure

Figure 30

Spatial resolution of an X-like cell at preferred and non-preferred orientations. The response measure was the amplitude of the fundamental component. The stimuli consisted of a 4 Hz drifting grating at 40% contrast at the preferred (closed squares) and the non-preferred (open hexagons) orientations. The spontaneous rate of the cell was zero.

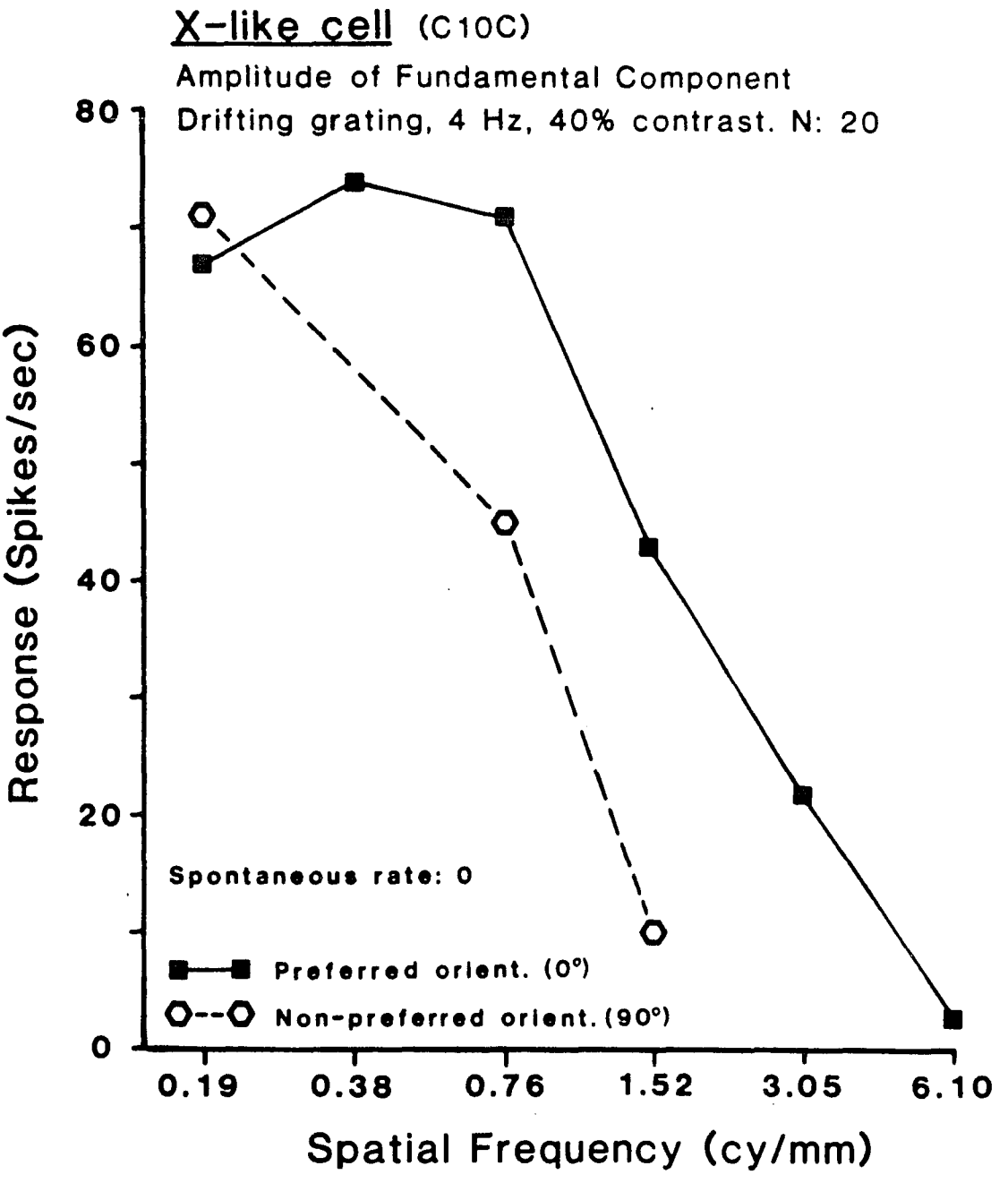
X-like cell (C10C)
Amplitude of Fundamental Component
Drifting grating, 4 Hz, 40% contrast. N: 20
Response (Spikes/sec)
80
60
40
20
0
Spontaneous rate: 0
Preferred orient. (0°)
Non-preferred orient. (90°)
0.19
0.38
0.76
1.52
3.05
6.10
Spatial Frequency (cy/mm)

Figure 31

Orientation tuning of an X-like cell with a circular receptive field. The response measure was the amplitude of the fundamental component. The responses of the cell to a 2 Hz drifting grating at various orientations, and at several spatial frequencies (a, b, and c), are shown. The contrast of each stimulus was 40 percent. The spatial frequency of the grating is given at the bottom of each figure. The dotted line in (a) represents the amplitude of the fundamental component to a stimulus of zero contrast.

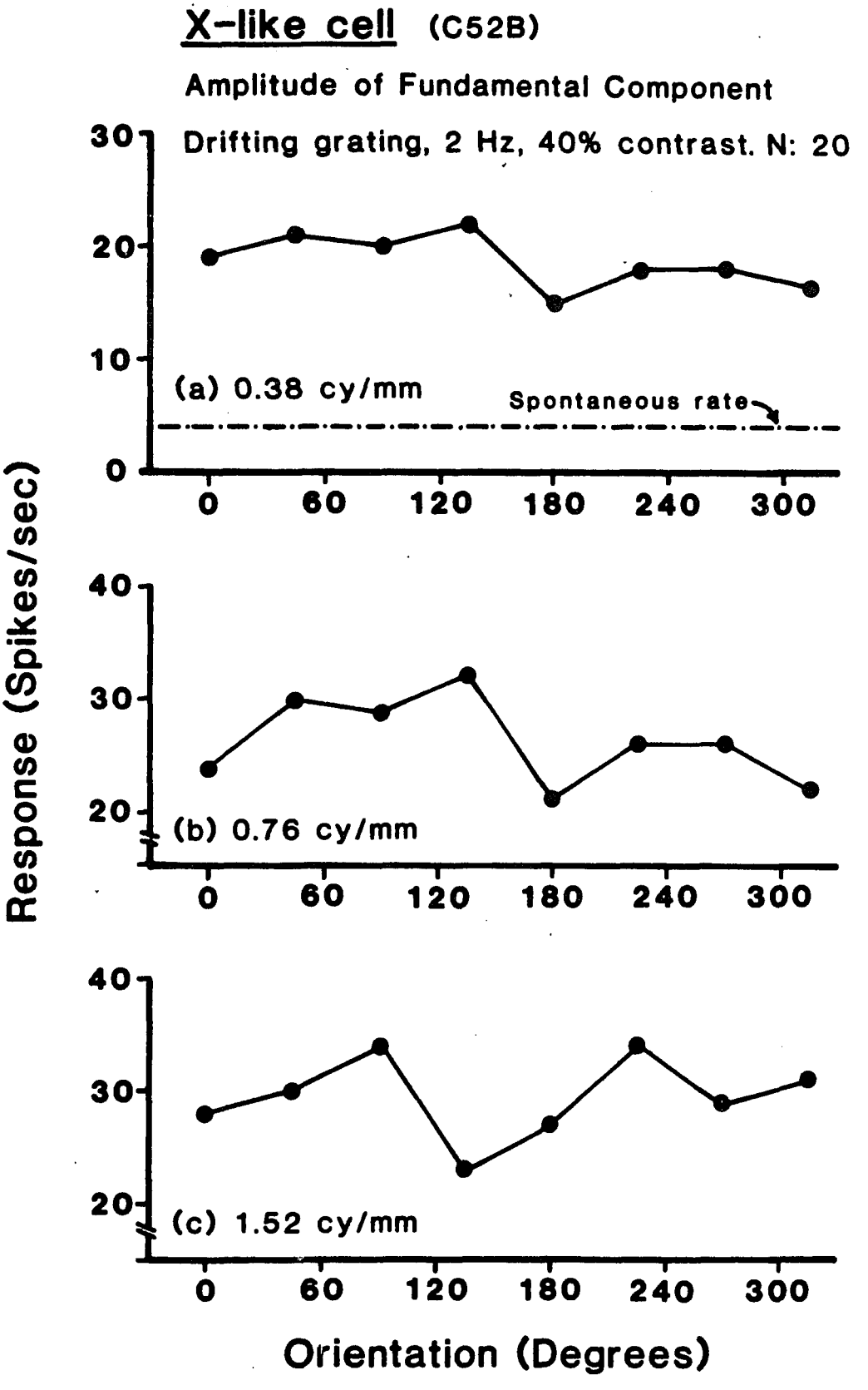
X-like cell (C52B)
Amplitude of Fundamental Component
Drifting grating, 2 Hz, 40% contrast. N: 20
30
20
10
0
(a) 0.38 cy/mm
Spontaneous rate
0
60
120
180
240
300
40
30
20
(b) 0.76 cy/mm
0
60
120
180
240
300
40
30
20
(c) 1.52 cy/mm
0
60
120
180
240
300
Response (Spikes/sec)
Orientation (Degrees)

was the amplitude of the fundamental component; the drift rate was 2 Hz and the contrast was 40 percent. The broken line represents the amplitude of the fundamental component when only mean luminance was present (i.e., spontaneous rate). As can be seen, there was little difference in the response across orientation, even at high spatial frequencies. However, at the highest spatial frequency (1.52 cy/mm), there did appear to be an irregularity in the function. This may reflect random variability in the response, and will be discussed below.

3.4.2 Y-like Cells.

Since Y-like cells are nonlinear, the most reliable measure of their overall response (including the nonlinear subunits) was max-min; the fundamental and second harmonic components of the cell's response were also calculated for comparison. All but one Y-like cell displayed orientation tuning. However, as in X-like cells, the degree of orientation tuning depended upon the spatial frequency of the stimulus. Figure 32 shows the orientation tuning of a Y-like cell and its dependence on spatial frequency. The response measure was the max-min response, the drift rate of the stimulus was 4 Hz, and the contrast for each stimulus is shown within each figure. The max-min response with no stimulus contrast is represented by the dashed line in Figures 32d, e. Thus, any response falling around this line could be attributed to noise in the firing pattern of the cell. As can be seen in this figure, at low spatial frequencies, the orientation tuning was small (Figure 32a), but as the spatial frequency increased, so

Figure 32

Orientation tuning of a Y-like cell. The response measure was the maximum response minus the minimum response. The responses of the cell to a 4 Hz drifting grating at various orientations, and at several spatial frequencies (a, b, c, d, and e), are shown. The spatial frequency and contrast of the grating are given at the bottom of each figure. The dashed line represents the max-min response to a grating of zero contrast.

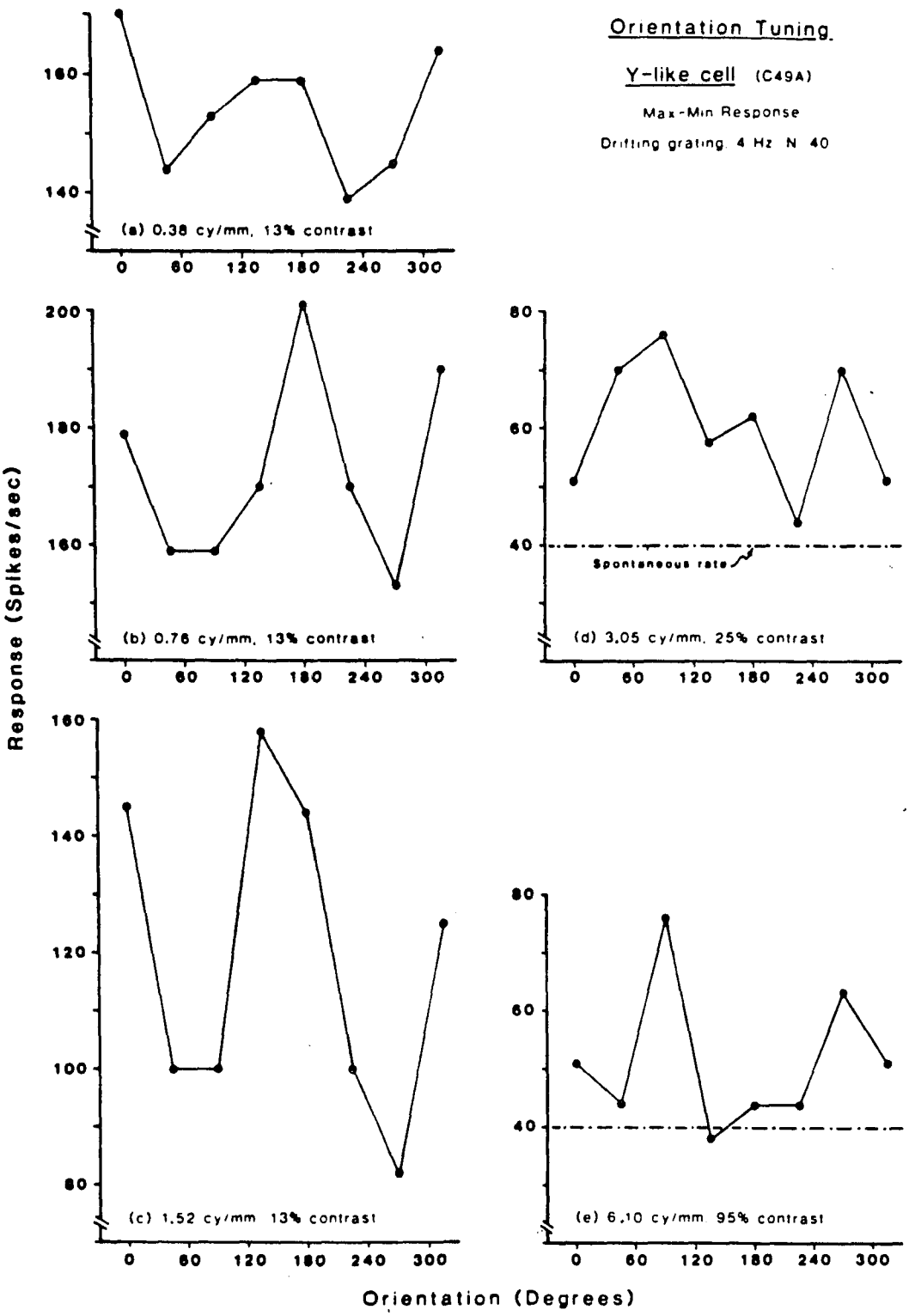
Orientation Tuning
Y-like cell (C49A)
Max-Min Response
Drifting grating 4 Hz N 40
(a) 0.38 cy/mm, 13% contrast
(b) 0.76 cy/mm, 13% contrast
(c) 1.52 cy/mm 13% contrast
(d) 3.05 cy/mm, 25% contrast
(e) 6.10 cy/mm 95% contrast
Spontaneous rate
Response (Spikes/sec)
Orientation (Degrees)
0
60
120
180
240
300

did the amount of orientation tuning (Figures 32b, c). At even higher spatial frequencies (Figures 32d, e), several preferred orientations were seen, and in some cases, the orientation of maximal response differed from the maximum at lower spatial frequencies. For example, at 0.76 cy/mm (Figure 32b), the preferred orientation was roughly 180 degrees, while the non-preferred orientation was at 90 degrees. The shape of the curve resembled a "w", which is what would be expected if the mechanism was elliptical and the maximum and minimum responses were orthogonal. The same holds true for 1.52 cy/mm (Figure 32c). However, at 3.05 cy/mm and 6.10 cy/mm (Figures 32d, e, respectively), the preferred orientation was not at 180 degrees but at 90 degrees; an orientation of 180 degrees at these high spatial frequencies actually produced the minimum response.

Another interesting distinction between the responses at low and high spatial frequencies was the shape of the function. At low spatial frequencies, the curve resembled a "w"; however, at the higher frequencies, there were actually several peaks and valleys in the function. This change in the orientation function at the higher spatial frequencies was not due the nonlinear subunits found in Y-like cells because this finding also occurred when the response measure was the fundamental component. There was also evidence for this unusual orientation tuning in X-like cells. Referring back to the X-like cell in Figure 31, the apparently random variability found in the function in Figure 31c could be due to the same phenomenon. It is interesting to note that at the lower spatial frequencies (Figure 31a) the function is relatively flat. If random fluctuation produced

the distortion in Figure 31c, then it should be evident in all the figures, which is not the case.

Figure 33 shows another Y-like cell which verifies that orientation tuning changes with spatial frequency and is maximal at intermediate frequencies. The response was max-min, the drift rate was 4 Hz, and the contrast of the gratings was 25 percent. The spontaneous rate is indicated by the dashed line. At low spatial frequencies, responses at the preferred and non-preferred orientations were similar, but as spatial frequency increased, the responses at the two orientations became disparate.

Eight out of fifteen Y-like cells tested displayed direction selectivity. As with orientation tuning, direction selectivity depended on the spatial frequency of the stimulus. However, the dependence on spatial frequency for direction selectivity was not the same as for orientation tuning. For example, the Y-like cell in Figure 34 clearly showed a direction preference at low spatial frequencies (Figure 34a) but not at higher spatial frequencies (Figure 34b). The response measure was max-min, the drift rate was 4 Hz and the contrast was 40 percent. The spontaneous rate is shown in Figure 34b by the dashed line and orientations 180 degrees from one another were superimposed on the abscissa. Note that in this cell there was orientation tuning at both spatial frequencies (since the functions were not horizontal straight lines) but there was no direction selectivity at the higher spatial frequency (i.e., responses to stimuli 180 degrees apart superimposed on one another). This finding implies that orientation and direction selectivity are two distinct phenomenon even though

Figure 33

Spatial resolution of a Y-like cell at the preferred and non-preferred orientations. The response measure was the maximum minus minimum response. The stimuli consisted of a 4 Hz drifting grating at 25% contrast at the preferred (closed squares) and the non-preferred (open hexagons) orientations. The dashed line represents the max-min response to a grating of zero contrast.

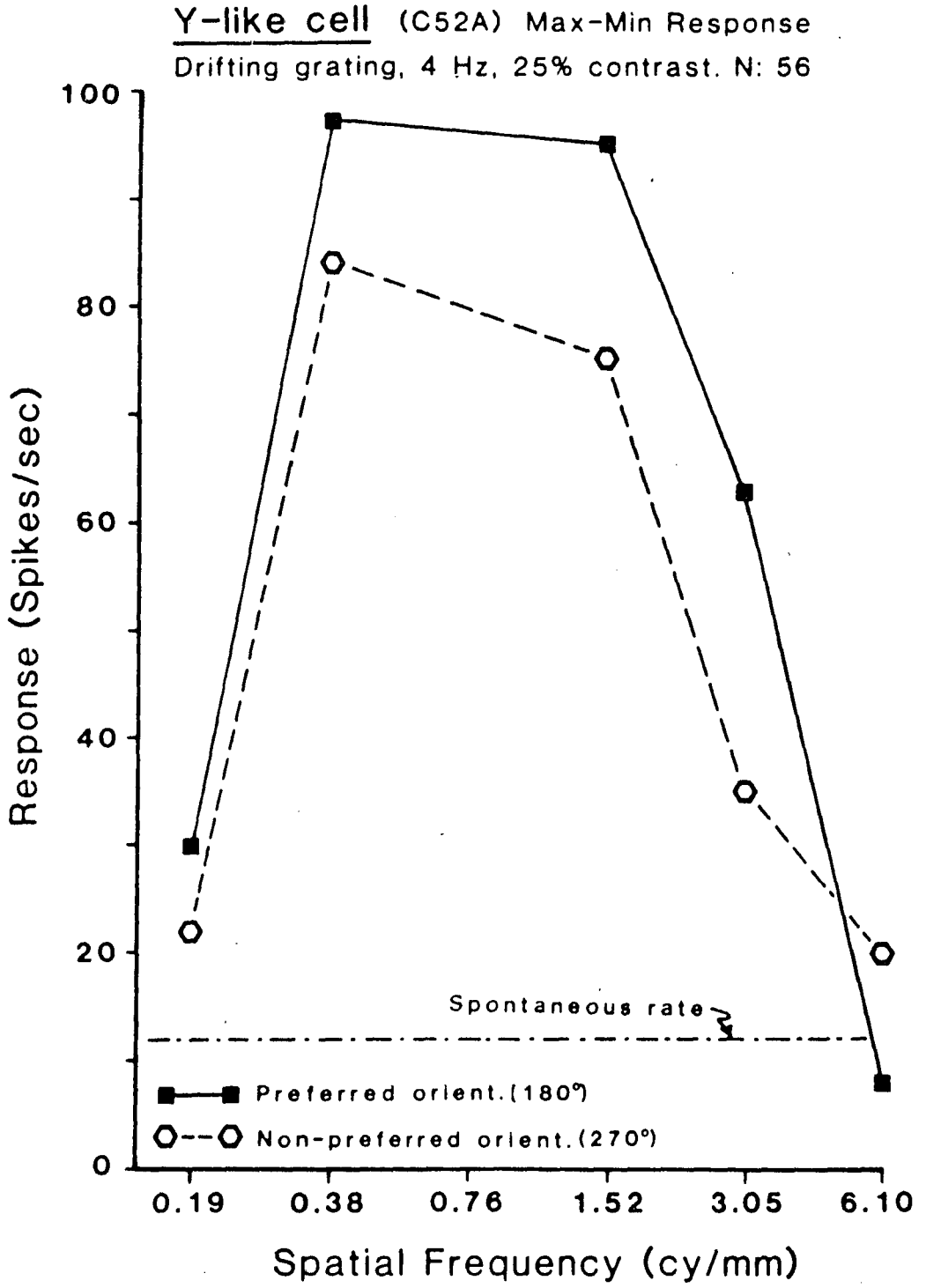
Y-like cell (C52A) Max-Min Response
Drifting grating, 4 Hz, 25% contrast. N: 56
Response (Spikes/sec)
100
80
60
40
20
0
Spontaneous rate
Preferred orient.(180°)
Non-preferred orient.(270°)
0.19
0.38
0.76
1.52
3.05
6.10
Spatial Frequency (cy/mm)

Figure 34

Orientation and direction selectivity of a Y-like cell. The response measure was the maximum minus minimum response. The responses of the cell to a 4 Hz drifting grating at various orientations, at two spatial frequencies (a and b), are shown. The contrast of each grating was 40 percent. The spatial frequency of the grating is given at the right of each figure. Orientation values 180 degrees out of phase are superimposed on the abscissa. The dashed line represents the max-min response to a grating of zero contrast. Note that at low spatial frequencies (0.38 cy/mm) the cell is both orientation and direction selective (a), but at high spatial frequencies (1.52 cy/mm) the cell is only orientation tuned (b).

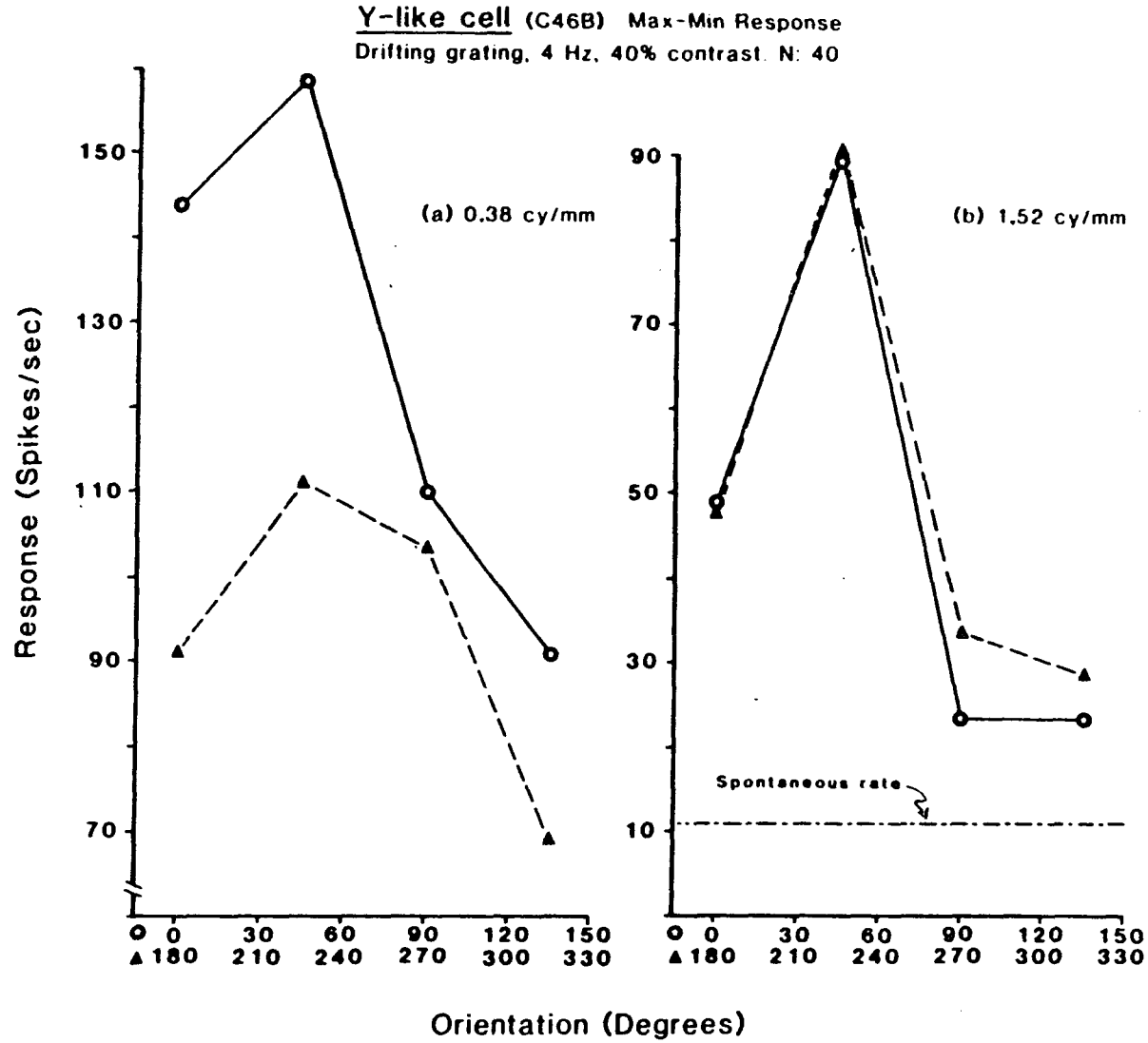
Y-like cell (C46B) Max-Min Response
Drifting grating, 4 Hz, 40% contrast. N: 40
(a) 0.38 cy/mm
(b) 1.52 cy/mm
Response (Spikes/sec)
150
130
110
90
70
90
70
50
30
10
Spontaneous rate
0 30 60 90 120 150
180 210 240 270 300 330
Orientation (Degrees)

they both depend on the spatial frequency of the stimulus.

To illustrate the distinction, Figure 35 displays the existence of orientation and direction selectivity in a Y-like cell for both the max-min response and the fundamental component. The stimulus was a drifting grating at 4 Hz and was presented at various contrasts. The responses to a zero contrast stimulus for the max-min response (Figures 35c, d) and the fundamental component (Figures 35f, g, h) are shown by dashed lines. Once again, gratings whose orientations were 180 degrees apart were superimposed on the abscissa to examine direction selectivity. At low spatial frequencies (Figures 35a, e), there was little orientation tuning but at intermediate spatial frequencies (Figures 35b, f), both orientation and direction selectivity became apparent. At higher spatial frequencies (Figures 35c, g) only orientation tuning was seen; at the highest spatial frequencies (Figures 35d, h) there was no direction selectivity but possibly the unusual orientation tuning seen in other cells. However, the responses were too close to the spontaneous rate to be sure. Since the findings hold for both the max-min response and the fundamental component, orientation and direction selectivity were probably not due to the nonlinear subunits found in Y-like cells' receptive fields.

3.4.3 W-like Cells.

Since W-like cells are also nonlinear, the max-min response was used to test for orientation and direction tuning. All W-like cells displayed orientation and direction selectivity, and both were dependent on the spatial frequency of the grating. Figures 36 and 37

Figure 35

Spatial frequency dependence of orientation and direction selectivity of a Y-like cell. The response measures are the maximum minus minimum response (a, b, c, and d) and the amplitude of the fundamental component (e, f, g, and h). The responses of the cell to a 4 Hz drifting grating at various orientations at several spatial frequencies are shown. The spatial frequency and contrast of the grating are given at the bottom of the max-min response figures. The arrows indicate that the pair of figures represent different response measures to the same stimulus (e.g., a and e result from the same stimulus). The dashed lines represent the response of the cell to a grating of zero contrast. Note that the max-min response is somewhat higher to a "dummy" stimulus than the fundamental component of the response, illustrating that there is more noise or variability in the max-min measure. Orientation values 180 degrees out of phase are superimposed on the abscissa. This figure demonstrates that orientation and direction selectivity are found in both the max-min response and the fundamental component.

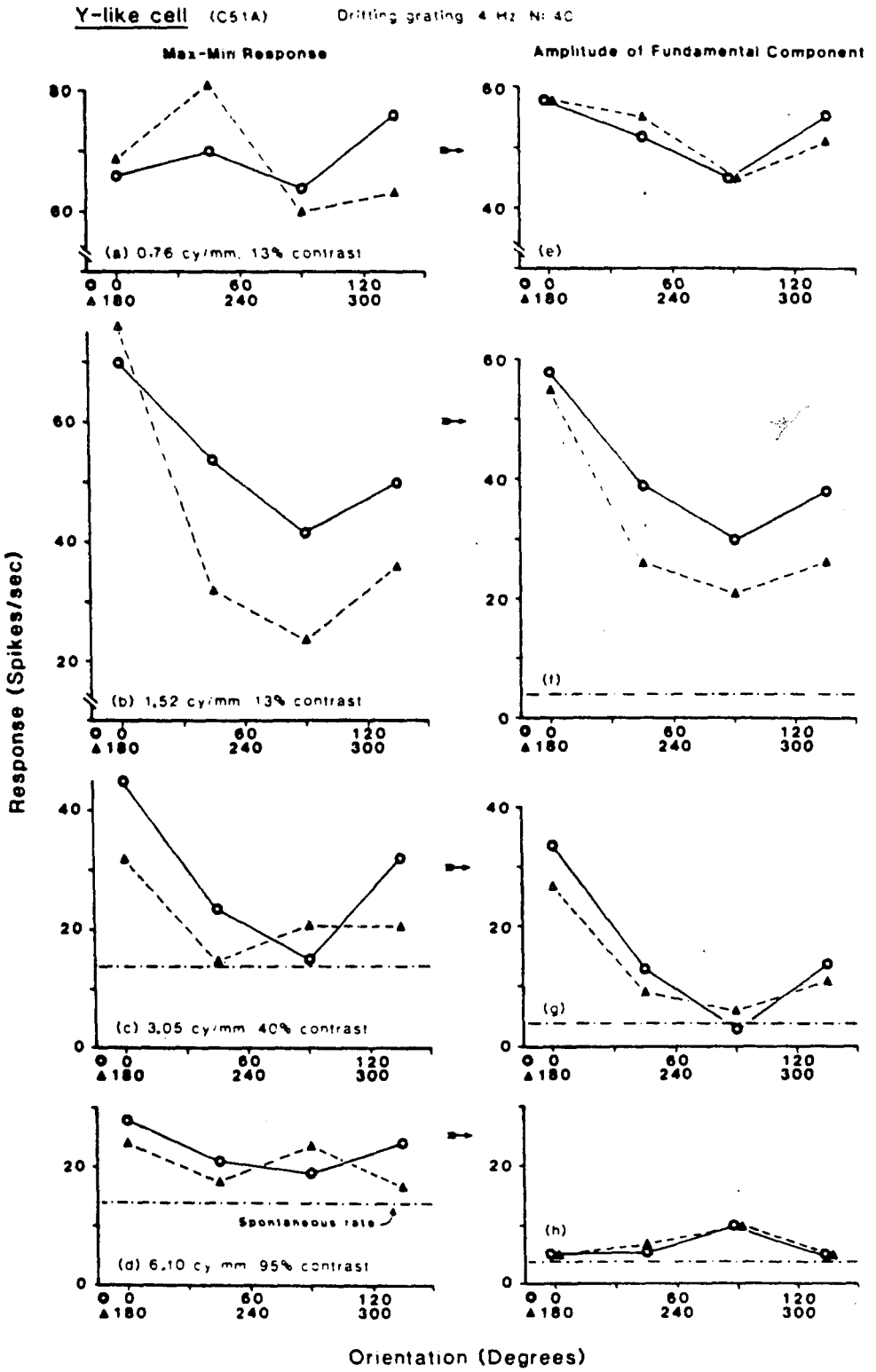
Y-like cell (C51A)
Drifting grating 4 Hz N: 40
Max-Min Response
Amplitude of Fundamental Component
(a) 0.76 cy/mm, 13% contrast
(b) 1.52 cy/mm 13% contrast
(c) 3.05 cy/mm 40% contrast
(d) 6.10 cy/mm 95% contrast
(e)
(f)
(g)
(h)
Spontaneous rate
Response (Spikes/sec)
Orientation (Degrees)

Figure 36

Orientation and direction selectivity of a W-like cell. The response measure was the maximum minus minimum response. The responses of the cell to a 2 Hz drifting grating at various orientations, at several spatial frequencies (a, b, and c), are shown. The contrast of each grating was 25 percent. The spatial frequency of the grating is given at the bottom of each figure. The dashed line in (a) represents the max-min response to a grating of zero contrast. Orientation values 180 degrees out of phase were superimposed on the abscissa.

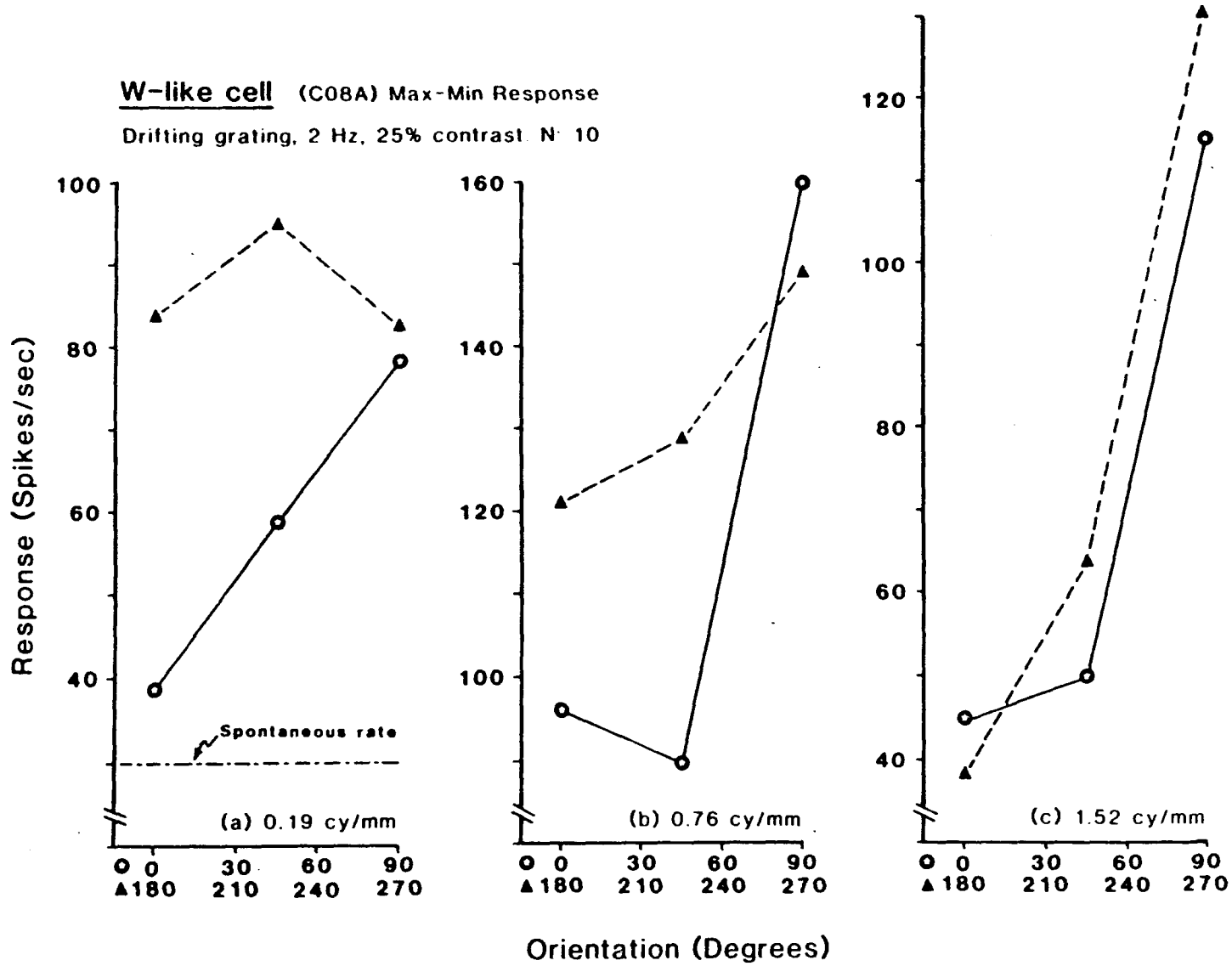
W-like cell (C08A) Max-Min Response
Drifting grating, 2 Hz, 25% contrast N: 10
Response (Spikes/sec)
Spontaneous rate
(a) 0.19 cy/mm
(b) 0.76 cy/mm
(c) 1.52 cy/mm
Orientation (Degrees)

Figure 37

Orientation and direction selectivity of two W-like cells. The response measure was the maximum minus minimum response. The responses of two cells to a 4 Hz drifting grating at various orientations, at several spatial frequencies, are shown. The spatial frequency and contrast of each grating are given at the bottom of each figure. Orientation values 180 degrees out of phase were superimposed on the abscissa. The max-min response of the first cell (a, b, and c) to a grating of zero contrast is represented by the dashed line in (c). The response of the second cell (d, e, and f) to a zero contrast grating was 15 spikes/sec.

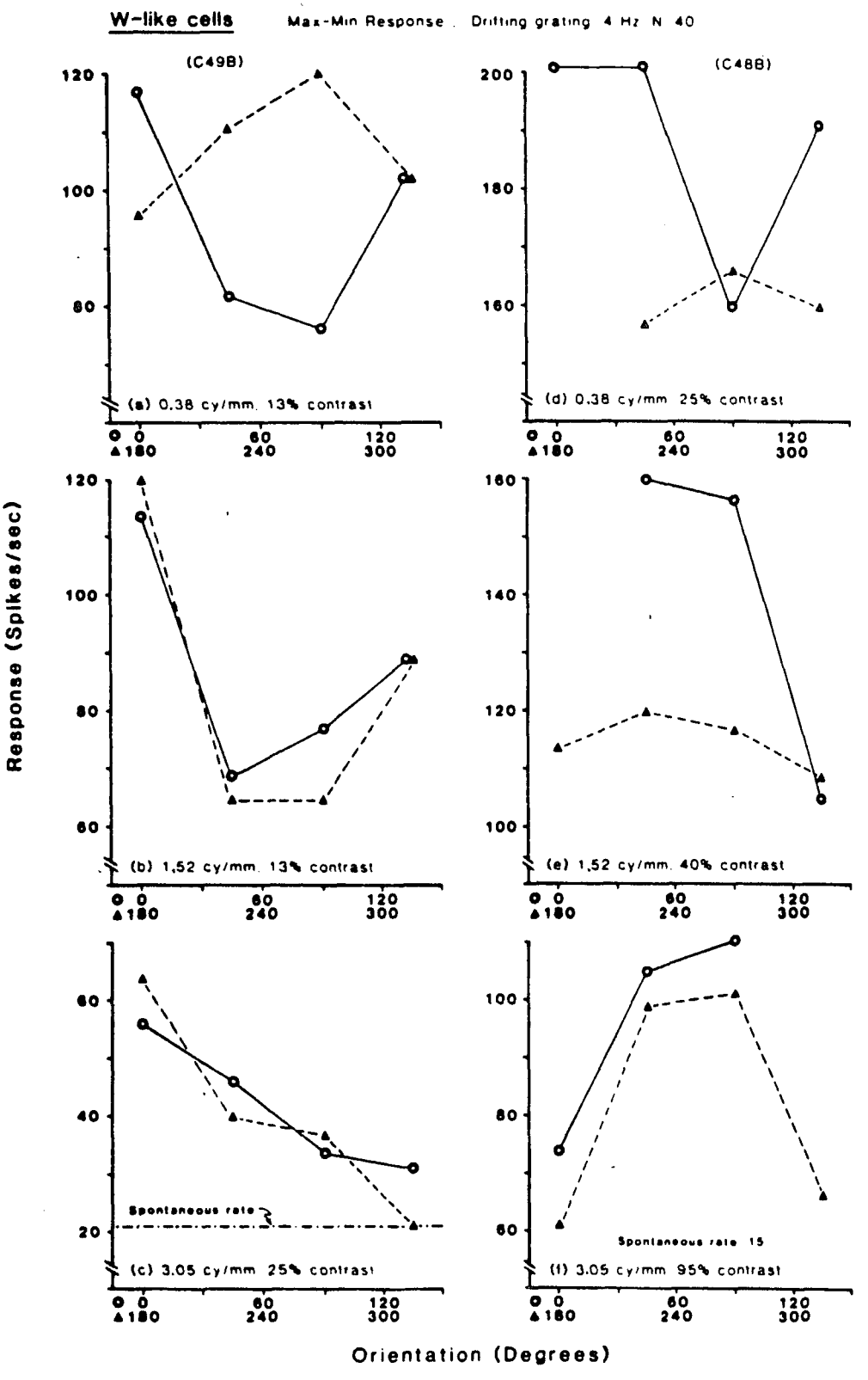
W-like cells
Max-Min Response . Drifting grating 4 Hz N 40
(C49B)
(C48B)
(a) 0.38 cy/mm. 13% contrast
(d) 0.38 cy/mm 25% contrast
(b) 1.52 cy/mm. 13% contrast
(e) 1.52 cy/mm. 40% contrast
(c) 3.05 cy/mm 25% contrast
(f) 3.05 cy/mm 95% contrast
Spontaneous rate
Spontaneous rate 15
Response (Spikes/sec)
Orientation (Degrees)

show typical responses of a W-like cell to drifting gratings at different orientations. In both figures (Figure 37 shows two cells), max-min is the response measure and the responses to gratings 180 degrees apart are superimposed. The drift rate was 2 Hz for Figure 36, and 4 Hz for Figure 37. The contrasts are indicated in each figure and the spontaneous rates are represented by the dashed line or indicated in the figure. Although W-like cells always displayed orientation tuning, there was very little consistency in the magnitude of the orientation tuning across spatial frequencies; there was no regular pattern as seen in X- and Y-like cells. Direction selectivity in W-like cells also displayed no consistent pattern across spatial frequencies. However, a spatial frequency could always be found where the cell was not direction selective and that usually was at a high spatial frequency. For example, in Figure 36a and b, there were both orientation and direction tuning but in Figure 36c (a higher spatial frequency) there was only orientation tuning. Similar results occurred in Figure 37; at low spatial frequencies the cell had both types of tuning (Figures 37a, d, e) but at higher spatial frequencies, there was only orientation tuning (Figures 37b, c, e, f). Finally, there was no indication that W-like cells possessed any of the unusual tuning at very high spatial frequencies found in Y- and possibly in X-like cells. Once again, the W-like cells' characteristics appear to be different from X- and Y-like cells.

3.5 Spatial and Spectral Properties.

To examine the relationship between spatial and spectral proper-

ties, each ganglion cell was classified along both spatial and spectral dimensions. Each cell was classified as X-, Y- or W-like based on its response to a contrast-reversal grating; cells were also classified as spectrally opponent or nonopponent as well as by the response of the L-cones to center stimulation ($L^+/-$, $L-/^+$ or $L^+/^+$ center cells). All spectral classifications were based on responses to monochromatic stimuli presented to the center (spot of light) and to the surround (annulus of light) of the cell's receptive field. (See Section 3.1 for details.)

A total of ninety cells were successfully classified by their spatial summation and spectral properties. To examine the relationship between spatial summation class (X-, Y-, and W-like) and spectral class ($L^+/-$, $L-/^+$, and $L^+/^+$ center) a 3 by 3 chi-square test of independence was calculated on the frequencies across the various categories. Table 1 shows the frequencies and percentages for each category. The results indicate that spatial summation class was independent of spectral class ($\chi^2(4) = 3.92$, $p > 0.05$). That is, a cell classified as X-like was just as likely to be an $L^+/-$, $L-/^+$, or $L^+/^+$ center cell; the same was true of Y- and W-like cells.

A 3 by 2 chi-square test for independence was performed on the frequencies of spatial summation class and spectral opponency. Results revealed that spatial summation was independent of the fact that a cell was spectrally opponent or nonopponent ($\chi^2(2) = 0.86$, $p > 0.05$). Table 2 provides the frequencies and percentages across the categories.

In summary, there does not appear to be any relationship

Table 1

Spatial Summation Class by Spectral Class

		Spectral Class			
		$L^+/-$	$L-/^+$	$L^+/^+$	Total
Spatial	X-like	4(24%)	7(41%)	6(35%)	17(19%)
Summation	Y-like	9(23%)	17(44%)	13(33%)	39(43%)
Class	W-like	14(41%)	13(38%)	7(21%)	34(38%)
	Total	27(30%)	37(41%)	26(29%)	

Table 2

Spatial Summation Class by Spectral Opponency

		Spectral Opponency		
		Opponent	Nonopponent	Total
Spatial	X-like	6(35%)	11(65%)	17(19%)
Summation	Y-like	11(28%)	28(72%)	39(43%)
Class	W-like	13(38%)	21(62%)	34(38%)
	Total	30(33%)	60(67%)	

between a cell's spatial summation properties and its spectral properties; X-, Y-, and W-like cells are equally likely to be spectrally opponent or nonopponent, and $L^+/-$, $L-/^+$, or $L^+/^+$ center cells. Although spatial summation classification was independent of the cell's spectral properties, other spatial properties, such as the S-CSF and sensitivity to contrast (contrast gain), were influenced by the cells' spectral properties.

3.5.1 S-CSF.

The S-CSFs of all the cells for which this information was available were entered into a data matrix and then sorted into the appropriate categories and averaged. All S-CSFs were normalized with respect to their own maximum sensitivity value. Only S-CSFs obtained with drifting gratings of 4 Hz were used to eliminate any spatio-temporal interactions (see Section 3.3). For the purpose of comparability, the response measure for all S-CSFs was the amplitude of the fundamental component. This provided information regarding the center and surround mechanisms only, which, at least for X- and Y-like cells, are similar; nonlinear subunits were excluded from the analysis. The normalized S-CSFs from the different cells were averaged, and the average renormalized to give the mean function for a particular classification of cells.

Average S-CSFs for X-, Y-, and W-like cells are shown in Figure 38. All three functions are typical in shape in that they are most sensitive to middle spatial frequencies, attenuate sharply at higher spatial frequencies and gradually decrease in sensitivity at

Figure 38

Average S-CSFs of X-, Y-, and W-like cells. The response measure was the amplitude of the fundamental component. The S-CSFs of X- (enclosed stars), Y-, (open stars), and W-like (asterisks) cells were determined by their responses to a 4 Hz drifting grating. Sensitivity for all Y- and W-like and most X-like cells were obtained by interpolation on the response vs. contrast curves to find the contrast necessary for a constant response amplitude. The sensitivity for some X-like cells was calculated directly from the response measure. Each average S-CSF was renormalized separately. The number of cells for each spatial summation class is given at the bottom of the figure. Error bars represent one standard error of the mean.

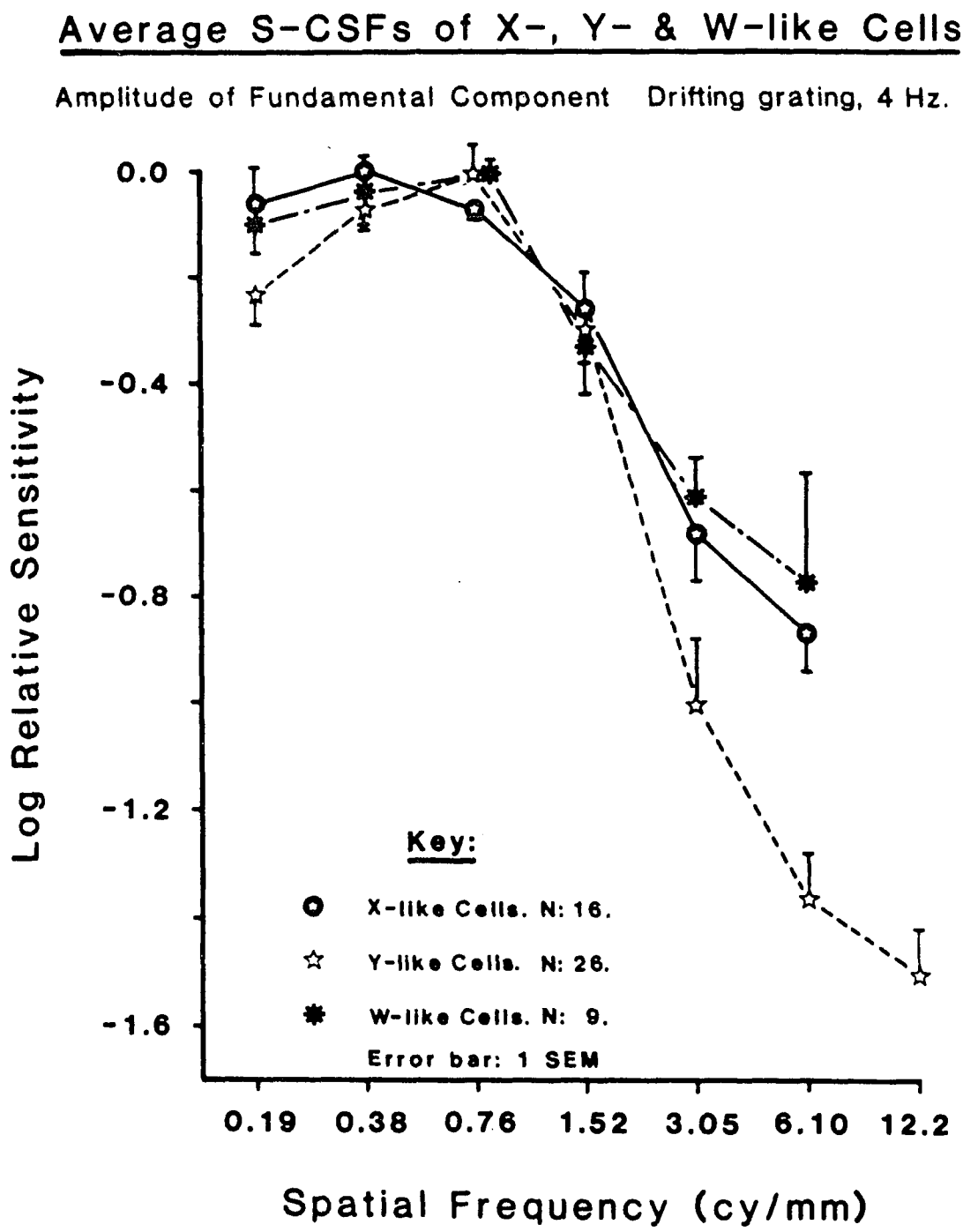
Average S-CSFs of X-, Y- & W-like Cells
Amplitude of Fundamental Component Drifting grating, 4 Hz.
0.0
-0.4
-0.8
-1.2
-1.6
Log Relative Sensitivity
Key:
X-like Cells. N: 16.
Y-like Cells. N: 26.
W-like Cells. N: 9.
Error bar: 1 SEM
0.19
0.38
0.76
1.52
3.05
6.10
12.2
Spatial Frequency (cy/mm)

lower spatial frequencies. It is clear from the figure that X- and W-like cells are relatively more sensitive at higher spatial frequencies than Y-like cells. The high-frequency cut-off, if one were to extrapolate, would be much lower for Y-like cells than for X- and W-like cells. Since the high frequency portion is due to the smallest subarea in the receptive field (i.e., the "center" for X- and Y-like cells) these findings suggest that the Y-like cell's center area is somewhat larger than the center of X-like cells. W-like cells clearly have a receptive field subarea similar in size to the X-like cell's center area; however, when examined in other species (Gordon and Shapley, 1978), W-like cells do not appear to possess the classic center and surround arrangement as in X- and Y-like cells.

Spectral Class. Figure 39 compares the average S-CSFs of X-like $L^+/-$, $L-/^+$, and $L^+/^+$ center cells. Although the $L^+/-$ and $L-/^+$ center cells' S-CSFs were similar in shape, the $L^+/-$ center cells' S-CSF was shifted to the higher spatial frequencies, both in their peak sensitivity and their sensitivity at higher spatial frequencies. Both of these results support the notion that $L^+/-$ center cells have a smaller receptive field center than the $L-/^+$ center cells. The $L^+/^+$ center cells also have better spatial resolution than $L-/^+$ and possibly, $L^+/-$ center cells, although it is not as obvious at the peak sensitivity. The S-CSF of the $L^+/^+$ center cells also appeared to be broader in its band-pass characteristics than both $L^+/-$ and $L-/^+$ center cells.

Similar, and more pronounced, differences occurred when the Y-like $L^+/-$, $L-/^+$, and $L^+/^+$ center cells were compared as shown in

Figure 39

Average S-CSFs of X-like cells by spectral class. The response measure was the amplitude of the fundamental component. The average S-CSFs of $L^+/-$ (closed circles), $L-/^+$ (open circles), and $L^+/^+$ (closed triangles) center cells were determined by their responses to a 4 Hz drifting grating. Sensitivity was obtained either by interpolation on the response vs. contrast curves to find the contrast necessary for a constant response amplitude or by using response measures directly. Each average S-CSF was renormalized separately. The number of cells for each spectral class is given at the bottom of the figure. Error bars represent one standard error of the mean.

Average S-CSFs of X-like Cells

Amplitude of Fundamental Component

Drifting grating, 4 Hz.

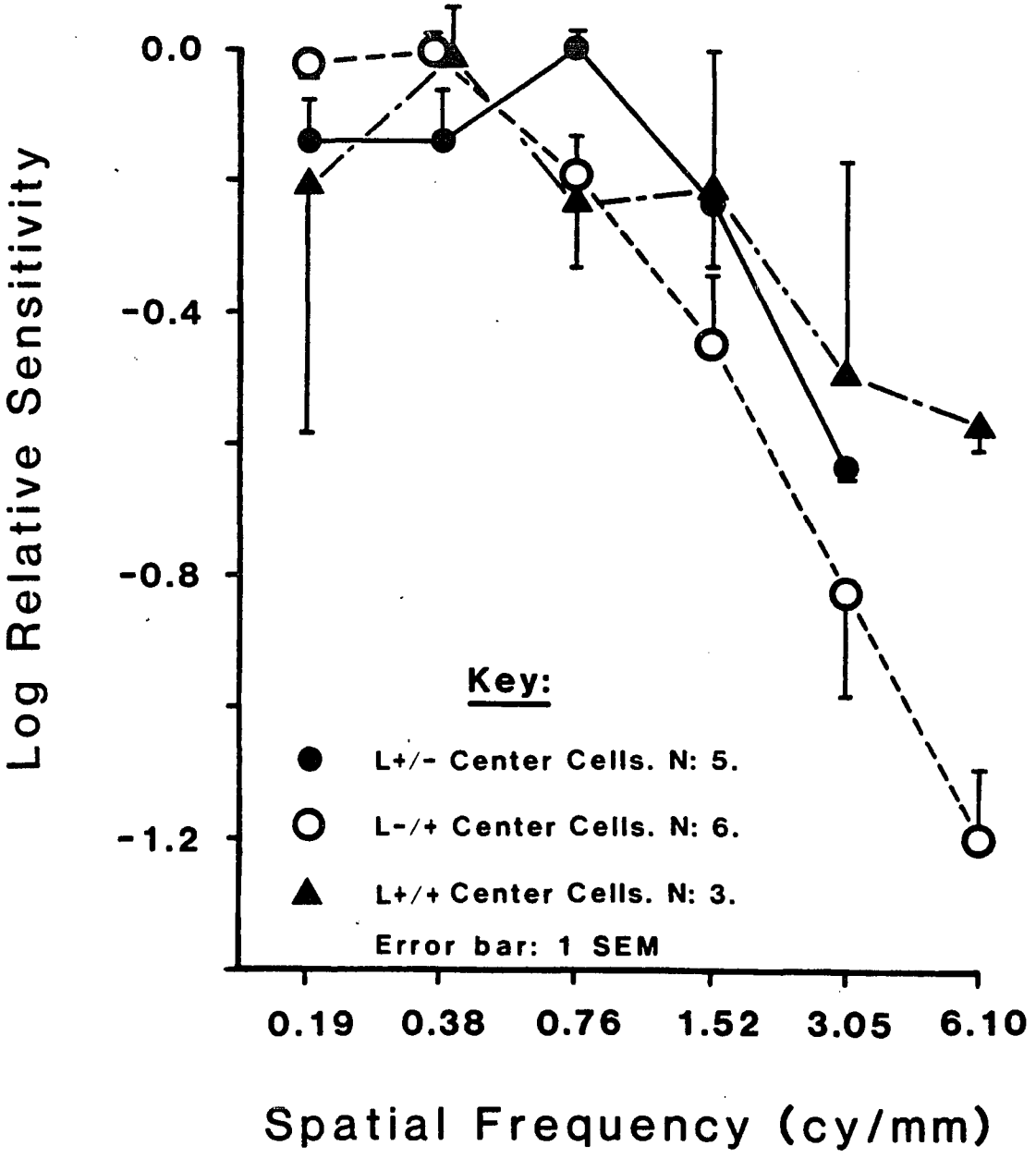

Figure 40

Average S-CSFs of Y-like cells by spectral class. The response measure was the amplitude of the fundamental component. The average S-CSFs of $L^+/-$ (closed circles), $L-/^+$ (open circles), and $L^+/^+$ (closed triangles) center cells were determined by their responses to a 4 Hz drifting grating. Sensitivity was obtained by interpolation on the response vs. contrast curves to find the contrast necessary for a constant response amplitude. Each average S-CSF was renormalized separately. The number of cells for each spectral class is given at the bottom of the figure. Error bars represent one standard error of the mean.

Average S-CSFs of Y-like Cells

Amplitude of Fundamental Component

Drifting grating, 4 Hz.

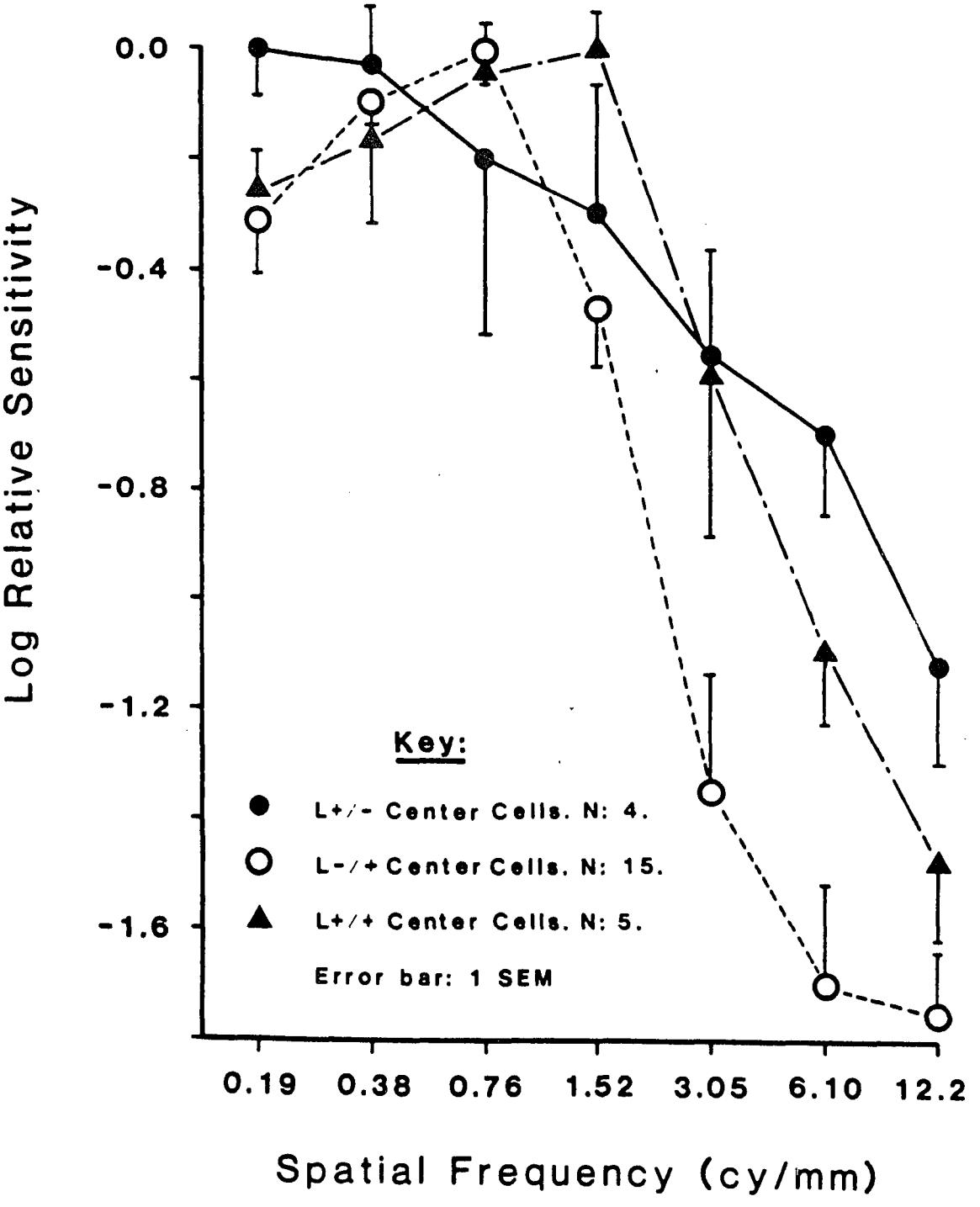

Figure 40. $L^+/-$ center cells' high frequency cut-off was much higher than that of $L-/^+$ center cells. However, unlike the X-like S-CSFs, the peak sensitivity of Y-like $L^+/-$ center cells' S-CSF was at a lower spatial frequency than the $L-/^+$ center cells' peak sensitivity. This could be due to the fact that there was a small number of $L^+/-$ center cells in the average S-CSFs. Also, these was much more variability in the responses of Y-like cells than in X-like cells.

In Figure 41, the average S-CSF of W-like cells for each spectral type is shown. Unlike X- and Y-like cells, there was virtually no difference in the S-CSFs across the spectral cell types. There was no difference in either the peak sensitivity or the relative sensitivity at high spatial frequencies between $L^+/-$ and $L-/^+$ center cells. The fact that there were no differences across spectral cell types for W-like cells while there were clear differences in the S-CSFs of the spectral types in X- and Y-like cells support the fact that W-like cells are functionally different from X- and Y-like cells.

To produce a clearer picture of the differences across spectral cell types (by increasing sample size), and since spatial summation class was independent of spectral class (see Section 3.5), the S-CSFs of the X- and Y-like cells were combined and compared across spectral class; W-like cells were not included in the averaging since they are clearly functionally different from X- and Y-like cells along this dimension. Figure 42 displays the results. $L^+/-$ and $L-/^+$ center cells were again relatively more sensitive at the higher spatial frequencies than $L-/^+$ center cells. The peak sensitivity of the $L-/^+$ center cells was also at a slightly lower frequency than both the $L^+/-$

Figure 41

Average S-CSFs of W-like cells by spectral class. The response measure was the amplitude of the fundamental component. The average S-CSFs of $L^+/-$ (closed circles), $L-/^+$ (open circles), and $L^+/^+$ (closed triangles) center cells were determined by their responses to a 4 Hz drifting grating. Sensitivity was obtained by interpolation on the response vs. contrast curves to find the contrast necessary for a constant response amplitude. Each average S-CSF was renormalized separately. The number of cells for each spectral class is given at the bottom of the figure. Error bars represent one standard error of the mean.

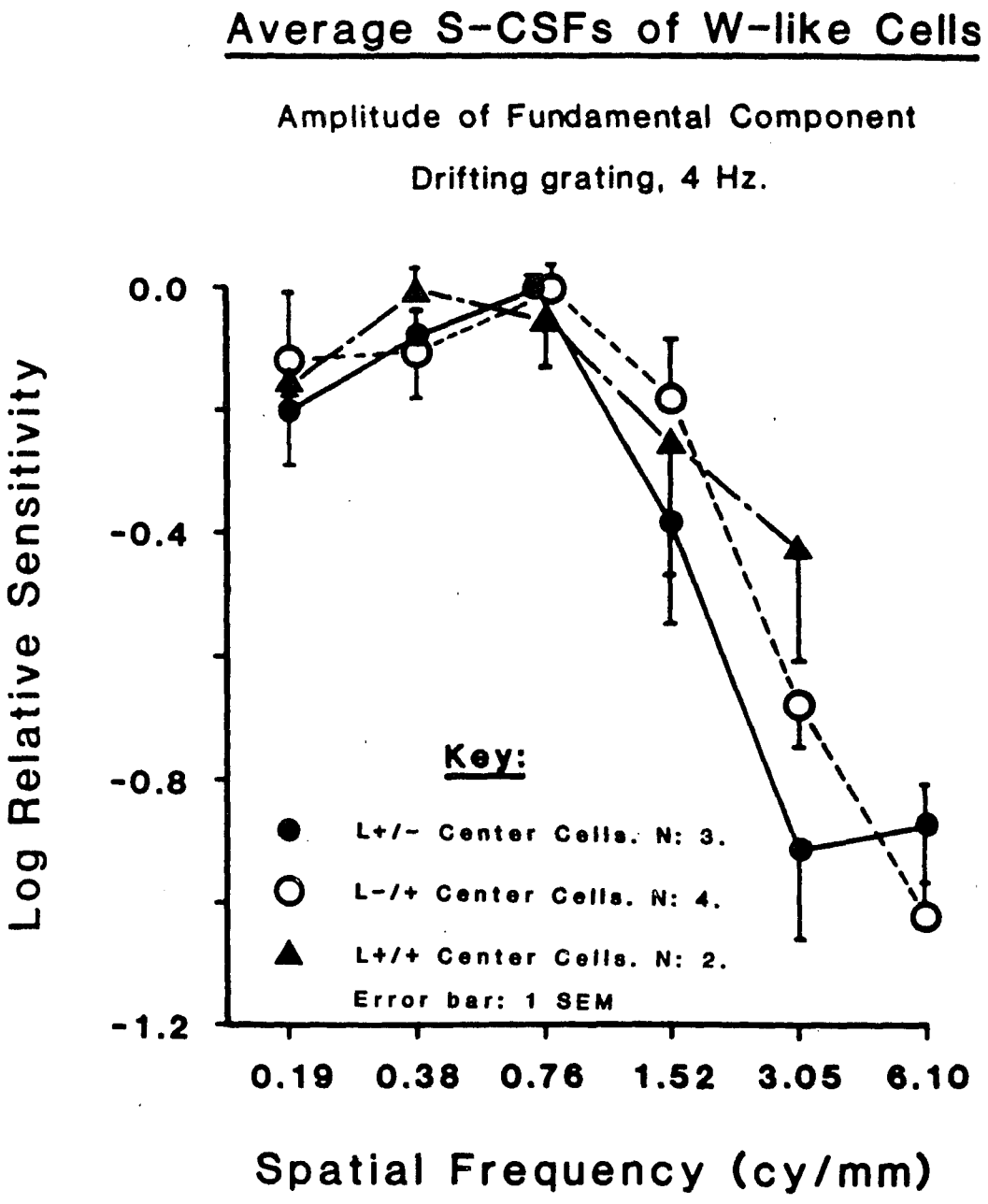
Average S-CSFs of W-like Cells
Amplitude of Fundamental Component
Drifting grating, 4 Hz.
Log Relative Sensitivity
0.0
-0.4
-0.8
-1.2
Key:
L+/- Center Cells. N: 3.
L-/+ Center Cells. N: 4.
L+/+ Center Cells. N: 2.
Error bar: 1 SEM
0.19
0.38
0.76
1.52
3.05
6.10
Spatial Frequency (cy/mm)

Figure 42

Average S-CSFs of X- and Y-like cells by spectral class. The response measure was the amplitude of the fundamental component. The average S-CSF of $L^+/-$ (closed circles), $L-/^+$ (open circles), and $L^+/^+$ (closed triangles) center cells were determined by their responses to a 4 Hz drifting grating. Sensitivity for all Y-like and most X-like cells were obtained by interpolation on the response vs. contrast curves to find the contrast necessary for a constant response amplitude. The sensitivity for some X-like cells was calculated directly from the response measure. Each average S-CSF was renormalized separately. The number of cells for each spectral class is given at the bottom of the figure. Error bars represent one standard error of the mean.

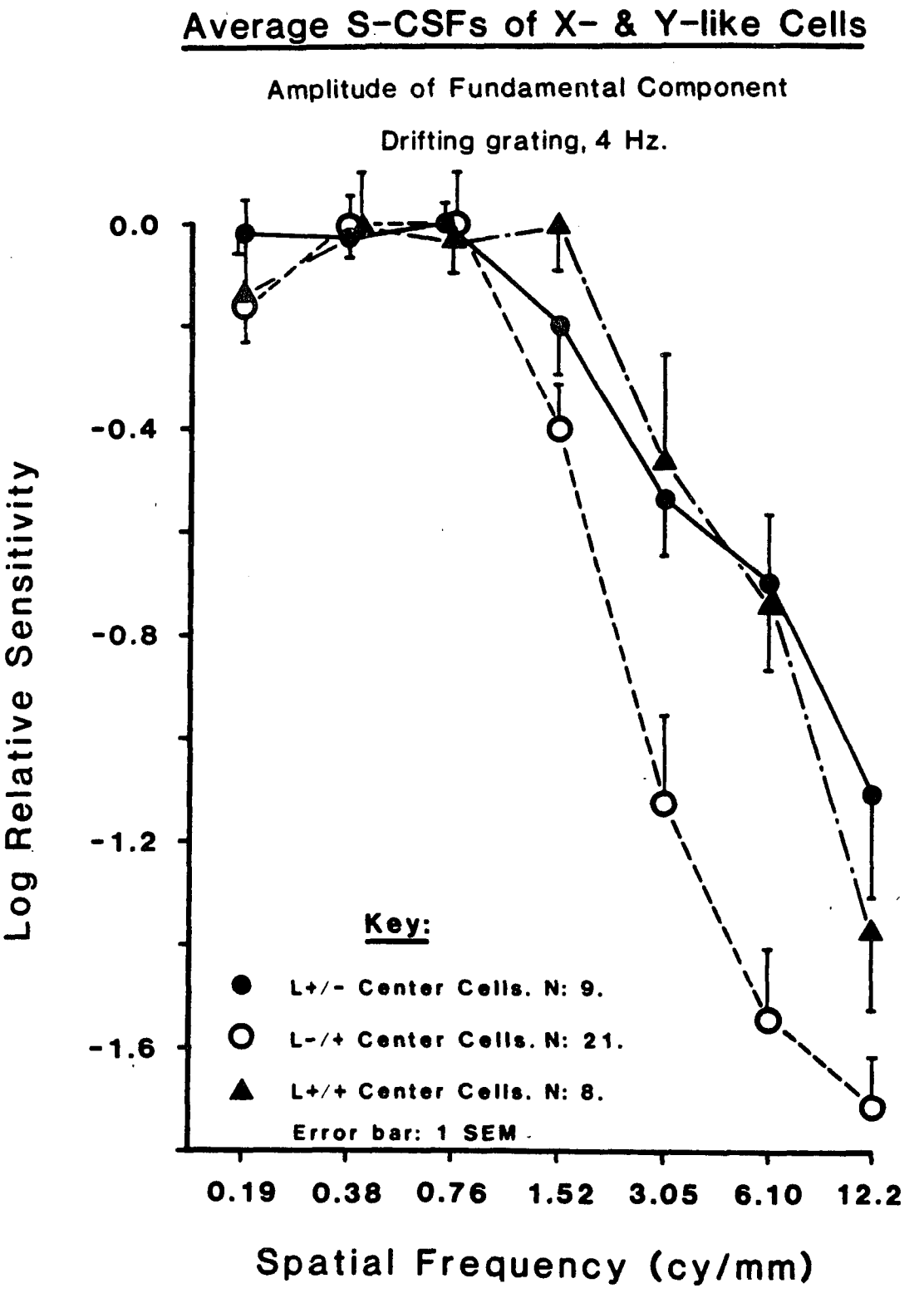
Average S-CSFs of X- & Y-like Cells
Amplitude of Fundamental Component
Drifting grating, 4 Hz.
0.0
-0.4
-0.8
-1.2
-1.6
Log Relative Sensitivity
Key:
L+/- Center Cells. N: 9.
L-/+ Center Cells. N: 21.
L+/+ Center Cells. N: 8.
Error bar: 1 SEM
0.19
0.38
0.76
1.52
3.05
6.10
12.2
Spatial Frequency (cy/mm)

and $L^+/^+$ center peaks; the $L^+/^+$ center cells had the largest shift to higher spatial frequencies.

In summary, it is clear that for X- and Y-like cells, $L^+/-$ center cells possess a smaller receptive field center than $L-/^+$ center cells. This is illustrated by the facts that $L^+/-$ center cells are relatively more sensitive to higher spatial frequencies than $L-/^+$ center cells and that their peak sensitivity is shifted slightly to higher frequencies. For the $L^+/^+$ center cells, it is apparent that their center area is also smaller than $L-/^+$ center and probably $L^+/-$ center cells. All of these conclusions correspond to the findings obtained by mapping the receptive field center with small spots of light (see Section 1.6.3). Finally, W-like cells continue to live up to their name -- they appear to be a class apart from the other spatial summation classes.

Spectral Opponency. S-CSFs were also compared as a function of spectral opponency. For both X- and Y-like cells, the S-CSF depended on whether the cell was spectrally opponent or nonopponent, at least for $L^+/-$ and $L-/^+$ center cells. Figure 43 compares the average S-CSFs of cells that were spectrally opponent and nonopponent. Since the S-CSFs of X- and Y-like cells were similar, they were averaged together. The response measure was the amplitude of the fundamental component and each curve was normalized to its own maximum sensitivity. There are two points worth noting in this figure: First, the spectrally opponent S-CSF was shifted to higher spatial frequencies in both the peak sensitivity and the high-frequency portion of the curve as compared with the spectrally nonopponent S-CSF. This suggests that the spectrally opponent cells possess a

Figure 43

Average S-CSFs of X- and Y-like cells by spectral opponency. The response measure was the amplitude of the fundamental component. The average S-CSFs of spectrally opponent (open hexagons) and spectrally nonopponent (closed hexagons) cells were determined by their responses to a 4 Hz drifting grating. Sensitivity values were determined as in Figure 42. Each average S-CSF was renormalized separately. The number of cells for each category is given at the bottom of the figure. Error bars represent plus or minus one standard error of the mean.

Average S-CSFs of X- & Y-like Cells by Spectral Opponency

Amplitude of Fundamental Component Drifting grating, 4 Hz.

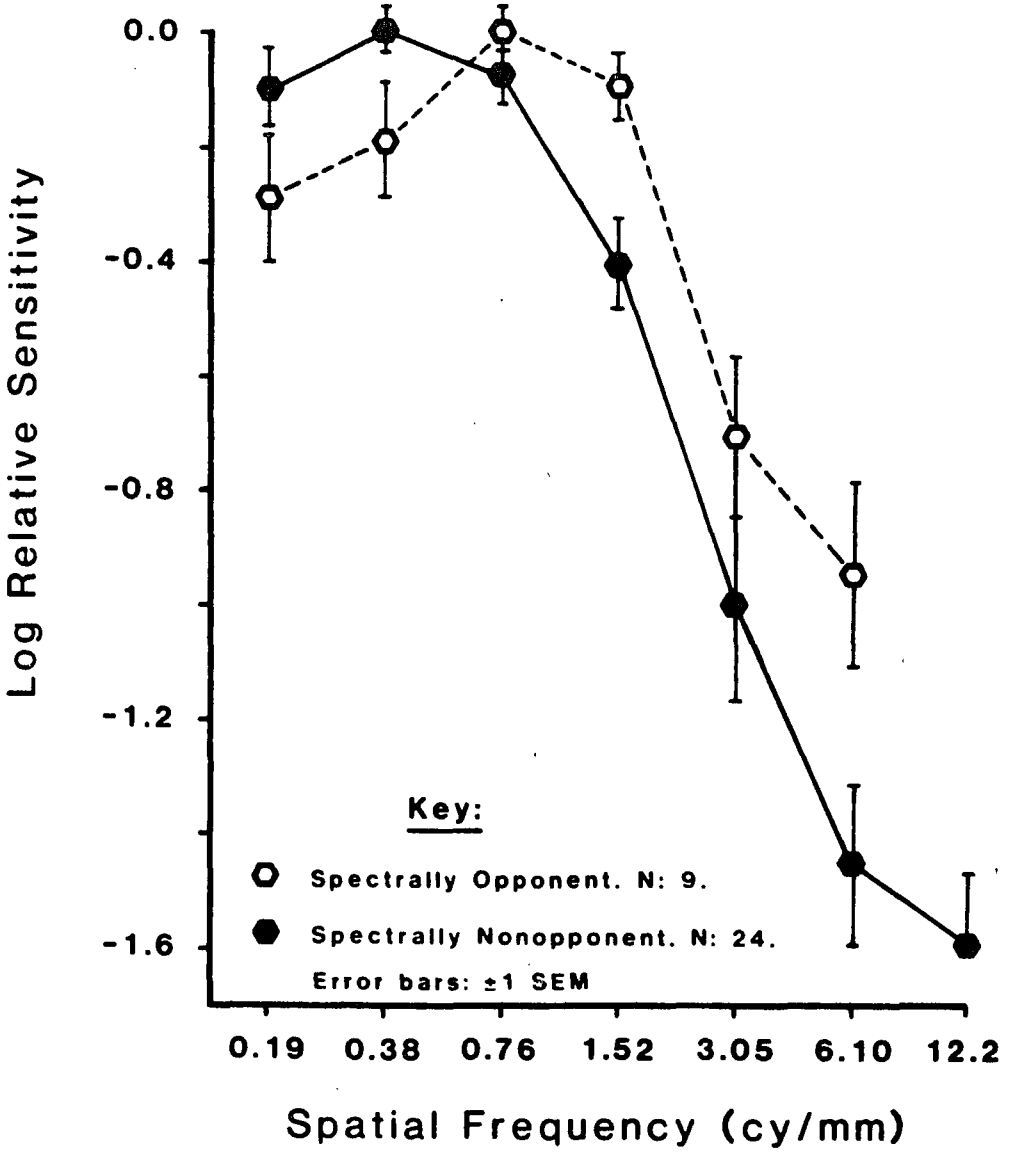

smaller receptive field center than spectrally nonopponent cells. Second, there was more low frequency attenuation in the spectrally opponent cells' function than in the nonopponent cells' S-CSF. This may be the result of not testing at lower spatial frequencies; sliding the spectrally opponent function to superimpose the peak sensitivities of the two curves shows that at the lowest spatial frequency tested (0.19 cy/mm) the curves are similar -- the most dramatic attenuation for both functions would occur at frequencies lower than 0.19 cy/mm. Regarding W-like cells, the sample size was too small and the variability across cells was too large to draw any conclusions.

Since both spectral class and spectral opponency/nonopponency appeared to influence the S-CSF of cells, each cell was sorted by both factors and then averaged. That is, spectrally opponent cells were divided into $L^+/-$, $L-/^+$ and $L^+/^+$ center types and average S-CSFs were calculated; the same was done for spectrally nonopponent cells. The major distinction between the spectrally opponent and nonopponent cells was that the nonopponent S-CSF reflected primarily the input of one cone type (L-cones) while the spectrally opponent S-CSF was the result of an overt interaction of at least two cone inputs. Note that the nonopponent cells are not necessarily driven by only one cone type, but that one input dominated the response. This was also true when the CRT display was used, since the L-cone input of spectrally nonopponent cells dominated the ganglion cell response across the spectrum. This was verified by the cell's response to monochromatic stimuli at various wavelengths and by the fact that when stimulated by the CRT display, the cell's response

modulation corresponded to its L-cone center component. For example, an $L^+/-$ center cell's response was in-phase with the sinusoidal temporal modulation of a uniform field (i.e., an increase in the cell's response with an increase in stimulus intensity).

The results are shown in Figure 44. X- and Y-like cells were combined; W-like cells were omitted from the calculations. For spectrally nonopponent (predominately L-cones) cells, there was a clear distinction across the spectral cell types (Figure 44a). $L^+/-$ and $L-/^+$ center cell types differed both in their sensitivities at high spatial frequencies and at the spatial frequency where sensitivity begins to decline (i.e., peak sensitivity). For spectrally opponent cells (Figure 44b) however, the shift in S-CSFs was not as apparent. Although there were slight differences at higher spatial frequencies, the peak sensitivities across the spectral cell types were the same.

3.5.2 Response to Contrast.

Recently, a new classification scheme has been introduced in an attempt to examine the relationship across the various cell classifications. This classification is based on the neuron's response to contrast (Kaplan and Shapley, 1984; 1986), and was examined in the goldfish ganglion cells in the following way: The response versus contrast function was obtained from the cell's responses to the peak spatial frequency of the S-CSF. The stimulus was a 4 Hz drifting grating and the contrast ranged from zero (dummy stimulus) to 95 percent. The response measure used for each cell was the amplitude of the fundamental component. The response vs. contrast function

Figure 44

Average S-CSFs of X- and Y-like cells by spectral class and spectral opponency. The response measure was the amplitude of the fundamental component. The average S-CSFs of $L^+/-$ (closed circles), $L-/^+$ (open circles), and $L^+/^+$ (closed triangles) center cells were calculated by their responses to a 4 Hz drifting grating. Spectrally nonopponent cells are shown in (a); spectrally opponent cells are shown in (b). Sensitivity was obtained as in Figure 42. Each average S-CSF was renormalized separately. The number for each category of cell types is given at the bottom of each figure. Error bars represent one standard error of the mean.

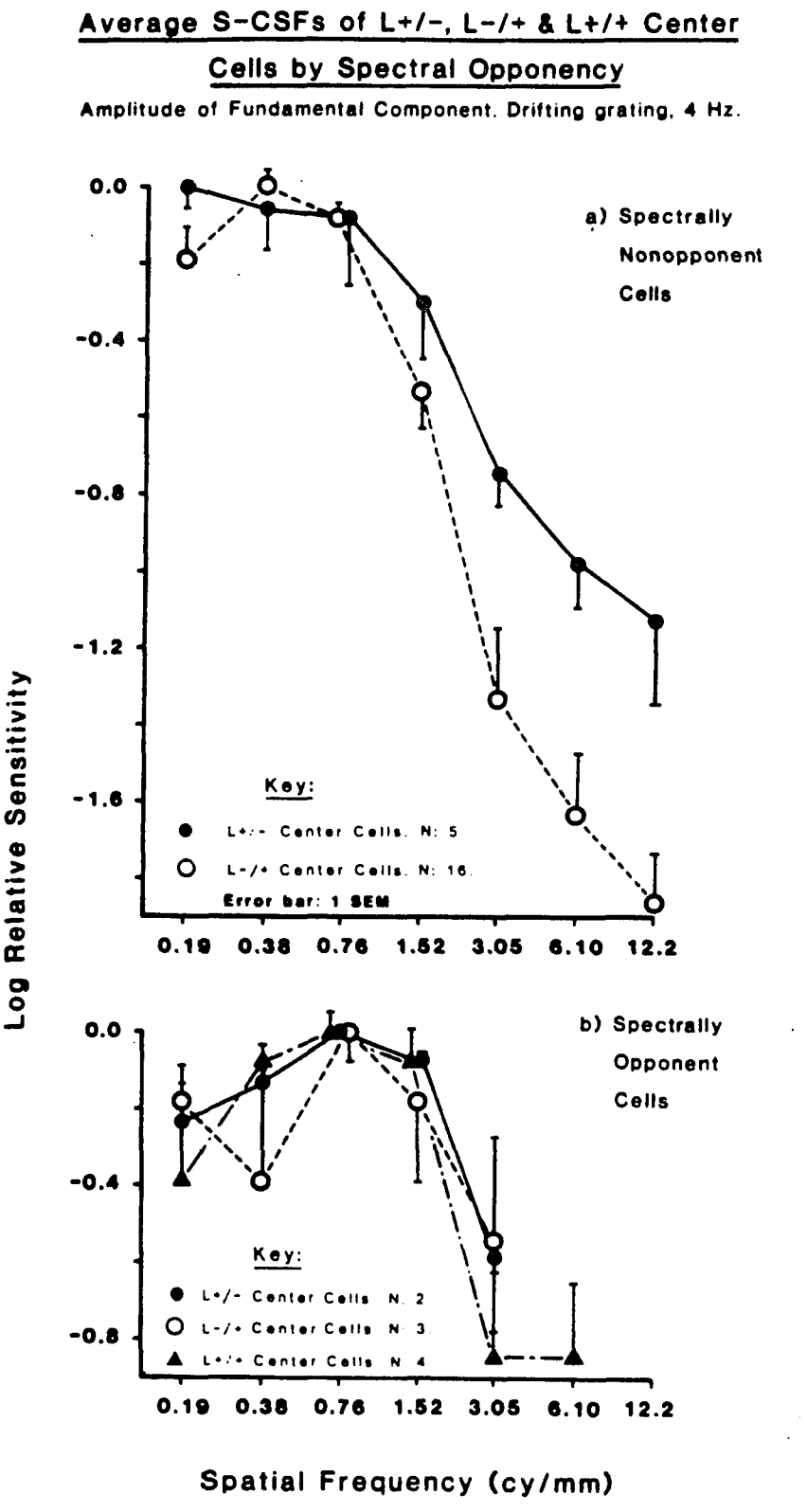
Average S-CSFs of L+/-, L-/+ & L+/+ Center Cells by Spectral Opponency
Amplitude of Fundamental Component. Drifting grating, 4 Hz.
a) Spectrally Nonopponent Cells
0.0
-0.4
-0.8
-1.2
-1.6
Key:
L+/- Center Cells. N: 5
L-/+ Center Cells. N: 16.
Error bar: 1 SEM
0.19 0.38 0.76 1.52 3.05 6.10 12.2
b) Spectrally Opponent Cells
0.0
-0.4
-0.8
Key:
L+/- Center Cells N: 2
L-/+ Center Cells N: 3
L+/+ Center Cells N: 4
0.19 0.38 0.76 1.52 3.05 6.10 12.2
Log Relative Sensitivity
Spatial Frequency (cy/mm)

for each cell was entered into a data matrix, sorted and averaged as described earlier for the average S-CSFs. Unfortunately, not all cells were presented with all contrasts, so many of the averaged response functions had an unequal number of data points. The number associated with each curve represents the total number of cells used in the calculations.

Figure 45 compares the contrast-response curves of $L^+/-$, $L-/^+$ and $L^+/^+$ center cells. In this figure, X- and Y-like cells were combined; W-like cells were omitted since no differences were found across spectral class for W-like cells. The response measure was the amplitude of the fundamental component. As can be seen, $L-/^+$ center cells were more sensitive to contrast than both $L^+/-$ and $L^+/^+$ center cells; in fact, by about 10% contrast their response saturated. For the $L^+/-$ center cells, the linear portion of the function extended over a wide range of contrasts -- there was little evidence of saturation in this function. $L^+/^+$ center cells possessed attributes of both $L^+/-$ and $L-/^+$ center cells. The linear portion of the function had a similar slope to $L^+/-$ center cells but saturated at the same contrast as $L-/^+$ center cells. Finally, there were differences in response saturation among the cell types. The $L^+/^+$ center cells' response saturated at about 40 spikes/sec while $L-/^+$ center cells reached 90 spikes/sec and the $L^+/-$ center cells' continued to respond at even higher rates.

Figure 46 compares the contrast-response curves sorted by spectral opponency. Once again, X- and Y-like cells were averaged together. There was clearly a difference between spectrally opponent

Figure 45

Average response vs. contrast curves of X- and Y-like cells by spectral class. The response measure was the amplitude of the fundamental component. The average response vs. contrast curves of $L^+/-$ (closed circles), $L-/^+$ (open circles), and $L^+/^+$ (closed triangles) center cells were determined by the cells' responses to a 4 Hz drifting grating at the spatial frequency of peak sensitivity for each cell. The number of cells for each spectral class is given at the bottom of the figure. Error bars represent one standard error of the mean.

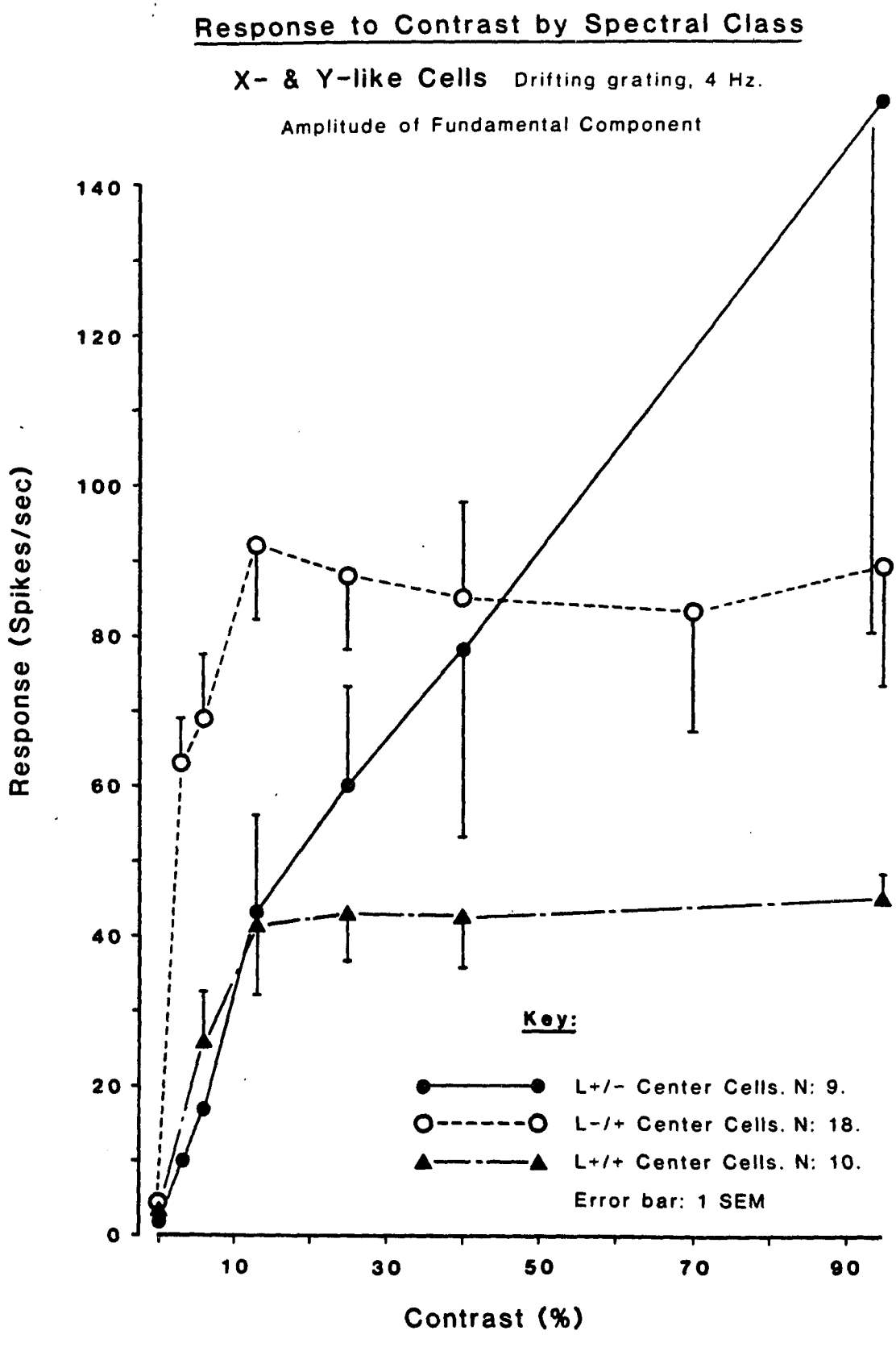
Response to Contrast by Spectral Class
X- & Y-like Cells Drifting grating, 4 Hz.
Amplitude of Fundamental Component
Response (Spikes/sec)
140
120
100
80
60
40
20
0
10
30
50
70
90
Contrast (%)
Key:
L+/- Center Cells. N: 9.
L-/+ Center Cells. N: 18.
L+/+ Center Cells. N: 10.
Error bar: 1 SEM

Figure 46

Average response vs. contrast curves of X- and Y-like cells by spectral opponency. The response measure was the amplitude of the fundamental component. The average response vs. contrast curves of spectrally nonopponent (closed hexagons) and spectrally opponent (open hexagons) cells were determined by the cells' responses to a 4 Hz drifting grating at the spatial frequency of peak sensitivity for each cell. The number of cells in each category is given at the bottom of the figure. Error bars represent plus or minus one standard error of the mean.

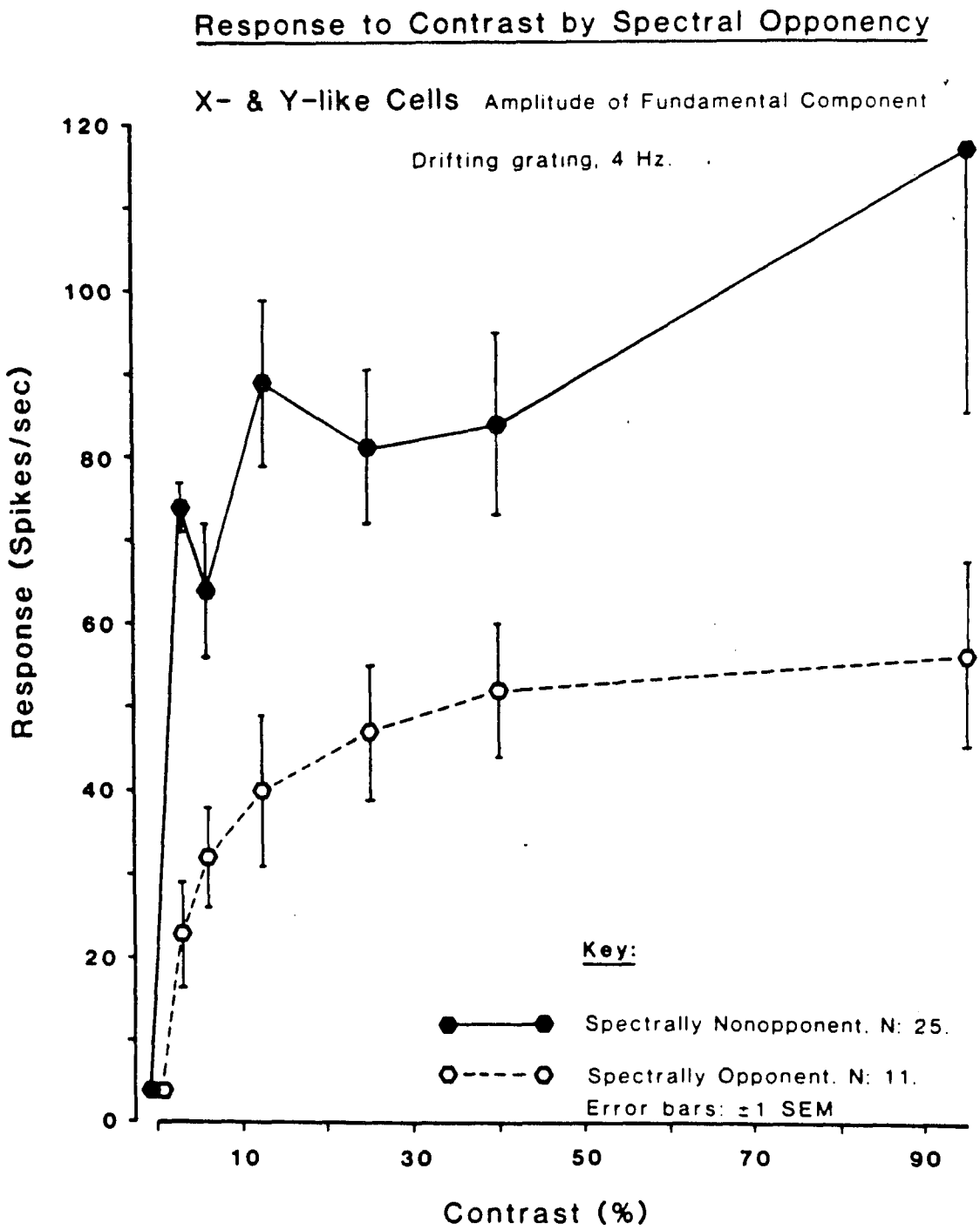
Response to Contrast by Spectral Opponency
X- & Y-like Cells Amplitude of Fundamental Component
Drifting grating, 4 Hz.
Response (Spikes/sec)
120
100
80
60
40
20
0
10
30
50
70
90
Contrast (%)
Key:
Spectrally Nonopponent. N: 25.
Spectrally Opponent. N: 11.
Error bars: ±1 SEM

and nonopponent cells. Spectrally nonopponent cells were much more sensitive to contrast (i.e., steeper slope) than spectrally opponent cells. There was also a difference in where the response saturated; spectrally nonopponent cells saturated at a much higher response rate than the spectrally opponent cells. These findings correspond to the division found in macaque neurons (Kaplan and Shapley, 1984; 1986). However, if spectral class is separated by spectral opponency as well, an interesting pattern emerges.

Figure 47 shows the contrast vs. response curves of $L^+/-$, $L-/^+$ and $L^+/^+$ center cells as a function of spectral opponency. As can be seen in Figure 47a, there was an obvious difference in spectrally opponent and nonopponent curves for $L^+/-$ center cells. The spectrally nonopponent cells were much more sensitive to contrast and saturated at a much higher response rate than the spectrally opponent cells. For $L-/^+$ center cells (Figure 47b), the difference between spectrally opponent and nonopponent cells was not as apparent. Although the slope of the nonopponent cells was slightly steeper, their response saturation values were similar; also, both curves saturated at the same contrast value. Regarding the $L^+/^+$ center cells (Figure 47c), there was no clear difference between the contrast-response curves. Therefore, a cell's sensitivity to contrast depends not only on whether the cell is spectrally opponent or nonopponent, but also on the cell's spectral class.

Figure 47

Average response vs. contrast curves of X- and Y-like cells by spectral opponency and spectral class. The response measure was the amplitude of the fundamental component. The average response vs. contrast curves of spectrally nonopponent (closed squares) and spectrally opponent (enclosed stars) cells for $L^+/-$ (a), $L-/^+$ (b), and $L^+/^+$ (c) center cells were determined by the cells' responses to a 4 Hz drifting grating at the spatial frequency of peak sensitivity for each cell. The number of cells in each category is given at the bottom of each figure. Error bars represent one standard error of the mean.

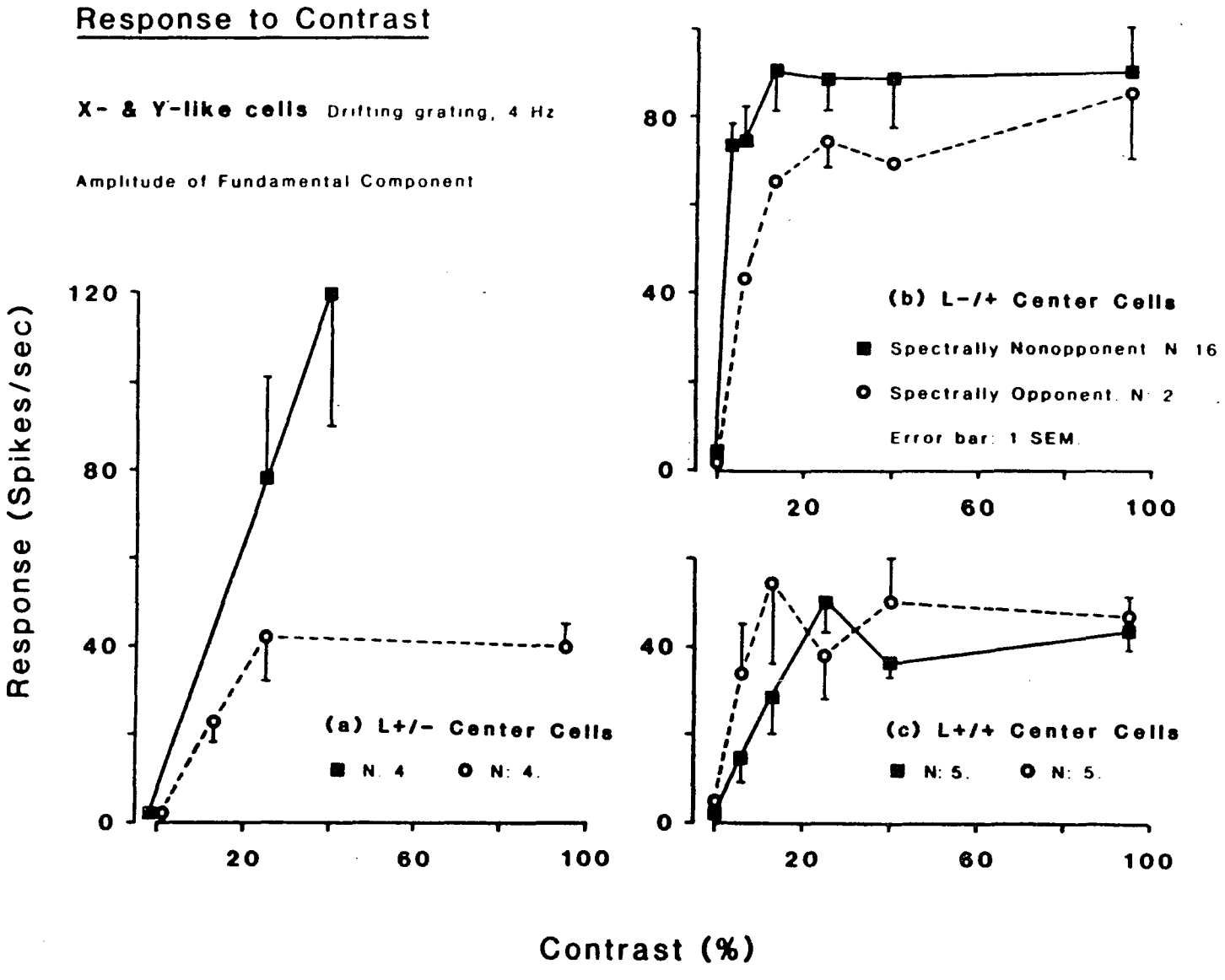
Response to Contrast
X- & Y-like cells Drifting grating, 4 Hz
Amplitude of Fundamental Component
Response (Spikes/sec)
120
80
40
0
20
60
100
(a) L+/- Center Cells
N: 4
N: 4.
(b) L-/+ Center Cells
Spectrally Nonopponent N: 16
Spectrally Opponent N: 2
Error bar: 1 SEM
(c) L+/+ Center Cells
N: 5.
N: 5.
Contrast (%)

3.6 Unusual Units.

3.6.1 Y-like Cells.

There was a small subclass of Y-like cells that gave an unusual response to drifting gratings. All of these cells (7 cells) were undoubtedly Y-like cells; they met all the criteria and were similar to all Y-like cells in their responses to a contrast-reversal grating. However, when a grating was drifted across the receptive field, their responses were very complex; the type of response depended on the spatial frequency of the grating. Figure 48 shows the response of such a cell at two spatial frequencies. The grating was drifted at 4 Hz with a contrast of 13 percent. The abscissa represents one stimulus cycle (250 msec) divided into 30 discrete bins (8.3 msec per time bin). The ordinate is the response rate per time bin averaged over 56 stimulus cycles. At the lower spatial frequency (Figure 48a), the response pattern was at double the stimulus frequency (i.e., most of the response was at the second harmonic), while at the high spatial frequency (Figure 48b), the response matched the temporal frequency of the stimulus (most of the response at the fundamental). This response pattern is the reverse of the typical Y-like cell response. Most Y-like cells' responses modulate at the stimulation rate at low spatial frequencies, but deviate from this pattern at high spatial frequencies. What is also puzzling is that for these unusual units, there is very little power at any other component other than 2f at low

Figure 48

Averaged response histograms of an unusual Y-like cell to a 4 Hz drifting grating at two different spatial frequencies. The contrast of the grating was 13 percent. The abscissa represents one complete stimulus cycle. Note that at 0.76 cy/mm (a) there is a clear doubling response, but at 3.05 cy/mm (b), the response modulates at the stimulus frequency.

Response Histogram of an Unusual Y-like Cell

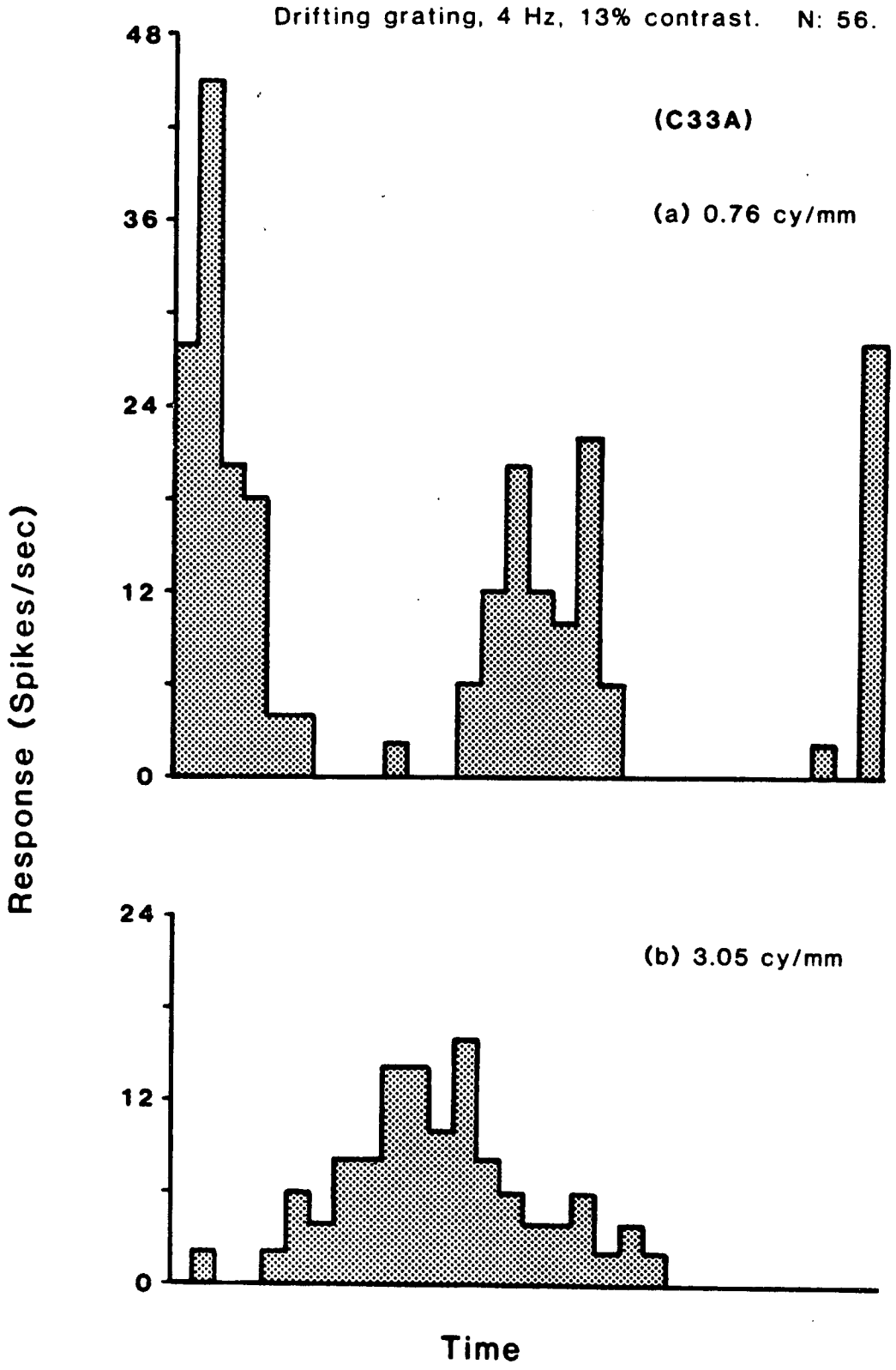

spatial frequencies. For typical Y-like cells, response to a drifting grating is never a pure doubling response.

Spatial resolution of a similar cell was determined for the max-min, the fundamental and the second harmonic components and is shown in Figure 49. The grating was drifted at a rate of 4 Hz and presented at 13% contrast. The ordinate is derived directly from the response measures and is therefore labelled log relative response (see Section 3.3.1). The spatial resolution of the max-min response was very broad-band with no low frequency attenuation (Figure 49a). However, the spatial tuning of the fundamental and second harmonic components separately (Figure 49b) were typical in their shape with respect to other S-CSFs. They were both sharply tuned and both possessed low frequency attenuation. They differed from the other functions in that the second harmonic component was more sensitive at low spatial frequencies than the fundamental component. (All values in the figure were normalized with respect to one maximum response; hence, the second harmonic component was more sensitive than the fundamental at lower spatial frequencies.) Also, the second harmonic spatial tuning was shifted towards the lower spatial frequencies. These components were clearly separate mechanisms, unlike the S-CSFs of typical Y-like cells where the second harmonic component, if found at low spatial frequencies, was usually a result of a low spontaneous rate or of overdriving of the cell's responses. If these three curves are superimposed on the same graph (Figure 49c), it is obvious that the max-min function was the result of the most sensitive mechanism (second harmonic at low spatial frequencies and fundamen-

Figure 49

S-CSFs of the various response components of an unusual Y-like cell. Each function (max-min (enclosed stars); amplitude of the fundamental component (closed circles); amplitude of the second harmonic component (open stars)) was derived from the responses of the cell to a 4 Hz drifting grating at 13% contrast. In (b), each value was normalized with respect to one maximum value; thus, the second harmonic component is more sensitive at low spatial frequencies than the fundamental component. In (c), the three response measures are superimposed. Note that the max-min response appears to be the result of the most sensitive component between the fundamental and second harmonic components.

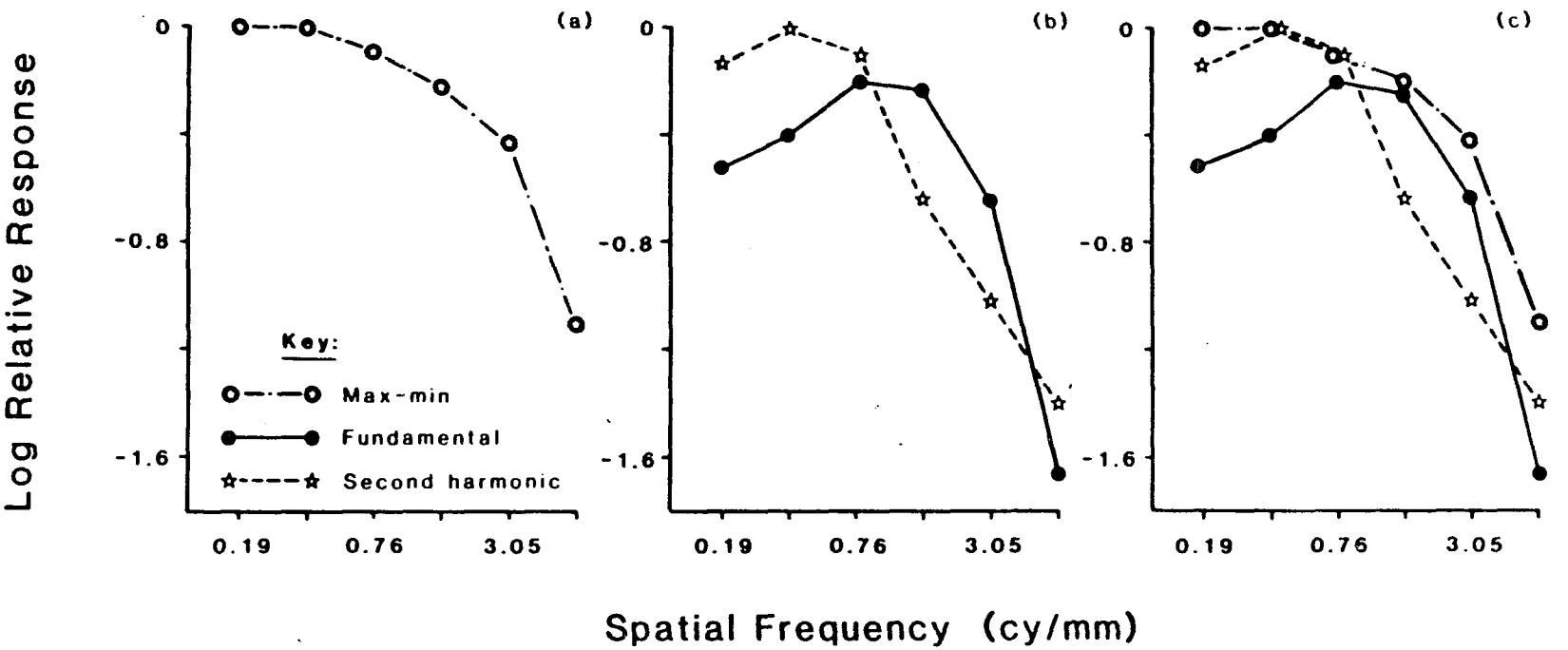
S-CSF of an Unusual Y-like Cell (C42B) Drifting grating, 4 Hz, 13% contrast. N: 30
Log Relative Response
0
-0.8
-1.6
(a)
(b)
(c)
Key:
Max-min
Fundamental
Second harmonic
0.19
0.76
3.05
Spatial Frequency (cy/mm)

tal at high spatial frequencies). The fact that there was a low frequency attenuation in both the fundamental and second harmonic components suggests that there was some antagonism within the receptive field.

To illustrate that this phenomemon was not due to the fact that response measures were used instead of sensitivity, Figure 50 shows a similar cell in which sensitivity was derived by interpolation on the response vs. contrast curves. The drift rate was 4 Hz, and the sensitivity values of the max-min response were normalized with respect to its maximum sensitivity, while the fundamental and second harmonic component values were normalized to one maximum value. Once again, the max-min response reflected the relative sensitivities of the fundamental and second harmonic components. The second harmonic component was more sensitive to lower spatial frequencies and all functions showed a low frequency attenuation.

Of the 7 Y-like cells that displayed these unusual characteristics 4 were spectrally nonopponent $L^{+}/^{+}$ center cells, 2 were spectrally opponent $L^{+}/^{-}$ center cells and one was a spectrally opponent $L^{-}/^{+}$ center cell. Thus, all of these cells had one thing in common -- all cells were capable of generating an ON-excitation and OFF-excitation response. This is obvious for the $L^{+}/^{+}$ center cells. For the spectrally opponent cells, a $^{+}/^{+}$ response would occur when two or more antagonistic cone mechanisms interacted. For example, an $L^{-}/^{+}$ and a $M^{+}/^{-}$ could produce an overall $^{+}/^{+}$ response, thus accounting for the frequency doubling when a drifting grating is presented. This is demonstrated in Figure 51. Figure 51 shows a peri-stimulus time his-

Figure 50

S-CSFs of another unusual Y-like cell. Each function (max-min, asterisks; amplitude of the fundamental component, closed circles; amplitude of the second harmonic component, open circles) was determined from the responses of the cell to a 4 Hz drifting grating. Sensitivity was obtained by interpolation on the response vs. contrast curves to find the contrast necessary for a constant response amplitude. The values of the fundamental and second harmonic components were normalized with respect to one maximum value; the max-min values were normalized separately from the other two measures. Once again, the max-min response appears to be a function of the most sensitive value of the fundamental and second harmonic components.

S-CSFs of Another Unusual Y-like Cell

(C40D) Drifting grating, 4 Hz. N: 40.

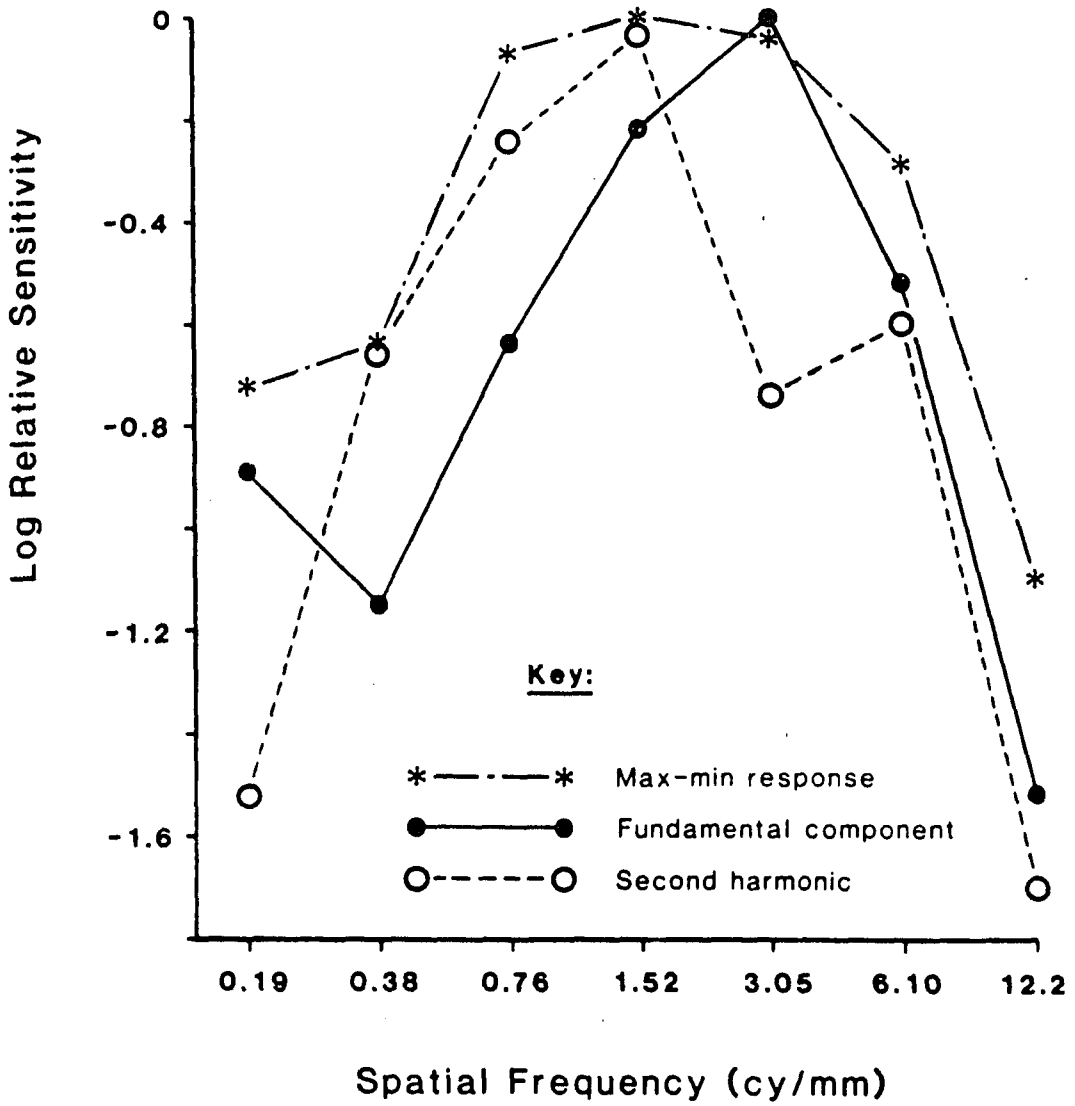

Figure 51

Spectral properties of an unusual Y-like cell. The responses to one second flashes of monochromatic spots (center; a, b, and c) and annuli (surround; d, e, and f) of light are shown. The bottom illustrations show the onset and offset of the stimulus. The three wavelengths (450 nm, (a) and (d); 510 nm, (b) and (e); 700 nm, (c) and (f)) represent the isoabsorption points along the L-cone spectrum. This cell was classified as an $L^{+/-}$ center cell since the response to a 700 nm spot of light presented to the center resulted in an ON-excitation response.

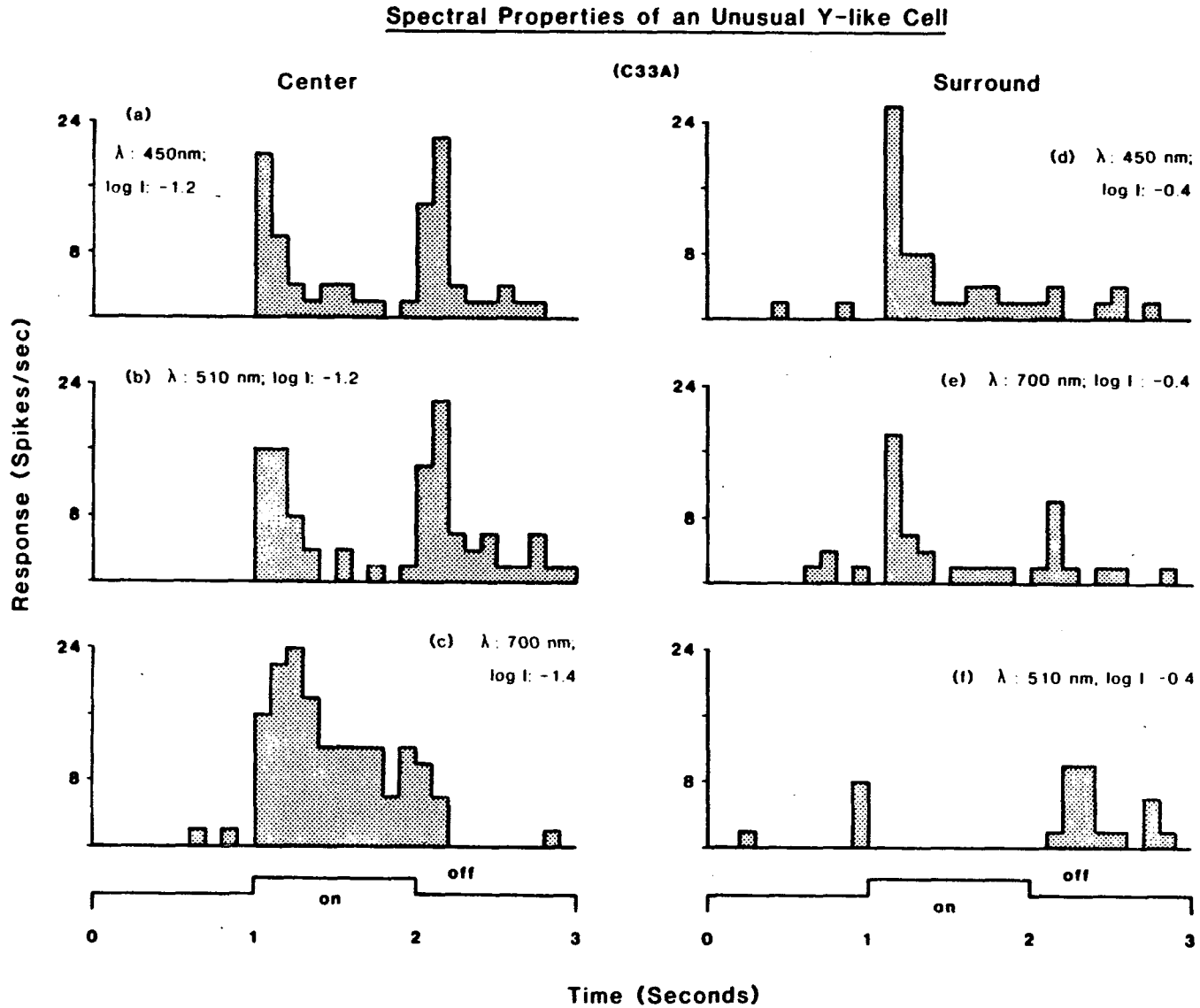
Spectral Properties of an Unusual Y-like Cell
(C33A)
Center
Surround
(a)
λ : 450nm;
log I: -1.2
(b) λ : 510 nm; log I: -1.2
(c) λ : 700 nm,
log I: -1.4
(d) λ : 450 nm;
log I: -0.4
(e) λ : 700 nm; log I : -0.4
(f) λ : 510 nm, log I -0.4
24
8
off
on
0
1
2
3
Response (Spikes/sec)
Time (Seconds)

togram of the responses of the cell shown in Figure 48 to monochromatic spots and annuli of light. (This cell was classified as an $L^+/-$ center cell.) The bars on the bottom of the figure represent the one second presentation of the stimulus. Responses one second prior to and one second after the stimulus are also shown. The response is in spikes per second. Figures 51a, b and c show the responses of the cell to a spot of light at three different wavelengths (450, 510 and 700 nm) at roughly equivalent intensities. These three wavelengths represent isoabsorption points of the L-cones; therefore, the responses would be similar if only the L-cones responded. The spontaneous rate is close to zero which is shown by the responses one second prior to the presentation of the stimulus. At 700 nm (Figure 51c), where only the L-cones are responsive, the cell responded with excitation to the stimulus onset and gradually decreased. This cell was classified as an $L^+/-$ center cell since its response to a long-wavelength center stimulus was ON-excitation. (The apparent response at the offset of the stimulus was merely the "on" response tapering off.) Comparing the response to the long-wavelength stimulus to the response to a 510 nm stimulus (Figure 51b), the response pattern of the cell differed. There was excitation to stimulus onset, but the response was much more transient than at 700 nm. Also, there was a very strong excitation response at stimulus offset. At this wavelength, the cell's response appeared $+/+$. A similar $+/+$ response pattern was found at 450 nm (Figure 51a). Since the $+/+$ response did not occur at 700 nm, where only the L-cones were sensitive, then the response at the shorter wavelengths must

have been due to more than one cone type. (The second cone type in this case was probably the M-cones since the responses at 450 and 510 nm were similar and the sensitivity of these cones to these wavelengths are roughly equivalent.)

Turning to the surround, this cell was clearly spatially opponent, since at 700 nm, the response was opposite to the center's response. There was an OFF-excitation to this wavelength and possibly an ON-inhibition, although the spontaneous rate was too low to be certain. However, at 510 nm, the response was ON-excitation and OFF-excitation. Again, the response at this wavelength must reflect the input of two cone types. Therefore, since the response was $^{+}/^{+}$ for both the center and surround, the response to a drifting grating would be twice the modulation frequency of the stimulus. However, this cannot be the sole explanation since several "typical" Y-like cells had $^{+}/^{+}$ responses to spectral stimuli (either $L^{+}/^{+}$ center or spectrally opponent cells), but never responded with twice the modulation frequency to a drifting grating stimulus. Finally, these cells all responded to a uniform sinusoidally modulated stimulus at the modulation frequency -- their response consisted mostly at the fundamental frequency.

3.6.2 W-like Cells.

There was also a subgroup of W-like cells that responded to a drifting grating at twice the stimulus modulation. However, their response pattern was not the same as the unusual Y-like cells. Their responses were not as strongly dependent on the stimulus' spatial

frequency as were those of Y-like cells. There was usually very little difference between the amplitudes of the fundamental and second harmonic components; one component did not dominate the response. The S-CSFs derived from the fundamental and second harmonic components usually corresponded with one another, which was not the case in the unusual Y-like cells. Figure 52a shows an example of the S-CSF of an unusual W-like cell. The S-CSFs of the max-min, the fundamental and second harmonic components are shown for comparison. The drift rate of the grating was 8 Hz. In general, most of these cells were very broad in their spatial tuning compared with other cells. Figure 52b shows the T-CSF of the same cell. Only the fundamental component was shown here since, as with the other cells, most of the response was contained at the fundamental component. Eleven of these unusual W-like cells were found; only 2 were $L^+/^+$ center cells and the remaining cells were either spectrally opponent or nonopponent. Therefore, these cells were not similar to the unusual Y-like cells, since the Y-like cells were either $L^+/^+$ center cells or spectrally opponent and their doubling response to the drifting grating could be accounted for by the number of mechanisms apparent in their receptive field.

3.6.3 Unusual Spectral Classes.

One final cell merits attention. This cell was the only cell positively identified L-/- center cell. This cell responded to long-wavelength light in the center portion of the receptive field by ON-inhibition and OFF-inhibition. This cell was classified as a Y-like

Figure 52

S-CSFs and T-CSF of an unusual W-like cell. Each S-CSF (a), max-min, (asterisks), amplitude of the fundamental component (closed circles) and the amplitude of the second harmonic component (open circles), was determined from the cell's response to a 8 Hz drifting grating. The response measure of the T-CSF (b) was the amplitude of the fundamental component. Sensitivity was obtained by interpolation on the response vs. contrast curves to find the contrast for a constant response amplitude. The fundamental and second harmonic components in (a) were normalized with respect to one maximum value.

S- & T-CSFs of an Unusual W-like Cell

(C02C) Drifting grating, 8 Hz. N: 60.

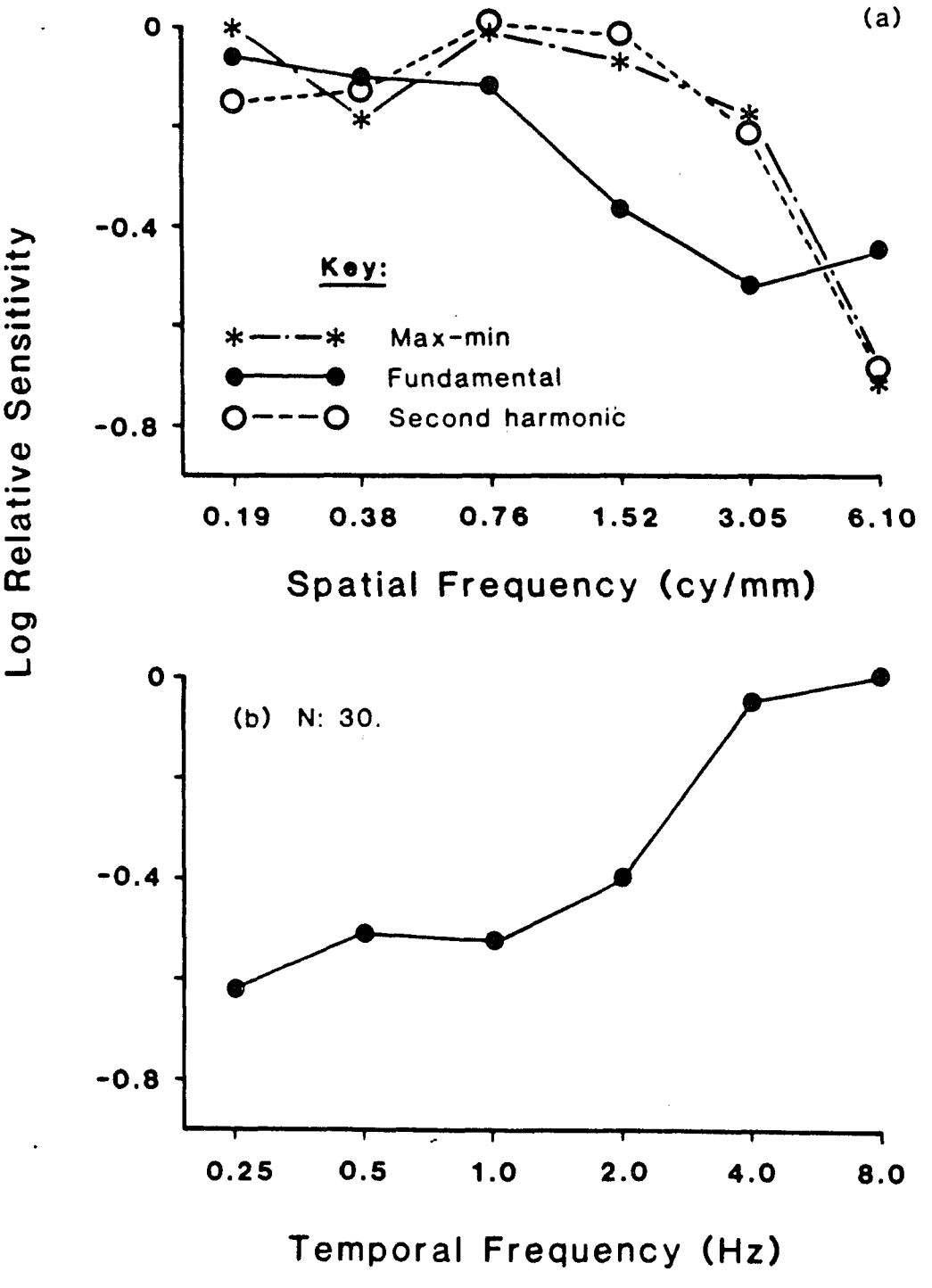

cell, possessed no spectral opponency and unfortunately, no information regarding a surround was obtained. The interesting thing about this cell occurred during the presentation of the spatial stimuli. When the stimulus was at mean luminance, the cell responded with a low, but obvious spontaneous rate. When a drifting grating was presented, the cell's response went to zero and remained at zero until the drifting stimulus was extinguished leaving the cell exposed to mean luminance. At this time, the cell's firing rate returned to spontaneous level. This cell could be classified as a "suppressed by contrast" cell like that found in frog ganglion cells (Lettvin, Maturana, McCulloch and Pitts, 1959). In retrospect, it seems quite possible that there may have been other L-/- center cells which were inadvertently passed by as cells that were unresponsive.

[4]
DISCUSSION

4.1 Spatial Processing

4.1.1 Spatial Summation

The most important finding of this project is that goldfish ganglion cells can be classified by their spatial summation properties. Using techniques that quantitatively assess a cell's spatial summation properties, goldfish ganglion cells can be classified as X-, Y-, or W-like cells. The response properties of these cells are virtually identical to the response properties and classification of cat ganglion cells. That this classification scheme is found in such disparate species suggests that these cell types perform some basic and necessary role in vision.

Using the same criteria as for cat X-cells, goldfish X-like cells are linear. Goldfish Y-like cells, for the most part, are similar to cat Y-cells in their response characteristics. Both cat Y-cells and goldfish Y-like cells respond to high spatial frequency, contrast-reversal gratings with twice the stimulus modulation frequency and display no null point. The nonlinearities of goldfish Y-like cells are most likely

due to small, nonlinear subunits, as in cat Y-cells (Hochstein and Shapley, 1976b). This hypothesis is supported by the fact that the nonlinearity is most apparent at high spatial frequencies where such small subunits are most responsive. Aside from this nonlinearity at high spatial frequencies, the fundamental response component of the Y-like cell behaves as in the X-like cell, suggesting that the organization of X- and Y-like cell receptive fields are similar, except that Y-like cells possess nonlinear subunits. These findings agree with what is known about cat ganglion cells (Enroth-Cugell and Robson, 1966; Hochstein and Shapley, 1976a,b).

However, cat Y- and goldfish Y-like cells' responses are somewhat different when the contrast-reversal grating consists of low spatial frequencies. Goldfish Y-like cells possess a null point at low spatial frequencies. Cat Y-cells, on the other hand, display a slight doubling response at the null position; however, when the grating is positioned away from the midposition of the receptive field, the response is dominated by the fundamental response component as in goldfish Y-like cells. Thus, although the nonlinear behavior of the cells in both species can be best explained by the presence of small, nonlinear subunits, there are qualitative differences in the subunits' properties. For the goldfish, the subunit responses appear to be nulled at low spatial frequencies along with the center and surround responses; for cat Y-cells, only the center and surround components are nulled at low spatial frequencies, leaving only the responses of the rectifying subunits.

Victor and Shapley (1979) have suggested that the subunits in

cat Y-cells result from the direct input of bipolar cells. It is possible that the differences between the species' subunits may be a reflection of the strength of the surround component of their bipolar cells. Although cat bipolar cells possess a center/surround organization, the response of the surround is relatively weak compared to the center response (see Rodieck, 1973). Thus, stimulating both the center and surround components (e.g., by presenting low spatial frequency gratings) will result in a net response predominated by the center component of the subunits. The surround does reduce the net response somewhat since the subunits' responses are attenuated at low spatial frequencies (Victor and Shapley, 1979); however, with low spatial frequency stimuli, the subunits are not nulled by the center and weak surround combination, and Y-cells will respond.

The surround component's antagonism to the center in goldfish bipolar cells is much stronger than that found in the cat (see Kaneko, 1970). Thus, at low spatial frequencies, the net result of stimulating both the centers and surrounds of all the subunits could produce a null response. With high spatial frequency stimuli, the surrounds of these subunits would be less sensitive, leaving predominately the center responses which would behave as the cat Y-cells.

This discrepancy in spatial summation across spatial frequencies between the goldfish and cat ganglion cells has been illustrated in studies which examined Ricco's law in ganglion cells. Both cat (Cleland and Enroth-Cugell, 1968) and goldfish (Easter, 1968) ganglion cells behaved similarly and obeyed Ricco's law when the stimuli consisted of one spot of increasing diameter. However, when Ricco's law

is examined in goldfish by using two spots in separate areas (both spots positioned well within Ricco's area as determined above), Ricco's law fails; two spots produced a greater response than predicted by Ricco's law (Easter, 1968). For cat ganglion cells, Ricco's law predicted the behavior for both one and two spot experiments (Cleland and Enroth-Cugell, 1968) (see Section 1.4.1). For the cat cells, since there is little surround influence within a bipolar cell or subunit, the net result of the ganglion cell is simply the combination of the center components of the subunits. Thus, both a large stimulus and several smaller stimuli (of the same total area on the receptive field) will activate the same number of subunits yielding identical results. In goldfish, however, the small spots will only activate the center portion of the subunits which will produce a greater response than will larger stimuli which stimulate both the center and surround components of the subunits.

The relationship between goldfish W-like cells and cat W-cells is more difficult to determine. Since it is relatively difficult to isolate and maintain stable recordings of cat W-cells from the optic tract, their properties have not been studied in as much detail as X- and Y-cells. Also, because of response variability across W-cells, it is difficult to find any common characteristics. The W-cell category in the cat is a "catch-all" classification -- a cell that is not an X- or Y-cell is categorized as a W-cell. This was also the case for the goldfish W-like cell category; cells that did not fulfill all the criteria for X-like and did not behave as Y-like were labelled W-like. One general characteristic all W-like cells possessed was that they

appeared to be "somewhere inbetween" X- and Y-like cells. For example, when a contrast-reversal grating was presented at a position away from the midpoint of the receptive field, the cell responded like an X-like cell. However, positioning the same stimulus closer to the middle of the receptive field, resulted in a Y-like cell response. The nonlinearities of W-like cells cannot be due to subunits like those found in Y-like cells, since the nonlinearities are found at all spatial frequencies. The one consistent finding on W-like cells is that, regardless of the stimulus, their responses are different from X- and Y-like cells under the same conditions. This is true for their orientation properties as well as for the influence of their spectral properties on spatial processing.

One possible explanation for the strange and variable behavior of W-like cells can be seen in similar cells found in the eel retina (Gordon and Shapley, 1978). Many goldfish W-like cells displayed response characteristics similar to the "not-X" cell found in the eel. To account for the responses of these "not-X" cells, Gordon and Shapley proposed a receptive field organization which is different from the center/surround organization of X- and Y-cells in the cat. The receptive fields of these cells consist of two slightly overlapping Gaussian distributions. One area responds with ON-excitation, the other with OFF-excitation. Both areas possess linear spatial summation, but prior to combining the responses of the two separate areas, the responses of each component are half-wave rectified. Therefore, once the responses are combined, the overall response of the cell is at twice the stimulus modulation. The degree of overlap of the areas

varies from cell to cell; there is no consistent pattern across these cells, thus accounting for the inconsistency within this classification. It is also interesting to note that Gordon and Shapley (1978) found that some "not-X" cells displayed S-CSFs with low frequency attenuation. They attributed this finding to the possibility of a "silent surround" (see Barlow, 1953). Some of the W-like cells in the goldfish also displayed low frequency attenuation in the S-CSF. It is quite likely that goldfish W-like cells and the eel "not-X" cells are similar in their receptive field organizations.

The fact that goldfish ganglion cells can be classified by their spatial summation properties confirms the results of Levine and Shefner (1979) and Levine (1980) who found that goldfish ganglion cells could be divided into X-like and not-X-like cells. Unfortunately, because of their technique to determine the cell's linearity (rotating a pinwheel of light within the center), they were only able to establish that a ganglion cell was either linear (X-like) or nonlinear (not-X-like). Also, in their studies, linearity was only examined for the center mechanism and not the entire receptive field. This project has elaborated on their findings by examining the nature of the nonlinearity of the not-X-like cells. These not-X-like cells can be subdivided into Y- and W-like based on their response properties. In addition, linearity was tested for both the center and surround mechanisms simultaneously. Despite these differences across the studies, the proportions of the various cell types in both studies are relatively similar. Levine and colleagues found approximately two-thirds (64%) of their cells to be not-X-like. In this study, if Y- and W-like cells

are combined into one "nonlinear" category, then 79% of the cells were nonlinear.

One possible reason for the slight differences in percentages across the studies, is that some W-like cells in the Levine studies could have been misclassified as X-like cells. In the present study, it was found that the responses of W-like cells could be very misleading unless examined with a wide range of stimuli. Since the nonlinearities of W-like cells (unlike Y-like cells) are most likely due to an overlap of two receptive field areas (Gordon and Shapley, 1978), the small, pinwheel stimulus, placed in the center of one field may not activate the other field; since each area possesses linear spatial summation, the cell behaves linearly.

On the other hand, the findings of this project are in disagreement with the findings of Spekreijse and van den Berg (1971) who found that all goldfish ganglion cells possessed linear spatial summation -- no cells behaved nonlinearly. The discrepancies between the present study (and the work of Levine) and Spekreijse and van den Berg (1971) probably are related to the types of stimuli used and the criteria for linearity. Spekreijse and van den Berg (1971) presented a large checkerboard pattern which was sinusoidally modulated out-of-phase with an adjacent checkerboard pattern. They were able to adjust the phase and contrast of each pattern to create a stimulus pattern that produced a "null" response from the ganglion cell.

Unfortunately, a large checkerboard, although it contains a large number of spatial frequencies, has most of its power at low spatial frequencies. Therefore, their stimulus consisted mostly of low spatial

frequencies. In the present study, it was found that a stimulus consisting of low spatial frequencies was insufficient to reveal the small, nonlinear subunits, and under these conditions, the cell would behave linearly. It is quite possible that the stimulus used in the Spekreijse and van den Berg (1971) study was insufficient to examine the nonlinear subunits found in Y-like cells and thus, these cells would be classified as linear.

This explanation does not account for the absence of W-like cells in their findings. However, remember that W-like cells were very difficult to classify (using contrast-reversal gratings, these cells appeared to be X-like unless examined with a variety of spatial positions). In their study, a cell was considered linear if, by adjusting the two adjacent stimuli, a null response occurred. Unfortunately, they adjusted the stimuli so that the two receptive field areas were equally sensitive. By using a sensitivity measure, any nonlinearities in the response are overlooked. Thus, by this criterion, all cells should behave linearly.

Turning back to the Levine studies (Levine, 1980; Levine and Shefner, 1979), their small, pinwheel stimulus must have contained spatial frequencies high enough to stimulate the nonlinear subunits in Y-like cells. Also, each stimulus series was presented at several different intensities to ensure that responses were consistent over a wide range of values.

In summary, it appears that the differences in studies of spatial summation of goldfish ganglion cells are due to the nature of the stimuli and the criteria used for determining linearity. One of the

purposes of the present study was to examine spatial summation processing in goldfish ganglion cells using the exact same stimuli and criteria as used in work on other species, primarily cat and monkey. By using these techniques, it has been found that spatial summation processing in goldfish ganglion cells is the same as in cat and monkey neurons.

4.1.2 Spatial Contrast Sensitivity.

Another component of a cell's spatial processing characteristics is its spatial filtering properties. These were determined by deriving each cell's S-CSF. From this information, it appears that goldfish ganglion cells possess spatial filtering characteristics similar to the neurons of other species. The goldfish ganglion cells' S-CSFs are at least qualitatively similar to the S-CSFs obtained from the neurons of cat and monkey. In most cases, the spatial filtering appears to be bandpass in that the neuron is most sensitive to middle spatial frequencies and less sensitive to higher and lower frequencies. The low frequency attenuation is presumed to be due to lateral inhibition since most neurons are comprised of a center and antagonistic surround receptive field areas.

Although the S-CSFs obtained from single neurons are similar in shape among the different species, there are some differences. The most important difference is found in the range of spatial frequencies to which the neuron is sensitive. Compared to the cat and the monkey S-CSFs, the goldfish S-CSF is shifted to much lower spatial frequencies, implying that the goldfish has poor acuity and is unable to

detect fine detail in its environment. Of course, this is not surprising since the underwater world of the goldfish consists of "blurred" images, devoid of any fine details.

This shift of the S-CSF of goldfish ganglion cells agrees with the psychophysically determined S-CSF of the goldfish (Northmore and Dvorak, 1979). It too, illustrates that goldfish spatial filtering is bandpass and is shifted to lower spatial frequencies compared to behavioral measures from the cat, monkey and man.

It is interesting to compare the psychophysical S-CSF to the physiological S-CSF of single neurons. For the goldfish, although the two functions are similar in shape, there are important differences. For example, despite the fact that the acuity limits of the two functions appear to be similar, there is a large discrepancy between the peak sensitivities of the psychophysical and physiological measures. The peak of the physiological curve is well below the peak of the behavioral function. This discrepancy between the psychophysical and physiological functions at the peak sensitivity but not at the high frequency cut-off implies that the ganglion cell S-CSFs have a wider bandwidth than the behavioral function. It is not entirely clear why there is this discrepancy between the bandwidths of the two measures. Perhaps, as in other species, the bandwidths of neurons in higher visual centers are narrower than those in lower centers. For example, cat cortical cells are much more narrowly tuned across spatial frequencies than LGN or ganglion cells (see Maffei, 1978). Another possibility is that the differences between the functions are a result of the stimulus used to derive the S-CSF. As was demon-

strated in this work, the characteristics of the S-CSF for an individual neuron depended on the stimulus parameters. The psychophysical S-CSFs were determined with static, sinusoidal gratings while in this project, S-CSFs were derived from responses to drifting sinusoidal gratings.

Another apparent difference between the goldfish and other animals is in the similarity of the acuity limits of X- and Y-like cells. In cat neurons, the differences in acuity limit between X- and Y-cells were much larger than in the goldfish. Although there was some indication that some goldfish ganglion cells were tuned to higher spatial frequencies (see Figure 20), the majority of X- and Y-like cells had similar functions. One explanation for the difference may be sampling bias due to the size of the recording electrode. For example, Shefner and Levine (1979) found systematic grouping of X-like and not-X-like cells depending on the group of electrodes they used. Since X-like cells probably have smaller cell bodies, they would be more difficult to isolate. (This also accounts for the difficulty in maintaining good isolation of X-like cells for long periods of time.) Thus, if an X-like cell were found, it was probably somewhat larger than the average X-like cell. The fact that only large X-like cells were isolated explains why the average S-CSF of X-like cells was only slightly shifted to higher spatial frequencies compared to Y-like cells. However, this cannot explain why most neurons, both X- and Y-like, had acuity limits which approached the behavioral limit. If only large neurons were isolated then they would have functions shifted to much lower spatial frequencies than the psychophysical values.

The differences between cat and goldfish ganglion cells must reside in differences in their receptive field components or inputs. The spatial resolution of a ganglion cell depends on the size of its receptive field center. For example, with retinal eccentricity, the receptive field centers of cat ganglion cells become larger and this is reflected in the spatial resolution of the cell; peripheral cells have lower high-frequency cut-offs than cells more centrally located (Cleland, Harding and Tulunay-Keesey, 1979). Also, at any one retinal location, Y-cells have poorer spatial resolution than X-cells (Cleland, et al., 1979; Hochstein and Shapley, 1976a). It is hypothesized that in the area centralis (where neurons have the best resolution), direct input from one bipolar cell constitutes the receptive field center of a ganglion X-cell. (The centers of these X-cells are about the same size as a Y-cell nonlinear subunit, also believed to be the result of a single bipolar cell input). Moving away from the area centralis, the receptive field centers become larger and therefore must receive more than one bipolar cell input, resulting in poorer spatial resolution.

Unlike the cat retina, the goldfish retina possesses no area centralis and is uniform throughout. Thus, within a spatial summation class, it is not surprising to find that the S-CSFs across neurons are similar. Thus, each goldfish ganglion cell probably receives a similar number of direct bipolar cell inputs to its receptive field center. The spatial resolution of each goldfish ganglion cell is too poor to be the result of a single bipolar cell input to its center. Goldfish X-like cells are probably most similar to the X-cells found in the cat peripheral retina which must also have multiple bipolar cell input to their

center mechanisms.

What is interesting is that the size of the goldfish Y-like cell center, unlike the cat Y-cell, appears to be the same as the size of its X-like cells. Thus, although the two cell types may serve different functions in visual processing, as is believed to be the case in the cat (i.e., X for acuity, Y for detection), the spatial resolution of the two systems in the goldfish is similar.

4.2 Difference of Gaussians Model

4.2.1 Evidence Supporting the Model

Since the receptive fields of goldfish ganglion cells consist of the same spatial organization (i.e., center and surround components) as other species, such as the cat, it was predicted that the S-CSFs of the goldfish cells would display the same characteristics. If the S-CSF of a neuron is a function of the interaction between the responses of the center and surround components, then any condition that changes the balance of this interaction would also be reflected in changes in the S-CSF. For the most part, this was found to be the case. For example, cells that displayed no antagonistic surround also had no low frequency attenuation in the S-CSF. The function appeared to be the result of the center mechanism only (see Section 1.5.1). The size of these receptive fields must be similar to the size of most receptive field center mechanisms since the high spatial frequency portion of the S-CSF of these cells corresponded to the functions obtained from cells with both a center and surround component.

This was supported by the fact that there was no response when the "surround" area was examined with flashes of light.

The exact nature of the center and surround mechanisms' influence on the cell's S-CSF was examined by obtaining S-CSFs of each component separately and comparing these functions to the cell's overall S-CSF. These findings confirmed the S-CSF model proposed by Enroth-Cugell and Robson (1984). Low frequency attenuation of the S-CSF is the result of antagonistic inputs from the center and surround; this antagonism occurs only when both mechanisms are responsive to the stimuli which, because of the low spatial tuning of the surround component, is found only at low spatial frequencies. At high spatial frequencies, the full field S-CSF and the center component S-CSF coincide suggesting that responses at high spatial frequencies are driven by the center mechanism only.

It has also been demonstrated that the center and surround components are not always antagonistic; in fact, under certain conditions they may be synergistic, enhancing sensitivity. This finding explains the variation of the S-CSF as a function of stimulus drift rate. At high spatial frequencies, there is little or no change in the shape of the S-CSF as a function of stimulus drift rate (at these frequencies there is only the response of the center -- there is no interaction of center and surround). The significant change occurs at low spatial frequencies, where increasing the temporal rate of the stimulus, produces less attenuation.

One possible explanation for this phenomenon is that the surround mechanism is less sensitive to high temporal frequencies and

therefore does not respond to the stimulus, producing no antagonism at low spatial frequencies. However, this cannot be the case since T-CSFs of the surround show that it is at least as sensitive as the center component and usually peaks at a temporal frequency which is higher than the center component peak. This is not surprising if one assumes that the ganglion cell surround receives its input from amacrine cells which appear to be well suited to respond to transient stimuli.

The best explanation is found by comparing the relative phase shifts of the center and surround components. At low temporal frequencies, the center and surround components are approximately 180 degrees out-of-phase. Stimulating both the center and surround components at low temporal frequencies produces an antagonism, and thus, less overall sensitivity. Therefore, at low temporal frequencies, or drift rates, the S-CSF will contain low frequency attenuation. However, as the temporal frequency of the stimulus is increased, the phase shift of both the center and surround components increases (that is, they become slower in following the stimulus) but at different rates. It is possible, and was always found to be the case in this study, that there could be a temporal frequency at which the center and surround responses are in-phase resulting in an increase in sensitivity when the entire receptive field is stimulated. At this temporal frequency, the S-CSF will have no low frequency attenuation since there is no center/surround antagonism. These results are similar to and support the work of Gouras and Zrenner (1979); they found that at high flicker rates the center and surround components

of rhesus monkey ganglion cells became synergistic. This phenomenon of center and surround interactions changing with temporal frequency has been demonstrated in Limulus (Ratliff, Knight and Graham, 1969) as well as in cat ganglion cells (Kaplan, et al., 1979).

4.2.2 Discrepancies in the Model

Although the difference of Gaussians model can account for a substantial portion of the results, it does fall short. The difference of Gaussians model assumes a receptive field with a circular center and surround arranged in a concentric fashion. The facts that many goldfish ganglion cells display orientation tuning and sometimes display direction selectivity are in direct contrast to the model. However, with a few minor modifications of the model, these results can be explained.

The orientation selectivity of many cells suggests that their receptive fields are not circular but elliptical. This is supported by the fact that the orientation producing the maximum response is orthogonal to the orientation of minimum response. However, since orientation tuning occurs primarily at high spatial frequencies, only the center needs to be elliptical. In cat ganglion cells, Levick and Thibos (1982) have suggested that only the center mechanism is elliptical while the surround component is circular; this has been supported by Soodak, et al. (1985). The goldfish center component may also be elliptical. Similarly, the goldfish ganglion cell receptive fields appear to be organized into smaller subunits as found in the cat (Soodak, et al., 1985). This is suggested by the finding that orien-

tation tuning changes drastically at very high spatial frequencies. As in the cat, these subunits are not the nonlinear subunits found only in Y-like cells, since orientation tuning occurs in X-like cells, and is also prominent in the fundamental response component of the Y-like cells' responses.

An elliptical center mechanism in goldfish ganglion cells is supported by the work of Levine and Zimmerman (1986). Not only do they find that the center portion of many goldfish ganglion cells is not circular, but they also find that the center portion consists of smaller subunits with different ON/OFF response patterns. Thus, a stimulus of appropriate high spatial frequency could activate these subunits and produce a response pattern different from a stimulus consisting of a lower spatial frequency in which the responses of these units are merely averaged.

Another modification of the difference of Gaussians model must be introduced to account for direction selectivity. Dawis, et al. (1984) have produced such a model, cleverly referred to as the "modified difference of Gaussians" model. The modification is that the center and surround components need not be concentric. By positioning the center component slightly off-axis with respect to the surround, it is possible to produce directionally selective cells, even in cells with linear spatial summation (X-cells). (All that is necessary for a directionally selective X-cell to produce a null response is that the spatial phase of the center and surround midpoints be 180 degrees apart.)

From this model, direction selectivity can be explained by differ-

ences in the phase relations between the center and surround responses. Because of the asymmetry, a stimulus moving in one direction could create a situation in which the center and surround responses are in-phase (producing a maximum response) while the same stimulus moving in the opposite direction will cause the center and surround responses to be out-of-phase (producing a minimum response).

There are two findings which support this model for goldfish ganglion cells. One finding is from the work of Levine and Zimmerman (1986) who found that the majority of goldfish ganglion cells possessed some form of inhomogenity. For example, surround component responses that were stronger on one side of the field or subareas with different response patterns located adjacent to one another. Any of these, with the appropriate stimuli, could produce a directionally selective response.

The second piece of evidence which supports this model stems from the fact that direction selectivity must be a function of the center/surround interaction. Thus, for stimuli that do not activate both mechanisms, there should be no direction selectivity. A consistent finding in this study is that for all cells examined, direction selectivity occurred only at the lower spatial frequencies. For example, in Figure 35, at the low spatial frequency, the cell displayed both orientation and direction selectivity; however, at the high spatial frequency, direction selectivity literally "disappeared", even though orientation tuning was still apparent. This was true for all the cells, including W-like cells. When the stimulus activates only one receptive

field component, there can be no interaction and thus, no direction selectivity. Note that this does not apply to orientation selectivity which further emphasizes the notion that orientation and direction selectivity are two independent phenomena produced by two different mechanisms. However, this model cannot entirely explain the dramatic direction selectivity found in many cells. An alternate, and perhaps coexistent, explanation stems from the work of Levick and colleagues in their research on the rabbit retina (e.g., Barlow, Hill and Levick, 1964).

It is somewhat puzzling why orientation and direction selectivity have not been reported in other studies of goldfish ganglion cells. The same is true for cat ganglion cells -- some studies report significant orientation tuning (Levick and Thibos, 1982; Soodak, et al., 1985) while others show no evidence (Kuffler, 1953) and suggest that the receptive fields are circular and concentric. One possibility is that the studies which found no orientation tuning used stimuli that were not adequate to examine the type of specialized tuning found in both the goldfish and cat ganglion cells. It is interesting, and most likely significant, that the studies which report orientation tuning used sinusoidal gratings of various spatial frequencies as stimuli. The other studies examined orientation and direction tuning with spots or bars of light which passed through the receptive field. Based on the findings of this study, it is quite clear that the tuning characteristics depended on the stimulus parameters. Since a bar of light consists of a variety of spatial frequencies, it is possible that any orientation or direction tuning will be obscured with this stimu-

lus. For an illustration of what could happen with a bar stimulus, refer to Figure 32. Assume that the stimulus presented contains the five spatial frequencies shown in the figure. Calculating the average response of the cell for each orientation the range of these mean values is about 23 spikes per second. Comparison of this value with the range in any graph in the figure shows that the responses are quite different for the two types of stimuli. Thus, the effects of orientation have been averaged out. A similar argument can be made for direction selectivity.

We now summarize the important aspects of goldfish ganglion cells. The majority of X- and Y-like cells appear to possess a center and surround organization. However, these receptive field components are not necessarily circular or concentric. Some cells may possess an elliptical center portion and a circular surround. It is also possible for a cell to possess a slightly elliptical surround as well. The receptive field centers are not necessarily concentric within the surround field. Some cells may have a center mechanism which is slightly displaced from a completely concentric organization. Although this modified difference of Gaussians model can adequately describe the behavior of a cell under most circumstances, one should also be aware that this model is not complete. The center and possibly the surround components are further divided into smaller subunits. For the most part, the responses of these subunits remain obscured and averaged into oblivion; however, with the appropriate stimuli (stimuli of high spatial frequency) these units can alter the response pattern of the cell.

The exact nature of the receptive field organization of the unusual Y-like cells is somewhat perplexing. Perhaps the best explanation is that these cells are special cases of "not-X" cells found in the eel (Gordon and Shapley, 1978) and should be classified as W-like even though their responses to contrast-reversal stimuli display Y-like properties. These Y-like cells, like the "not-X" cells, appear to possess separate ON and OFF overlapping areas. The ON and OFF mechanisms can be a function of either the ON/OFF responses of $L^+/^+$ center cells or spectral opponency (e.g., $L^+/^-$ and $M^-/^+$). Another feature that these cells may possess is that one area is smaller than the other. Also, since these cells behave like Y-like cells to contrast-reversal grating, they must also contain the small, nonlinear subunits.

Finally, like the eel "not-X" cells, each area must summate linearly and separately as well as half-wave rectify prior to combination. With this configuration, the cell's response to a contrast-reversal grating of low spatial frequency will be linear, but at high spatial frequency, the response will double due to the nonlinear subunits. Regarding the cell's S-CSF, at low spatial frequencies, both areas respond with half-wave rectification and out-of-phase, producing a doubling response. However, at high spatial frequencies, the responses of the larger area will diminish leaving only the smaller mechanism to respond; even with the rectification, the fundamental component will dominate the response.

Regarding the unusual W-like cells, their responses are similar to the responses found in the "not-X" category in the eel and there-

fore, probably consist of the receptive field model of two overlapping areas and half-wave rectification prior to combination as proposed by Gordon and Shapley (1978).

4.3 Spectral Contributions to Spatial Processing

4.3.1 Spatial Summation

Another important outcome of this project is the finding that spatial summation is independent of a cell's spectral properties. The significance of these results is that each spatial summation class contains cells that provide color information (spectrally opponent cells) and cells that do not provide color information (spectrally nonopponent cells). Also, each spatial summation class contains cells that are activated by light ($L^+/-$ center cells), cells activated by the removal of light ($L-/^+$ center cells) and cells which provide information regarding transient illumination ($L^+/^+$ center cells). The independence of these classifications suggests that these categories also have a functional independence to one another. If one were to assume that each spatial summation class serves a particular visual function then it would be necessary for each class to contain a color channel as well as an achromatic one. For example, suppose that the role of X-like cells (as many have suggested) is for visual acuity and Y-like cells' role is to provide visual information to the eye movement center (see Section 1.4.2). If it were the case that only X-like cells were spectrally opponent, then all information to the eye movement center (Y-like cells) would be achromatic. A more efficient system would be

for both functional classes to contain both color and noncolor information. The same argument applies to the ON and OFF channels, if they indeed perform separate functions (see below).

4.3.2 Influence of Spectral Properties on Other Spatial Processing

Although the spectral properties of a cell are independent of its spatial summation properties, the spectral properties did affect other spatial properties, such as the S-CSF and its sensitivity to contrast.

S-CSF. As predicted, there were differences in S-CSFs as a function of the spectral class of X- and Y-like cells. $L^+/-$ and $L^+/^+$ center cells had S-CSFs which were relatively more sensitive to higher spatial frequencies than $L-/^+$ center cells. This implies that the $L^+/-$ and $L^+/^+$ center cells have a smaller center diameter than $L-/^+$ center cells, confirming the findings of earlier work in which the receptive field centers were mapped using small spots of light (Macy and Easter, 1981; Schellart and Spekreijse, 1976). The agreement between the results obtained with spots of light and the results from the S-CSFs further supports the difference of Gaussians model and the usefulness of the S-CSF. Since the size of the center determines the high frequency portion of the S-CSF, any differences in center size should also be reflected in the S-CSF; this was found to be the case.

Another interesting finding concerns the influence of the cell's spectral properties when the S-CSFs of spectrally opponent and nonopponent cells are compared. It was found that spectrally opponent cells' S-CSFs were shifted to higher spatial frequencies than

those of spectrally nonopponent cells. Although it may not be entirely clear why this should be the case, the difference of Gaussians model, based on what is known about the receptive field organization of goldfish ganglion cells, would predict the same results.

Referring back to Figure 3, an example of a spectrally opponent (Figure 3a) and spectrally nonopponent (Figure 3b) receptive fields are shown. Figure 3a is redrawn and shown in Figure 53a. Figure 53a shows the receptive field map of a typical spectrally opponent cell. The letters refer to the maximally effective wavelengths and the signs associated with the letters refer to an excitatory (+) or inhibitory (-) response. The two inner circles correspond to the center while the large, outer circle represents the surround. The smaller portion of the center consists of an excitatory Red-component and an inhibitory Green-component. The inhibitory component extends beyond the smaller excitatory component and forms the outer ring of the center. Figure 53b shows the sensitivity profile of the two center mechanisms; each profile is represented by a Gaussian distribution. Figure 53c is the resulting profile of the difference of the two Gaussian functions. The interaction between the antagonistic Red- and Green-components has made the center Red-component smaller. Thus, spectrally opponent cells have functionally smaller centers resulting in better spatial resolution and a shift in the S-CSF towards higher spatial frequencies. This "shrinking" of the receptive field center will occur whenever both components are responsive to the stimulus, for example, white light or any stimulus that stimulates both the Red- and Green-components.

Figure 53

Spatial organization of a spectrally opponent goldfish ganglion cell receptive field. (a) Receptive field map of a spectrally opponent goldfish ganglion cell. The outer area of the center (-G) is enlarged in this figure to illustrate a point; it is actually much smaller than depicted (see Figure 3a for the appropriate dimensions). (b) Sensitivity profiles of the center chromatic mechanisms; the curves represent Gaussian distributions. (c) Sensitivity profile of the difference of Gaussians of the center mechanisms presented in (b). See text for details.

Spatial Organization of Goldfish Ganglion Cell Receptive Fields (Spectrally Opponent Cells)

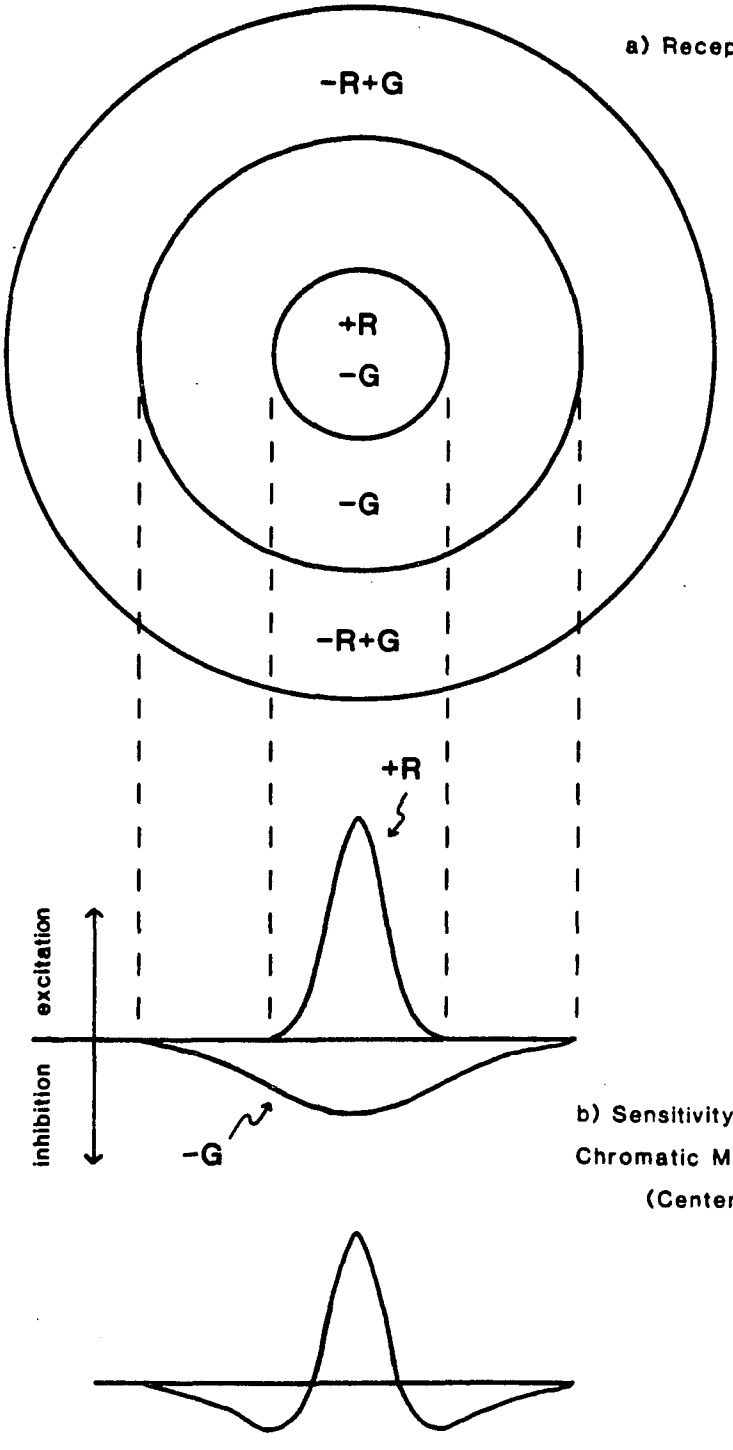

The fact that there are no differences across spectral classes for spectrally opponent cells (Figure 44b) suggests that the interaction between the center components reduces the effective size of the center similarly across the spectral cell classes. The interaction "shrinks" the size of the center to similar sizes across the $L^+/-$, $L-/^+$ and $L^+/^+$ center cell types and thus, the S-CSFs do not differ. For spectrally nonopponent cells (Figure 44a), the center probably consists of only the Red-component, and the S-CSF is solely a function of this component's dimensions. Therefore, the differences in the two S-CSFs reflect the differences in the Red-component center size across spectral class.

Sensitivity to Contrast. Another spatial property that was influenced by the cell's spectral properties was its sensitivity to contrast. For both X- and Y-like cells, sensitivity to contrast was affected by both the spectral type of the cell and whether the cell was spectrally opponent or nonopponent.

Turning first to the influence of spectral opponency on sensitivity to contrast, it was found that spectrally opponent cells were less sensitive to contrast than spectrally nonopponent cells; this agrees with findings in macaque ganglion cells (Kaplan and Shapley, 1982; 1984; 1986). From a theoretical viewpoint, the distinction seems appropriate. If one assumes that spectrally nonopponent cells provide information regarding intensity of luminance changes in the environment, then they should be very sensitive to contrast. Spectrally opponent cells, the most likely candidates for color information, should be less concerned with intensity variations or luminance con-

trast.

From a functional perspective, the difference of Gaussians model predicts that spectrally opponent cells would be less sensitive to contrast than nonopponent cells. Referring back to Figure 53, the result of the difference of Gaussians (Figure 53c) of spectrally opponent cells is not only to reduce the size of the receptive field center, as discussed above, but also to reduce the overall sensitivity of the center mechanism; thus making the cell less sensitive to contrast.

Regarding the differences in sensitivity to contrast across the spectral classes, it was found that L-/+ center cells were more sensitive to contrast than both L+/- and L+/+ center cells. It was also found that the L-/+ center cells saturated at a faster rate than the other two spectral classes. The sensitivity to contrast of L+/+ center cells appears to be the result of a combination of the ON and OFF responses. At low contrasts, these cells behave like L+/- center cells, but saturate at the same contrast as L-/+ center cells. This hybrid response is not surprising since it has been shown anatomically that L+/+ center cells (ON/OFF) receive input from both ON-center and OFF-center type bipolar cells in the inner plexiform layer (Famiglietti, et al., 1977).

Differences in sensitivity to contrast between L+/- and L-/+ center cells suggest different roles for these cell types in the visual process. For example, at scotopic levels, a substantial portion of goldfish OFF ganglion cells were found to have a lower quantum-to-spike ratio and signal-to-noise ratio than both ON and ON/OFF ganglion cells (Falzett, Nussdorf and Powers, 1987). Their findings

suggest that these OFF cells were more sensitive to light than the other cell types. In addition, the psychophysical and OFF cell thresholds were similar while ON cell thresholds differed from both.

Although the present study was performed under photopic conditions, it is quite possible that the role of L-/+ center cells is to detect slight changes in intensity or contrast. The fact that OFF channels are more sensitive to contrast than ON channels have also been demonstrated in humans using visual evoked potentials (Zemon, Gordon and Welch, 1986). On the other hand, the L+/- center cells' function may be for spatial resolution or acuity. This is supported by the fact that the linear portion of the response vs. contrast function covers a large range of contrasts and that the function saturates at very high contrasts. Also, L+/- center cells have smaller receptive field centers and are thus better suited for spatial resolution than L-/+ center cells.

The interaction between spectral class and spectral opponency on the sensitivity to contrast can be explained by the fact that any antagonism between similar components will reduce the overall sensitivity of the cell. Thus, for spectral classes of L+/-, L-/+ and L+/+ center cells, the presence of spectral opponency reduced the sensitivity to contrast. For the L+/+ center cells, spectral opponency has little effect since the ON/OFF components already produced antagonism resulting in a decrease in overall sensitivity to contrast.

4.4 The Big Picture

Perhaps the most striking conclusion one can draw from the

results of this project is the similarity of the responses of goldfish ganglion cells to the ganglion cell responses of other species. Whenever the same quantitative experiments are performed on cat and goldfish ganglion cells, the findings are remarkably similar. They both have the same spatial classes; their responses are a function of spatio-temporal properties and orientation of the stimulus. Even the microstructure of their receptive fields is similar in that they both consist of small, unique subunits and asymmetries. Given that the two species examined are so evolutionarily diverse suggests that these properties are essential in visual processing.

In comparing the effects of the spectral properties on spatial processing, one must turn one's focus to the monkey. When compared, goldfish ganglion cells produce findings similar to monkey ganglion cells. Specifically, spectral opponency has the same effect on the cell's sensitivity to contrast in both goldfish and monkey ganglion cells (Kaplan and Shapley, 1982; 1984; 1986). The influence of spectral class on sensitivity to contrast has not yet been examined in monkey ganglion cells, but it would not be surprising if results similar to the goldfish were found.

It is also believed that when the influence of spectral properties on other spatial processing is examined, they too will concur with the findings in goldfish. To illustrate this statement, data obtained from Thorell, et al. (1984) have been redrawn and shown in Figure 54. The data represents the S-CSFs of two cells located in the VI area of the macaque visual cortex. The stimulus consisted of luminance-varying gratings of 33% contrast. One cell was classified as "double-

Figure 54

S-CSFs of two cells in VI area of macaque visual cortex. One cell has been classified as a single-opponent cell (closed triangles), the other classified as double-opponent (open stars). The stimulus in both cases, consisted of a luminance-varying drifting grating of 33 percent contrast. Each function has been normalized separately. The data points were obtained from figures 12a and 12b from Thorell, et al. (1984) and replotted in one figure; the solid and dashed lines have been redrawn.

S-CSFs of Monkey Cortical Cells by Spectral Opponency

Drifting grating, 33% contrast.

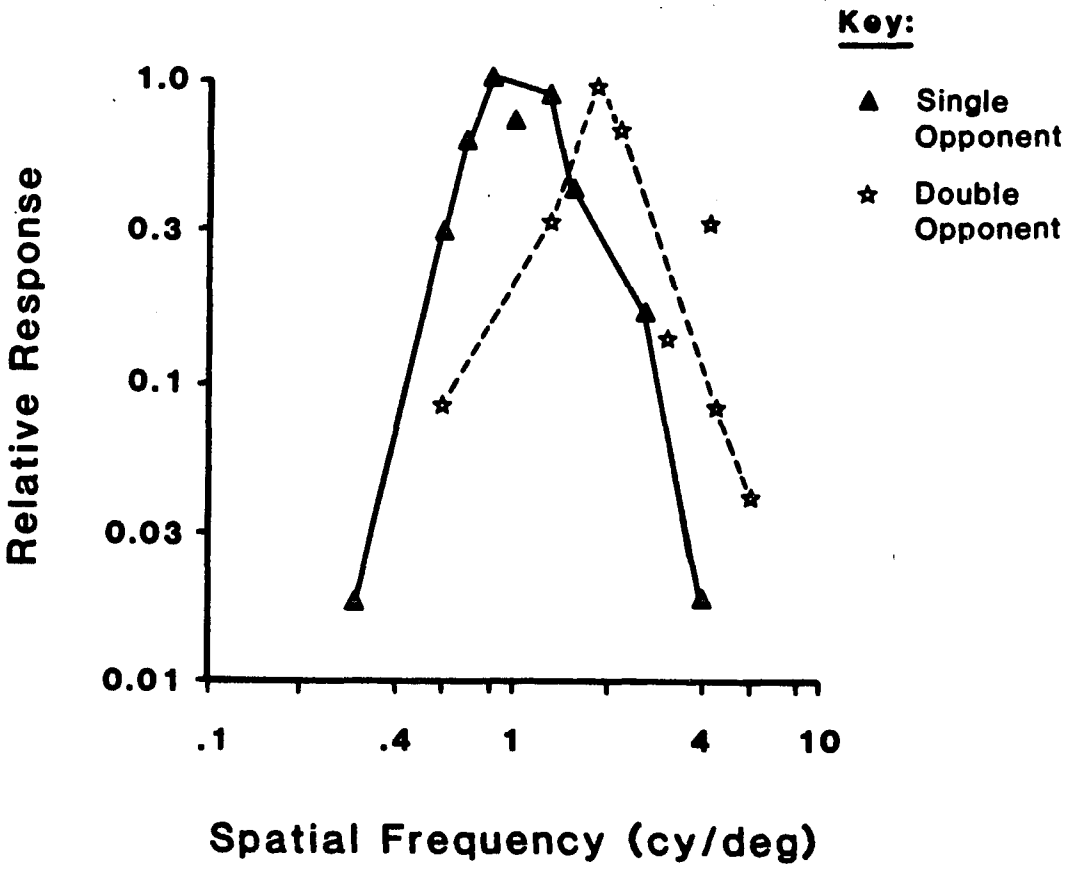

opponent" and the other, "single-opponent" (e.g., +R center/-G surround). Since the grating varies only in luminance, the single-opponent cell is functionally the same as a goldfish spectrally nonopponent cell. The monkey double-opponent cell, of course, corresponds to the goldfish ganglion cell equivalent. The S-CSFs of these cells are very similar to the results obtained from the goldfish cells (see Figure 43). Although each curve in the monkey data is represented by only one cell, the similarity to the goldfish data is quite striking.

This project attempted to examine the spatial and spectral properties of goldfish ganglion cells. To do so, each cell was examined and classified under a variety of dimensions; some were spatial dimensions (e.g., spatial summation, response to contrast), others were spectral categories (e.g., spectral class, spectral opponency). It was hoped that from these different classifications, a small subset (ideally one) could have been used to predict and explain the responses of each cell under a wide range of conditions. Unfortunately, it is not that simple. There is no one dimension that can predict the response pattern of a ganglion cell. For example, knowing that the cell is an X-like cell does not provide any information regarding its spectral properties or the shape of its S-CSF. Also, if the S-CSF displays no low frequency attenuation, it could be because there is no surround or because the temporal pattern of the stimulus has invoked a center and surround synergism. In order to understand the response pattern of the cell, one must know several characteristics -- one or two will not be adequate. However, once the various parame-

ters of the cell are known, as in this study, its response to the various stimuli can be understood.

The concentric center and antagonistic surround receptive field organization is no longer completely adequate to explain a cell's response pattern. This model was useful in explaining behavior when the stimulus consisted of stationary spots or slowly moving bars of light. However, as vision research progressed and the visual stimulus became somewhat more complex and dynamic, so did the cell's responses. The center and surround can be antagonistic to some stimuli and synergistic to others; spectrally opponent cells' antagonistic color components can interact and enhance the cell's spatial resolution; a cell can provide orientation and direction information for some stimuli but not for others. All of which leads to the following conclusion: In order to understand the behavior of a neuron, one must examine its spatial, temporal and spectral properties.

4.5 Where do we go from here?

One goal of this project was to bring the spatial processing of goldfish ganglion cells "up to date". The general subdivision of ganglion cells into X, Y, and W categories appears to hold across vertebrate species. These cells clearly exist in the goldfish and their properties seem to be the same as in mammals. This increases the usefulness of the goldfish as a "model vertebrate" system. The goldfish also offers some distinct advantages over other species: First, the goldfish, unlike most mammals, has well-developed color vision. Second, the spectral sensitivities of its cones are well separated so

that, unlike in monkeys, it is relatively simple to isolate responses driven by single cone types and to ask what are their separate contributions to spatial and temporal processing. Third, compared with the mammalian retina, the isolated goldfish retina is easier to maintain, and the responses of more distal cells that provide inputs to the ganglion cells are easier to record.

In terms of future research, perhaps a more detailed and focused approach is the next step. This project attempted to examine a wide range of visual processing. Such a global approach was necessary to provide a framework for more specific and detailed projects.

One such project would be a more detailed investigation of the center and surround inputs to the overall S-CSF. Because the center and surround fields overlap, it is impossible to stimulate the entire area of one component without stimulating the other. For example, any stimulus that stimulates the center must inevitably stimulate the middle portion of the surround. This was the case in this project as well; the stimulus areas for this study were chosen to maximize the influence of one area, while minimizing the input from the other. Since there is no simple way to avoid this interaction, it would be interesting to examine the S-CSFs as the size of the stimulus area is varied. For instance, one could restrict the stimulus pattern to 0.5, 1.0, 2.0 mm, etc. diameters and derive S-CSFs for the center and surround and compare them to the full field S-CSF as in this study. Presumably, as the stimulus area becomes smaller, there is less influence of the surround and the response is mostly the result of the center input. To illustrate the role of the center and surround

Figure 55

Effect of stimulus area on the S-CSFs of the center and surround components of an X-like cell. The response measure was the amplitude of the fundamental component. The stimulus consisted of a 2 Hz drifting grating at 40% contrast. Each response value was normalized with respect to one maximum. The dotted line in each figure represents the response of the cell to a zero contrast stimulus (i.e., spontaneous level). The full field S-CSF (closed circles) is shown in both figures for comparison. Open stars refer to the response to a grating restricted to either a 1 mm by 1 mm (a) or a 0.5 mm by 0.5 mm (b) square centered on the receptive field; enclosed stars represent the response of the cell to a grating restricted to the surrounding portion of the full aperture. In all cases, the portion of the receptive field not stimulated by the grating was maintained at mean luminance.

Effect of Stimulus Area on S-CSFs X-like cell (C52B) Amplitude of Fundamental Component N: 20.

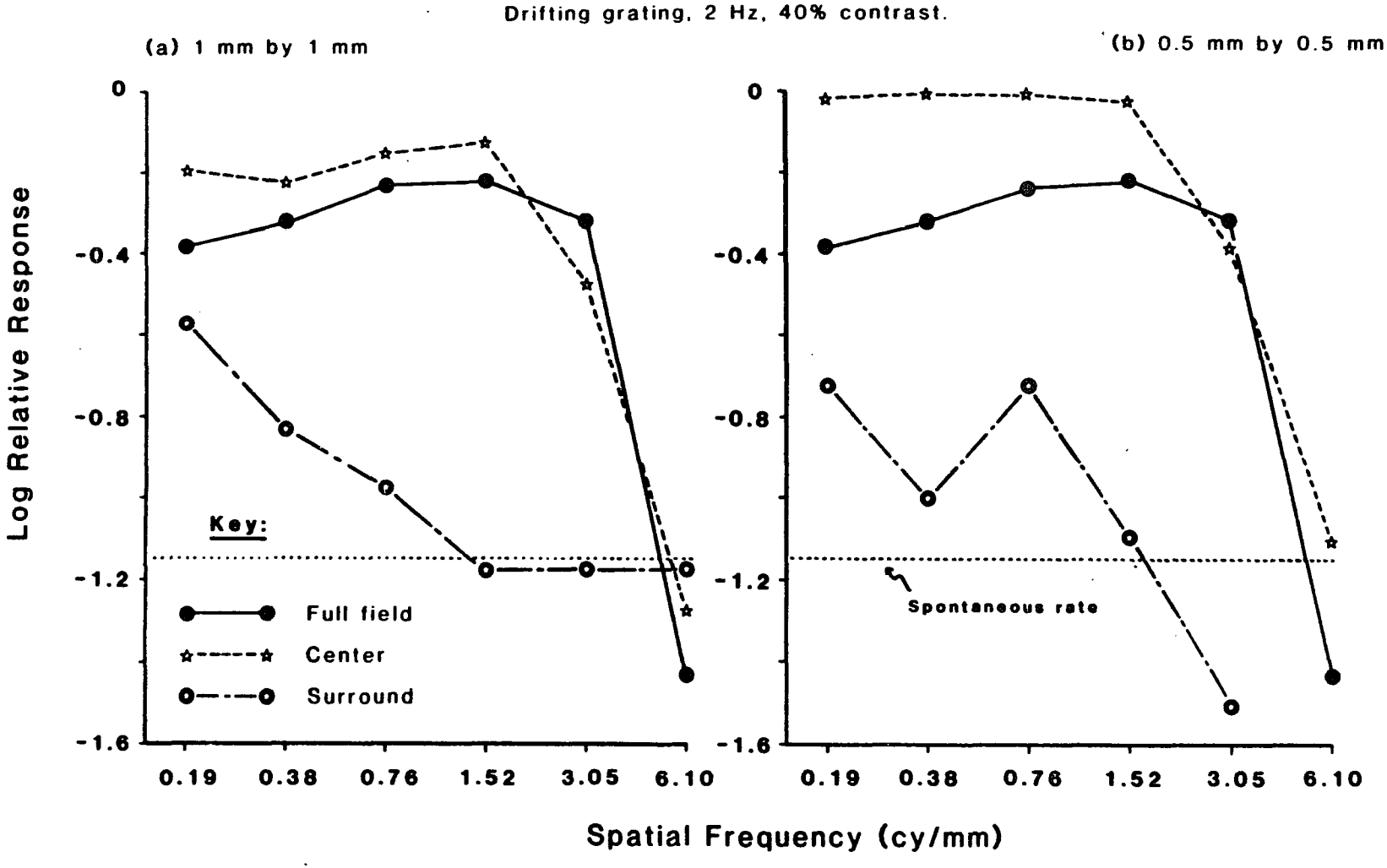

interactions as a function of stimulus area, Figure 55 shows some pilot work on an X-like cell. S-CSFs were obtained from the full field, the center only, and the surround only. In Figure 55a, the sinusoidal grating was restricted to a 1 mm by 1 mm square; in Figure 55b, the grating was presented in a 0.5 mm by 0.5 mm square. For surround stimulation only, the stimulus consisted of the full field area with a center plug of the appropriate size. The overall mean luminance was the same for all areas. The response measure was the amplitude of the fundamental component and the stimulus consisted of a 2 Hz drifting grating at 40 percent contrast. The full field S-CSF was derived only once but shown in each figure for comparison. Although the values at high spatial frequencies are most like due to noise (the horizontal dotted line represents the cell's response to a zero contrast grating), it is obvious that when the stimulus area is smaller (Figure 55b), the center component dominates the response. Comparing the S-CSFs of the center and the full field with a larger stimulus area (Figure 55a), there is some low frequency attenuation in the full field S-CSF as well as in the center component; at low spatial frequencies in this figure the response of the surround function is relatively strong and the center function may also contain a surround contribution. However, with a smaller stimulus area, the center displays no low frequency attenuation and the surround response is not as strong.

Another set of experiments that can be used to examine the interaction of the center and surround, is to derive S-CSFs at different mean luminances. As demonstrated in cat ganglion cells, at low

luminance levels, the response of the surround diminishes (Barlow, et al., 1957); thus low frequency attenuation should decrease (Enroth-Cugell and Robson, 1966). One could also examine the spatio-temporal interactions under the different luminance conditions to obtain a more complete understanding of the center and surround interactions.

Finally, one could examine the spatial and temporal characteristics of the separate cone channels. Although there is evidence from human psychophysics that the L- and M-channels are spatially and temporally similar (Cavonius and Estevez, 1975; Green, 1968; 1969; Kelly, 1974; Mollon and Krauskopf, 1973), there is also evidence to suggest that the S-channel may have poorer spatial (Cavonius and Estevez, 1975; Green, 1968; Kelly, 1974) and temporal resolution (Boynton and Whitten, 1975). To examine this, one must be able to isolate the separate cone mechanisms prior to examining the spatial and temporal properties. This could be accomplished by the use of chromatic adaptation or the technique of "silent substitution" (see Estevez and Spekreijse, 1982). Chromatic adaptation is a technique in which an intense, spectrally restricted, light is presented to the retina which selectively adapts or desensitizes the cone mechanism(s) one wishes to eliminate. The problem with chromatic adaptation lies in the fact that the spectral sensitivities of the cone types overlap particularly at the shorter wavelengths. Thus, although it is possible to eliminate the M- and L-cones with an intense "yellow" light and examine the S-cone input, it would be difficult to chromatically adapt the S-cones and not also adapt the M- and L-cones. Another problem

with chromatic adaptation is the phenomenon of cross-adaptation. That is, adapting one cone channel, may alter the sensitivity or responses of the isolated cone channel (see Wisowaty and Boynton, 1980).

Silent substitution is an alternative method to isolate cone types. In this technique, two wavelengths of light are chosen so that the two cone types one wishes to eliminate are equally sensitive. Alternating these two stimuli in succession produces no change in response for these two cone inputs. However, if a third cone input is present and the two stimuli are not iso-absorption values for that cone type, there will be a response modulation when the two stimuli are interchanged. Unfortunately, for silent substitution to be effective, the stimuli must be chosen with great precision; any variation can produce large discrepancies in the responses. This can be accomplished only if the cone spectra are accurately known. Although there are problems with both methods, any information regarding the spatio-temporal processing of the cone types would prove interesting.

Appendix

CONVERTING CYCLES PER MILLIMETER TO CYCLES PER DEGREE

In this section, the operations used to convert cycles per millimeters on the retina to cycles per degree are described. This conversion is necessary to compare the electrophysiological spatial contrast sensitivity function (S-CSF) of single neurons to the goldfish psychophysical S-CSF determined by Northmore and Dvorak (1979).

The procedure is based on the values obtained from the schematic eye of the goldfish (Charman and Tucker, 1973). They derived the "standard" values from fish ranging in body length from 5 to 9 centimeters and body weight between 3 and 10 grams. Their schematic eye reflects values of a 8.5 centimeter fish weighing 10 grams.

Based on the assumptions of thick-lens theory and the fact that the goldfish lens is roughly spherical, the principle and nodal points are located in the center of the lens, the important value for our purpose is the distance from the receptors to the lens nodal point or the second focal length. Charman and Tucker (1973) found this value to be 2.87 millimeters in water. (In air, it is slightly different at 2.51 millimeters.) From this value, the appropriate conversion value can be determined in the following manner:

Suppose an object is imaged on the retina so that the image cov-

ers one millimeter of the retina. In bisecting this image with a line perpendicular to the retina extending to the second nodal point of the lens, a right triangle is formed (see Figure 56). Two sides of this triangle are known since one side is one-half of the one millimeter image on the retina, and another side is the second focal length. From these two values, the angle θ can be determined:

$$\tan \theta = \text{one-half image size} / \text{second focal length} \qquad (A.1)$$

Substituting the known values into equation A.1:

$$\tan \theta = 0.5 \text{ mm} / 2.87 \text{ mm} \qquad (A.2)$$

giving:

$$\tan \theta = 0.17422 \qquad (A.3)$$

and solving for θ:

$$\theta = \arctan 0.17422 \qquad (A.4)$$

yielding:

$$\theta = 9.88 \text{ degrees} \qquad (A.5)$$

Since θ represents only half of the entire image length, a one

Figure 56

Schematic of the goldfish eye. The values are from Charman and Tucker (1973).

Goldfish Schematic Eye

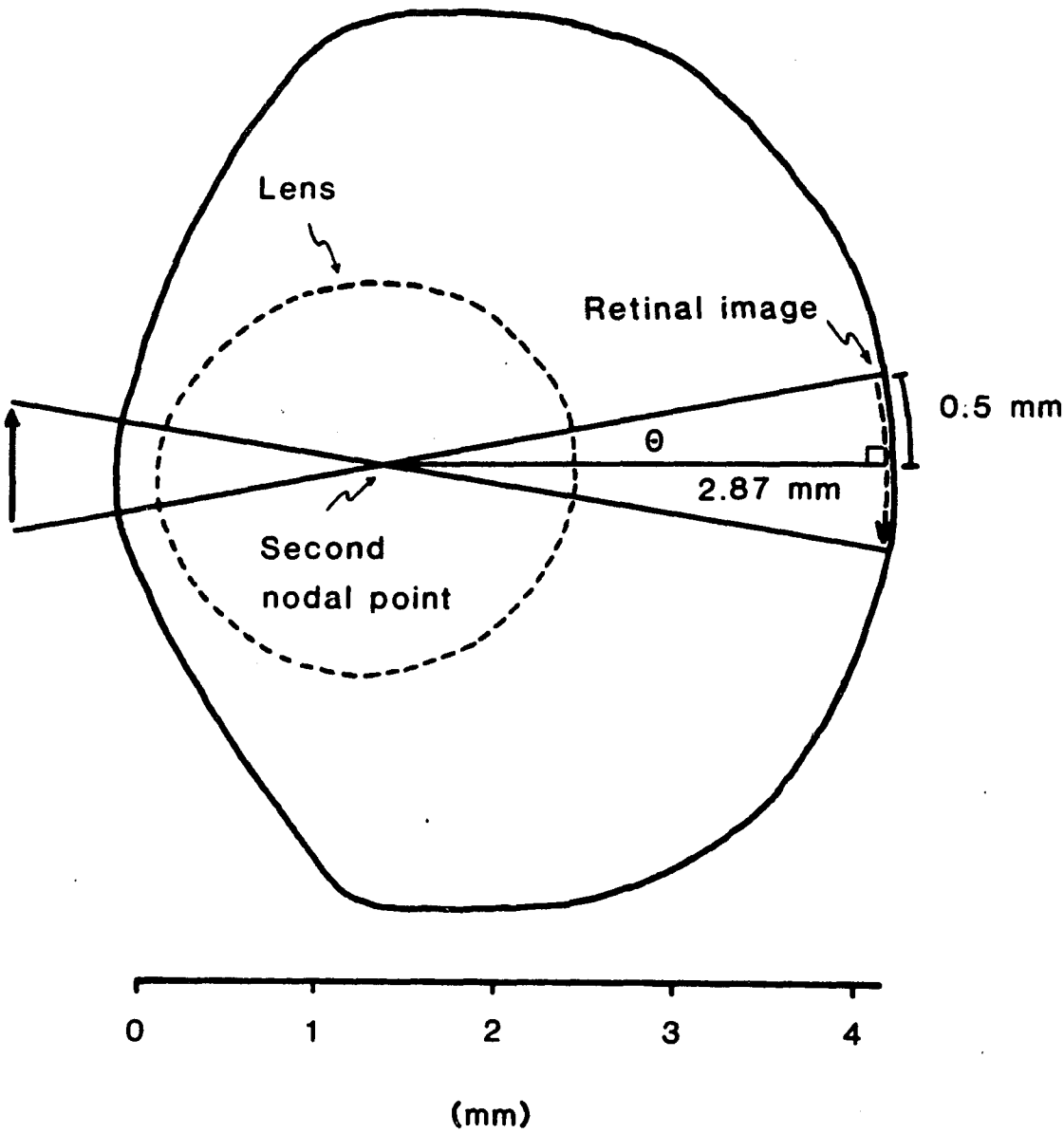

millimeter image on the retina has double this angular subtense to yield 19.76 degrees. Therefore, the conversion factor is 20 degrees per millimeter on the retina.

However, the schematic goldfish eye values were calculated from a standard fish 8.5 centimeters in length. Since the goldfish lens diameter is positively correlated with body length (Easter, Johns and Bouman, 1977), the length of the fish used in the measurements could affect the values of the lens diamenter and hence the conversion value. Macy and Easter (1981) have shown that the distance on the retinal surface per degree of visual angle varies as a function of the lens diameter. Because of this, they have derived a general equation which adjusts for the difference in lens diameter. This "Retinal Magnification Factor (RMF) can be computed as follows:

$$\text{RMF } (\mu m/deg) = 20.5 \times \text{lens diameter (mm)} \qquad (A.6)$$

Referring back to the schematic eye, the lens diameter for the standard fish is 2.40 millimeters. Substituting this value into equation A.6 gives a RMF of 49.2 microns per degree. Converting to degrees per millimeter yields 20.3 or approximately 20 degrees per millimeter; this agrees with the value determined above.

To determine the appropriate RMF of the fish used in this study, the lens diameters of ten eyes used in this study were measured. Each lens was measured immediately following enucleation with vernier calipers (Manstat; Type 6911). The average lens diameter was found to be 2.58 millimeters (SD = 0.23). Substituting this value

into equation A.6 produces a conversion value of 18.91 or 19 degrees per millimeter. Therefore, the conversion value used in this project to convert cycles per millimeter on the retina to cycles per degree of visual angle was 19 degrees per millimeter.

References

Charman, W.N., & Tucker, J. (1973). The optical system of the goldfish eye. Vision Research, 13, 1-8.

Easter, S.S., Jr., Johns, P.R. & Bauman, L.R. (1977). Growth of the adult goldfish eye - 1. Optics. Vision Research, 17, 460-477.

Northmore, D.P.M., & Dvorak, C.A. (1979). Contrast sensitivity and acuity of the goldfish. Vision Research, 19, 255-261.

REFERENCES

Abramov, I., & Gordon, J. (1973). Vision. In E.C. Carterette & M.P. Friedman (Eds.), Handbook of Perception: Vol. 3. Biology of Perceptual Systems (pp. 327-357). New York: Academic Press.

Abramov, I., & Levine, M.W. (1972). The effects of carbon dioxide on the excised goldfish retina. Vision Research, 12, 1881-1895.

Abramov, I., & Levine, M.W. (1975). On the lack of lateral inhibition within the receptive fields of goldfish retinal ganglion cells. Vision Research, 15, 791-798.

Adams, A.J. (1970). Chromatic, spatial and temporal influences on single ganglion cell responses of the in vivo goldfish retina. Unpublished doctoral dissertation, Indiana University.

Ali, M.A. (1975). Retinomotor responses. In M.A. Ali (Ed.), Vision in Fishes: New Approaches in Research: Vol. 1 (pp. 313-355). New York: Plenum Press.

Avery, J.A., Bowmaker, J.K., Djamgoz, M.E.A., & Downing, J.E.G. (1982). Ultra-violet sensitive receptors in a freshwater fish. Journal of Physiology, 334, 23P.

Barlow, H.B. (1953). Summation and inhibition in the frog's retina. Journal of Physiology, 119, 69-88.

Barlow, H.B., Fitzhugh, R., & Kuffler, S.W. (1957). Change of organization in the receptive fields of the cat's retina during dark adaptation. Journal of Physiology, 137, 338-354.

Barlow, H.B., Hill, R.M., & Levick, W.R. (1964). Retinal ganglion cells responding selectively to direction and speed of image motion in the rabbit. Journal of Physiology, 173, 377-407.

Barlow, H.B., & Mollon, J.D. (1982). The Senses. Cambridge: Cambridge University Press.

Baylor, D.A., & Fuortes, M.G.F. (1970). Electrical responses of single cones in the retina of the turtle. Journal of Physiology, 207, 77-92.

Baylor, D.A., & Hodgkin, A.L. (1973). Detection and resolution of visual stimuli by turtle photoreceptors. Journal of Physiology, 234, 163-198.

Beauchamp, R.D., & Daw, N.W. (1972). Rod and cone input to single goldfish optic nerve fibers. Vision Research, 12, 1201-1212.

Beauchamp, R.D., & Lovasik, J.V. (1973). Blue mechanism response of single goldfish optic nerve fibers. Journal of Neurophysiology, 36, 925-939.

Boycott, B.B., & Dowling, J.E. (1969). Organization of the primate retina: Light microscopy. Philosophical Transactions of the Royal Society of London, 255, 109-184.

Boynton, R.M., & Whitten, D.N. (1970). Visual adaptation in monkey cones: Recordings of late receptor potentials. Science, 170, 1423-1426.

Boycott, B.B., & Wassle, H. (1974). The morphological types of ganglion cells of the domestic cat's retina. Journal of Physiology, 240, 397-419.

Braddick, O., Campbell, F.W., & Atkinson, J. (1978). Channels in vision: basic aspects. In R. Held, H.W. Leibowitz & Teuber, H.-L. (Eds.), Handbook of Sensory Physiology: Vol. VIII. Perception (pp. 3-38). Berlin: Springer-Verlag.

Bridges, C.D.B. (1967). Spectroscopic properties of porphyropsins. Vision Research, 7, 349-369.

Bridges, C.D.B. (1972). The rhodopsin-porphyropsin visual system. In H.J.A. Dartnall (Ed.), Handbook of Sensory Physiology: Vol. VII. Photochemistry of Vision (pp. 417-480). Berlin: Springer-Verlag.

Brown, K.T., & Wiesel, T.N. (1959). Intraretinal recording with micropipette electrodes in the intact cat eye. Journal of Physiology, 149, 537-562.

Burkhardt, D.A. (1977). Responses and receptive-field organization of cones in perch retinas. Journal of Neurophysiology, 40, 53-62.

Byzov, A.L., & Trifonov, Yu.A. (1968). The response to electric stimulation of horizontal cells in the carp retina. Vision Research, 8, 817-822.

Cajal, S.R. (1893). 'La retine des vertebres' translated by D. Maguire & R.W. Rodieck. In R.W. Rodieck's (1973): The Vertebrate Retina. San Fransisco: W.H. Freeman & Co.

Cavonius, C.R., & Estevez, O. (1975). Contrast sensitivity of individual colour mechanisms of human vision. Journal of Physiology, 248, 649-662.

Charman, W.N., & Tucker, J. (1973). The optical system of the goldfish eye. Vision Research, 13, 1-8.

Cleland, B.G., Dubin, M.W., & Levick, W.R. (1971). Sustained and transient neurones in the cat's retina and lateral geniculate nucleus. Journal of Physiology, 217, 473-496.

Cleland, B., & Enroth-Cugell, C. (1966). Cat retinal ganglion cell responses to changing light intensities: sinusoidal modulation in the time domain. Acta Physiologica Scandinavica, 68, 365-381.

Cleland, B.G., & Enroth-Cugell, C. (1968). Quantitative aspects of sensitivity and summation in the cat retina. Journal of Physiology, 198, 17-38.

Cleland, B.G., Harding, T.H., & Tulunay-Keesey, U. (1979). Visual resolution and receptive field size: examination of two kinds of cat retinal ganglion cells. Science, 205, 1015-1017.

Cleland, B.G., & Levick, W.R. (1974a). Brisk and sluggish concentrically organized ganglion cells of the cat's retina. Journal of Physiology, 240, 421-456.

Cleland, B.G., & Levick, W.R. (1974b). Properties of rarely encountered types of ganglion cells in the cat's retina and an overall classification. Journal of Physiology, 240, 457-492.

Cleland, B.G., Levick, W.R., & Wassle, H. (1975). Physiological identification of a morphological class of cat retinal ganglion cells. Journal of Physiology, 248, 151-171.

Cooley, J.W., & Tukey, T.W. (1965). An algorithm for the machine calculation of complex Fourier series. Mathematics of Computations, 19, 297-301.

Cronly-Dillon, J.R. (1964). Units sensitive to direction of movement in goldfish optic tectum. Nature, 203, 214-215.

Daw, N.W. (1967a) Color coded units in the goldfish retina. Unpublished doctoral dissertation, The Johns Hopkins University, Baltimore.

Daw, N.W. (1967b) Goldfish retina: organization for simultaneous color contrast. Science, 158, 942-944.

Daw, N.W. (1968). Colour coded ganglion cells in the goldfish retina: extension of their receptive fields by means of new stimuli. Journal of Physiology, 197, 567-592.

Daw, N.W., & Beauchamp, R.D. (1972). Unusual units in the goldfish optic nerve. Vision Research, 12, 1849-1856.

Dawis, S., Shapley, R., Kaplan, E., & Tranchina, D. (1984). The receptive field organization of X-cells in the cat: spatiotemporal coupling and asymmetry. Vision Research, 24, 549-564.

de Monasterio, F.M. (1978). Center and surround mechanisms of opponent-color X and Y ganglion cells of retina of macques. Journal of Neurophysiology, 41, 1418-1434.

de Monasterio, F.M., Gouras, P., & Tolhurst, D.J. (1976). Spatial summation, response pattern and conduction velocity of ganglion cells of the rhesus monkey retina. Vision Research, 16, 674-678.

Derrington, A.M., & Lennie, P. (1982). The influence of temporal frequency and adaptation level on receptive field organization of retinal ganglion cells in cat. Journal of Physiology, 333, 343-366.

DeTesta, A.S. (1966). Morphological studies on the horizontal and amacrine cells of the teleost retina. Vision Research, 6, 51-59.

De Valois, R.L., & De Valois, K.K. (1975). Neural coding of color. In E.C. Carterette & M.P. Friedman (Eds.), Handbook of Perception: Vol. 5. Seeing (pp. 117-166). New York: Academic Press.

Dreher, B., Fukuda, Y., & Rodieck, R.W. (1976). Identification, classification and anatomical segregation of cells with X-like and Y-like properties in the lateral geniculate nucleus of old-world primates. Journal of Physiology, 258, 433-452.

Dowling, J.E. (1970). Organization of vertebrate retinas. Investigative Ophthalmology and Visual Science, 9, 655-680.

Dowling, J.E., Ehinger, B., & Hedden, W.L. (1976). The interplexiform cell: a new type of retinal neuron. Investigative Ophthalmology and Visual Science, 15, 916-926.

Easter, S.S., Jr. (1967). Excitation and adaptation in the goldfish retina: a microelectrode study. Unpublished doctoral dissertation, The Johns Hopkins University; Baltimore.

Easter, S.S., Jr. (1968). Excitation in the goldfish retina: evidence for a non-linear intensity code. Journal of Physiology, 195, 253-271.

Enroth-Cugell, C., & Pinto, L.H. (1972a). Properties of the surround response mechanism of cat retinal ganglion cells and center-surround interaction. Journal of Physiology, 220, 403-439.

Enroth-Cugell, C., & Pinto, L.H. (1972b). Pure central responses from off-center cells and pure surround responses from on-center cells. Journal of Physiology, 220, 441-464.

Enroth-Cugell, C., & Robson, J.G. (1966). The contrast sensitivity of retinal ganglion cells of the cat. Journal of Physiology, 187, 517-552.

Enroth-Cugell, C., & Robson, J.G. (1984). Functional characteristics and diversity of cat retinal ganglion cells: Basic characteristics and quantitative description. Investigative Ophthalmology and Visual Science, 25, 250-267.

Enroth-Cugell, C., Robson, J.G., Schweitzer-Tong, D.E. & Watson, A.B. (1983). Spatio-temporal interactions in cat retinal ganglion cells showing linear spatial summation. Journal of Physiology, 341, 279-307.

Estevez, O., & Spekreijse, H. (1982). The 'silent substitution' method in vision research. Vision Research, 22, 681-691.

Falzett, M., Nussdorf, J.D. & Powers, M.K. (1987). Responsivity and absolute sensitivity of retinal ganglion cells in goldfish of different sizes, when measured under "psychophysical" conditions. Manuscript submitted for publication.

Famiglietti, E.V., Jr., Kaneko, A. & Tachibana, M. (1977). Neuronal architecture of on and off pathways to ganglion cells in the carp retina. Science, 198, 1267-1269.

Famiglietti, E.V., Jr., & Kolb, H. (1976). Structural basis for ON- and OFF-center responses in retinal ganglion cells. Science, 194, 193-195.

Fukuda, Y., & Stone, J. (1974). Retinal distribution and central projections of X-, Y-, and W-cells of the cat's retina. Journal of Neurophysiology, 37, 749-772.

Fukurotani, K., & Hashimoto, Y. (1984). A new type of S-potential in the retina of cyprinid fish: the tetraphasic spectral response. Investigative Ophthalmology and Visual Science, 19(Suppl.), 118.

Gordon, J., & Shapley, R.M. (1978). Contrast sensitivity and spatial summation in frog and eel retinal ganglion cells. In J.C. Armington, J. Krauskopf & B.R. Wooten (Eds.), Visual Psychophysics and Physiology (pp. 315-329). New York: Academic Press.

Gouras, P. (1968). Identification of cone mechanisms in monkey ganglion cells. Journal of Physiology, 199, 533-547.

Gouras, P. (1969). Antidromic responses of orthodromically identified ganglion cells in monkey retina. Journal of Physiology, 204, 407-419.

Gouras, P., & Zrenner, E. (1979). Enhancement of luminance flicker by color-opponent mechanisms. Science, 205, 587-589.

Green, D.G. (1968). The contrast sensitivity of the colour mechanisms of the human eye. Journal of Physiology, 196, 415-429.

Green, D.G. (1969). Sinusoidal flicker characteristics of the color-sensitive mechanisms of the eye. Vision Research, 9, 591-601.

Grusser, O.-J., Schaible, D. & Vierkany-Glathe, J. (1970). A quantitative analysis of the spatial summation of excitation within the receptive field centers of retinal neurons. Pflugers Archives, 319, 101-121.

Hammond, P. (1973). Contrasts in spatial organization of receptive fields at geniculate and retinal levels: centre, surround and outer surround. Journal of Physiology, 228, 115-137.

Hammond, P. (1974). Cat retinal ganglion cells: size and shape of receptive field centres. Journal of Physiology, 242, 99-118.

Harosi, F.I. (1976). Spectral relations of cone pigments in goldfish. Journal of General Physiology, 68, 65-80.

Harosi, F.I., & Hashimoto, Y. (1983). Ultraviolet visual pigment in a vertebrate: a tetrachromatic cone system in the dace. Science, 222, 1021-1023.

Harris, C.M., & Abramov, I. (1983). Linearizing the z-axis of an oscilloscope display. Behavior Research Methods & Instrumentation, 15, 662.

Hartline, H.K. (1938). The response of single optic nerve fibers of the vertebrate eye to illumination of the retina. American Journal of Physiology, 121, 400-415.

Hartline, H.K., & McDonald, P.R. (1947). Light and dark adaptation of single photoreceptor elements in the eye of Limulus. Journal of Cellular and Comparative Physiology, 30, 225-254.

Hashimoto, Y., & Inokuchi, M. (1981). Characteristics of second order neurons in the dace retina: physiological and morphological studies. Vision Research, 21, 1541-1550.

Hawryshyn, C.W., & Beauchamp, R.D. (1985). Ultraviolet photosensitivity in goldfish: an independent U.V. retinal mechanism. Vision Research, 25, 11-20.

Hester, F.J. (1968). Visual contrast thresholds of the goldfish (Carassius auratus). Vision Research, 8, 1315-1336.

Hitchcock, P.F., & Easter, S.S., Jr., (1984). Morphology and quantitative differentiation of retinal ganglion cells in the goldfish. Society for Neuroscience Abstracts, 10, 465.

Hitchcock, P.F., & Easter, S.S., Jr., (1986). Retinal ganglion cells in goldfish: a qualitative classification into four morphological types, and a quantitative study of the development of one of them. Journal of Neuroscience, 6, 1037-1050.

Hochstein, S., & Shapley, R.M. (1976a). Quantitative analysis of retinal ganglion cell classifications. Journal of Physiology, 262, 237-264.

Hochstein, S., & Shapley, R.M. (1976b). Linear and nonlinear spatial subunits in Y cat retinal ganglion cells. Journal of Physiology, 262, 265-284.

Hubel, D.H., & Wiesel, T.N. (1968). Receptive fields and functional architecture of monkey striate cortex. Journal of Physiology, 195, 215-243.

Ishida, A.T., Stell, W.K. & Lightfoot, D.O. (1980). Rod and cone inputs to bipolar cells in goldfish retina. Journal of Comparative Neurology, 191, 315-335.

Jacobson, M., & Gaze, R.M. (1964). Types of visual response from single units in the optic tectum and optic nerve of the goldfish. Quarterly Journal of Experimental Physiology, 49, 199-209.

Kaneko, A. (1970). Physiological and morphological identification of horizontal, bipolar and amacrine cells in goldfish retina. Journal of Physiology, 207, 623-633.

Kaneko, A. (1971a). Electrical connexions between horizontal cells in the dogfish retina. Journal of Physiology, 213, 95-105.

Kaneko, A. (1971b). Physiological studies of single retinal cells and their morphological identification. Vision Research, (Suppl. 3), 17-26.

Kaneko, A. (1973). Receptive field organization of bipolar and amacrine cells in the goldfish retina. Journal of Physiology, 235, 133-153.

Kaneko, A. (1979). Physiology of the retina. Annual Review of Neuroscience, 2, 169-191.

Kaneko, A., & Hashimoto, H. (1969). Electrophysiological study of single neurons in the inner nuclear layer of the carp retina. Vision Research, 9, 37-55.

Kaneko, A., & Tachibana, M. (1981). Retinal bipolar cells with double colour-opponent receptive fields. Nature, 293, 220-222.

Kaplan, E., Marcus, S. & So, Y.T. (1979). Effects of dark adaptation on spatial and temporal properties of receptive fields in cat lateral geniculate nucleus. Journal of Physiology, 294, 561-680.

Kaplan, E., & Shapley, R.M. (1982). X and Y cells in the lateral geniculate nucleus of macaque monkeys. Journal of Physiology, 330, 125-143.

Kaplan, E., & Shapley, R.M. (1984). The primate retina contains 2 groups of ganglion cells, with high and low contrast sensitivity. Investigative Ophthalmology and Visual Science, 25(Suppl.), 120.

Kaplan, E., & Shapley, R.M. (1986). The primate retina contains two types of ganglion cells, with high and low contrast sensitivity. Proceedings of the National Academy of Sciences, USA, 83, 2755-2757.

Kelly, D.H. (1974). Spatio-temporal frequency characteristics of color-vision mechanisms. Journal of the Optical Society of America, 64, 983-990.

Kolb, H. (1970). Organization of the outer plexiform layer of the primate retina: electron microscopy of Golgi-impregnated cells. Philosophical Transactions of the Royal Society of London, 258, 261-283.

Kock, J.-H., & Reuter, T. (1978). Retinal ganglion cells in the crucian carp (Carassius carassius). II. Overlap, shape and tangential orientation of dendritic trees. Journal of Comparative Neurology, 179, 549-568.

Kuffler, S.W. (1953). Discharge patterns and functional organization of mammalian retina. Journal of Neurophysiology, 16, 37-68.

Lettvin, J.Y., Maturana, H.R., McCulloch, W.S. & Pitts, W.H. (1959). What the frog's eye tells the frog's brain. Proceedings of the Institute of Radio Engineers, 47, 1940-1951.

Levick, W.R., & Thibos, L.N. (1982). Analysis of orientation bias in cat retina. Journal of Physiology, 329, 243-261.

Levine, M.W. (1972). An analysis of spatial summation in the receptive fields of goldfish retinal ganglion cells. Unpublished doctoral dissertation. Rockefeller University: New York.

Levine, M.W. (1982). Retinal processing of intrinsic and extrinsic noise. Journal of Neurophysiology, 48, 992-1010.

Levine, M.W., & Abramov, I. (1975). An analysis of spatial summation in the receptive fields of goldfish retinal ganglion cells. Vision Research, 15, 777-789.

Levine, M.W., & Shefner, J.M. (1979). X-like and not X-like cells in goldfish retina. Vision Research, 19, 95-97.

Levine, M.W., & Zimmerman, R.P. (1986). Evidence for local circuits within the receptive fields of retinal ganglion cells. Manuscript submitted for publication.

Linsenmeier, R.A., Frishman, L.J., Jakiela, H.G. & Enroth-Cugell, C. (1982). Receptive field properties of X and Y cells in the cat retina derived from contrast sensitivity measurements. Vision Research, 22, 1173-1183.

Lockhart, M., & Stell, W.K. (1979). Invaginating telodendria: a pathway for color-specific interconnections between goldfish cones. Investigative Ophthalmology and Visual Science, 19(Suppl.), 82.

Mackintosh, R.M. (1981). Short-wavelength cone input to the spectrally-opponent ganglion cells in the isolated goldfish retina. Unpublished doctoral dissertation, New School for Social Research: New York.

Mackintosh, R.M., Bilotta, J. & Abramov, I. (1987). Contributions of short-wavelength cones to goldfish ganglion cells. In press: Journal of Comparative Physiology A.

Macy, A., & Easter, S.S., Jr. (1981). Growth-related changes in the size of receptive field centers of retinal ganglion cells in goldfish. Vision Research, 21, 1498-1504.

Maffei, L. (1978). Spatial frequency channels: neural mechanisms. In R. Held, H.W. Leibowitz & Teuber, H.-L. (Eds.), Handbook of Sensory Physiology: Vol. VIII. Perception (pp. 39-66). Berlin: Springer-Verlag.

Maffei, L., & Cervetto, L. (1968). Dynamic interactions in retinal receptive fields. Vision Research, 8, 1299-1303.

Maffei, L., & Fiorentini, A. (1973). The visual cortex as a spatial frequency analyser. Vision Research, 13, 1255-1267.

Marc, R.E. (1977). Chromatic patterns of cone photoreceptors (1976 Glenn A. Fry Award Lecture). American Journal of Optometry and Physiological Optics, 54, 212-225.

Marc, R.E., & Sperling, H.G. (1976). Chromatic organization of the goldfish cone mosaic. Vision Research, 16, 1211-1224.

Marks, W.B. (1965). Visual pigments of single goldfish cones. Journal of Physiology, 178, 14-32.

Milkman, N., Shapley, R.M. & Schick, G. (1978). A microcomputer based visual stimulator. Behavior Research Methods and Instrumentation, 10, 539-545.

Mollon, J.D., & Krauskopf, J. (1973). Reaction time as a measure of the temporal response properties of individual colour mechanisms. Vision Research, 13, 27-40.

Naka, K., & Ohtsuka, T. (1975). Morphological and functional identifications of catfish retinal neurons. II. Morphological identification. Journal of Neurophysiology, 38, 72-91.

Naka, K., & Rushton, W.A.H. (1966a). S-potentials from colour units in the retina of fish (Cyprinidae). Journal of Physiology, 185, 536-555.

Naka, K., & Rushton, W.A.H. (1966b). An attempt to analyse colour reception by electrophysiology. Journal of Physiology, 185, 556-586.

Naka, K., & Rushton, W.A.H. (1966c). S-potentials from luminosity units in the retina of fish (Cyprinidae). Journal of Physiology, 185, 578-599.

Neumeyer, C. (1985). An ultraviolet receptor as a fourth receptor type in goldfish color vision. Naturwissenschaften, 72, 162-163.

Northmore, D.P.M., & Dvorak, C.A. (1979). Contrast sensitivity and acuity of the goldfish. Vision Research, 19, 255-261.

O'Bryan, P.M. (1973). Properties of the depolarizing synaptic potential evoked by peripheral illumination in cones of the turtle retina. Journal of Physiology, 235, 207-223.

Ratliff, F. (1965). Mach Bands: Quantitative Studies on Neural Networks in the Retina. San Francisco: Holden-Day.

Ratliff, F., Knight, B.W. & Graham, N. (1969). On tuning and amplification by lateral inhibition. Proceedings of the National Academy of Sciences, 62, 733-740.

Raynauld, J.-P. (1969). Rod and cone responses of ganglion cells in goldfish retina: a microelectrode study. Unpublished doctoral dissertation, The Johns Hopkins University: Baltimore.

Raynauld, J.-P. (1972). Goldfish retina: sign of the rod input in opponent color ganglion cells. Science, 177, 84-85.

Raynauld, J.-P. (1975). A model for the ganglionic receptive field organisation. In M.A. Ali (Ed.), Vision in Fishes: New Approaches in Research: Vol. 1(pp. 91-98). New York: Plenum Press.

Riemslag, F.C.C., & Schellart, N.A.M. (1978). Evoked potentials and spike responses to moving stimuli in the optic tectum of goldfish. Journal of Comparative Physiology A, 128, 13-20.

Robson, J.G. (1975). Receptive fields: neural presentation of the spatial and intensive attributes of the visual image. In E.C. Carterette & M.P. Friedman (Eds.), Handbook of Perception: Vol. 5. Seeing(pp. 81-116). New York: Academic Press.

Rodieck, R.W. (1965). Quantitative analysis of cat retinal ganglion cell response to visual stimuli. Vision Research, 5, 583-601.

Rodieck, R.W. (1973). The Vertebrate Retina. San Francisco: W.H. Freeman & Co.

Rodieck, R.W. (1979). Visual pathways. Annual Review of Neuroscience, 2, 193-225.

Rodieck, R.W., & Stone, J. (1965). Analysis of receptive fields of cat retinal ganglion cells. Journal of Neurophysiology, 28, 833-849.

Rosen, P., Levine, M.W., Rossetto, M. & Abramov, I. (1970). Instrumentation and techniques - a system for controlling the light output of a monochromator by any simple function and for temporally modulating the intensity. Behavior Research Methods and Instrumentation, 2, 297-300.

Rushton, W.A.H. (1965). The Ferrier Lecture, 1962: Visual adaptation. Proceedings of the Royal Society, Series B, 162, 20-46.

Saito, T., Kondo, H. & Toyoda, J. (1979). Ionic mechanisms of two types of on-center bipolar cells in the carp retina. 1. The reponses to central illumination. Journal of General Physiology, 73, 73-90.

Saito, T., Kujiraoka, T. & Yonaha, T. (1983). Connections between photoreceptors and horseradish peroxidase-injected bipolar cells in the carp retina. Vision Research, 23, 353-362.

Sakai, H., & Naka, K. (1983). Synaptic organization involving receptor, horizontal and ON- and OFF-center bipolar cells in the catfish retina. Vision Research, 23, 339-351.

Schellart, N.A.M. (1973). Dynamics and statistics of photopic ganglion cell responses in isolated goldfish retina. Unpublished doctoral dissertation, University of Amsterdam: Netherlands.

Schellart, N.A.M., & Spekreijse, H. (1972). Dynamic characteristics of retinal ganglion cell responses in goldfish. Journal of General Physiology, 59, 1-21.

Schellart, N.A.M., & Spekreijse, H. (1976). Shapes of receptive field centers in optic tectum of goldfish. Vision Research, 16, 1018-1020.

Schiller, P.H., & Malpeli, J.G. (1977). Properties and tectal projections of monkey retinal ganglion cells. Journal of Neurophysiology, 40, 428-445.

Scholes, J.H. (1975). Colour receptors and their synaptic connexions in the retina of a cyprinid fish. Philosophical Transactions of the Royal Society of London, 270, 61-118.

Scholes, J.H. (1976). Neuronal connections and cellular arrangement in the fish retina. In F. Zettler & R.E. Weiler (Eds.), Neural Principles in Vision (pp. 63-93). Berlin: Springer-Verlag.

Shapley, R.M., & Enroth-Cugell, C. (1984). Visual adaptation and retinal gain controls. Progress in Retinal Research, 3, 263-346.

Shapley, R.M., & Gordon, J. (1978). The eel retina: ganglion cell classes and spatial mechanisms. Journal of General Physiology, 71, 139-155.

Shapley, R.M., & Lennie, P. (1985). Spatial frequency analysis in the visual system. Annual Review of Neuroscience, 8, 547-583.

Shefner, J.M., & Levine, M.W. (1977). Interactions between rod and cone systems in the goldfish retina. Science, 198, 750-753.

Shefner, J.M., & Levine, M.W. (1979). A comparison of properties of goldfish retinal ganglion cells as a function of lighting conditions during dissection. Vision Research, 19, 83-89.

Sirovich, L., & Abramov, I. (1977). Photopigments and pseudopigments. Vision Research, 17, 5-16.

Snodderly, D.M. (1969). Manufactoring platinum microelectrodes. Unpublished manuscript.

Soodak, R.E. (1986). Two-dimensional modeling of visual receptive fields using Gaussian subunits. Proceedings of the National Academy of Sciences, USA, 83, 9259-9263.

Soodak, R.E., Shapley, R.M. & Kaplan, E. (1985). Unusual orientation tuning in the LGN and perigeniculate nucleus of the cat. Investigative Ophthalmology and Visual Science, 26(Suppl.), 264.

Soodak, R.E., Shapley, R.M. & Kaplan, E. (1987). Orientation tuning of receptive field subunits in Y cells of the cat. Manuscript submitted for publication.

Spekreijse, H., & Norton, A.L. (1970). The dynamic characteristics of color-coded S-potentials. Journal of General Physiology, 56, 1-15.

Spekreijse, H., & van den Berg, T.J.T.P. (1971). Interaction between colour and spatial coded processes converging to retinal ganglion cells in goldfish. Journal of Physiology, 215, 679-692.

Spekreijse, H., Wagner, H.G. & Wolbarsht, M.L. (1972). Spectral and spatial coding of ganglion cells responses in goldfish retina. Journal of Neurophysiology, 35, 73-86.

Stell, W.K. (1967). The structure and relationships of horizontal cells and photoreceptor-bipolar synaptic complexes in goldfish retina. American Journal of Anatomy, 121, 401-424.

Stell, W.K. (1972). The morphological organization of the vertebrate retina. In M.G.F. Fuortes (Ed.), Handbook of Sensory Physiology: Vol. VII. Physiology of Photoreceptor Organs (pp. 111-213). Berlin: Springer-Verlag.

Stell, W.K. (1975). Horizontal cell axons and axon terminals in goldfish retina. Journal of Comparative Neurology, 159, 503-520.

Stell, W.K. (1978). Inputs to bipolar cell dendrites in goldfish retina. Sensory Processes, 2, 339-349.

Stell, W.K. (1980). Photoreceptor-specific synaptic pathways in goldfish: a world of colour, a wealth of connections. In G. Verriest (Ed.), Colour Vision Deficiencies: Vol. V. (pp. 1-12). London: Hilger.

Stell, W.K., & Harosi, F.I. (1976). Cone structure and visual pigment content in the retina of the goldfish. Vision Research, 16, 647-657.

Stell, W.K., Ishida, A.T. & Lightfoot, D.O. (1977). Structural basis for on- and off-center responses in retinal bipolar cells. Science, 198, 1269-1271.

Stell, W.K., & Kock, J.-H. (1983). Structure, development and visual acuity in the goldfish retina. In S.R. Hilfer & J.B. Sheffield (Eds.), Molecular and Cellular Basis of Visual Acuity (pp. 79-105). New York: Spinger-Verlag.

Stell, W.K., & Lightfoot, D.O. (1975). Color-specific interconnections of cones and horizontal cells in the retina of the goldfish. Journal of Comparative Neurology, 159, 473-502.

Stone, J., & Fabian, M. (1968). Summing properties of the cat's retinal ganglion cell. Vision Research, 8, 1023-1040.

Stone, J., & Fukuda, J. (1974). Properties of cat retinal ganglion cells: a comparison of W-cells with X- and Y-cells. Journal of Neurophysiology, 37, 722-748.

Svaetichin, G. (1953). The cone action potential. Acta Physiologica Scandinavica, 29(Suppl.), 565-600.

Thorell, L.G., De Valois, R.L. & Albrecht, D.G. (1984). Spatial mapping of monkey VI cells with pure color and luminance stimuli. Vision Research, 24, 751-769.

Thorpe, S.A. (1971). Behavioral measures of spectral sensitivity of the goldfish at different temperatures. Vision Research, 11, 419-433.

Tomita, T. (1966). Electrophysiological study of the mechanisms subserving color coding. Cold Spring Harbor Symposium of Quantitative Biology, 30, 559-566.

Tomita, T. (1972). Light-induced potential and resistance changes in vertebrate photoreceptors. In M.G.F. Fuortes (Ed.), Handbook of Sensory Physiolgy: Vol. VII. Physiology of Photorecptor Organs (pp. 483-511). Berlin: Springer-Verlag.

Trifonov, Yu.A. (1968). Study of synaptic transmission between the photoreceptor and horizontal cell by electrical stimulation of the retina. Biofizika, 13, 809-817.

Tuttle, J.R., & Scott, L.C. (1978). X-like and Y-like ganglion cells in the Necturus retina. Investigative Ophthalmology and Visual Science, 17(Suppl.), 128.

van Dijk, B.W., & Spekreijse, H. (1984a). Color fundamentals deduced from carp ganglion cell responses. Vision Research, 24, 211-220.

van Dijk, B.W., & Spekreijse, H. (1984b). Linear color opponency in carp retinal ganglion cells. Vision Research, 24, 1865-1872.

Victor, J.D., & Shapley, R.M. (1979). The nonlinear pathway of Y ganglion cells in the cat retina. Journal of General Physiology, 74, 671-689.

Wagner, H.G., MacNichol, E.F., Jr. & Wolbarsht, M.L. (1960). The response properties of single ganglion cells in the goldfish retina. Journal of General Physiology, 43, 45-62.

Walls, G.L. (1942). The Vertebrate Eye and Its Adaptive Radiation. New York: Hafner Pub. Co.

Wartzok, D., & Marks, W.B. (1973). Directionally selective visual units recorded in the optic tectum of the goldfish. Journal of Neurophysiology, 36, 588-604.

Werblin, F.S., & Dowling, J.E. (1969). Organization of the retina of the mudpuppy Necturus maculosus: II. Intra-cellular recording. Journal of Neurophysiology, 32, 339-355.

Wiesel, T.N., & Hubel, D.H. (1966). Spatial and chromatic interactions in the lateral geniculate body of the rhesus monkey. Journal of Neurophysiology, 29, 1115-1156.

Wisowaty, J.J., & Boynton, R.M. (1980). Temporal modulation sensitivity of the blue mechanism: measurements made without chromatic adaptation. Vision Research, 20, 895-909.

Witkovsky, P., & Dowling, J.E. (1969). Synaptic relationships in the plexifomr layers of the carp retina. Z. Zellforsch, 100, 60-82.

Wolbarsht, M.L., & Wagner, H.G. (1963). Glass-insulated platinum microelectrodes: design and fabrications. In H. Bostem (Ed.), Medical Electronics (pp. 510-515). Liege: University of Liege Press.

Zemon, V., Gordon, J., & Welch, J. (1986). ON- and OFF-center pathways in humans examined using VEPs. Investigative Ophthalmology and Visual Science, 27(Suppl.), 280.